NorthWest Research Associates, Inc.
P.O. Box 3027 • Bellevue, WA 98009-3027

NWRA-CR-00-R226 1 November 2000

Decadal Variability and Temperature Trends in the Middle Atmosphere from Historical Rocketsonde Data

FINAL REPORT
for:
Contract No. NASW-97010

Prepared by:
Dr. Timothy J. Dunkerton
Principal Investigator
NorthWest Research Associates, Inc.

Prepared for:
National Aeronautics and Space Administration
Goddard Space Flight Center
Office of Headquarters Operations, Code 210.H
Greenbelt, MD 20771

14508 N.E. 20th Street • Bellevue, WA 98007-3713 • (425) 644-9660 • FAX (425) 644-8422

TABLE OF CONTENTS

Abstract

Observational studies were performed using historical rocketsonde data to investigate long-term temperature trends, solar-cycle variations, and interactions between tropical and extratropical latitudes in the middle atmosphere. Evidence from tropical, subtropical, and midlatitude North American rocketsonde stations indicated a consistent downward trend over 25 years, with a solar cycle component superposed. The trend is about -1.4 to-2.0 K per decade and the amplitude of the decadal oscillation is about1.1 K. Prior to trend derivation it was necessary for us to correct temperatures for aerodynamic heating in the early years. The empirically derived correction profile agrees well with a theoretical profile of Krumins and Lyons. A study was also performed of the correlation between equatorial winds and north polar temperatures in winter, showing that the entire stratospheric wind profile near the equator -- including the quasi-biennial oscillation (QBO) and stratopause semiannual oscillation (SAO) -- is important to the extratropical flow, not merely the QBO component as previously thought. A strong correlation was discovered between winter polar temperatures and equatorial winds in the upper stratosphere during the preceding September, suggesting a role for the second cycle of the SAO.

Further investigation of the Arctic Oscillation demonstrated a significant downward propagation of this mode from the mesosphere to the troposphere in winter. The statistical significance of this relationship was established. Finally, a contemporary and comprehensive review of the quasi-biennial oscillation was prepared for publication, reporting results from a 1998 workshop on the QBO.

STUDIES USING ROCKETSONDE DATA

GEOPHYSICAL RESEARCH LETTERS, VOL. 25, NO.17, PAGES 3371-3374, SEPTEMBER 1, 1998

Middle atmosphere cooling trend in historical rocketsonde data

Timothy J. Dunkerton, Donald P. Delisi, and Mark P. Baldwin

Northwest Research Associates, Bellevue, Washington

Abstract. Data from the historical rocketsonde network demonstrate that significant cooling of the upper stratosphere and lower mesosphere (~30–60 km) occurred in northern midlatitudes of the western hemisphere and in the tropics during 1962–1991. The downward trend of temperature averaged over this layer was about -1.7 K/decade and temperatures were apparently modulated by the solar cycle with amplitude ~1.1 K. The trend was a function of height and somewhat larger in the lower mesosphere relative to the middle and upper stratosphere.

Introduction

Cooling of the middle atmosphere is expected in response to the increasing concentration of greenhouse gases of anthropogenic origin. This signature is the largest and theoretically the most obvious component of climate change. Detection of a temperature trend above 10 hPa, however, is compromised by a number of problems including poor spatial and temporal coverage, instrument calibration, and inhomogeneities within each dataset. Nevertheless, there is general agreement that significant cooling has occurred over the last 2–3 decades. The observational evidence includes measurements from the Stratospheric Sounding Unit (SSU) [*Nash and Edge*, 1989], the historical rocketsonde network [*Angell*, 1987, 1991; *Golitsyn et al.*, 1996, and references therein], and Rayleigh lidar [*Hauchecorne et al.*, 1991; *Keckhut et al.*, 1995]. There is also indirect evidence of cooling in sodium lidar data suggesting a hydrostatic contraction of the atmosphere below ~95 km [*Clemesha et al.*, 1992], and a possible increase of noctilucent cloud sightings in the summer mesosphere [*Thomas*, 1991].

Identification of a climate trend distinct from natural interdecadal variability will require much more data than are currently available. Nevertheless, it is likely that observations in the modern era (1950s and thereafter) will play a pivotal role in the detection of human influence, having been acquired in a time period when such an effect might be first observable. Data from the historical rocketsonde network provide the longest continuous evidence of cooling in the upper stratosphere and lower mesosphere (~1962–1991). In order to make optimum use of these data it has been necessary for us to assemble the dataset from various sources and to carefully analyze the data for possible biases and inhomogeneities.

Paper number 98GL02385.
0094-8534/98/98GL-02385$05.00

Data Analysis

Data from the historical rocketsonde network (World Data Center 'A') including North American stations and a few tropical sites for the period 1969–1991 were obtained from the National Center for Atmosphere Research, supplemented by additional data from the Climate Prediction Center (Mel Gelman, personal communication) and National Climatic Data Center. These data are comprised of individual rocket soundings accompanied by rawinsonde data from the same stations. For the period before 1969 we obtained pre-processed data formerly utilized by scientists of the meteorology group at Control Data Corporation (David Venne, personal communication). These data were originally acquired from rocket soundings but had been processed

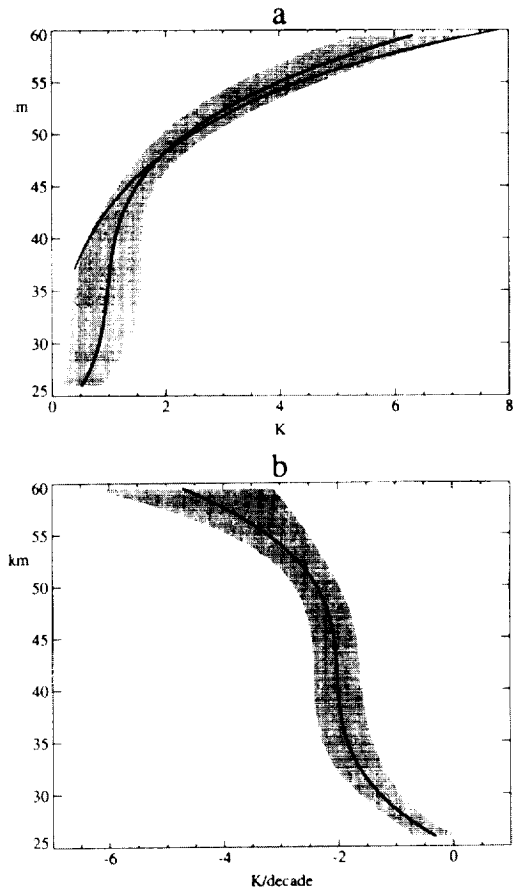

Figure 1. (a) Average of empirical temperature correction profiles (black line) plus or minus one standard deviation (shading). The standard correction is also shown (gray line). (b) Average profile of temperature trend, after the average correction was applied to stations individually, plus or minus one standard deviation (shading).

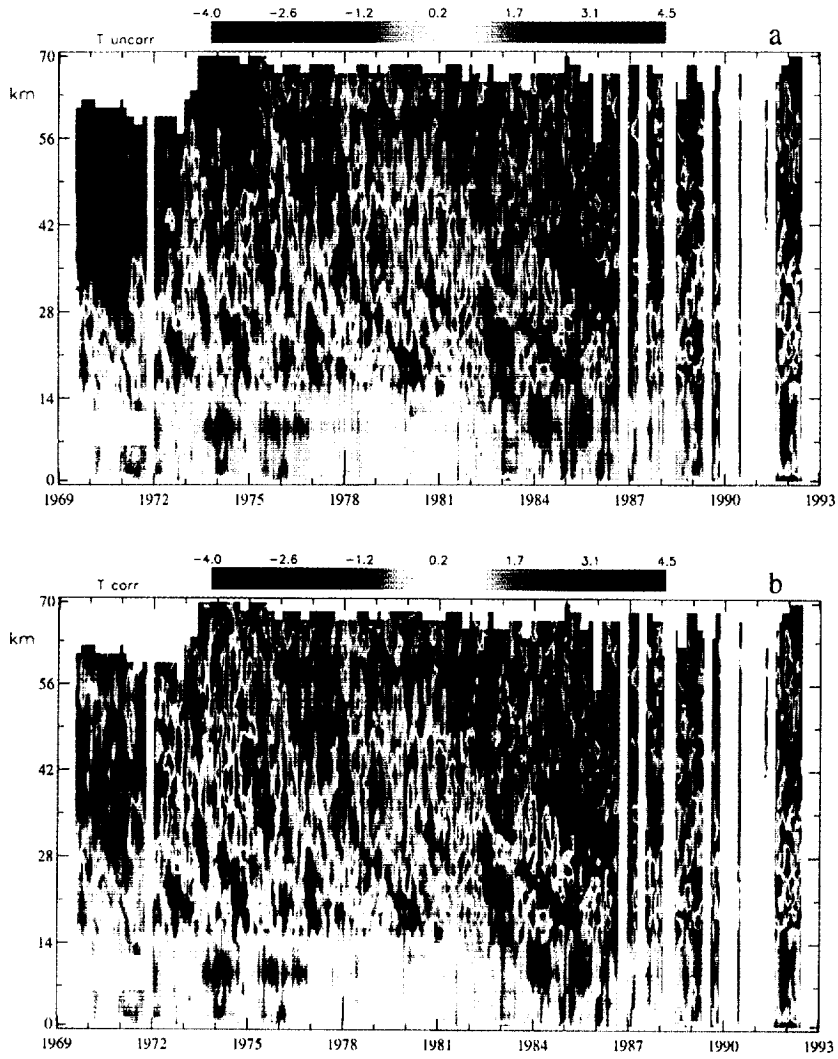

Figure 2. Time-height cross section of monthly mean deseasonalized temperature at Kwajalein. (a) Uncorrected and (b) corrected data are shown with the same color scale. At Kwajalein, the transition to corrected data occurred in April 1975. Units: K.

onto a regular vertical grid at 2 km intervals. The preprocessed data were obtained by us through 1982, and were found to agree with the original data in their period of overlap. Of the 22 stations included in this rocketsonde network, 17 provide data for more than 10 years and 9 provide data for more than 20 years. Data at most stations were analyzed but in this letter we focus attention on six of these lying either in western hemisphere midlatitudes or tropics:

Ascension (14.8°W, 8.6°S),
Kwajalein (167.4°E, 8.4°N),
Barking Sands (159.9°W, 22.0°N),
Cape Kennedy (80.7°W, 28.3°N),
Point Mugu (119.5°W, 34.1°N),
and
Wallops Island (75.7°W, 37.5°N).

Their location outside the winter polar vortex is such that interannual variability is relatively small.

Angell [1987, 1991] compared rawinsonde and rocketsonde temperatures at 26–35 km and concluded that, because of a sharp apparent cooling of rockets with respect to rawinsondes in the early 1970s, the rocket trend at that time was spurious. This is consistent with a suggestion by *Johnson and Gelman* [1985], who examined data from the North American network in the band 25–55°N. Our analysis shows that individual stations did not exhibit this cooling at the same time, and the spurious 'trend' really amounts to a near-discontinuity in measured temperature. We examined header information for soundings at tropical and midlatitude stations and determined that the spurious jump was due primarily to a change from uncorrected to corrected temperatures (to account for aerodynamic heating, etc.) rather than an instrumental change (e.g., Arcasonde to Datasonde). In this letter we therefore display temperature data using all instrument types. Included in the dataset are a few measurements obtained from falling spheres. The sphere data are colder, generally falling outside the range of observed layer-mean temperatures, but are relatively few in number and do not affect the results significantly.

In order to utilize uncorrected data before the early 1970s it is necessary to subtract a positive temperature correction profile. The standard correction is doc-

umented in *Krumins and Lyons* [1972]. For comparison, we chose instead to derive empirical correction profiles for each station in the following manner. Biennial-mean deseasonalized temperature profiles were obtained immediately before and after the switch from uncorrected to corrected data at each station (the biennial interval chosen to minimize effects of the quasi-biennial oscillation). We then assumed that the two biennial-mean profiles should have been equal apart from a linear trend. The empirical correction profile and final trend estimate were obtained at each level by iterating this procedure a few times until convergence. The average correction profile is shown in Figure 1a, and agrees well with the standard correction, except at lower levels where the empirical correction is about 1 K. Both corrections increase with altitude near the stratopause in approximately exponential fashion; the scale height is about 7.9 km for the standard correction, close to a density scale height. For the purpose of plotting data above 60 km, where our derivation of empirical correction would be unreliable, the correction profile was extrapolated using a constant scale height.

Application of the average correction to uncorrected data reduces the net trend over the entire record but does not eliminate either the trend or an apparent solar cycle influence as demonstrated below. The average trend of the six stations as a function of height is shown in Figure 1b: approximately -2 K/decade in the upper stratosphere, increasing to in excess of -4 K/decade in the lower mesosphere.

Results

Monthly mean uncorrected and corrected temperatures at Kwajalein are shown in Figures 2a and 2b, respectively. These figures display rawinsonde data below 3.7 scale heights (~25 hPa), rocketsonde data above 4.7 scale heights (~9 hPa), and a linear blend of the two in their region of overlap. Prominent features include descending phases of the quasi-biennial oscillation, an apparent decadal variation coinciding with the solar cycle (with maximum temperature near solar maximum and vice versa), and a cooling trend throughout the record. Note the apparent positive correlation with the solar cycle: e.g., solar maxima occurred around 1969, 1981, and 1990; solar minima occurred around 1976 and 1986. A transient effect of the El Chichón eruption in 1982 was prominent at Kwajalein in the middle half of this year with warming in the lower stratosphere and cooling aloft as documented by *Dunkerton and Delisi* [1991]. A cooling trend was present at most levels of the middle atmosphere, whereas the apparent solar influence was seen primarily above 35 km.

Figure 3a compares rawinsonde and corrected rocketsonde temperatures averaged vertically in their region of overlap, at five stations. At each location the two datasets agree reasonably well, especially the high-frequency variability; however, there was a brief period near 1970–71 when rocket temperatures were anomalously high by about 2 K, and another interval after 1984 when rockets were slightly cool by about 1–2 K. These discrepancies affect the trend estimates, which range from -0.19 to -0.73 K/decade for rawinsondes, and from -0.81 to -1.33 K/decade for rocketsondes. The downward trend is real, but possibly exaggerated in rocketsonde data. At higher levels, there is good agreement between stations concerning both the downward trend and apparent solar influence, as shown in Figure 3b. Here, temperatures are averaged vertically over the layer 4.1–7.9 scale heights (approximately 28–56 km) . Over the last 25 years, downward trends of magnitude -1.38 to -2.01 K/decade are obtained after correction. Amplitude of the decadal oscillation is ~1.1 K.

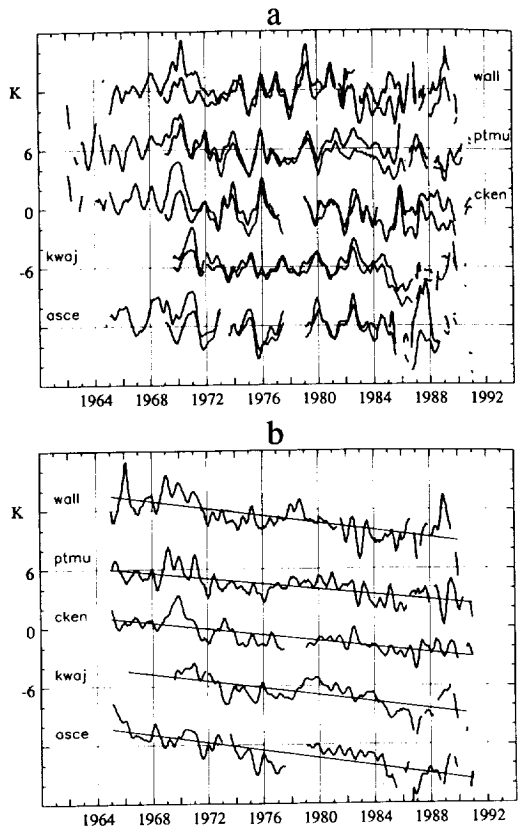

Figure 3. (a) Layer-mean temperature at 3.7-4.7 scale heights for five stations, derived from corrected rocketsonde data (black line) and rawinsonde data (gray line). (b) Layer-mean rocketsonde temperature at 4.1-7.9 scale heights. A linear least-squares fit to each series is also shown (light solid).

Figure 4 shows the average of the individual station data shown in Figure 3b. Data are plotted only when three or more stations have data in a given month. The dashed straight line is the linear least-squares fit through two solar cycles, starting at the solar minimum in 1965 and ending at the solar minimum in 1986. The slope of this line is -1.76 K/decade. The solid straight line is the linear least-squares fit through two solar cycles, starting at the solar maximum in 1969 and ending at the solar maximum in 1990. The slope of this line is -1.69 K/decade. The 10.7 cm solar flux is shown in the bottom part of this figure. Several interesting features are notable. For example, the data show a positive correlation with the solar flux, indicating an apparent solar cycle in the height-averaged temperature data. It should be recognized that the apparent solar signal is small and is best seen when the data are averaged vertically and data from several stations are blended together; the significance of this result should not be overstated. The data also show a reasonably constant trend over nearly three decades (in the sense that similar trends are obtained using subintervals within this

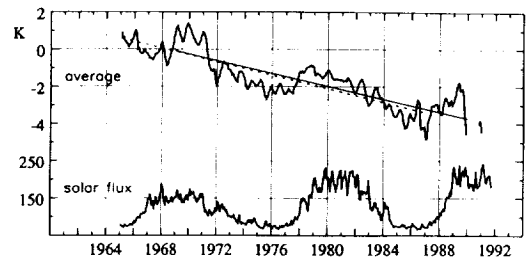

Figure 4. Average of layer-mean temperatures at 4.1-7.9 scale heights for the five stations of Figure 3. Trendlines between solar maxima (solid) and solar minima (dashed) are superposed.

record stretching over two solar cycles). This result appears to validate the temperature correction method even though the break points occurred at different times depending on location. For comparison, using only one solar cycle [e.g., *OTP*, 1988], the trends for solar minimum to solar minimum are -2.53 and -1.92 K/decade, and the trends for solar maximum to solar maximum are -1.93 and -1.28 K/decade.

Conclusion

Data from the historical rocketsonde network demonstrate that significant cooling of the upper stratosphere and lower mesosphere (~30–60 km) occurred in northern midlatitudes of the western hemisphere and in the tropics during 1962–1991. The downward trend of temperature data averaged over this layer was about -1.7 K/decade and temperatures were apparently modulated by the solar cycle with amplitude ~1.1 K. The trend was a function of height and somewhat larger in the lower mesosphere relative to the middle and upper stratosphere.

Uncorrected temperature data prior to the early 1970s require the user to correct for aerodynamic heating and other heat transfer effects; the date before which correction is required varies from station to station. Correction profiles derived empirically are similar to the standard correction, increasing with altitude approximately in exponential fashion with a scale height close to that of atmospheric density. The magnitude of derived temperature trend depends on the application of a suitable correction to early data; this is the most salient issue for trend studies using these data. The overall behavior of temperature time series does not depend significantly on thermistor type (e.g., Arcasonde or Datasonde) since instrumental changes were relatively few and most variability was observed in periods of time monitored by the same instrument. Other factors not discussed here such as measurement time of day and agreement with adjacent rawinsonde might alter the trend estimate, but our investigation (to be reported separately) indicates that these are relatively minor effects.

Putting our results in a larger context, although evidence of similar cooling has been found in other datasets [e.g., *Golitsyn et al.*, 1996], it is likely that temperature trends associated with climate change are not globally or hemispherically uniform but contain a dynamical component associated with planetary waves and induced mean meridional circulation. Further analysis of existing ground-based and satellite datasets and synthesis with newer methods of observation (e.g., lidar) will help to clarify the nature of the climate change signal as affected by atmospheric dynamics.

Acknowledgments. This research was supported by the National Aeronautics and Space Administration, Contract NASW-97010, and by the National Oceanic and Atmospheric Administration, Grant NA76GP0354.

References

Angell, J.K., Rocketsonde evidence for a stratospheric temperature decrease in the Western hemisphere during 1973-85. *Mon. Wea. Rev., 115*, 2569-2577, 1987.

Angell, J.K., Stratospheric temperature change as a function of height and sunspot number during 1972-89 based on rocketsonde and radiosonde data. *J. Climate, 4*, 1170-1180, 1991.

Clemesha, B.R., D.M. Simonich, and P.P. Batista, A long-term trend in the height of the atmospheric sodium layer: possible evidence for global change. *Geophys. Res. Lett, 19*, 457-460, 1992.

Dunkerton, T.J., and D.P. Delisi, Anomalous temperature and zonal wind in the tropical upper stratosphere, 1982/1983. *J. Geophys. Res., 96*, 22,631-22,641, 1991.

Golitsyn, G.S., A.I. Seminov, N.N. Shefov, L.M. Fishkova, E.V. Lysenko, and S.P. Perov, Long-term trends in the middle and upper atmosphere. *Geophys. Res. Lett., 23*, 1741-1744, 1996.

Hauchecorne, A., M.-L. Chanin, and P. Keckhut, Climatology and trends of the middle atmospheric temperature (33-87 km) as seen by Rayleigh lidar over the south of France. *J. Geophys. Res., 96*, 15,297-15,309, 1991.

Johnson, K.W., and M.E. Gelman, Trends in upper stratospheric temperatures as observed by rocketsondes (1965-1983). *Middle Atmosphere Program, Handbook for MAP*, Vol. 18, S. Kato, ed., 1985.

Keckhut, P., A. Hauchecorne, and M.L. Chanin, Midlatitude long-term variability of the middle atmosphere: trends and cyclic episodic changes. *J. Geophys. Res., 100*, 18887-18897, 1995.

Krumins, M.V., and W.C. Lyons, Corrections for the upper atmosphere temperature using a thin film loop mount. *NOLTR 72-152*, Naval Ordnance Laboratory, White Oak, Silver Spring, Maryland, 1972.

Nash, J., and P.R. Edge, Temperature changes in the stratosphere and lower mesosphere 1979-1988 inferred from TOVS radiance observations. *Adv. Space Res.,9*, 333-341, 1989.

OTP, Report of the International Ozone Trends Panel 1988. WMO, Global Ozone Research and Monitoring Project, Report No. 18., 1988.

Thomas, G.E., Mesospheric clouds and the physics of the mesopause region. *Rev. Geophys., 29*, 553-575, 1991.

T. J. Dunkerton, D. P. Delisi, and M. P. Baldwin, Northwest Research Associates, P.O. Box 3027, Bellevue, WA 98009. e-mail: tim@nwra.com; don@nwra.com; mark@nwra.com

(Received April 22, 1998; revised July 9, 1998; accepted July 15, 1998.)

Q. J. R. Meteorol. Soc. (2000), **127**, pp. 1–999

The Influence of the Equatorial Upper Stratosphere on Northern Hemisphere Stratospheric Sudden Warmings

By L.J. GRAY[1]* S.J. PHIPPS[1], T.J. DUNKERTON[2], M.P. BALDWIN[2], E.F. DRYSDALE[1] and M.R. ALLEN[1]

[1] *Rutherford Appleton Laboratory, UK*
[2] *Northwest Research Associates, USA*

(Received 1 January 2000; revised 31 December 2000)

SUMMARY

Equatorial winds in the stratosphere are known to influence the frequency of stratospheric sudden warmings. Sudden warmings, in turn, influence the Earth's climate both through their direct influence on polar temperatures and through the temperature dependence of ozone depletion in the lower stratosphere. The conventional (Holton-Tan) explanation for the equatorial influence on stratospheric warmings is in terms of the equatorial winds in the lower stratosphere (~20-30 km) acting as a wave-guide for mid-latitude planetary wave propagation. This study employs stratospheric temperature analyses and equatorial rocketsonde wind data extending to 58 km to diagnose the relationship between the Northern Hemisphere polar temperatures and equatorial zonal winds at all height levels in the stratosphere. In addition to the recognised Holton-Tan relationship linking the polar temperatures to the quasi biennial oscillation in equatorial winds in the lower stratosphere, a strong influence from equatorial winds in the upper stratosphere is found. We suggest that this may be associated with the rate of onset of the westerly phase of the semi annual oscillation in the upper stratosphere, although the observations alone cannot provide a conclusive, causal relationship. The main diagnostic tools employed are correlation studies and composite analysis. The need for continued high quality, equatorial wind measurements at all stratospheric levels is also stressed.

KEYWORDS: Stratosphere Quasi biennial oscillation Semi annual oscillation Northern hemisphere winter Stratospheric warming Interannual variability

1. INTRODUCTION

The Northern Hemisphere (NH) stratospheric winter circulation displays substantial inter-annual variability (Labitzke 1982). Some winters are extremely disturbed and are accompanied by stratospheric sudden warmings, in which the polar temperature increases by 20°C or more in just a few days (Andrews *et al.* 1987). In contrast, other winters have fewer warming events and the polar vortex remains cold and undisturbed. Variability associated with stratospheric warmings is the primary source of variability in the NH winter lower stratosphere. The variability of NH winter stratospheric temperatures is also closely coupled to the Arctic Oscillation, the leading mode of variability in the troposphere (Thompson and Wallace 1998, Baldwin and Dunkerton 1999, Ramaswamy et al. 2000).

Global, annual-mean temperatures in the lower stratosphere have fallen by ~0.6°C per decade over recent decades (e.g. Pyle *et al.* 1999). It is important to characterise natural variability if we are to assess how much of the observed temperature trend is directly related to human activity. It is also important because temperature directly influences the processes that lead to ozone trends in this region. Stratospheric warmings result in a weak, disturbed vortex with warm temperatures and substantial downward transport of ozone-rich air. Conversely, a strong, stable vortex with cold temperatures will result in large chemical ozone loss (due to the temperature-dependence of the destruction reactions) and weak transport of ozone (Chipperfield and Jones 1999). A number of studies have found evidence for long-term changes in the stratospheric circulation, including a

* Corresponding author: Rutherford Appleton Laboratory, Chilton, Didcot, Oxon., OX11 0QX, UK.

strengthening of the Arctic vortex (Zurek *et al.* 1996) and changes in the NH geopotential heights (Labitzke and van Loon 1995). Any such changes would also influence the long-term trends in ozone and temperature (Hood *et al.* 1997).

Although stratospheric sudden warmings have been observed and documented for many years, the factors that control their variability are not well understood. An essential requirement for their development is the presence of quasi-stationary planetary wave disturbances. These waves are generated in the troposphere and propagate vertically and horizontally into the stratosphere, where they can be of sufficient amplitude to displace the vortex away from the pole. These waves are the main mechanism for heat transfer to the polar region and associated with each vortex displacement there is a rapid increase in temperature at the pole.

The dependence of the winter-time average polar temperature and vortex strength on the phase of the quasi biennial oscillation (QBO) in the lower stratosphere was noted nearly twenty years ago (Holton and Tan 1980, 1982). The QBO is an oscillation of the equatorial zonal wind in the lower stratosphere. They oscillate between easterlies and westerlies with an average period of 28 months. The maximum amplitude of the oscillation is around 25-30km. When the equatorial winds at 20-30 km are in an easterly phase, the northern polar vortex is generally warmer, more disturbed by waves and disruption of the vortex by major mid-winter warmings is more likely (see also Dunkerton and Baldwin 1991, Baldwin and Dunkerton 1998). The conventional explanation for this equatorial influence on polar temperatures is that the QBO winds in the lower stratosphere influence the background mean flow, which then affects the propagation of planetary scale waves (e.g. O'Sullivan and Young 1992; O'Sullivan and Dunkerton 1994; Hamilton 1998; Niwano and Takahashi 1998; Baldwin *et al.* 2000). More specifically, the QBO winds in the lower stratosphere determine the position of the zero wind line near the equator, which acts as a wave-guide for the planetary wave propagation. This results in enhanced poleward heat transfer during an easterly QBO phase and weaker transfer during a westerly phase.

While this mechanism is generally accepted, it has also been recognised that this pattern of 'warm disturbed easterly phase' / 'cold undisturbed westerly phase' does not always hold up, particularly in late winter (Hamilton 1998; Baldwin et al. 2000). Labitzke and van Loon (1988) and Naito and Hirota (1997) have noted that the periods when the Holton-Tan relationship holds up well coincide with periods when the 11-year solar sunspot cycle is at its minimum phase (defined, for example, by the 10.7cm solar flux). Conversely, it appears to substantially weaken or reverse during periods of solar maximum. While the solar cycle / QBO link and the solar cycle / NH polar temperature link has been studied extensively (e.g. Labitzke and van Loon 1988; Gray and Dunkerton 1990; Teitelbaum and Bauer 1990; Salby and Shea 1991; Dunkerton and Baldwin 1992; Kodera 1991, 1993, 1995; Balachandran and Rind 1995; Rind and Balachandran 1995; Labitzke and van Loon 1996; Naito and Hirota 1997; Haigh 1999; Shindell *et al.* 1999), the precise mechanism that relates (1) the solar cycle, whose primary influence is in the region of the equatorial stratopause (~50 km), (2) the QBO, which has its maximum amplitude in the lower equatorial stratosphere (~20-30 km) and (3) the winter-time lower stratospheric polar temperatures, has yet to be clearly elucidated.

In this paper, we aim to explore the possible links between these three phenomena by examining the relationship between polar temperatures and equatorial winds using an equatorial wind data set that measures much higher than the radiosonde dataset more usually employed. While the radiosonde observations extend to ~20-30km, the rocketsonde dataset employed in this study extends to 58km (Dunkerton and Delisi 1997; Dunkerton *et al.* 1998). The rocketsonde dataset thereby includes not only the lower

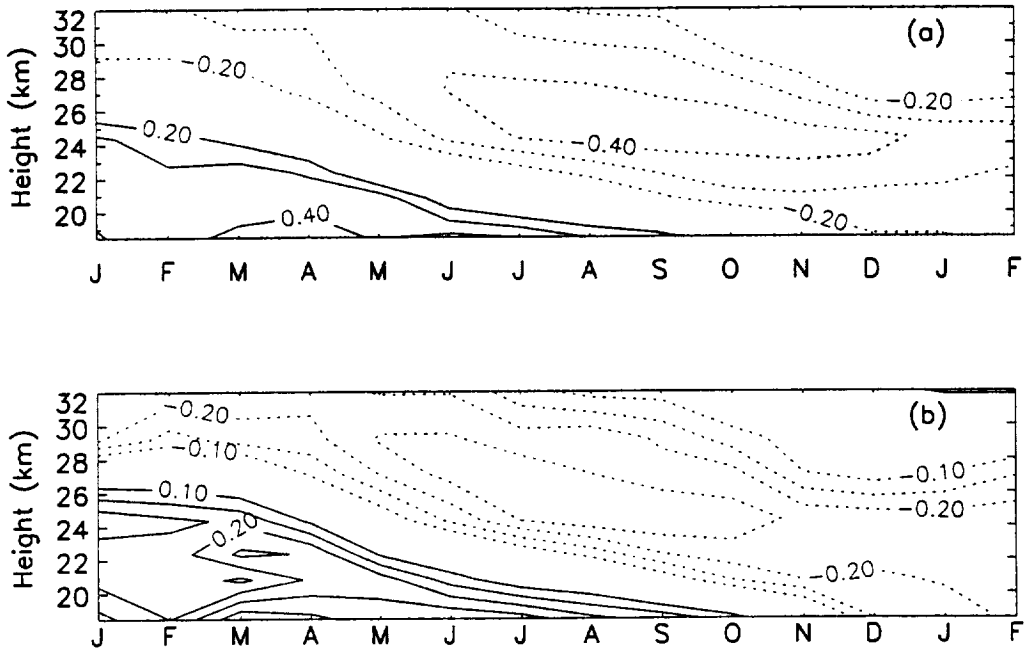

Figure 1. Correlation for the periods (a) 1964/65 - 89/90 and (b) 1955/56 - 1998/99 between JF North Polar (NP) temperature at 24km and monthly-averaged equatorial wind in each month from January of the previous year to February of the same year. Contour interval is 0.1. Dotted contours denote negative values. Shading indicates values are significant at the 95% confidence level (no values were significant at the 99% confidence level). For details of the significance test applied, see appendix A. NP temperatures are from the Berlin stratospheric analyses. Equatorial winds are from radiosonde ascents.

stratospheric winds (20-30km) usually associated with the observed QBO modulation of the polar temperatures but also the higher altitudes that encompass the stratopause region, where the direct solar influence is greatest. In section 2 we briefly review the results of correlations between NP temperatures and the lower stratospheric winds from the radiosonde dataset. In section 3 the rocketsonde dataset is described and a detailed analysis is presented of the relationships between NP temperatures and equatorial winds at all heights to 58km using the rocketsonde dataset. This analysis includes correlation studies, regression analyses, and composite studies. The main conclusions of the study are presented in section 4.

2. Radiosonde Analysis

Figure 1a shows the correlation over 24 winters (1964-90) between the January-February average (JF) North Polar (NP) temperature and the equatorial zonal winds (u_{eq}) from radiosonde observations in each month from January of the previous year to February of the same year. We choose to use JF temperature since most major midwinter warmings occur in these months. The polar temperatures are anti-correlated with the lower stratospheric equatorial winds in the previous months with the region of maximum correlation gradually descending through the atmosphere with time, corresponding to the descent of the QBO winds. This pattern is consistent with the mechanism described above (hereafter referred to as the Holton-Tan mechanism), with easterly (negative) wind anomalies associated with warm (positive) temperature anomalies and vice versa. For the 26-year period 1964-90, the maximum correlation coefficients are of order -0.4. However,

when the correlation is repeated using data from 43 winters (1955-99, see figure 1b), which is the full extent of the available radiosonde data, the maximum correlation drops to only ~-0.25.

Figure 2a shows the actual JF north polar temperatures and corresponding lower stratospheric equatorial wind for the period 1964-90 that were used to determine the correlations of figure 1a. It shows that the Holton-Tan relationship of negative correlation between the two signals is present for certain periods but not others. For example, the two signals are anti-correlated during the periods 1965-68, 1971-78 and 1986-88, but in the intervening years either the opposite is true (e.g. 1969, 1980 and 1984-85) or there is no apparent relationship (e.g. 1982-83). It is these latter periods that degrade the correlation, resulting in the relatively low correlations seen in figure 1a. A scatter plot of the data (figure 2b) further demonstrates the weakness of the resulting correlation.

It is possible that the difference in maximum correlation displayed by the analysis of the two different time periods in figure 1 can be understood as the difference in the relative number of solar minima and maxima in the two selected time periods (Labitzke and van Loon 1988; Naito and Hirota 1997). While the 1955/90 period encompasses an equal number of solar minimum and solar maximum periods, the 1964/90 period has a slightly larger influence from solar minimum than solar maximum periods.

3. Rocketsonde Analysis

(*a*) *The data*

Regular rocketsonde ascents were made from Kwajalein (8°N) during the period 1969-90 and from Ascension Island (8°S) during the periods 1962-77 and 1979-89. Occasional gaps of up to a few months duration are present in both records. In order to obtain a single, unbroken time series of equatorial winds, the monthly-averaged data from the two stations were first de-seasonalised. This was done by calculating and subtracting the climatological monthly mean at each height and at each station. Gaps of up to three months duration in the records for each station were then filled by linear interpolation. For those heights and months when data were available for both stations, the two data sets were then combined by averaging them together. When data were only available from one station, that data was used. In this way, an unbroken time series of de-seasonalised 'equatorial' (8°S–8°N averaged) winds was achieved from January 1964 to February 1990 for the height region 20-58 km.

Figure 3a shows the time-height cross-section of the raw monthly-averaged data from Kwajalein. The QBO is the dominant signal in the lower stratosphere (20-35 km). The maximum amplitude of the oscillation is around 25 km, with the wind varying between -30 ms^{-1} and +20 ms^{-1}. Above 35 km the semi-annual oscillation (SAO), with a period of six months, dominates. Figure 3b shows the combined Kwajalein and Ascension Island data set, which is derived from the de-seasonalised data as described above. (Note that the SAO has been removed by the deseasonalising process). The QBO period has been further highlighted in figure 3c using a 9-60 month bandpass filter.

(*b*) *Correlation studies*

Using the combined de-seasonalised rocketsonde wind data (figure 3b), we have carried out a correlation study to examine the link between the equatorial winds and the Northern Hemisphere polar temperature in winter. Figure 4 shows the strength of the correlation between the observed JF North Polar temperature at 24km from the Berlin stratospheric analyses (courtesy K. Labitzke) and the rocket-sonde equatorial winds at

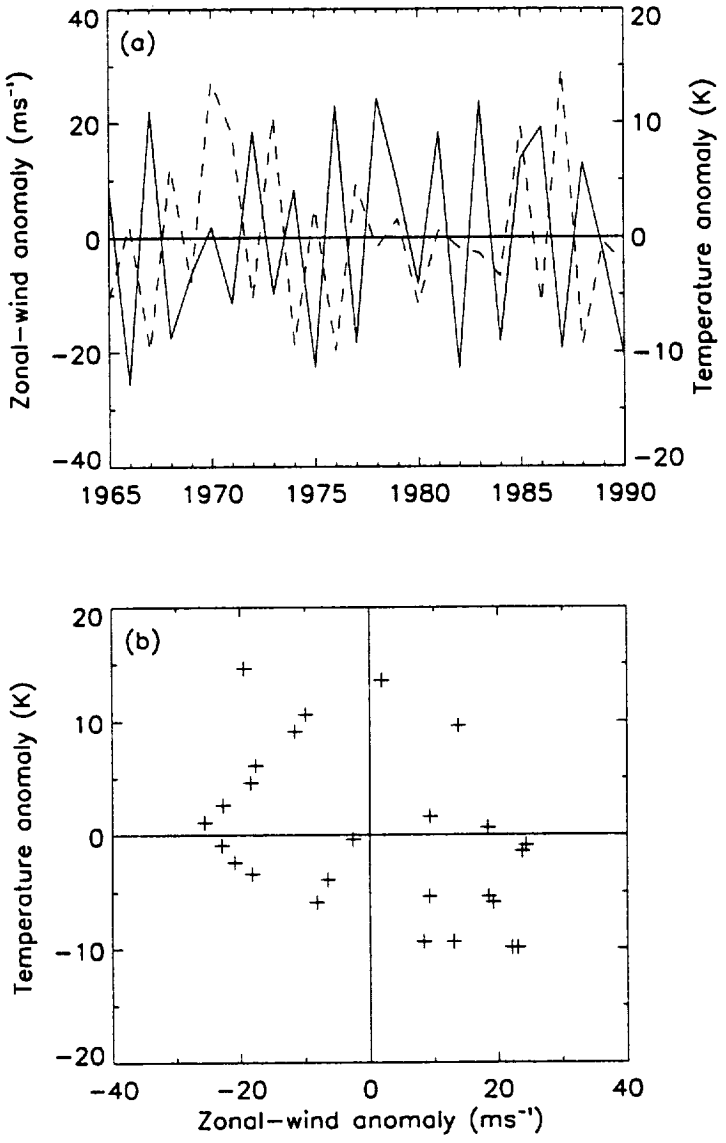

Figure 2. (a) Time-series of JF North Polar temperature anomaly (K) at 24km ($\sim 30hPa$) (dotted line) and equatorial wind anomaly (ms^{-1}) at 24km in the preceding December (solid line). (b) Scatter plot of the data.

each height and month leading up to January/February (i.e. identical to figure 1a but using the rocketsonde data). Note first the negative correlation of ~0.4 at 20-35 km which slowly propagates downwards with time. This was the correlation noted by Holton and Tan nearly 20 years ago and is virtually identical to the results of the correlations using radiosonde wind data (figure 1a).

However, there is also significant correlation at higher levels. In the 30-50 km region there is a positive correlation of ~0.3-0.4, also descending slowly with time. This change in sign of the correlation with height reflects the next incoming phase of the equatorial wind QBO (see figure 3). Above 50 km, there is a region of relatively high correlation in

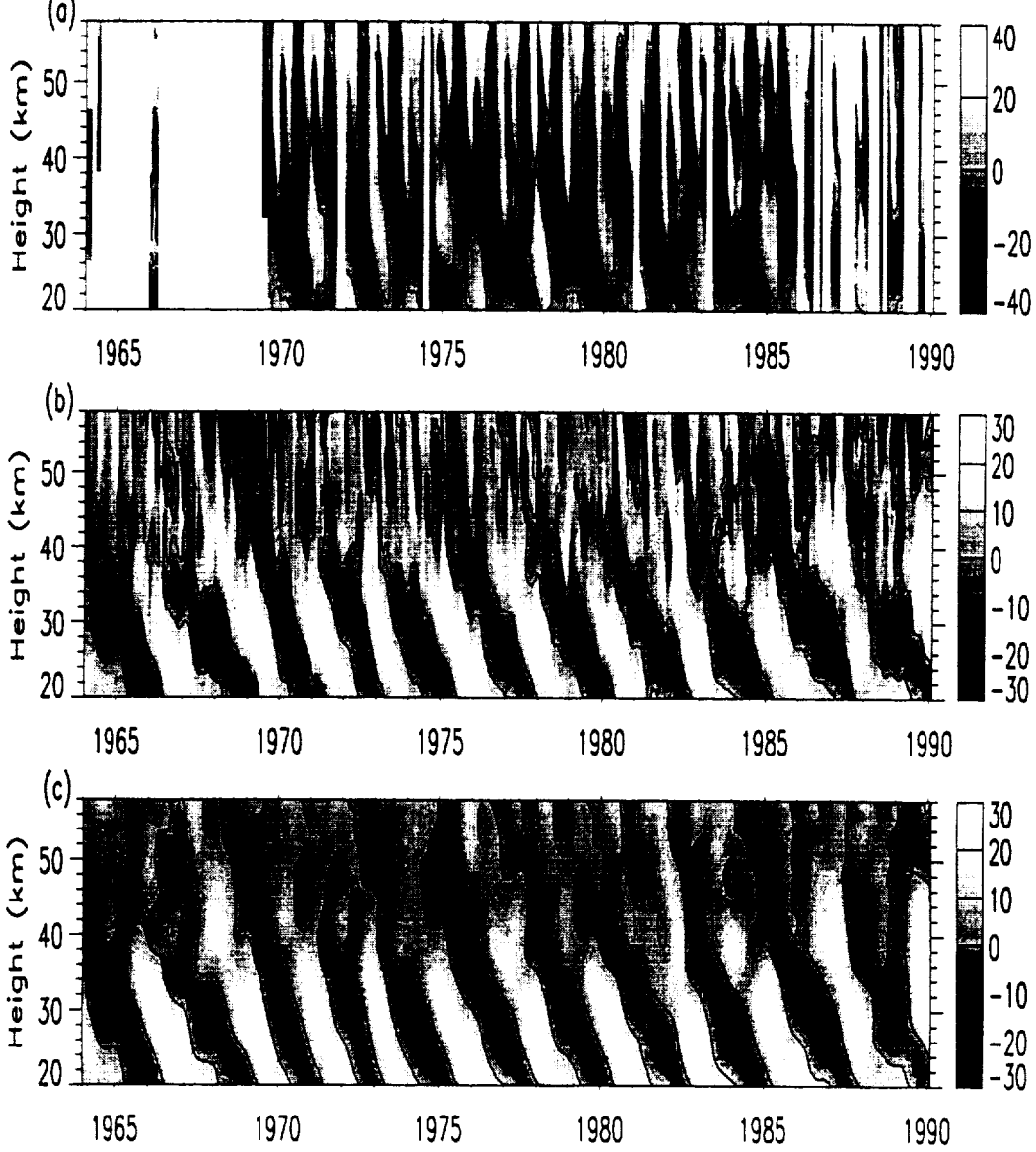

Figure 3. (a) Monthly-averaged zonal wind (ms^{-1}) derived from rocketsonde ascents at Kwajalein (8°N). (b) De-seasonalised monthly-averaged zonal wind dataset derived by combining data from both Kwajalein and Ascension Island as described in the text. (c) As in panel (b) after passing through a 9-60 month bandpass filter. Zero value is denoted by contour line.

September/October. At 52 km in September, the correlation exceeds -0.6 and is significant at the 99% confidence level. We note here that there can be no suggestion that this high correlation is simply a response of the equatorial winds to the winter polar warming, since the strongest correlation is found with the previous September, 4-5 months before the major warming takes place.

(c) *Regression analyses*

Linear regression analyses were carried out in order to assess the effectiveness of

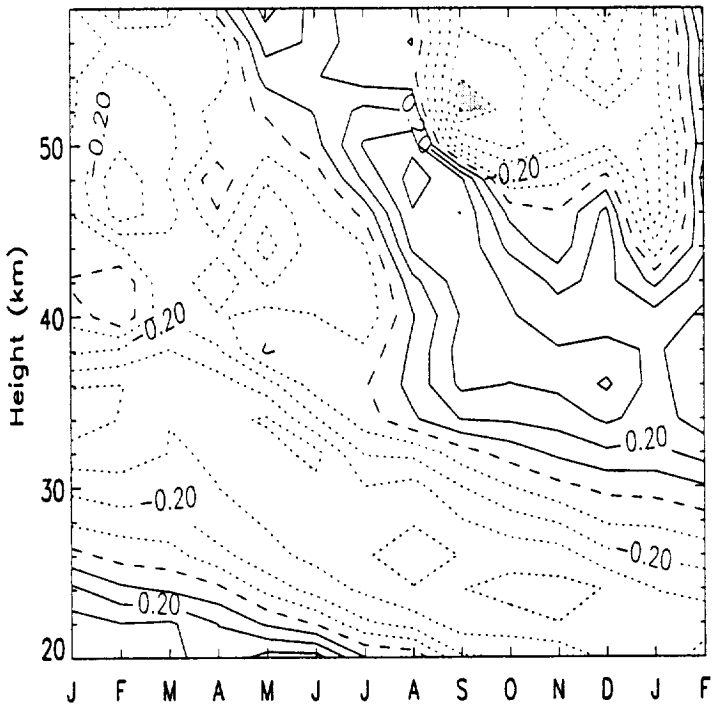

Figure 4. As figure 1 but using rocketsonde data that extends to 58km instead of radiosonde data. Light and dark shading denote regions where values are significant at the 95% and 99% confidence levels respectively.

the rocketsonde equatorial winds (u_{eq}) at different heights and in different months as a predictor of the winter-time polar temperature. Initially, simple linear regression was used to fit the JF NP temperature to u_{eq} at (a) 24km in December (as an indicator of the phase of the QBO in the lower stratosphere), and (b) 52km in September. The best fit to u_{eq} at 52 km was found to describe 37% of the variance in the polar temperature. By contrast, the best fit to u_{eq} at 24km was found to describe only 16% of the variance.

A series of multiple linear regressions was then carried out in order to find the two parameters that best predict the polar temperature. In each analysis, u_{eq} for a given height and month was employed as a fixed parameter, while u_{eq} for every other available height and month was used in turn as the second parameter. In this way, we sought to maximise the amount of the variance in the polar temperature that could be described. In the first such analysis, u_{eq} at 24km in December was employed as the fixed parameter. It was found that u_{eq} at 52 km in September was most effective as the second parameter, with a total of 41% of the variance in the polar temperature being described.

Repeating the analysis with u_{eq} at 52 km in September as the fixed parameter, it was found that the most effective second parameter was u_{eq} at 48 km in the same month. A total of 51% of the variance in the polar temperature was described. This is an interesting result on two accounts. Firstly, the greatest additional contribution did not come from the lower stratosphere - the region in which the Holton-Tan mechanism is at work. Secondly, the two parameters consist of the equatorial wind immediately above and immediately below 50 km in September. In figure 4 it can be seen that there is a sharp change in the sign of the correlation at this point. This suggests that the vertical gradient of the wind at ~ 50 km in September may be in some way linked to the North

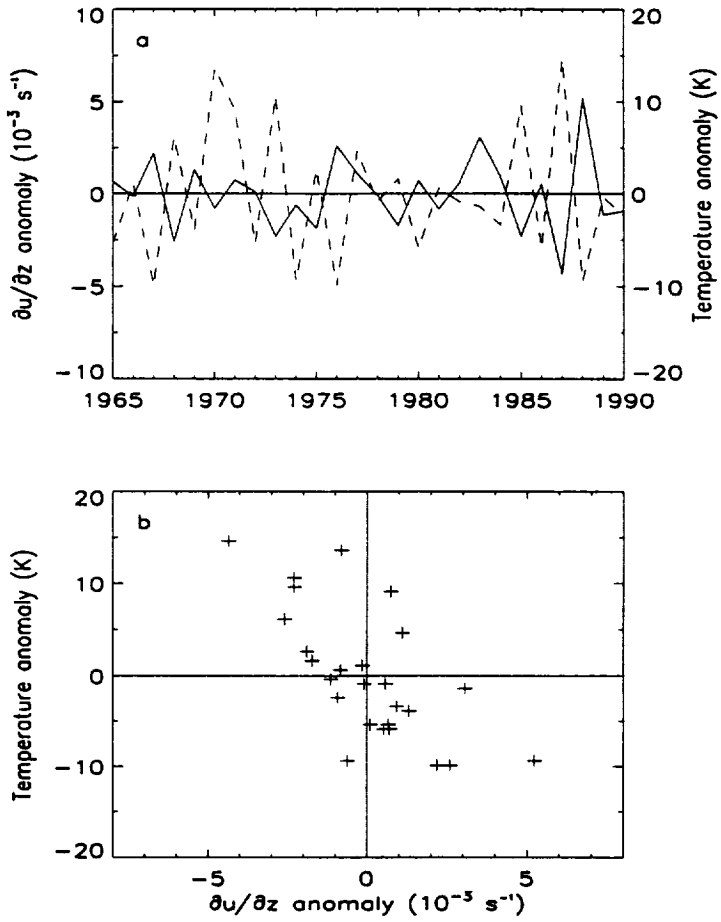

Figure 5. As figure 2 except solid line shows du_{eq}/dz (x$10^{-3}s^{-1}$) at 50km in the previous September.

Polar temperature in the following winter.

In order to investigate this link further, the vertical gradient of zonally-averaged zonal wind du_{eq}/dz was derived from the raw rocketsonde data using centred differences. These values were then de-seasonalised and combined in the same manner as that described above for the equatorial winds. The correlation between the JF North Polar temperature and du_{eq}/dz was found to peak at 50km in September, with a correlation of -0.68. Using simple linear regression it was found that du_{eq}/dz at 50 km in September could describe 46% of the variance in the JF North Polar temperature. The above multiple linear regression was repeated, using du_{eq}/dz at 50 km in September as the fixed parameter and all possible values of both u_{eq} and du_{eq}/dz as the second parameter. It was found that u_{eq} at 44km in October was most effective as the second parameter, with a total of 62% of the variance in the polar temperature being described.

These results suggest a link between the JF polar temperature and the equatorial wind and its vertical gradient in the upper stratosphere in the preceeding September/October. This strong link is evident in figure 5a, which shows the JF polar temperatures for 1965-90, overlaid by du_{eq}/dz at 50 km in the preceeding September. The two signals are reasonably well anti-correlated over most of the period. A comparison of the

scatter-plot of the data (figure 5b) with the corresponding plot in figure 2b for the lower stratospheric winds (u_{eq} at 24km) clearly demonstrates that the relationship between the JF polar temperature and du_{eq}/dz at 50km is stronger than with u_{eq} at 24km.

(*d*) *Composites*

In figure 6 we show a series of latitude - height 'composite differences' of JF winds using daily wind data derived from the National Centers for Environmental Prediction / National Center for Atmospheric Research (NCEP/NCAR) 1200 UTC heights and temperatures (Kalnay et al. 1996). Firstly, composites were derived by averaging together the JF wind distributions from the five warmest and five coldest Northern Hemisphere winters between 1964/65 and 1989/90. The appropriate years were selected on the basis of the North Polar temperatures at 24km. We do this to highlight the differences in the JF wind distribution between years in which major warmings have occurred and those in which they have not. The 'cold' composite minus the 'warm' composite is shown in figure 6a. During cold winters the westerly polar vortex is less disturbed by planetary waves and their accompanying warming events and hence there is a strong, high-latitude westerly anomaly, with maximum composite differences of 35 ms^{-1} at 32 km ($\sim$ 10 hPa). There is a small westerly anomaly at the equator, consistent with the Holton-Tan mechanism, peaking at around 11 ms^{-1}.

Secondly, the wind distributions were composited on the basis of the direction of the equatorial wind at 24 km in January. These composites test the Holton-Tan mechanism whereby the polar temperatures and vortex are influenced by the equatorial wind in the lower stratosphere. The 'west QBO' minus 'east QBO' composite differences in figure 6b show a high latitude westerly wind anomaly peaking at $\sim$ 15 ms^{-1} at 32km, consistent with a stronger westerly polar jet during the westerly phase of the QBO at 24km.

Finally, composites were constructed on the basis of du_{eq}/dz at 50km in September. The difference between the 'large shear' and 'small shear' years has a maximum amplitude of $\sim$25 ms^{-1} at high latitudes (figure 6c). Hence, years with stronger than average vertical wind shear near the equatorial stratopause tend to be characterised by a cold, more stable westerly polar vortex, and vice versa. These composites confirm that, while by no means accounting for the full amplitude of the differences in figure 6a, the composite differences based on du_{eq}/dz at 50km in September are substantially larger than the composite differences constructed using the 24km equatorial winds.

In figure 7 we show the height-time evolution of the equatorial wind from the NCEP analyses for the 'warm' and 'cold' composites described above, and the difference between them. The major feature of the equatorial wind series between 40-60 km is the semi-annual oscillation (SAO), in which the equatorial wind direction reverses from easterly to westerly and back again on a time-scale of approximately 6 months. September is the onset of a westerly phase at around 50km. There is a notable difference in the nature of this westerly phase between the 'warm' and 'cold' composites. In the 'warm' composite, the westerly phase extends deeper in the atmosphere, with the zero wind line at its lowest extent in November reaching $\sim$30km compared with only $\sim$ 40km in the 'cold' composite. This is a result of a more rapid descent of the westerly phase during September and October. The vertical wind shear at $\sim$ 50km in September reflects this difference, being weaker in the 'warm' composite than in the 'cold' composite (as we have already noted in the discussion of figure 6c above).

Figure 7 suggests that the difference between the warm and cold composites may be associated with the relative strength and penetration of the SAO westerly phase around September/October. The westerly phase of the SAO arises as a result of energy deposition by westerly-phase vertically propagating equatorial waves e.g. gravity and

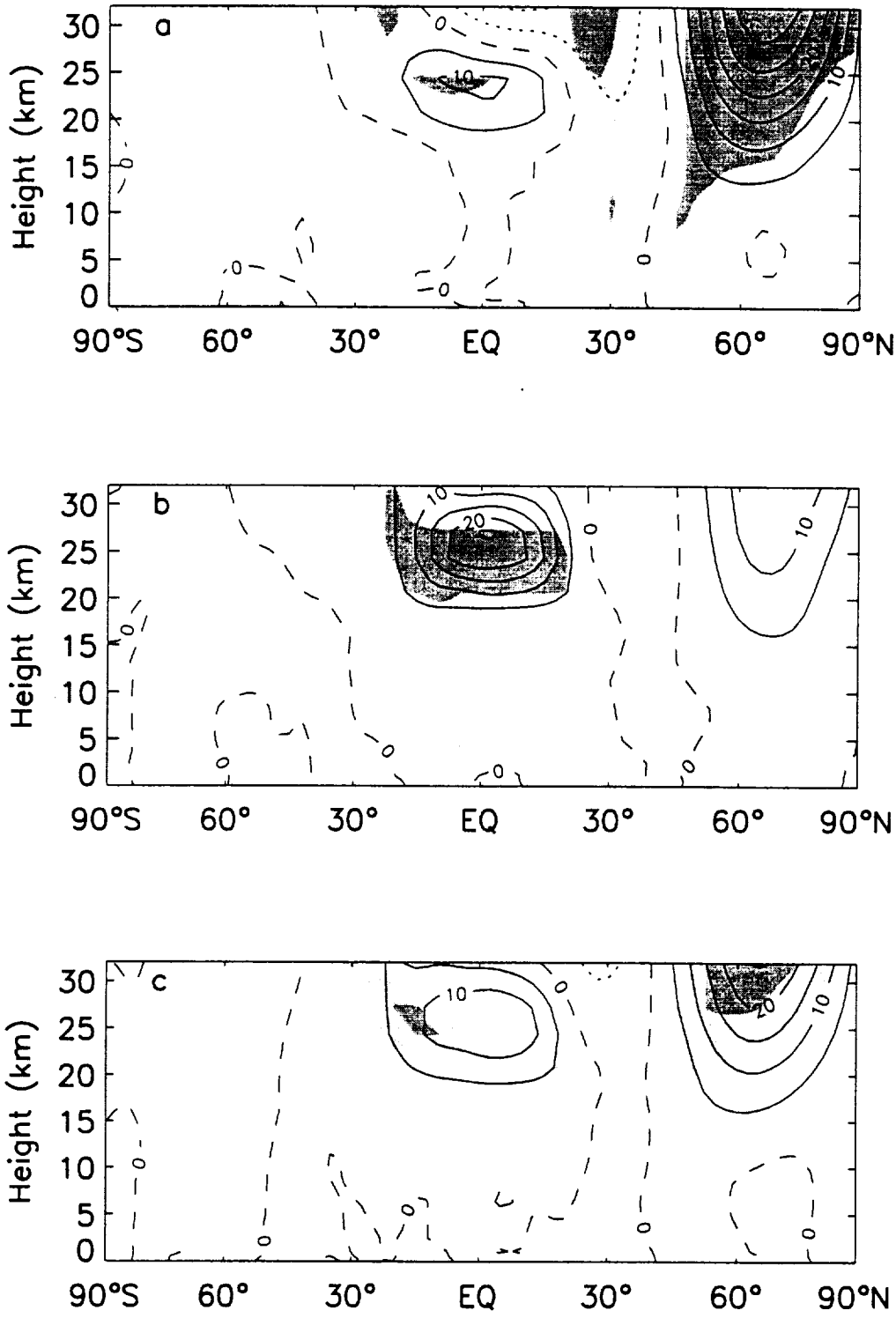

Figure 6. Latitude-height distributions of JF zonally-averaged zonal wind (ms^{-1}) from the NCEP analyses for the period 1964/65 - 1989/90. (a) composite difference of 5 coldest minus 5 warmest NH winters as determined by the 30 hPa JF NP temperatures, (b) composite difference of 5 most westerly minus 5 most easterly QBO phase based on equatorial winds at 24km in the previous December, (c) composite difference of 5 strongest minus 5 weakest du_{eq}/dz at 50km in the previous September. Contour interval is 5 ms^{-1}. Negative (easterly) values are denoted by dotted contours. Light and dark shading denote regions where values are significant at the 95% and 99% confidence levels respectively. The significances of the values were tested by performing a Student's t-test on the difference between the two mean wind distributions.

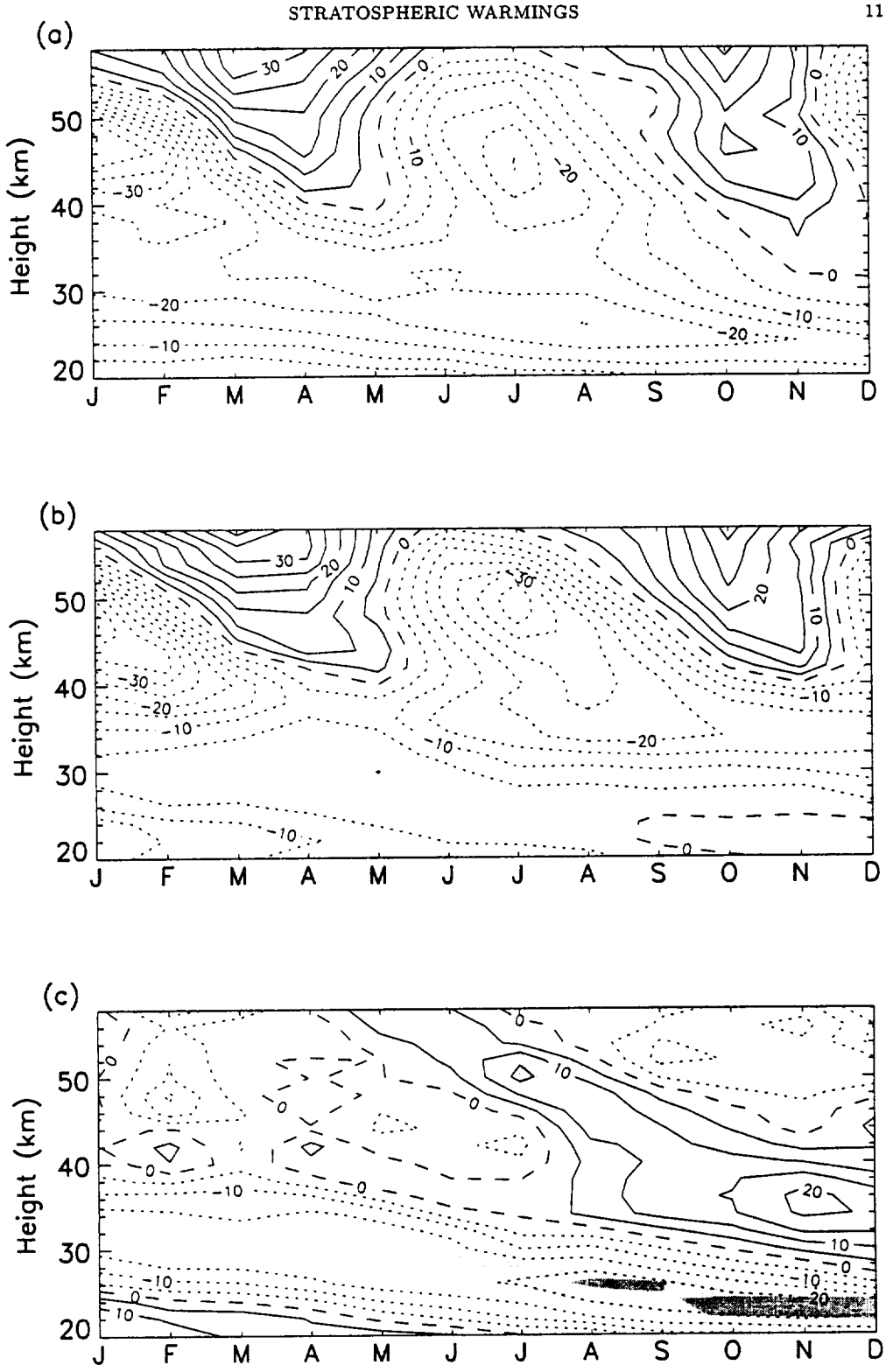

Figure 7. Time-series of monthly-averaged, zonally-averaged zonal wind at the equator (ms^{-1}) derived from the NCEP analyses. (a) Composite of 5 warmest NH winters, as determined using 30 hPa NP temperatures, (b) As for panel (a) but for the 5 coldest winters. (c) The difference between the two composites i.e. panel (a) minus panel (b). Contour interval is 5 ms^{-1}. Negative (easterly) values are denoted by dotted contours. Light and dark shading denote regions where values are significant at the 95% and 99% confidence levels respectively. The significances of the values were tested by performing a Student's t-test on the difference between the two mean wind distributions.

Kelvin waves (Andrews *et al.* 1997). These waves are able to propagate relatively easily through lower stratospheric easterlies. However, when the waves reach heights ($\sim$ 50km) where the background zonal winds are of similar magnitude and direction to their own phase speeds, the waves are unable to propagate further. They are dissipated and their energy is transferred to the background flow, thus forcing the local background flow even more westerly. In this way, the westerly SAO phase gradually descends through the atmosphere with time. The rate of descent of the westerly phase, and hence the vertical wind shear at 50km, is therefore dependent on the QBO in the lower stratosphere (Lindzen and Holton, 1968; Gray and Pyle 1989; Hirota *et al.* 1991; Kennaugh *et al.* 1997), since the relative ease of vertical propagation of the westerly-phase waves depends on the wind speed and direction in the lower stratosphere. Strong easterlies at 20-30 km allow enhanced penetration and hence more effective westerly forcing higher up (and vice versa). The resulting QBO modulation has been observed at mesospheric levels in the HRDI wind observations (Burrage *et al.* 1996) and is evident in figure 3c which shows a weak QBO signal extending into the upper stratosphere. It is for this reason that we see evidence of a QBO-like variation in du_{eq}/dz at 50 km in figure 5 and a fairly substantial westerly anomaly at the equator in the composite difference of figure 6c, similar to that in figure 6b.

4. Conclusions

We have presented evidence for a dependence of the North Polar temperature on the equatorial wind and its vertical shear in the upper stratosphere in the previous September/October. This dependence appears to be related to the timing of onset of the westerly phase of the SAO. The evidence provided here strongly suggests an influence on polar winter temperatures from the upper stratosphere, in addition to that from the lower stratospheric QBO. This upper height region also coincides with the region of the atmosphere where the solar cycle is believed to exert its strongest influence. While a data correlation study such as this cannot, on its own, establish a causal relationship nor provide the mechanism for this relationship (if, indeed, one exists) it nevertheless suggests that a better understanding of the equatorial upper stratosphere, its relationship to the QBO lower down and to the polar lower stratosphere will be essential if we are to fully understand the nature of the equatorial influence on polar temperatures and hence on the Earth's climate. The study also highlights the need for continued high quality wind measurements of the equatorial upper atmosphere. The 1990s have been an unusual decade, with very few mid-winter warmings, which may be an indicator of climate change. Unfortunately, our analysis could not be extended into the 1990s because of the lack of adequate equatorial wind data in the region 40-60 km.

Appendix

In figures 1 and 4 the significance of each point on the correlation plot was tested by calculating the value of the statistic: $t = r\sqrt{\frac{N-2}{1-r^2}}$, where r is the correlation between the two time-series and N is the number of data points in the time-series. In the null case of no correlation, this statistic is distributed like Student's t-distribution with N-2 degrees of freedom (Press et al. 1992). In order to compensate for the autocorrelation of the wind data, the effective sample size N_e was substituted for N, where $N_e = N$ unless $\rho_1 > 0$ when $N_e = N\left\{\frac{1-\rho_1}{1+\rho_1}\right\}$ and ρ_1 is the lag-one autocorrelation coefficient (Wilks 1995).

ACKNOWLEDGEMENTS

We thank Prof. K. Labitzke for provision of the Berlin Stratospheric temperature analyses and Dr. B. Naujokat for the equatorial radiosonde data. This work was supported by the U.K. Natural Environment Research Council.

REFERENCES

Andrews, D. G., Holton, J. R. and Leovy, C. B. 1987 *MIDDLE ATMOSPHERE DYNAMICS*, Academic Press, London

Balachandran, N. K. and Rind, D. 1995 Modeling the effects of UV variability and the QBO on the troposphere stratosphere system. Part I: The middle atmosphere. *J. Climate*, **8**, 2058–2079

Baldwin, M. P. and Dunkerton, T. J. 1998a Biennial, quasi biennial and decadal oscillations of potential vorticity in the northern stratosphere. *J. Geophys. Res.*, **103**, 3919–3928

Baldwin, M. P. and Dunkerton, T. J. 1998b Quasi biennial modulations of the southern hemisphere stratospheric polar vortex. *Geophys. Res. Letts.*, **25**, 3343–3346

Baldwin, M. P. and Dunkerton, T. J. 1999 Propagation of the Arctic Oscillation from the stratosphere to the troposphere. *J. Geophys. Res.*, **104**, 30,937–30,946

Baldwin, M. P. et al. 2000 The quasi biennial oscillation. *Submitted to Rev. Geophys.*

Chipperfield, M. P. and Jones, R. L. 1999 Relative influence of atmospheric chemistry and transport on Arctic ozone trends. *Nature*, **400**, 551–554

Dunkerton, T. J. and Baldwin, M. P. 1991 Quasi biennial modulation of planetary scale fluxes in the Northern Hemisphere winter. *J. Atmos. Sci.*, **48**, 1043–1061

Dunkerton, T. J. and Baldwin, M. P. 1992 Modes of interannual variability in the stratoshere. *Geophys. Res. Letts.*, **19**, 49–52

Dunkerton, T. J. and Delisi, D. P. 1997 Interaction of the quasi biennial oscillation and the stratopause semiannual oscillation. *J. Geophys. Res.*, **102**, 26,107–26,116

Dunkerton, T. J., Delisi, D. P. and Baldwin, M. P. 1998 Middle atmosphere cooling trend in historical rocketsonde data. *Geophys. Res. Letts.*, **25**, 3371–3374

Gray, L. J. and Dunkerton, T. J. 1990 Seasonal Cycle Modulations of the Equatorial QBO. *J. Atmos. Sci.*, **47**, 2431–2451

Gray, L. J. and Pyle, J. A. 1989 A two dimensional model of the quasi-biennial oscillation of ozone. *J. Atmos. Sci.*, **46**, 203–220

Haigh, J. D. 1999 A GCM study of climate change in response to the 11-year solar cycle. *Quart. J. Roy. Met. Soc.*, **125**, 871–892

Hamilton, K. 1998 Effects of an imposed quasi biennial oscillation in a comprehensive troposphere stratosphere mesosphere general circulation model. *J. Atmos. Sci.*, **55**, 2393–2418

Hirota, I., Sakurai, T. and Gille, J. C. 1991 Kelvin waves near the equatorial stratopause as seen in SBUV ozone data.*J. Meteorol. Soc. Jpn.*, **69**, 179–186

Holton, H. and Tan, H.-C. 1980 The influence of the equatorial quasi-biennial oscillation on the global circulation at 50 mb. *J. Atmos. Sci.*, **37**, 2,200–2,208

Holton, H. and Tan, H.-C. 1982 The quasi-biennial oscillation in the Northern Hemisphere lower stratosphere. *J. Meteor. Soc. Jpn.*, **60**, 140–148

Hood, L. L., McCormack, J. P. and Labitzke, K. 1997 An investigation of dynamical contributions to midlatitude ozone trends in winter. *J. Geophys. Res.*, **102**, 13,079–13,093

Kalnay, M. E. et al. 1996 The NCEP/NCAR Reanalysis Project. *Bull. Am. Meteorol. Soc.*, **77**, 437–471

Kennaugh, R., Ruth, S. L. and Gray, L. J. 1997 Modeling quasi-biennial variability in the semi-annual double peak. *J. Geophys. Res.*, **102**, 16169–16187

Kodera, K.	1991	The solar and equatorial QBO influences on the stratospheric circulation during the early Northern Hemisphere winter. *Geophys. Res. Lett.*, **18**, 1023–1026
Kodera, K.	1993	Quasi decadal modulation of the influence of the equatorial quasi biennial oscillation on the north polar stratospheric temperatures. *J. Geophys. Res.*, **98**, 7245–7250
Kodera, K.	1995	On the origin and nature of the interannual variability of the winter stratospheric circulation in the Northern Hemisphere. *J. Geophys. Res.*, **100**, 14,077–14,087
Labitzke, K.	1982	On the interannual variability of the middle stratosphere during the northern winters. *J. Meteorol. Soc. Jpn.*, **60**, 124–139
Labitzke, K. and van Loon, H.	1988	Association between the 11-year solar cycle, the QBO and the atmosphere. Part I: the troposphere and stratosphere in Northern Hemisphere in winter. *J. Atmos. Terr. Phys.*, **50**, 197–206
Labitzke, K. and van Loon, H.	1995	A note on the distribution of trends below 10 hPa: the extratropical northern hemisphere. *J. Meteorol. Soc. Jpn.*, **73**, 883–889
Labitzke, K. and van Loon, H.	1996	The signal of the 11-year sunspot cycle in the upper troposphere lower stratosphere. *Space Sci. Revs.*, **80**, 393–410
Lindzen, R. S. and Holton, J. R.	1968	A theory of the quasi biennial oscillation. *J. Atmos. Sci.*, **25**, 1095–1107
Naito, Y. and Hirota, I.	1997	Interannual variability of the northern winter stratospheric circulation related to the QBO and the solar cycle. *J. Meteorol. Soc. Jpn.*, **75**, 925–937
Niwano, M. and Takahashi. M.	1998	The influence of the equatorial QBO on the Northern Hemisphere winter circulation of a GCM. *J. Meteorol. Soc. Jpn.*, **76**, 453–461
O'Sullivan, D. and Dunkerton, T. J.	1994	Seasonal development of the extratropical QBO in a numerical model of the middle atmosphere. *J. Atmos. Sci.*, **51**, 3706–3721
O'Sullivan, D. and Young, R. E.	1992	Modeling the quasi biennial oscillation's effect on the winter stratospheric circulation. *J. Atmos. Sci.*, **49**, 2437–2448
Press, W. H., Teukolsky, S. A., Vetterling, W. T. and Flannery, B. P.	1992	*Numerical Recipes in FORTRAN: The Art of Scientific Computing*. Cambridge University Press
Pyle, J. A. et al.	1999	*STRATOSPHERIC OZONE* DETR report no. 99EP0458, London
Ramaswamy, V. et al.	2000	Stratospheric temperature changes: observations and model simulations. *Submitted to Rev. Geophys.*
Rind, D. and Balachandran, N. K.	1995	Modeling the effects of UV variability and the QBO on the troposphere stratosphere system. Part II: The troposphere. *J. Climate*, **8**, 2080–2095
Salby, M., Callaghan, P. and Shea, D.	1997	Interdependence of the tropical and extra-tropical QBO: relationship to the solar cycle versus a biennial oscillation in the stratosphere. *J. Geophys. Res.*, **102**, 29,789–29,798
Salby, M. and Shea, D.	1991	Correlations between solar activity and the atmosphere: an unphysical explanation. *J. Geophys. Res.*, **96**, 22,579–22,595
Shindell, D. T., Rind, D., Balachandran, N. K., Lean, J. and Lonergan, P.	1999	Solar cycle variability, ozone and climate, *Science*, **284**, 305–308
Teitelbaum, H. and Bauer, P.	1990	Stratospheric temperature eleven year variation: solar cycle effect or stroboscopic effect? *Ann. Geophys.*, **8**, 239–242

Thompson, D. W. J. and Wallace, J. M. 1998 The Arctic Oscillation in the wintertime geopotential height and temperature fields. *Geophys. Res. Letts.*, **25**, 1297–1300

Wilks, D. S. 1995 *Statistical Methods in the Atmospheric Sciences,* Academic Press, San Diego, California

Zurek, R. W., Manney, G. L., Miller, A. J., Gelman, M. E. and Nagatani, R. M. 1996 Interannual variability of the north polar vortex in the lower stratosphere during the UARS mission. *Geophys. Res. Letts.*, **23**, 289–292

STUDIES OF THE ARCTIC OSCILLATION

Propagation of annular modes from the mesosphere to the Earth's surface

Mark P. Baldwin & Timothy J. Dunkerton

Northwest Research Associates, 14508 NE 20th Street, Bellevue, WA 98007-3713, USA

'Annular modes' are deep, longitudinally symmetric patterns which dominate the circulation variability of both hemispheres from the Earth's surface to the mesosphere[1,2]. These ring-like patterns are characterised by fluctuations in pressure of one sign over the polar caps and the opposite sign at low latitudes. Their simple structure appears to be a fundamental fluid dynamical consequence of the Earth's size and rotation rate[3]. More than two decades of global satellite observations allow us to examine the time-height development of the annular modes. Here we present the first observations that show that fluctuations in the annular modes often begin in the lower mesosphere and propagate downward, over a period of up to three months, to affect surface weather and climate patterns. These results show that variations in the stratospheric annular modes are coupled to the surface, and that in the upper stratosphere, the two hemispheres are coupled. Perturbations and trends in the circulation of the stratosphere and mesosphere, which may be caused by natural variability, increasing greenhouse gases, ozone depletion, volcanic aerosols, or 11-year solar variability, may have a larger influence on surface weather and climate trends than has been recognised.

Variability in the circulation of the stratosphere (~11–48 km) and lower mesosphere is largest during the winter, when the cold, cyclonic polar vortex varies in strength and is disturbed by planetary-scale waves. These waves originate in the troposphere, transport momentum upward, and interact with the stratospheric flow. In the Northern Hemisphere, where planetary wave amplitudes are larger, the process of wave-mean interaction can lead to the sudden and dramatic slowing and reversal of the westerly polar vortex, even in midwinter (called a major stratospheric warming). The southern vortex is colder, stronger, and is less disturbed by waves.

Theory[4,5], observations[6], and modelling experiments[7] show not only that the circulation of the troposphere and stratosphere are coupled, but that the influence on the mean flow tends to be downward, even while circulation changes are driven by tropospheric waves that propagate upward. Stratospheric circulation anomalies alter the propagation of wave energy from the troposphere, and the resulting changes to the flow tend to burrow downward, often into the troposphere. This 'downward control'[4] has important implications for long-term climate variability. Surface weather and climate appear to be sensitive to the state of the stratosphere, and the stratosphere is sensitive to changes in the concentrations of greenhouse gases, ozone, and volcanic aerosols. Annular modes provide a conceptual model with which to examine and quantify the observed circulation changes which span the troposphere and stratosphere.

Upward propagating planetary-scale waves are ducted by a waveguide which depends on the longitudinally averaged westerly wind, $\bar{u}$. Anomalies (defined as deviations from the average climatology) in the stratospheric $\bar{u}$ field act to refract upward propagating planetary waves, alter the locations where wave energy is deposited, and initiate a positive feedback in which the waves are refracted at successively lower altitudes[8]. Variations in $\bar{u}$ tend to occur over deep layers in the vertical, are of opposite sign at high and low latitudes[9,10], and correspond to changes in the annular modes because $\bar{u}$ varies as the north-south gradient of geopotential height surfaces.

Annular modes provide a better measure of vertical coupling to the troposphere than longitudinally averaged fields[6], such as $\bar{u}$. The use of geopotential height surfaces to define the annular modes has the advantage of providing a three-dimensional picture of vertical coupling. The annular modes are typically defined within the troposphere as the leading empirical orthogonal function (EOF) of slowly varying (e.g. monthly mean) cold-season geopotential anomalies. The surface, or 1000-mbar, northern annular mode (NAM, Fig. 1i) is known as the 'Arctic Oscillation'[11] and its southern counterpart is the southern annular mode (SAM). The NAM pattern is robust, in that it is insensitive to the details of the calculation (months or data levels used, temporal averaging, data set, etc.)[6]. Over the Atlantic sector, it is recognised as the North Atlantic Oscillation[12] (NAO); it has been argued that NAO and annular mode are two paradigms describing a single phenomenon[13]. Variations in the NAM index are related to hemispheric-scale effects not just on weather patterns, but on extreme weather events such as heavy rainfall, snow, wind, and droughts[14].

We extend the concept of the annular modes into the lower mesosphere (Fig. 1) by defining the annular modes as the leading EOF for each of 26 pressure levels from 1000 to 0.316 mbar (~57 km). We use November–April data to define the cold season in the Northern Hemisphere, but September–December in the Southern Hemisphere (the time during which the southern vortex is decreasing in size and is susceptible to influence from upward propagating planetary-scale waves). The annular modes (Fig. 1) account for 20–30% of the (90-day low-pass filtered) temporal variance of geopotential height in the troposphere, but more than half the variance above the tropopause. The smaller variability of the Southern Hemisphere stratospheric circulation results in a smaller amplitude of the SAM, approximately ⅔ that of the NAM.

We define a daily index of the annular modes for each level by regressing daily geopotential anomalies onto the annular mode pattern for each level. The resulting indices are similar to the principal component time series from the EOF analysis, but have daily resolution spanning the entire data record (Fig. 2). The troposphere in both hemispheres experiences many fluctuations in the annular modes that are evanescent above the tropopause. However, events during the cold seasons often show deep, strong coupling from the lower mesosphere to the surface. The tendency is for such events to be initiated at the highest levels. Such downward propagation is seen here for the first time above 10 mbar and in the Southern Hemisphere. The Northern Hemisphere shows more consistent vertical coupling and downward propagation of the annular mode, which is to be expected because the northern vortex can break down at any time during the winter. Stratospheric warmings correspond to a weak polar vortex, shown in red[6]. Typically, these events begin in the mesosphere and propagate downward over a period of a few weeks, often (but not always) reaching the Earth's surface. The negative anomalies (red) are more likely to penetrate into the troposphere.

The time scale for events in the Southern Hemisphere is somewhat longer and corresponds to the breakdown of the polar vortex during spring. As the vortex is reduced in size, begin-

ning in August-September, anomalies in the SAM tend to move slowly downward over a period of 2–3 months. Vacillations in the SAM are not as consistent as the NAM, nor are they confined entirely to the cold season. Although the NAM has a very small amplitude during the warm season, the SAM[15], in both the troposphere and stratosphere, has substantial fluctuations throughout the year.

The northern winter of 1998–1999 was the only winter ever to experience two major midwinter stratospheric warming events (Fig. 3). The alternating, descending positive and negative anomalies (shown with no time filtering) provide a striking illustration of the balance between wave-mean interaction as the vortex is diminished during two warming events, and radiative cooling (aided by nonlinear wave-wave interactions[16]) as the vortex rebuilds during the following weeks. The wave-mean interaction process appears to be similar to that which drives the descending easterly and westerly wind regimes of the quasi-biennial oscillation (QBO) in the equatorial stratosphere. Both phases of the QBO are forced by a broad spectrum of equatorial waves. A similar wave-driven oscillation has been observed in the stratosphere of Jupiter[17] and has been hypothesised to occur in the interior of the sun[18]. In each of these phenomena vertically propagating waves produce an orderly, downward propagating oscillation from chaotic forcing. The annual cycle allows only brief windows during which the modes descend, but 'perpetual January' GCM simulations[7] show irregular, alternating, descending wind regimes (vacillation cycles).

Anomalies in $\bar{u}$ are observed[19,20] and simulated[21] to move northward as they descend over a period of ~2 months, corresponding particularly well to stratospheric warmings. Since the NAM pattern is much tighter at 10 mbar than at 1 mbar, corresponding anomalies in 10-mbar $\bar{u}$ are found at higher latitudes. For each level we calculated the geostrophic wind anomaly of the longitudinally averaged SAM and NAM. As the NAM (Fig. 4b) descends, maximum wind anomalies are found at lower levels and higher latitudes, beginning at ~50°N and reaching ~70°N in the lower stratosphere. Downward propagation of the NAM corresponds to northward and downward propagation of zonal wind anomalies. Even though the latitudinal structure of the NAM is fixed and cannot describe northward propagation at a fixed level, the vertical structure of the NAM provides a partial explanation for this propagation. In the southern hemisphere the scale of the SAM pattern also changes in the vertical, so a similar, but smaller, effect is seen (Fig. 4a).

Ozone depletion and increasing greenhouse gases are expected to cool the stratosphere, increase the strength of the stratospheric polar vortex, and influence the phase of the Arctic Oscillation[22,23,24]. We examine the relationship between annular mode indices at 10 and 1000 mbar, for each hemisphere (the observational record in the Northern Hemisphere (Fig. 5) permits analysis to 10 mbar since 1958[6]). The correlations (0.54 in the Northern Hemisphere, 0.66 in the Southern Hemisphere) do not prove cause and effect, but do suggest that a trend in the strength of the stratospheric polar vortex would be mimicked at the surface, as has been simulated in GCMs[24,25]. Previous modelling studies have demonstrated that a trend in the Arctic Oscillation may also be caused by land use changes[26], raising the question of the relative influence on climate of tropospheric and stratospheric forcing. The NAM and SAM indices tend to vary together in the upper stratosphere above 5 mbar (Fig. 5c) This suggests that either the same forcing is acting on both hemispheres, the hemispheres are linked dynamically, or both.

Our results indicate that perturbations to the temperature and wind fields of the stratosphere and mesosphere can affect surface weather and climate. Such perturbations occur on a variety of time scales, due to natural variability, volcanic eruptions, the 11-year solar cycle, ozone depletion, and increasing concentrations of greenhouse gases. Wave-mean interaction provides a mechanism whereby changes to the flow at high levels and low atmospheric densities (the mesosphere contains less than 0.1% of the mass of the atmosphere) can be amplified and communicated downward. We also find evidence of inter-hemispheric coupling of the annular modes in the upper stratosphere.

Methods

Data

At 10 mbar and below we use National Centers for Environmental Prediction (NCEP) 'reanalysis' data. Prior to 11 July, 1993 from 6.81 to 1 mbar we use TOVS geopotential thickness fields added to the NCEP 10-mbar field. After 11 July, 1993, up to 0.316 mbar we use UKMO thickness fields above 10 mbar.

Acknowledgements

We thank J.R. Holton for comments on the manuscript. This work was supported by NASA's SR&T Program for Geospace Science, NASA's ACMAP Program, and the National Science Foundation.

Correspondence and requests for materials should be addressed to M.P.B. (e-mail: mark@nwra.com).

[1] Limpasuvan, V., & Hartmann, D.L. Eddies and the annular modes of climate variability. *Geophys. Res. Lett.* **26**, 3133–3136 (1999).
[2] Thompson, D.W.J., & Wallace, J.M. Annular modes in the extratropical circulation. Part I: Month-to-month variability. *J. Climate* **13**, 1000–1016 (2000).
[3] Williams, G.P. Planetary circulations: 3. Terrestrial quasi-geostrophic regime. *J. Atmos. Sci.* **36**, 1409–1435 (1979).
[4] Haynes, P.H., C.J. Marks, M.E. McIntyre, T.G. Shepherd, & Shine, K.P. On the "downward control" of extratropical diabatic circulation by eddy-induced mean zonal forces. *J. Atmos. Sci.* **48**, 651–678 (1991).
[5] Hartley, D.E., J.T. Villarin, R.X. Black, & Davis, C.A. A new perspective on the dynamical link between the stratosphere and troposphere. *Nature* **391**, 471–474 (1998).
[6] Baldwin, M.P., & Dunkerton, T.J. Downward propagation of the Arctic Oscillation from the stratosphere to the troposphere *J. Geophys. Res.* **104**, 30,937–30,946 (1999).
[7] Christiansen, B. A model study of the dynamic connection between the Arctic Oscillation and stratospheric vacillations, *J. Geophys Res.*, submitted, 2000.
[8] Shindell, D.T., Schmidt, G.A., Miller, R.L., & Rind, D. Northern hemisphere winter climate response to greenhouse gas, ozone, solar and volcanic forcing, *J. Geophys. Res.*, submitted (2000).
[9] Nigam, S. On the structure of variability of the observed tropospheric and stratospheric zonal-mean wind. *J. Atmos. Sci.* **47**, 1799–1813 (1990).
[10] Baldwin, M. P., X. Cheng, & Dunkerton, T. J. Observed correlations between winter-mean tropospheric and stratospheric circulation anomalies. *Geophys. Res. Lett.* **21**, 1141–1144 (1994).
[11] Thompson, D.W.J., & Wallace, J.M. The Arctic Oscillation signature in the wintertime geopotential height and temperature fields. *Geophys. Res. Lett.* **25**, 1297–1300 (1998).
[12] Hurrel, J.W. Decadal trends in the North Atlantic Oscillation regime temperatures and precipitation. *Science* **269**, 676–679 (1995).
[13] Wallace, J.M., North Atlantic Oscillation / Annular Mode: Two paradigms – One Phenomenon. *Quart. J. Royal Met. Soc.* **126**, 1–15 (2000).
[14] Thompson, D.W.J., & Wallace, J.M. Regional climate impacts of the Northern Hemisphere annular mode and associated climate trends. *Nature* **404**, submitted (2000).
[15] Fyfe, J.C., & Manzini, E. The influence of the stratospheric circulation on the annular modes of climate variability in a middle atmosphere model. *J. Geophys. Res.*, submitted (2000).
[16] Andrews, D.G., Holton, J.R., and Leovy, C.B. Middle Atmosphere Dynamics, Academic Press, p288, 1987.
[17] Leovy, C.B., Friedson, A.J., & Orton, G.S. The quasiquadrennial oscillation of Jupiter's equatorial stratosphere. *Nature* **354**, 380–382 (1991).
[18] Gough, D.O., & McIntyre, M.E. Inevitability of a magnetic field in the Sun's radiative interior *Nature* **394**, 755–757 (1998).
[19] Kodera, K., Y. Kuroda, & Pawson, S. Stratospheric sudden warmings and slowly propagating zonal-mean zonal wind anomalies. *J. Geophys. Res.*, **105**, submitted. (2000).
[20] Dunkerton, T.J. Midwinter deceleration of the subtropical mesospheric jet and interannual variability of the high-latitude flow in UKMO analyses. *J. Atmos. Sci.* **57**, submitted (2000).
[21] Kodera, K., & Kuroda, Y. A mechanistic model study of slowly propagating coupled stratosphere-troposphere variability *J. Geophys. Res.* submitted (2000).
[22] Hartmann, D.L., J.M. Wallace, V. Limpasuvan, D.W.J. Thompson, and J.R. Holton, Can ozone depletion and global warming interact to produce rapid climate change?, *Proceedings of the National Academy of Sciences* **97**, 1412–1417 (2000).
[23] Corti, S, Molenari, F., & Palmer, T.N. Signature of recent climate change in frequencies of natural atmospheric circulation regimes, *Nature* **398**, 799–802 (1999).
[24] Shindell, D.T., Miller, R.L., Schmidt, G.A. & Pandalfo, L. Simulation of recent northern winter climate trends by greenhouse-gas forcing, *Nature* **399**, 452–455 (1999).
[25] Shindell, D.T, Schmidt, G.A., Miller, R.L., and Rind, D. Northern Hemisphere winter climate response to greenhouse gas, ozone, solar and volcanic forcing, *J. Geophys. Res.* Submitted (2000).
[26] Chase, T.N., Pielke Sr., R.A., Kittel, T.G.F., Nemani, R.R., & Running, S.W. Simulated impacts of historical land cover changes on global climate in northern winter. *Climate Dynamics* **16**, 93–105 (2000).

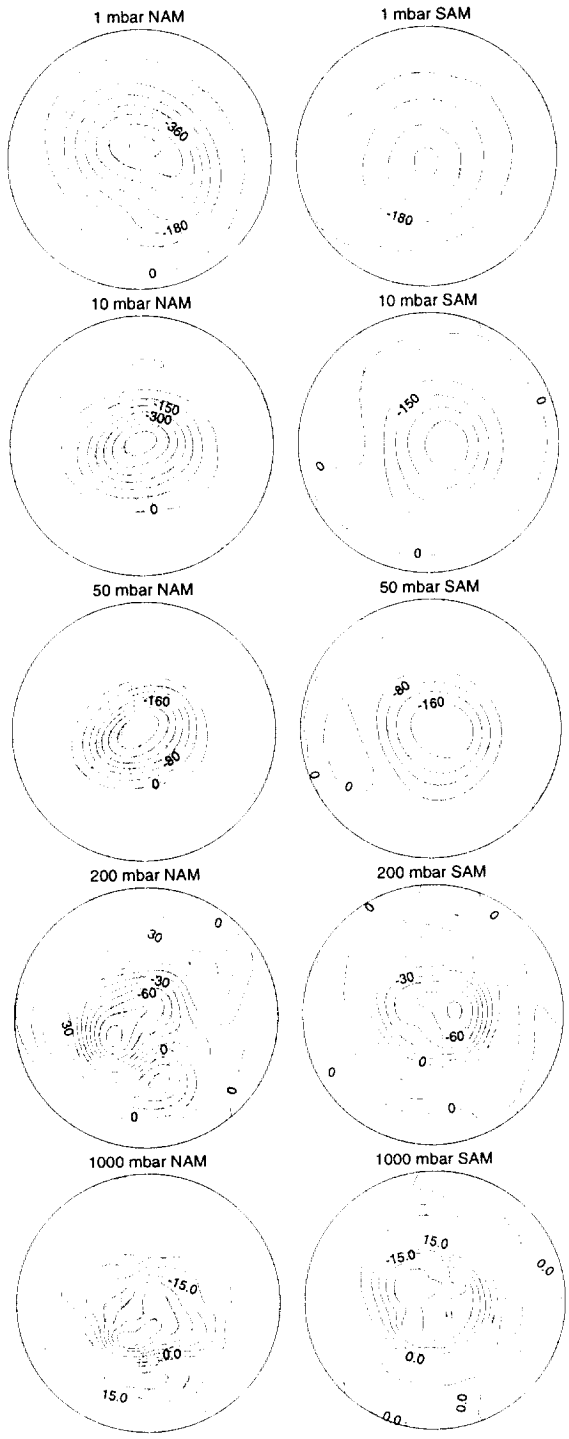

Figure 1 Northern (left) and Southern (right) annular mode patterns in geopotential height (m). The patterns represent the first EOF of 90-day low pass filtered anomalies for November–April in the Northern Hemisphere and September–December in the Southern Hemisphere.

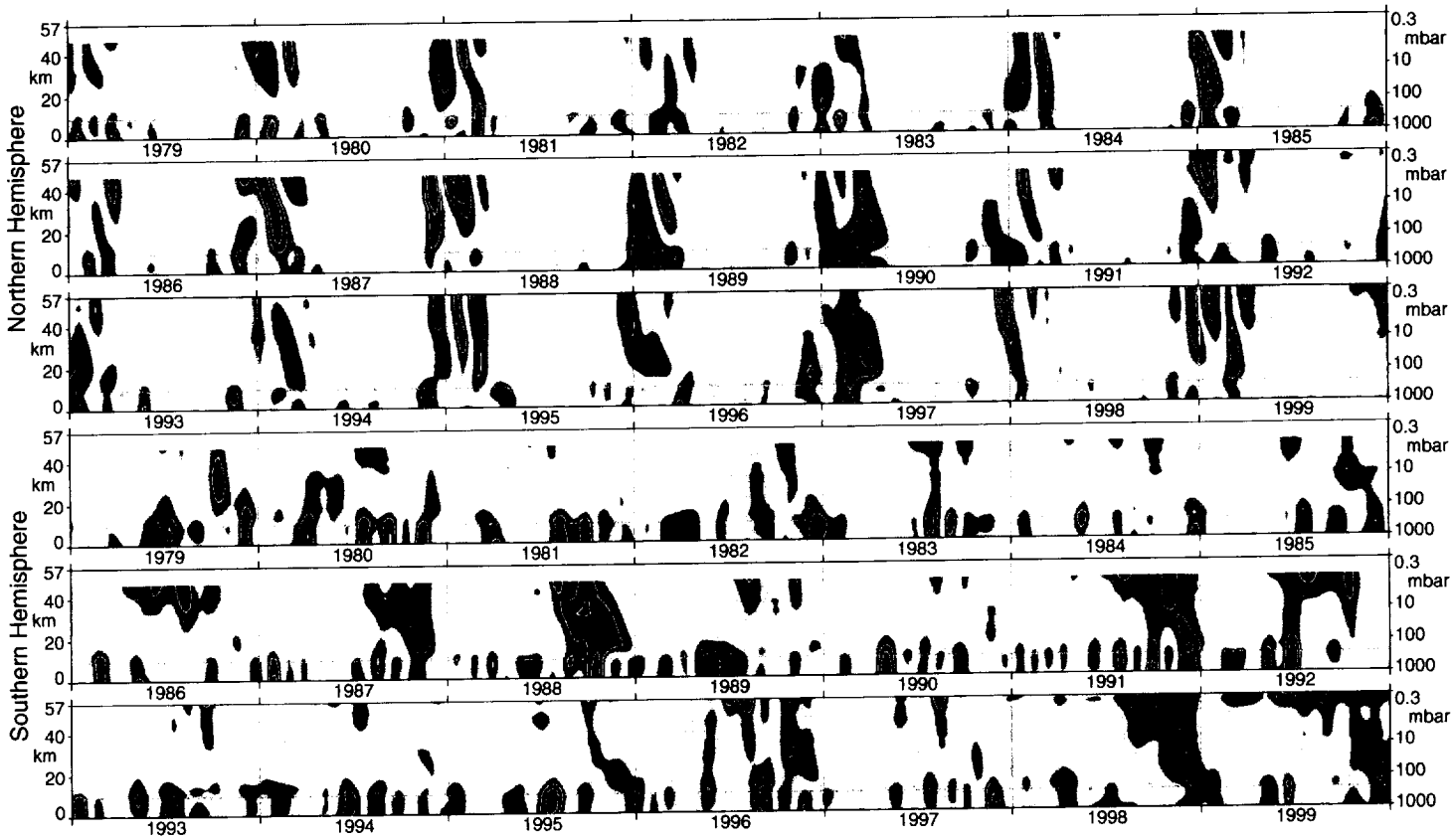

Figure 2 Time-height development of the NAM (top 3 panels) and SAM (bottom 3 panels) during 1979–1999. The indices have been 45-day low pass filtered. The indices are nondimensional, with a value of 1.0 corresponding to the patterns in Figure 1. The contour interval is 0.5, with values between -0.5 and 0.5 unshaded.

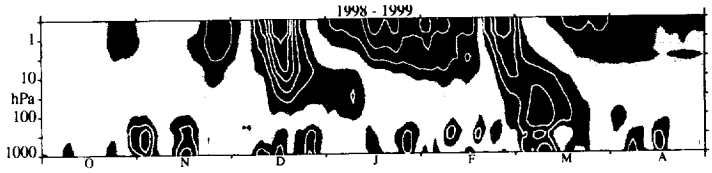

Figure 3 As in Figure 2, but unfiltered NAM index for the winter of 1998–1999.

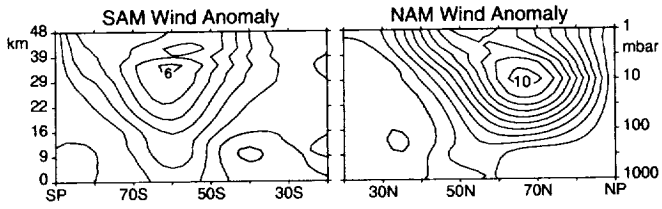

Figure 4 Geostrophic wind anomalies, $\bar{u}$ (ms^{-1}) corresponding to the longitudinally averaged annular modes in Figure 1. **a**, SAM. **b**, NAM.

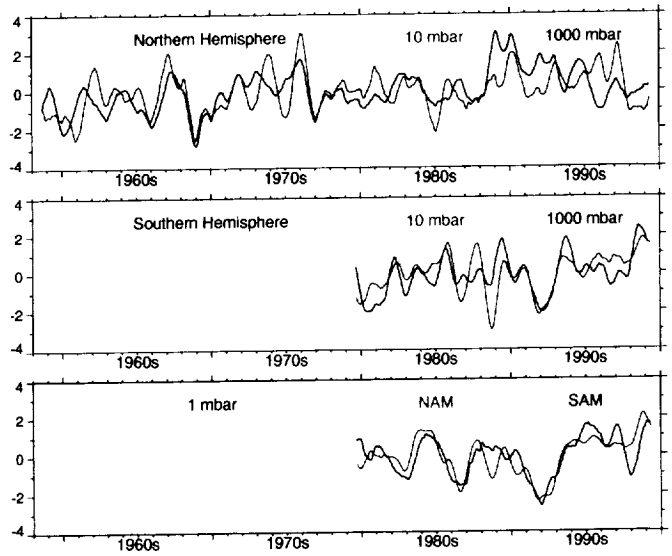

Figure 5 Comparison of NAM and SAM indices. All time series have been smoothed with a triangular filter (250-day half width). **a**, Northern Hemisphere 1000 mbar (black) and 10 mbar(red) ; **b**, as in **a**, but Southern Hemisphere; **c**, Comparison of 1-mbar NAM (black) and SAM (red).

Submitted to the *Journal of Geophysical Research*, 2000.

Nonlinearity in the stratospheric response to external forcing

Nathan P. Gillett
Department of Physics, University of Oxford, Oxford, UK.

Mark P. Baldwin
Northwest Research Associates, Bellevue, Washington.

Myles R. Allen
Space Science and Technology Department, Rutherford Appleton Laboratory, Didcot, UK.

Abstract

The leading mode of variability of the lower atmosphere circulation in the Northern Hemisphere is a largely zonally symmetric mode known as the Arctic Oscillation. We calculate Arctic Oscillation (AO) indices on a range of levels from 1000 to 10hPa by means of a principal component analysis of NCEP daily geopotential height anomalies. We find the apparent downward propagation of anomalies noted by other authors to be statistically significant compared to a red noise model. By examining histograms of these indices for each month, we note that the distribution of the index is generally close to Gaussian in the troposphere. In the stratosphere, however, the index is negatively skewed in the winter, and positively skewed in the spring. We conclude that the positive skewness in April results from the coexistence of distinct summer and winter circulation states, and by examining polar stratospheric temperatures we conclude that the negative skewness in January is due to the radiatively-determined limit on the vortex strength. This radiative limit responds only slowly to anthropogenic forcing, whereas changes in planetary wave forcing could have a large impact on the number of warm events. This leads to the hypothesis that the vortex strength may respond nonlinearly to anthropogenic forcing, which is supported by an observed change in the shape of the histograms of 20-200hPa AO indices in January over the past 40 years. In view of the downward propagation discussed, we speculate that this nonlinearity extends to the tropospheric response.

1. Introduction

The leading mode of variability in the Northern Hemisphere troposphere and stratosphere is an approximately zonally symmetric pattern known as the Arctic Oscillation [*Thompson and Wallace*, 1998]. This pattern, conventionally defined as the first empirical orthogonal function (EOF) of cold season sea level pressure, has an index which is closely associated with the more regional North Atlantic Oscillation [*Wallace*, 2000]. *Thompson and Wallace* [1998] describe how the AO index is closely correlated with the strength of the stratospheric polar vortex, and this relationship is explored more fully by *Baldwin and Dunkerton* [1999], who perform a principal component analysis on the geopotential height field on five levels from 1000 to 10hPa. It has long been known that warming events propagate downwards in the stratosphere [e.g. *Murray*, 1960], but *Baldwin and Dunkerton* [1999] were the first to note such downward propagation in a zonal index, with anomalies of both signs traveling from the 10hPa level to the surface in around three weeks. However, they do not assess the statistical significance of this result. Such an analysis is called for since they examine a signal with a 20-day lag in 90-day low pass filtered data. Since the publication of *Baldwin and Dunkerton* [1999] such downward propagation has also been noted by *Yamazaki and Shinya* [1999] and P. McCloghrie (pers. comm.) in GCMs. *Shindell et al.* [1998] suggest that Arctic Oscillation anomalies may propagate downwards by means of an interaction between upward propagating planetary waves and the mean flow. This suggestion is supported by the work of *Kuroda and Kodera* [1999] who note that zonal wind anomalies appear first in the mid-latitude stratosphere, and propagate polewards and downwards. They show the Eliassen-Palm flux, and note that it is consistent with the downward propagation resulting from a wave/mean-flow interaction.

Many authors have analysed geopotential height datasets by computing probability density functions (PDFs) of the system in the phase-space of one or more principal components. The field most often analysed is 500hPa geopotential height in the Northern Hemisphere winter. Both *Hansen and Sutera* [1992] and *Corti et al.* [1999] note apparent multimodality in the first principal component of this field in a model and observations respectively. By contrast *Kimoto and Ghil* [1993] and *Cheng and Wallace* [1993] find the PDF to be unimodal, but significantly different from a Gaussian, by comparison with a red noise model. The skewness of Northern Hemisphere winter tropospheric geopotential height has been analysed on a gridpoint basis by *Nakamura and Wallace* [1991]. They find positive skewness to the north of the stormtrack, and negative skewness to its south. *Baldwin and Dunkerton* [1999] mention that the skewness of the Arctic Oscillation index at 10hPa is slightly negative overall, but they do not consider how this skewness changes through the year, or indeed whether it is significantly different from zero. We estimate PDFs of the daily Arctic Oscillation indices for each month on a range of levels between 1000 and 10hPa, and test for skewness and departures from Gaussian. The reason the issue of multimodality in the climate system is considered important is because it could lead to nonlinearity in the response to an external forcing [*Palmer*, 1999]. However, we note that multimodality is not a requirement for such a response, and a nonlinear stratospheric response could lead to a nonlinear tropospheric response even if tropospheric distributions are Gaussian.

Histograms of temperature at 30hPa over the North Pole for each month were shown by *Labitzke* [1982]. As well as a seasonal cycle in the mean, the winter months having the lowest temperatures, these PDFs exhibit a seasonal cycle in variability, with a variability maximum in February, and much less variability in the summer months. This is due to the fact that in summer, prevailing easterly winds in the stratosphere prohibit the upward propagation of planetary waves from the troposphere [*Charney and Drazin*, 1961]. The PDFs also exhibit considerable positive skewness in December and January. *Labitzke* [1977] describes how warmings of the polar stratosphere, corresponding to a weakened vortex, are generally associated with a strengthening of the wavenumber one disturbance to the geopotential height field. Canadian warmings in particular are associated with a strengthening of the Aleutian High and a displacement of the vortex towards Siberia. We examine the shape of the vortex when the AO index is particularly high and low in this study, to look for evidence of such phenomena and to find physical explanations for the shape of the PDFs.

The Arctic Oscillation index at the surface has recently exhibited an upward trend which is statistically significant when compared to a red noise model [*Thompson et al.*, 2000], and when compared to control variability in a GCM [*Gillett et al.*, 2000]. There has been an accompanying increase in the strength of the stratospheric polar vortex [e.g. *Graf et al.*, 1998; *Thompson et al.*, 2000], which is consistent with a cooling of the polar stratosphere due to ozone depletion and greenhouse gases [*Perlwitz and Graf*, 1995; *Shindell et al.*, 1998]. These results are supported by several GCM modelling studies, which have shown that anthropogenic forcing causes an increase in the AO index at the surface [*Shindell et al.*, 1999; *Fyfe et al.*, 1999; *Paeth et al.*, 1999]. *Corti et al.* [1999] note a change in the shape of the distribution of the first two principal components of 500hPa geopotential height over the past

forty years, consistent with a 'regime transition' view of climate change [*Palmer*, 1999]. We look for evidence of such a change in the distribution of the AO index in both the troposphere and stratosphere, which could signify a nonlinear response to external forcing.

2. Downward Propagation of the Arctic Oscillation

We followed the method of *Baldwin and Dunkerton* [1999] to derive AO indices on a range of levels from 1000 to 10hPa by means of an EOF analysis of NCEP geopotential heights (see Appendix for more details). *Baldwin and Dunkerton* [1999] calculate the 20-day lag correlation between the 90-day low-pass filtered Arctic Oscillation index at 10hPa and successive levels downwards to the surface, and note an apparent downward propagation. In order to assess the significance of these results we calculated the lagged cross correlation between the unfiltered 10 and 1000hPa indices, and compared our results with a two-channel AR(1) model, constructed as follows:

$$\mathbf{x}_t = \mathbf{A}\mathbf{x}_{t-1} + \mathbf{Q}\mathbf{z}_t \qquad (1)$$

where $\mathbf{x}_t$ is a 2-element vector representing the AO index at the 10 and 1000hPa levels at time t, $\mathbf{A}$ is a 2×2 matrix of AR coefficients, $\mathbf{Q}$ is a symmetric 2×2 matrix, and $\mathbf{z}_t$ is a 2-element vector of uncorrelated unit variance Gaussian noise [*Priestley*, 1981] (equivalent to a POP model [*von Storch et al.*, 1995]). By post-multiplying by $\mathbf{x}_{t-1}^T$ and taking expectations we obtain the estimator $\hat{\mathbf{A}} = \mathbf{R}(1)\mathbf{R}(0)^{-1}$ where $E[\hat{\mathbf{A}}] = \mathbf{A}$. $\mathbf{R}(s)$ consists of the auto- and cross-covariances of the two indices at lag s, estimated from the observed AO indices. By post-multiplying by $\mathbf{x}_t^T$ and taking expectations, we find that $\hat{\mathbf{Q}}\hat{\mathbf{Q}}^T = \mathbf{R}(0) - \mathbf{R}(1)\mathbf{R}(0)^{-1}\mathbf{R}(1)^T$. If we are to avoid building the downward propagation into our noise model, since it is its existence that we are to test, then we must set the off-diagonal elements of $\hat{\mathbf{A}}$ to be equal. This was accomplished here by setting both to the mean of the two. Having evaluated $\hat{\mathbf{A}}$ and $\hat{\mathbf{Q}}$, we generated a 1000-member Monte Carlo ensemble using this model. This method generates an ensemble of pairs of red noise series, each with the same variance and lag-1 autocorrelation as the 10 and 1000hPa indices respectively, and with the same lag-0 cross-correlation.

In order to use our noise model to assess significance, it was important to ensure that it was spectrally realistic. With daily sampling there were wide discrepancies between the AO spectra and red noise, but these discrepancies were reduced as the sampling interval was increased at the expense of a reduction in sample size. We subsampled at 5 day intervals, which gave reasonable agreement with a red noise spectrum for those periods important for our hypothesis testing of less than about two months (figures 1a and 1b), but our results regarding downward propagation were insensitive to the exact sampling interval chosen. A comparison of the observed spectra with those of the noise model (figures 1a and 1b) shows remarkably good agreement at 1000hPa at periods up to two years, whilst the 10hPa index appears to follow a power law other than that of an AR(1) model. This is interesting, but not of direct relevance to the present investigation, and will be pursued elsewhere. The discrepancy between the AO index at 1000hPa and the AR(1) model at periods longer than two years is consistent with *Thompson et al.* [2000]'s findings that the observed trend in the surface AO is significant compared with a red noise model.

The cross-correlation function of the 10 and 1000hPa indices is shown in figure 1c. This function is asymmetric, having much larger amplitude at negative lag, which corresponds to the 10hPa index leading the 1000hPa index, or downward propagation. The grey band shown in figure 1c represents the range between the 2.5th and 97.5th percentiles of our noise model. It may clearly be seen that the observed lagged cross-correlation is significantly greater than that of the noise model for lags of around 15 - 40 days, peaking at 20 days, which agrees closely with the time for propagation from 10hPa to the surface of around three weeks noted by *Baldwin and Dunkerton* [1999]. In order to form a parametric estimate of the significance of the result, we calculated the ratio of the area under the cross-correlation function at positive lags to the area at negative lags, and compared with the noise model. Using this test the downward propagation result is significant at the 99% level.

3. PDFs of daily Arctic Oscillation Indices

Spectra and cross-correlations only provide information on the first and second moments of the distributions, so in order to look in more detail at the statistics of the AO indices, we plotted histograms for each month on four levels (figure 2). The Arctic Oscillation is derived based on anomalies from the seasonal cycle, so in each case the histograms are centred on zero. However, a clear seasonal cycle in variance may be seen at all levels. In the troposphere the seasonal cycle in variance is relatively smooth, with a minimum in July and a maximum in January. In the stratosphere, by contrast, there is an abrupt transition from the variable winter regime to the summer regime with very little variance, which generally occurs

in April and is known as the final warming [*Godson and Lee*, 1958]. The low variance observed in summer occurs because prevailing easterly winds in the stratosphere prohibit the upward propagation of planetary waves from the troposphere [*Charney and Drazin*, 1961]. Generally our histograms appear similar in form to those of the North Pole 30hPa temperature shown by *Labitzke* [1982]. This is to be expected since the AO index is anti-correlated with polar stratospheric temperatures [*Thompson and Wallace*, 2000].

Several authors have suggested that the first principal component of Northern Hemisphere geopotential height may be multimodal at 500hPa [*Hansen and Sutera*, 1992; *Corti et al.*, 1999], even when only monthly data are used. However, we find no significant multimodality in these AO indices on any level, based on daily data (apparent multiple maxima in our histograms result from the limited sample, and are not significant). In the troposphere, the PDFs are generally not significantly skewed (when tested against a noise model following the approach in section 2), and departures from Gaussian are small. In the stratosphere, however, the PDFs exhibit negative skewness in December and January and positive skewness in April. The reasons for these departures from normality are examined in the following sections. Departures from Gaussian were generally found to be largest at 70hPa (figure 2), and for this reason we show results for this level in the following analysis. However the main conclusions hold over all the stratospheric levels considered from 150 to 10hPa.

3.1. April results

The AO index in April exhibits strong positive skewness in the stratosphere, most notably at 70hPa (figure 2). From figure 3 we can conclude that the final warming is most likely to occur in April. The final warming is associated with a transition to easterly mean flow, which prohibits the upward propagation of planetary waves, dramatically reducing stratospheric variability, and rendering summer and winter states physically distinct [*Charney and Drazin*, 1961]. Figure 3 shows the large change in variance which is associated with the final warming, and which usually occurs in April. We thus conclude that it is the superposition of PDFs corresponding to the summer and winter states, which we expect to be distinct on physical grounds, which leads to the positive skewness of the AO PDF in April.

3.2. January results

The AO index in January (and less markedly in December) exhibits negative skewness in the stratosphere, as may be clearly seen in figure 2. However, an examination of figure 3 shows that, unlike in April, this non-normality is not due to a one-way transition between two distinct states: the PDF changes little through the month. Since temporal variations in the circulation offered no insight into the causes of the skewness, we turned to its spatial characteristics, by examining the form taken by the vortex on days at the extremes of the distribution. We took the 5% of the days with the lowest 70hPa index for this month, and the 5% of the days with the highest index (as indicated by the shading in figure 4a), and plotted a contour of the 70hPa surface for each day in both cases (figures 4b and 4c respectively). We show the full flow rather than anomalies to aid physical interpretation. It is apparent that on the days with large positive AO index the vortex is centred close to the pole, and the pattern of geopotential height is almost symmetric, as might be expected. By contrast, when the index is negative, and the vortex is warm, its centre is generally displaced south towards Eurasia, but there is large variation between individual days. This shift of the vortex towards Eurasia which occurs during sudden warmings is consistent with a strengthening of the Aleutian High as discussed by e.g. *Labitzke* [1977]; *Baldwin and Holton* [1988].

The spatial patterns of the strong and weak vortex states do not in themselves explain why the PDFs are skewed, but the difference in variability within the samples may help to do so. Whilst the weak vortex states are very different to one another, the strong vortex states in January are all very similar. For comparison, similar contour plots were produced for the strong and weak vortex states in April (figures 5b and 5c). A different contour height is used because the mean vortex state is weaker. It is notable that whilst the general form of the strong and weak vortex flows is similar in both months, the strong vortex states in January are much more similar to each other than those in April. We might thus hypothesise a physical limit to the strength of the vortex in January, or correspondingly to polar stratospheric temperature, since this is closely correlated with the mode [*Thompson and Wallace*, 2000]. In principle, such a limit exists: in the absence of dynamical heating mainly by planetary waves, the winter polar stratosphere would cool to its radiatively determined state [*Shine*, 1987]. Based on monthly data, *Shine* [1987] concludes that mean stratospheric temperatures around the North Pole are not strongly influenced by this radiative limit, in contrast to temperatures near the South Pole. However although the mean temperatures are not close to the radiatively determined limit, those on individual days may be. We tested this hypothesis by comparing daily 70hPa North Pole temperatures from the NCEP reanaly-

sis with radiatively determined temperatures. These differ from radiative equilibrium temperatures, in that they take account of the seasonal cycle. The difference is significant in the winter stratosphere due to the long radiative cooling timescales associated with low temperatures. We use radiatively determined temperatures updated from *Shine* [1987] using the ozone climatology described in *Shine* [1989] and other small improvements. Note that calculated temperatures depend on the set-up of the model used, for example, the position of the lower boundary and the fact that the ozone climatology is that of a radiatively determined state. Thus, the radiatively determined temperatures used here should be regarded as approximate.

The NCEP polar temperatures at 70hPa show a minimum in January, and as expected, the temperatures are strongly anti-correlated with the AO index on the same level (r=-0.87 in January, and r=-0.73 in April). Histograms of the 70hPa polar temperature thus show the opposite skewness to those of the AO index (figure 6), and the apparent cutoff at low temperatures in January is even more marked than the corresponding cutoff at high AO index values. The radiatively determined temperature for the middle of the month, interpolated to 70hPa at the North Pole is shown in each case for comparison. These are of course lower than the actual temperatures observed, since dynamical effects act to heat the polar winter stratosphere. However, in January (figure 6b) the lowest temperatures are only about 5K warmer than the radiatively determined temperature, which is small compared to the total range of around 50K. Note that at the onset of the vortex in October (figure 6a), when the stratosphere is relatively undisturbed, the mean 70hPa temperature is over 10K warmer than the radiatively determined temperature. Thus given the long radiative timescale, we would expect the stratosphere to be considerably warmer in January than the radiatively determined state even if it remained undisturbed from October. Further, the mean circulation leads to some dynamic heating even in the absence of planetary waves, which also prevents the limit from being reached.

A similar comparison of the 70hPa North Pole temperatures was carried out for April (figure 6c). Here the radiatively determined temperature is much colder than the mean observed temperature (38K versus 21K in January), so it causes no corresponding cutoff in the PDF. Thus the radiatively determined state is indeed likely to act to limit negative fluctuations in stratospheric temperature or positive AO anomalies, and is likely to be the cause of the observed skewness in January. We also found that the mean observed temperature in January at 70hPa is closer to the radiatively determined temperature than at any of the higher levels we considered (the model used to compute radiatively determined temperatures is not applicable to lower levels). This is consistent with the cutoff of AO and temperature PDFs being most pronounced here.

An obvious extension of this work would be to apply the same analysis to Southern Hemisphere geopotential heights, where conditions are much closer to the radiatively determined state during the winter [*Shine*, 1987]. However, the Southern Hemisphere annular mode exhibits much less coupling between the troposphere and stratosphere in this season, and hence the EOF-analysis method used in the Northern Hemisphere cannot be applied directly. Further, data are only available from 1979, making it difficult to identify changes in the distribution of the indices. However, other approaches do allow an annular mode to be identified, and its properties will be discussed in future work.

4. Changes in the Arctic Oscillation PDFs

As mentioned in section 1, over the past thirty years the Northern Hemisphere stratosphere has exhibited a cooling trend over the pole, accompanied by an increase in the strength of the vortex. In order to examine this effect in our data we computed the difference in the means of the AO index for each month over the periods 1958-1977 and 1978-1997. We assessed the significance of our results by comparison with a Monte Carlo ensemble of 1500 series generated with an AR(1) model. Noise parameters were estimated from the 5-day subsampled AO index. The difference in mean AO index is plotted where significant in figure 7a. It may be seen that changes in the AO index are positive and largest in January both near the surface and in the stratosphere. Smaller changes are also found in November, December and August. Based on thirty years of monthly SLP data, *Thompson et al.* [2000] also noted positive trends in these months, but attributed significance to the trends in January, February, March and August.

Greenhouse gas increases and ozone depletion together act to cool the stratosphere radiatively. The former effect is dominant in winter, but is only expected to account for a change in the radiatively determined state of around 0.5K/decade in the region we consider, leading to a difference between the means of the two halves of the record of order 1K (K. Shine, pers. comm.). However a second mechanism by which vortex strength is effected by anthropogenic forcing is discussed by *Shindell et al.* [1999]. Cooling of the polar stratosphere and warming of the tropical upper troposphere causes an increased meridional temperature gradient in the region of the tropopause, and an associated change in the vertical shear of the zonal wind. This change tends to deflect high-latitude plane-

tary waves southwards, reducing their heating effect on the polar stratosphere, and reducing the number of sudden warmings. If this mechanism has been important in determining the response of the stratospheric circulation to anthropogenic forcing, we might expect the number of warm vortex days in the "tail" to decrease, while the peak at positive vortex states stays in much the same place, changing the shape of the PDF. Owing to the fact that in January the vortex is coldest and the negative skewness is largest, we would expect this effect to be strongest in this month. Of the levels on which the radiatively determined temperature was available, 70hPa had temperatures closest to this limit, so changes in the shape of the PDF might be expected to be largest here. We thus plot histograms of the daily 70hPa AO index and North Pole temperature in January for each half of the record, 1958-1977 and 1978-1997 (figure 8). Both histograms show that the number of weak vortex events (sudden warmings) is lower in the second half of the record than in the first, whilst the broad maximum of the distribution has moved relatively little. The limiting effect is clearest in the polar temperatures, which are most directly limited by the radiatively determined state. Such a change in the distribution of stratospheric polar temperatures in January has since been noted in a stratosphere-resolving GCM in response to stratospheric ozone depletion (S. Rossier, pers. comm.), which has a similar effect on planetary wave propagation to a greenhouse gas increase [*Shindell et al.*, 2000].

We tested the significance of the change in the shape of the AO PDFs by subtracting the mean AO index of each half, and computing the Kolmogorov-Smirnov statistic for the two distributions (figure 7b). This statistic is just the maximum difference between the two cumulative distributions. We evaluated the significance of these results by comparison with our Monte-Carlo noise ensemble. Our results indicate that the change in the shape of the PDF in January is significant against red noise between 200 and 20hPa at the 95% level. Thus the shape of the PDF of the Arctic Oscillation index is changing in January as well as its mean. This is consistent with the hypothesis that the main response to forcing has been through the southward deflection of planetary waves, which has reduced the number of sudden warmings, whilst the strong vortex states, limited by the slowly changing radiatively determined state, have changed little. We might thus eventually expect the former effect to saturate, so that no sudden warmings occur in January, leaving the vortex strength correspondingly less sensitive to further increases in forcing. Such a saturation of response has been noted in a GCM by *Shindell et al.* [2000]. This could explain the discrepancy between the observed AO sensitivity to forcing and that of GCMs with poor stratospheric resolution [*Gillett et al.*, 2000], whose unperturbed winter stratospheres are often already close to the radiatively-determined state, an issue we pursue elsewhere.

5. Conclusion

While we find PDFs of the AO index to be Gaussian-like in the troposphere, in contrast to the results of *Corti et al.* [1999], we note that nonlinearity in the stratospheric response to forcing could make the tropospheric response nonlinear through its downward influence. This hypothesis is supported by our finding that the downward propagation of AO anomalies in the NCEP reanalysis noted by *Baldwin and Dunkerton* [1999] is statistically significant, and that the AO exhibits significant departures from normality in the stratosphere. In April PDFs of the AO index in the stratosphere are positively skewed, with a narrow variance peak corresponding to days on which the final warming has occurred, and a tail to positive AO index, corresponding to days when the winter vortex persists. In January, when the polar stratosphere is dynamically heated by planetary wave activity, the observed negative skewness is associated with the limit on vortex strength corresponding to the radiatively determined state. Whilst this state changes only slowly in response to anthropogenic forcing, the southward deflection of planetary waves by the changed vertical shear of zonal wind could lead to a large reduction in the number of warming events, changing the distribution of the index. Using a KS-test and a Monte-Carlo ensemble of red noise series, we found that there has indeed been a significant change in the shape of the PDF between 200 and 20hPa in January between the periods 1958-1977 and 1978-1997, consistent with our hypothesis. As the planetary wave deflection effect saturates (when there are no more sudden warmings), we would expect a change in the sensitivity of the mean vortex strength to anthropogenic forcing. In view of the downward influence we observe, we speculate that as greenhouse gas concentrations further increase, the tropospheric Arctic Oscillation may also show a reduced sensitivity to the forcing, with implications for surface climate change.

Appendix: Calculation of AO Indices

We use the National Center for Environmental Prediction/National Center for Atmospheric Research (NCEP/NCAR) Reanalysis [*Kalnay et al.*, 1996] geopotential heights and temperatures, available as daily averages on a $2.5° \times 2.5°$ grid on 17 levels from 1000 to 10hPa for the years 1958-1997. By comparison with other data sources, J. Perlwitz (pers. comm.) concluded that the stratospheric data are un-

reliable in summer and in the tropics, but that northward of 20°N they are reliable for the study of large-scale circulation patterns in the lower stratosphere. However, we note that changes in the observations assimilated around 1979 may influence higher moments of the AO indices, and it would be prudent to verify these results using other reanalyses as they become available. Following the method of *Baldwin and Dunkerton* [1999], an EOF analysis was first performed on 90-day low-pass filtered DJF geopotential height anomalies on five levels (1000, 300, 100, 30 and 10hPa) over the region northward of 20°N. The data on each level were normalised separately by dividing by the standard deviation, and an equal-area grid was used. Spatial patterns for each of the 17 levels were then recovered by regressing geopotential height data onto the first principal component from the EOF analysis. Indices at each level were obtained by regressing the geopotential heights onto each of these spatial patterns. These are referred to by *Baldwin and Dunkerton* [1999] as 'AO signature time series', but we use the term 'AO indices' for simplicity.

References

Baldwin, M. P. and T. J. Dunkerton, Propagation of the Arctic Oscillation from the stratosphere to the troposphere, *J. Geophys. Res.*, *104*, 30937–30946, 1999.

Baldwin, M. P. and J. R. Holton, Climatology of the stratospheric polar vortex and planetary wave breaking, *J. Atmos. Sci.*, *45*, 1123–1142, 1988.

Charney, J. G. and P. G. Drazin, Propagation of planetary-scale disturbances from the lower into the upper atmosphere, *J. Geophys. Res.*, *66*, 83–109, 1961.

Cheng, X. and J. M. Wallace, Cluster analysis of the Northern Hemisphere wintertime 500-hpa height field: Spatial patterns, *J. Atmos. Sci.*, *50*, 2674–2696, 1993.

Corti, S., F. Molteni, and T. N. Palmer, Signature of recent climate change in frequencies of natural atmospheric circulation regimes, *Nature*, *398*, 799–802, 1999.

Fyfe, J. C., G. J. Boer, and G. M. Flato, The Arctic and Antarctic Oscillations and their projected changes under global warming, *Geophys. Res. Lett*, *26*, 1601–1604, 1999.

Gillett, N. P., G. C. Hegerl, M. R. Allen, and P. A. Stott, Implications of changes in the Northern Hemisphere circulation for the detection of anthropogenic climate change, *Geophys. Res. Lett*, *27*, 993–996, 2000.

Godson, W. L. and R. L. Lee, High level fields of wind and temperature over the Canadian Arctic, *Beitr. Phys. Atmos.*, *31*, 40–68, 1958.

Graf, H. F., I. Kirchner, and J. Perlwitz, Changing lower stratospheric circulation: The role of ozone and greenhouse gases, *J. Geophys. Res.*, *103*, 11251–11261, 1998.

Hansen, A. R. and A. Sutera, Structure in the phase space of a general circulation model deduced from empirical orthogonal functions, *J. Atmos. Sci.*, *49*, 320–326, 1992.

Kalnay, E. et al., The NCEP/NCAR 40-year reanalysis project, *Bull. Amer. Met. Soc.*, *77*, 437–471, 1996.

Kimoto, M. and M. Ghil, Multiple flow regimes in the Northern Hemisphere winter. Part I: Methodology and hemispheric regimes, *J. Atmos. Sci.*, *50*, 2625–2643, 1993.

Kuroda, Y. and K. Kodera, Role of planetary waves in the stratosphere-troposphere coupled variability in the Northern Hemisphere winter, *Geophys. Res. Lett*, *26*, 2375–2378, 1999.

Labitzke, K., Interannual variability of the winter stratosphere in the Northern Hemisphere, *Mon. Wea. Rev.*, *105*, 762–770, 1977.

Labitzke, K., On the interannual variability of the middle stratosphere during the Northern winters, *J. Meteor. Soc. Japan*, *60*, 124–138, 1982.

Murray, F. W., Dynamic stability in the stratosphere, *J. Geophys. Res.*, *65*, 3273–3305, 1960.

Nakamura, H. and J. M. Wallace, Skewness of the low-frequency fluctuations in the tropospheric circulation during the Northen Hemisphere winter, *J. Atmos. Sci.*, *48*, 1441–1448, 1991.

Paeth, H., A. Hense, R. Glowienka-Hense, S. Voss, and U. Cubasch, The North Atlantic Oscillation as an indicator for greenhouse-gas induced regional climate change, *Climate Dynamics*, *15*, 953–960, 1999.

Palmer, T. N., A nonlinear dynamical perspective on climate prediction, *J. Climate*, *12*, 575–591, 1999.

Perlwitz, J. and H. F. Graf, The statistical connection between tropospheric and stratospheric circulation of the Northern Hemisphere in winter, *J. Climate*, *8*, 2281–2295, 1995.

Priestley, M. B., *Spectral analysis and time series*, volume 2, 685–687 pp., Academic Press, London, 1981.

Shindell, D. T., R. L. Miller, G. Schmidt, and L. Pandolfo, Simulation of the Arctic Oscillation trend by greenhouse forcing of a stratospheric model, *Nature*, *399*, 452–455, 1999.

Shindell, D. T., D. Rind, and P. Lonergan, Increased polar stratospheric ozone losses and delayed eventual recovery owing to increasing greenhouse-gas concentrations, *Nature*, *392*, 589–592, 1998.

Shindell, D. T., G. A. Schmidt, R. L. Miller, and D. Rind, Northern hemisphere winter climate response to greenhouse gas, ozone, solar and volcanic forcing, *J. Geophys. Res.*, 2000. submitted.

Shine, K. P., The middle atmosphere in the absence of dynamical heat fluxes, *Quart. J. Roy. Met. Soc.*, *113*, 603–663, 1987.

Shine, K. P., Sources and sinks of zonal momentum in the middle atmosphere diagnosed using the diabatic circulation, *Quart. J. Roy. Met. Soc.*, *115*, 265–292, 1989.

Thompson, D. W. J. and J. M. Wallace, The Arctic Oscillation signature in the wintertime geopotential height and temperature fields, *Geophys. Res. Lett*, *25*, 1297–1300, 1998.

Thompson, D. W. J. and J. M. Wallace, Annular modes in the extratropical circulation Part I: Month to month variability, *J. Climate*, *5*, 1000–1016, 2000.

Thompson, D. W. J., J. M. Wallace, and G. C. Hegerl, Annular modes in the extratropical circulation Part II: Trends, *J. Climate*, *5*, 1018–1036, 2000.

von Storch, H., G. Bürger, R. Schnur, and J.-S. von Storch, Principal oscillation patterns: A review, *J. Climate*, *8*, 377–400, 1995.

Wallace, J. M., North Atlantic Oscillation / Annular Mode: Two paradigms - One phenomenon, *Quart. J. Roy. Met. Soc.*, 2000. in press.

Yamazaki, K. and Y. Shinya, Analysis of the Arctic Oscillation simulated by a GCM, *J. Meteor. Soc. Japan*, *77*, 1287–1298, 1999.

M. R. Allen, Space Science and Technology Department, Rutherford Appleton Laboratory, Chilton, Didcot OX11 0QZ, UK. (e-mail: m.r.allen@rl.ac.uk)

M. P. Baldwin, Northwest Research Associates, 14508 NE 20th Street, Bellevue, WA 98007-3713. (e-mail: mark@nwra.com)

N. P. Gillett, Atmospheric, Oceanic and Planetary Physics, Clarendon Laboratory, Parks Road, Oxford OX1 3PU, UK. (e-mail: gillett@atm.ox.ac.uk)

This preprint was prepared with AGU's LaTeX macros v5.01. File aochange pp formatted May 25, 2000.

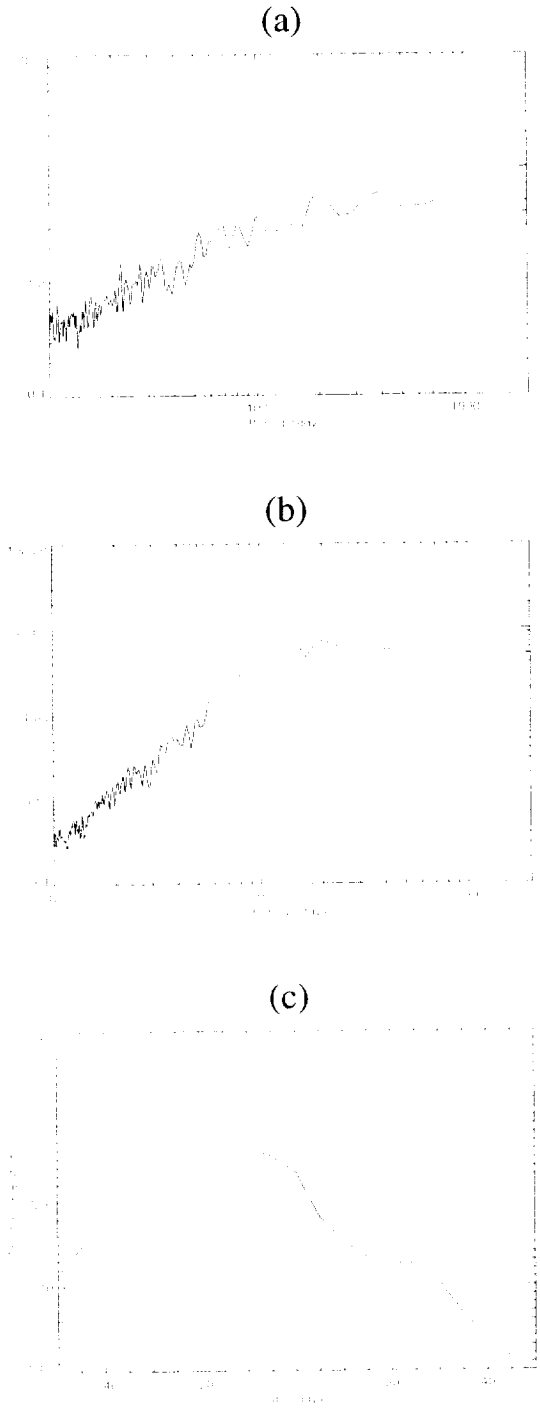

Figure 1. Power spectra of 5-day subsampled AO index at (**a**) 1000hPa, (**b**) 10hPa, and (**c**) their cross-correlation function. In each case the range between the 2.5th and 97.5th percentiles of the bivariate AR(1) model is shown by a grey band. In **c** negative lag corresponds to the 10hPa index leading the 1000hPa index.

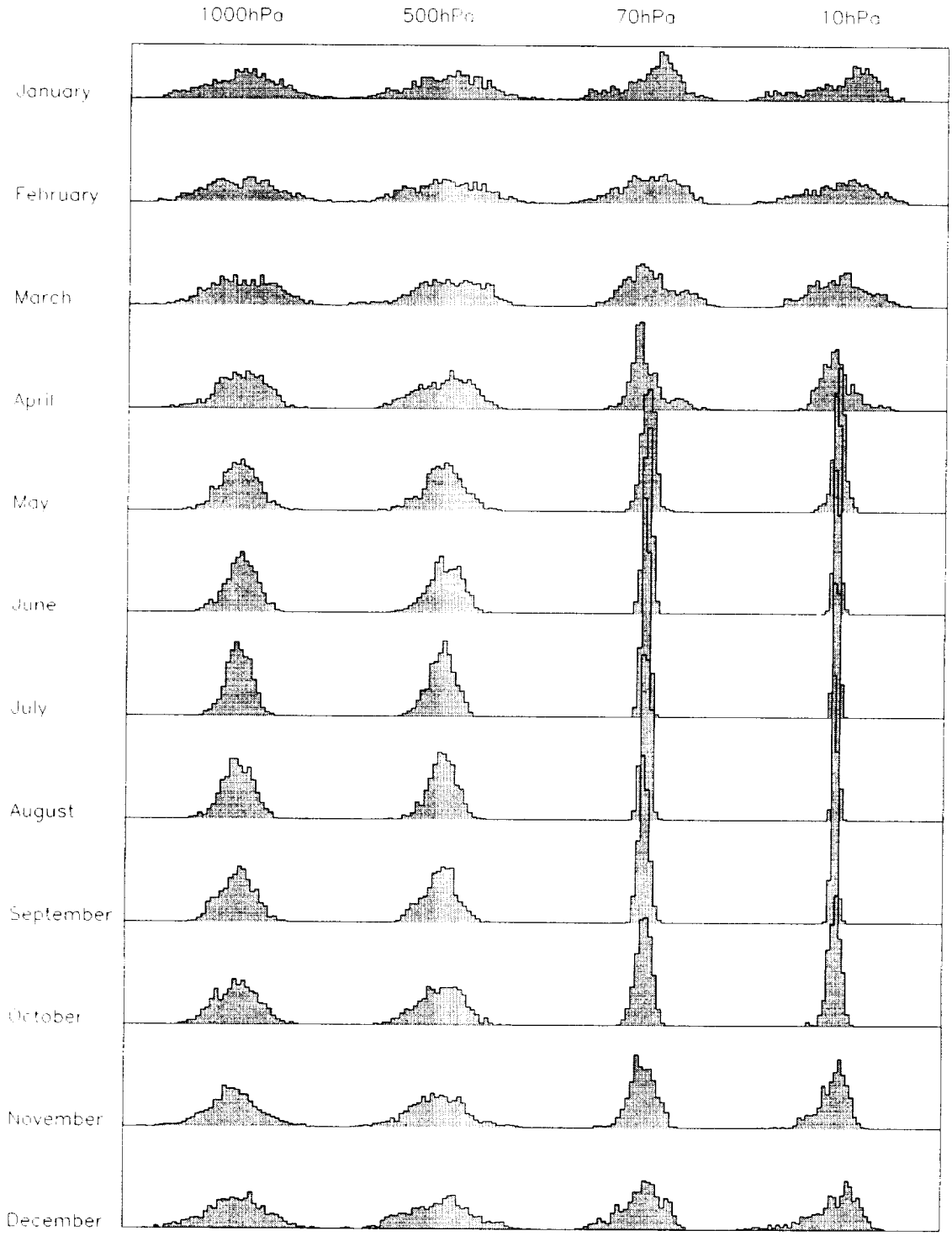

Figure 2. Histograms of daily AO indices on four levels for each month for the years 1958-1997.

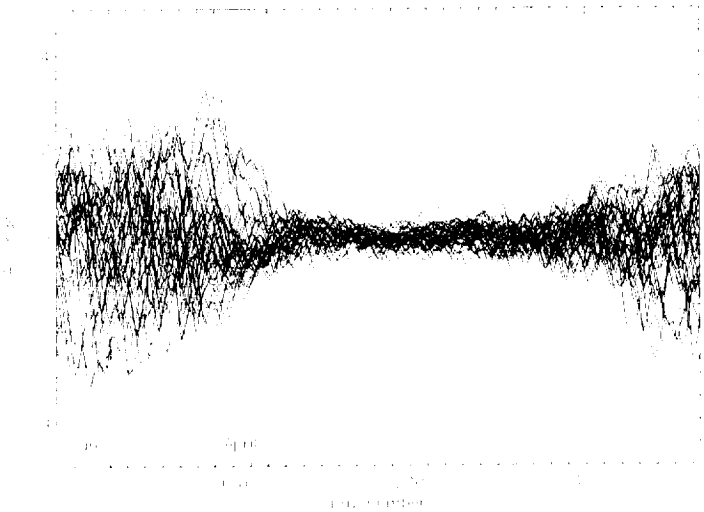

Figure 3. 70hPa AO index for each year 1958-1997 plotted against day number. Note that the index is based on deseasonalised geopotential heights. Skewness in January and April is visible as clustering above and below zero respectively.

(a)

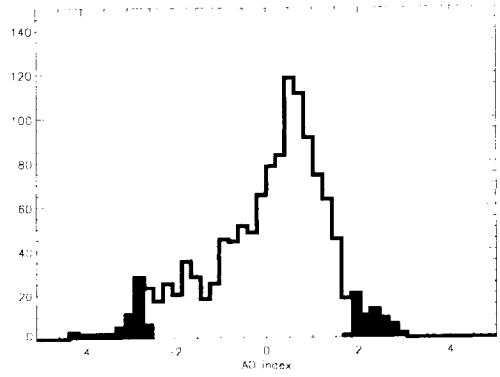

(b)

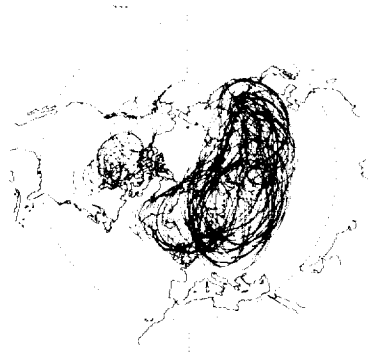

(c)

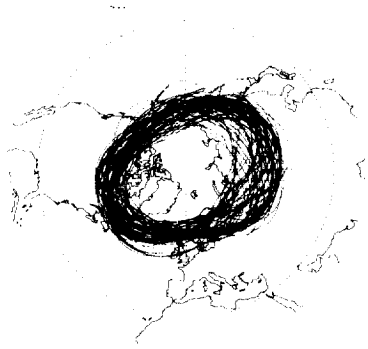

Figure 4. **a** is an enlarged version of the histogram of AO index at 70hPa in January shown in figure 2. The light shaded region represents the 5% of days with the lowest AO index, and the 17.75km contour of 70hPa geopotential height on all these days is plotted in panel **b**. The dark shaded region corresponds to the 5% of days with the highest AO index, and the associated 17.75km contours of 70hPa height are shown in **c**.

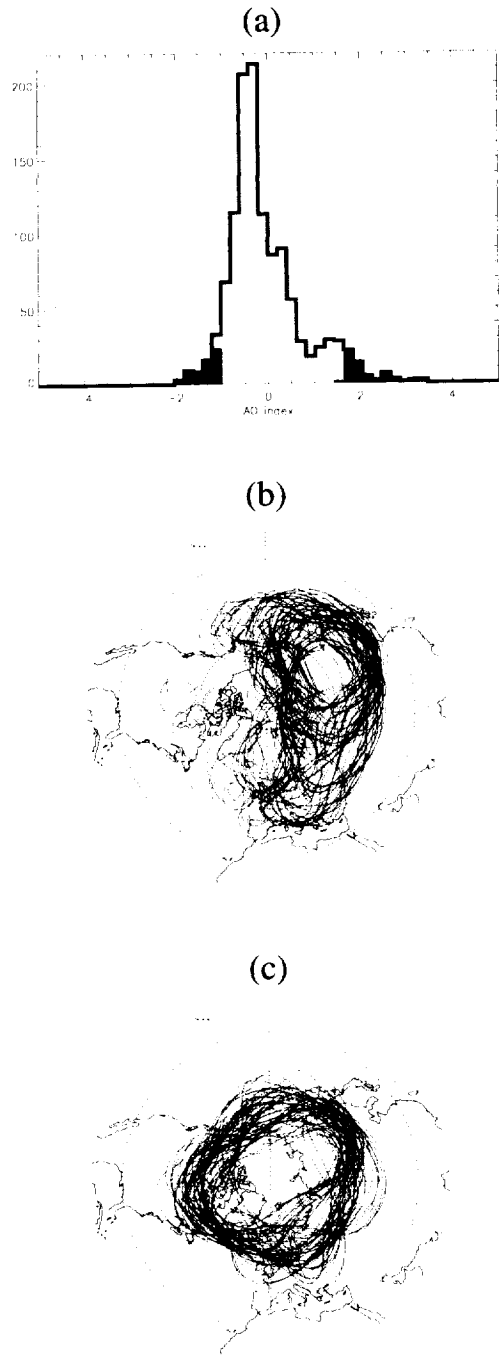

Figure 5. As figure 4, but for April. The 18.2km contour of 70hPa geopotential height is shown in panels **b** and **c**.

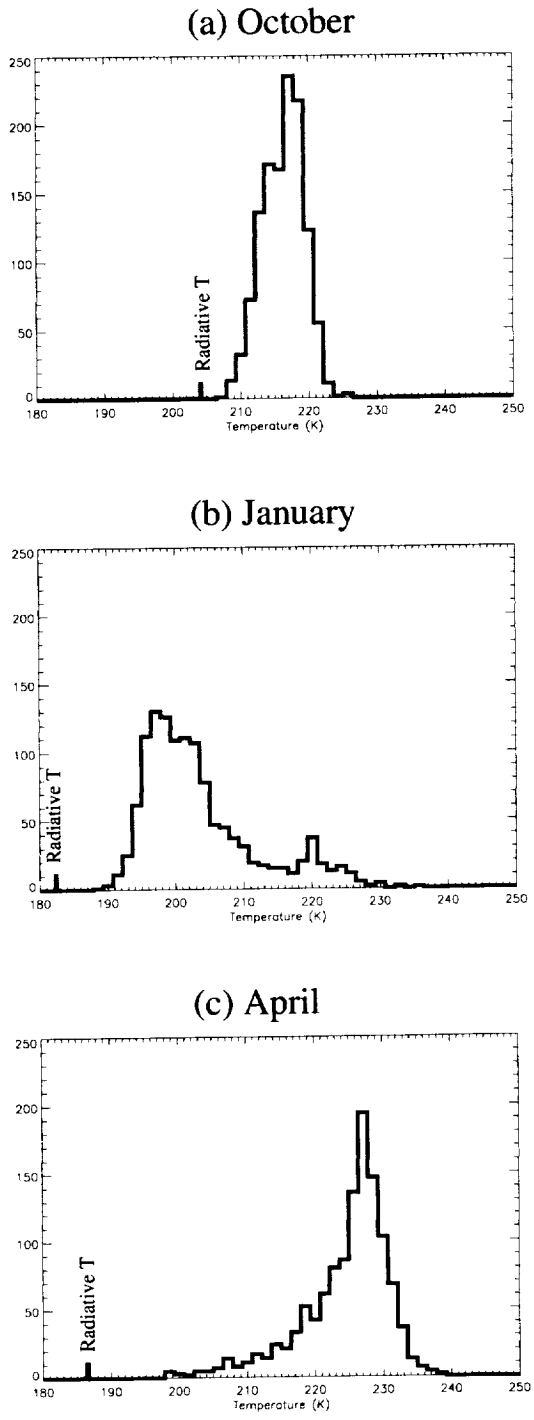

Figure 6. Histograms of daily NCEP 70hPa North Pole temperature over the period 1958-1997 in (**a**) October, (**b**) January, and (**c**) April. The corresponding radiatively determined temperatures are shown for comparison.

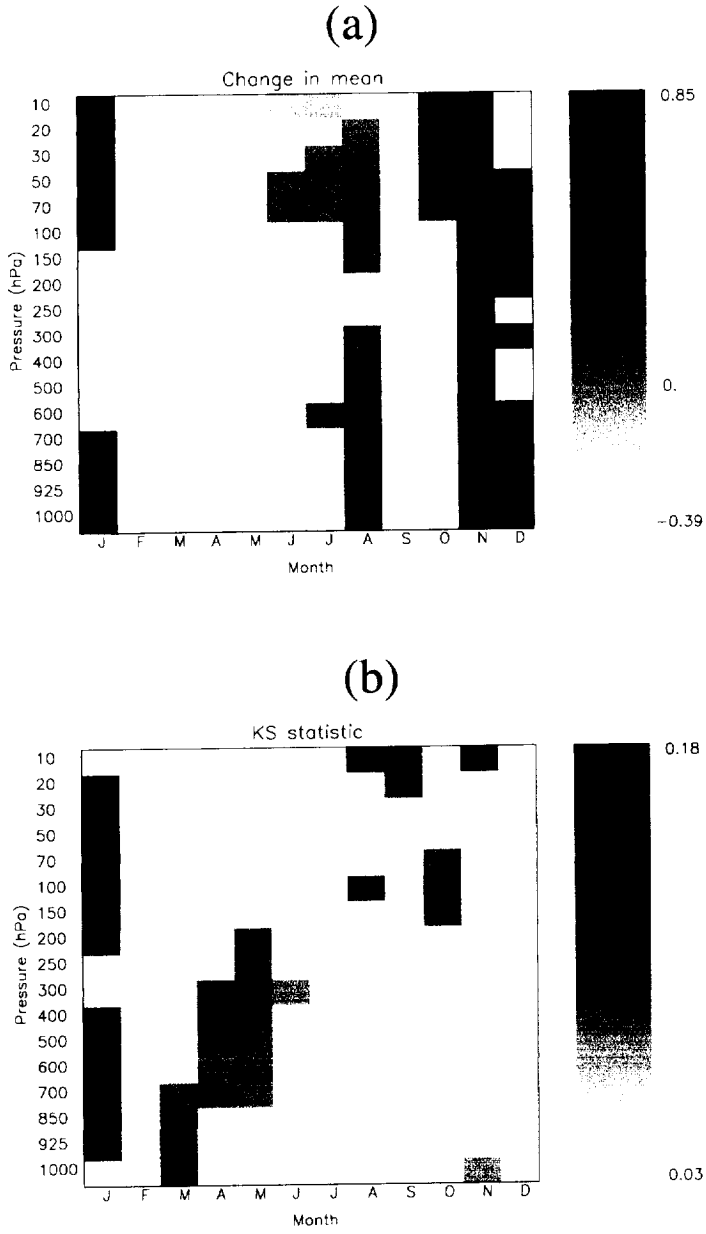

Figure 7. **a** shows the change in the mean AO index between the periods 1958-1977 and 1978-1997, only plotted where <95% or >95% of those in the noise model. **b** shows the KS-statistic, a measure of the difference between the AO index distributions of the two periods, independent of the change in the mean, and only plotted where significant at the 95% level.

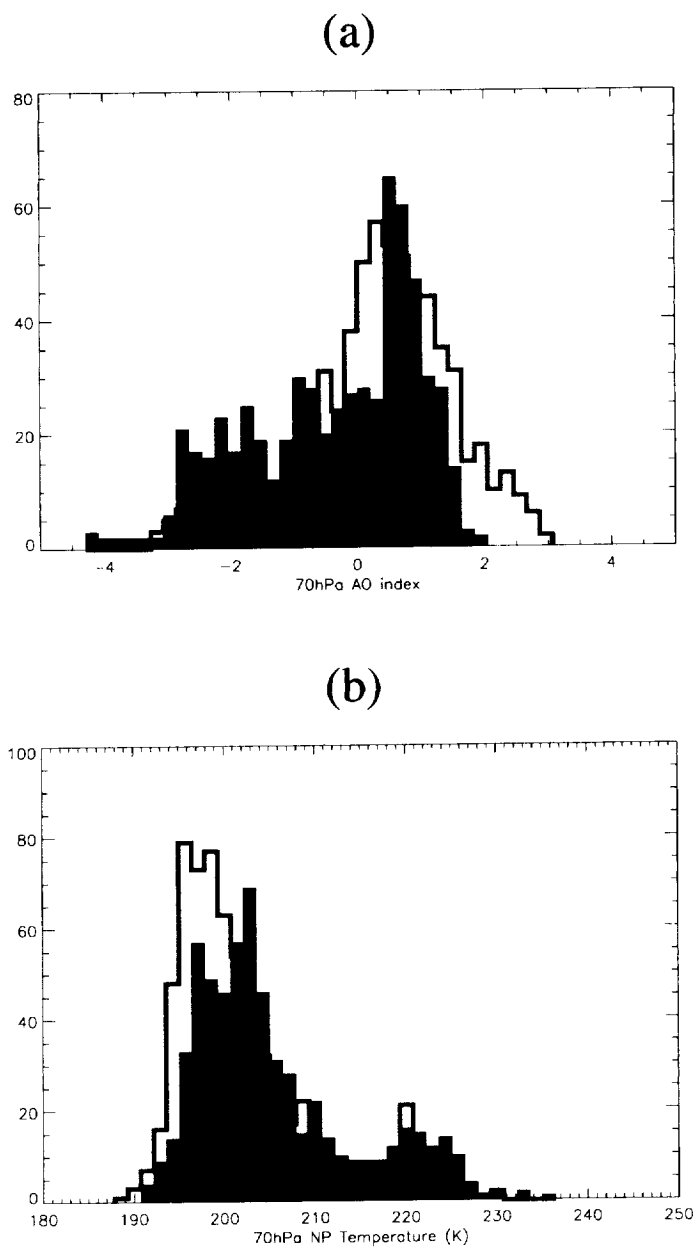

Figure 8. Histograms of the daily January 70hPa AO index (**a**) and North Pole temperature (**b**) for 1958-1977 (dark shaded) and 1978-1997 (grey line).

REVIEW ARTICLE ON THE QBO

Submitted to *Reviews of Geophysics*, October 1999

Revised, August 2000

THE QUASI-BIENNIAL OSCILLATION

M.P. Baldwin,[1] L.J. Gray,[2] T.J. Dunkerton,[1] K. Hamilton,[3]
P.H. Haynes,[4] W.J. Randel,[5] J.R. Holton,[6] M.J. Alexander,[7] I. Hirota,[8] T. Horinouchi,[9]
D.B.A. Jones,[10] J.S. Kinnersley,[11] C. Marquardt,[12] K. Sato,[8] and M. Takahashi[13]

ABSTRACT

The quasi-biennial oscillation (QBO) dominates the variability of the equatorial stratosphere (~16–50 km) and is most easily seen as downward propagating easterly and westerly wind regimes, with a variable period averaging approximately 28 months. From a fluid dynamical perspective, the QBO is a fascinating (and perhaps the premier) example of a coherent, oscillating mean flow that is driven by vertically propagating waves with periods unrelated to that of the resulting oscillation. Although the QBO is a tropical phenomenon, it affects the stratospheric flow from pole to pole by modulating the effects of extratropical waves. The QBO affects variability in the mesosphere near 85 km by selectively filtering waves that propagate upward through the equatorial stratosphere, and even appears to affect the strength of Atlantic hurricanes. Indeed, study of the QBO is inseparable from the study of atmospheric wave motions that drive it and are modulated by it. The effects of the QBO are not confined to atmospheric dynamics. Chemical constituents, such as ozone, water vapor, and methane, are affected by circulation changes, in both hemispheres, induced by the QBO. There are also substantial QBO signals in many of the shorter-lived chemical constituents. Through modulation of extratropical wave propagation, the QBO has an effect on the breakdown of the wintertime stratospheric polar vortices and severity of high-latitude ozone depletion. The polar vortex in the stratosphere tends to affect surface weather patterns, providing a mechanism for the QBO to have a small effect at the Earth's surface. As more data sources (e.g., wind and temperature measurements from both ground-based systems and satellites) become available, the effects of the QBO can be more precisely assessed.

This review covers the current state of knowledge of the tropical QBO, its extratropical dynamical effects, chemical constituent transport, and effects of the QBO in the troposphere and above the stratosphere. It is intended to provide a broad overview of the QBO and its effects to researchers outside the field, as well as a source of information and references for specialists. The history of research on the QBO is discussed only briefly, and the reader is referred to several historical review papers. The basic theory of the QBO is summarized, and tutorial references are provided.

[1] NorthWest Research Associates, Inc., Bellevue, WA, USA
[2] Rutherford Appleton Lab, Chilton, Didcot, Oxon, UK
[3] Geophysical Fluid Dynamics Lab/NOAA, Princeton, NJ, USA
[4] DAMTP, University of Cambridge, Cambridge, UK
[5] National Center for Atmospheric Research, Boulder, CO, USA
[6] Dept. of Atmospheric Sciences, University of Washington, Seattle, WA, USA
[7] NorthWest Research Associates, Inc., CoRA Division, Boulder, CO, USA
[8] Dept. of Geophysics, Kyoto University, Kyoto, Japan
[9] Radio Atmospheric Science Center, Kyoto University, Kyoto, Japan
[10] Dept. of Earth and Planetary Sciences, Harvard University, Cambridge, MA, USA
[11] Dept. of Applied Mathematics, University of Washington, Seattle, WA, USA
[12] GFZ Potsdam, Potsdam, Germany
[13] Center for Climate System Research, University of Tokyo, Tokyo, Japan

1. INTRODUCTION

1.1. The discovery of the Quasi-Biennial Oscillation (QBO)

The first observations of equatorial stratospheric winds were made when it was discovered that debris from the eruption of Krakatau (1883) circled the globe from east to west in a period of about two weeks; these winds became known as the "Krakatau easterlies." (For a more complete review of the discovery of the QBO, and advances in observations and theory, the reader is referred to *Maruyama* [1997] and *Labitzke and van Loon* [1999]). In 1908 the German meteorologist Berson launched balloons from tropical Africa and found winds blowing from west to east at about 15 km, near the tropopause, which became known as the "Berson westerlies." For nearly 50 years there were only sporadic balloon observations [*Hamilton*, 1998a] to contradict the existence of equatorial stratospheric *easterly* winds overlying *westerly* winds. *Palmer* [1954] used upper air sounding data, gathered to study nuclear testing at the Marshall Islands, to find that the transition between the "Berson westerlies" and "Krakatau easterlies" varied from month to month and year to year. However, the data were insufficient to show any periodicity. By using observations from Christmas Island (2.0°N), *Graystone* [1959] contoured two years of wind speeds in the time-height plane, which showed gradually descending *easterly* (italicized terms are defined in the Glossary) and *westerly* wind regimes. (Note: The meteorological term "easterlies" describes winds that blow from the east, while "westerlies" blow from the west. Unfortunately, the terms "*eastward*" (to the east) and "*westward*" (to the west) are used commonly in discussions of wave propagation and flow, and have the opposite meaning of easterly and westerly. Throughout this review we will use both descriptions, as found in the literature.)

Discovery of the QBO must be credited to the independent work of R.J. Reed in the United States and R.A. Ebdon in Great Britain. In a paper entitled "The Circulation of the Stratosphere" presented at the 40th anniversary meeting of the American Meteorology Society, Boston, January 1960, Reed announced the discovery, using Canton Island data (2.8°S) of "alternate bands of easterly and westerly winds which originate above 30 km and which move downward through the stratosphere at a speed of about 1 km per month." Reed pointed out that the bands "appear at intervals of roughly 13 months, 26 months being required for a complete cycle." *Ebdon* [1960] also used data from Canton Island, spanning 1954–1959, to show that the wind oscillation had an apparent two-year period. *Ebdon and Veryard* [1961] used additional data from Canton Island (January 1954–January 1960) at 50 hPa (hectopascals, equal to millbars) to show that the wind fluctuated with a period of 25–27 months, rather than exactly two years. They extended the earlier study of Ebdon to include other equatorial stations and concluded that the wind fluctuations occurred simultaneously around the equatorial belt, and estimated that the wind regimes (when the equatorial winds are easterly or westerly) took about a year to descend from 10 hPa to 60 hPa. *Veryard and Ebdon* [1961] extended this study to find a dominant period of 26 months and observed similar fluctuations in temperature.

With the observation of a longer-period cycle starting in 1963, *Angell and Korshover* [1964] coined the term "quasi-biennial oscillation," which gained acceptance and was abbreviated "QBO." Many of the dynamical aspects of the QBO are best illustrated by a time-height cross-section of monthly-mean equatorial *zonal* (longitudinal) wind (Figure 1). Ideally, such a diagram would be of the zonally-averaged zonal wind, but the approximate longitudinal symmetry of the QBO allows rawinsonde (balloon) observations from a single station near the equator to be sufficient. The alternating wind regimes repeat at intervals that vary from 22 to 34 months, with an average period of slightly more than 28 months. Westerly shear zones (in which westerly winds increase with height) descend more regularly and rapidly than easterly shear zones. The amplitude of ~20 ms^{-1} is nearly constant from 5 hPa to 40 hPa, but decreases rapidly as the wind regimes descend below 50 hPa. Rawinsonde observations are used up to 10 hPa, and rocketsondes (meteorological rockets) above. The QBO amplitude diminishes to less than 5 ms^{-1} at 1 hPa, near the stratopause. The amplitude of the QBO is approximately Gaussian about the equator with a 12 degree half width and little phase dependence on latitude within the tropics [*Wallace*, 1973]. Although the QBO is definitely not a biennial oscillation, there is a tendency for a seasonal preference in the phase reversal [*Dunkerton*, 1990] so that, for example, the onset of both easterly and westerly winds regimes occurs mainly during Northern Hemisphere (NH) late spring at the 50-hPa level. Perhaps the three most remarkable features of the QBO that any theory must explain are (1) the quasi-biennial periodicity, (2) the occurrence of zonally symmetric westerly winds at the equator (conservation of angular momentum does not allow advection to create an equatorial westerly wind maximum), and (3) the downward propagation without loss of amplitude.

1.2. The search for an explanation of the QBO

At the time of discovery of the QBO, there were no observations of tropical waves and there was no theory predicting their existence. The search for an explanation for the QBO initially involved a variety of other causes: some internal feedback mechanism, a natural period of atmospheric oscillation, an external process, or some combination of these mechanisms. All these attempts failed to explain features such as the downward propagation and maintenance of the amplitude of the QBO as it descends (energy density grows as the winds descend).

Apparently, zonally asymmetric wave forcing is required to explain the equatorial westerly wind maximum. *Wallace and Holton* [1968] tried to drive the QBO in a numerical model through heat sources or through extratropical *planetary waves* propagating into the equator. They showed rather conclusively that lateral momentum transfer by planetary waves could not explain the downward propagation of the QBO without loss of amplitude. They made the crucial realization that the only way to reproduce the observations was to have a driving force (a momentum source) which actually propagates downward with the mean equatorial winds.

Booker and Bretherton's [1967] seminal paper on the absorption of *gravity waves* at a *critical level* provided the spark that would lead to an understanding of how the QBO is driven (see *Lindzen* [1987] for a historical review of the development of the theory of the QBO). It was Lindzen's leap of insight to realize that gravity waves could drive a QBO with descending shear zones. *Lindzen and Holton* [1968] showed how a QBO could be driven by a broad spectrum of vertically-propagating (propagating to the east or west) gravity waves. The crucial step in the understanding of the QBO was the realization that vertically propagating waves could provide the necessary momentum flux and that the periodicity could arise through an internal mechanism arising from a two-way feedback between the waves and the background flow. The first part of the feedback is the effect of the background flow on the propagation of the waves (and hence on the momentum fluxes). The second part of the feedback is the effect of the momentum fluxes on the background flow. *Lindzen and Holton* [1968] demonstrated explicitly, using a two dimensional (2-D) model in which the behavior and effect of the waves was parameterized in a simple way, that the feedback gave rise to an oscillation with a downward propagating pattern of easterly and westerly winds. An important corollary to their work was that the period of the oscillation was controlled in part by the wave momentum fluxes and hence, a range of periods was possible. The fact that the observed oscillation had a period close to a subharmonic of the annual cycle was, therefore, a pure coincidence.

It was a bold assertion to ascribe the forcing of the QBO to eastward and westward propagating gravity waves, considering that only the westward waves had been observed. The theory of equatorial waves was first developed during the late 1960s, in parallel with the theory of the QBO. The solutions included a *Rossby* mode, and a mode which became known as the *mixed Rossby-gravity* mode. A third solution, an eastward-propagating gravity mode in the zonal wind only, was called the equatorial *Kelvin* mode. *Maruyama* [1967] displayed observations consistent with the mixed Rossby-gravity mode. *Wallace and Kousky* [1968] first showed observations of equatorial Kelvin waves in the lower stratosphere, and noted that the wave produced an upward flux of westerly momentum which could account for the westerly acceleration associated with the QBO.

Lindzen [1970] showed that mixed Rossby-gravity waves, through a mechanism involving the *Coriolis* force acting on meridional parcel displacements, contribute a net easterly force. Thus, the potential existed for the QBO to be driven by a combination of mixed Rossby-gravity waves, which would contribute easterly forces, and Kelvin waves, which would contribute westerly forces. *Holton and Lindzen* [1972] refined the *Lindzen and Holton* [1968] model by demonstrating, in a one-dimensional (1-D) model, a QBO driven by vertically-propagating Kelvin and mixed Rossby-gravity waves. The observed amplitudes of these waves, though small, were arguably (given the paucity of equatorial wave observations) large enough to drive the QBO. The Holton and Lindzen mechanism continued to be the accepted paradigm for the QBO for more than two decades.

The conceptual model of the QBO, which formed the basis of the *Lindzen and Holton* [1968] model, was strongly supported by the famed laboratory experiment of *Plumb and McEwan* [1978], which used a salt-stratified fluid contained in a large annulus. The bottom boundary of the annulus consisted of a flexible membrane that oscillated up and down to produce vertically propagating gravity waves traveling clockwise and counterclockwise around the annulus. For waves of sufficient amplitude, a wave-induced mean flow regime was established that was characterized by downward progressing periodic reversals of the mean flow. This experiment, which remains one of the most dramatic laboratory analogues of a large-scale geophysical flow, showed that the theoretical paradigm for the QBO was consistent with the behavior of a real fluid system.

While the observed amplitudes of Kelvin and mixed Rossby-gravity waves are sufficient to drive a QBO in idealized models of the atmosphere, *Gray and Pyle* [1989] found it necessary to increase the wave amplitudes by a factor of three to achieve a realistic QBO in a full radiative-dynamical-photochemical model. *Dunkerton* [1997] pointed out that the observed rate of tropical upwelling (about 1 km per month) effectively requires that the QBO wind regimes propagate downward much faster than was thought because the whole of the tropical stratosphere is moving upward as the QBO propagates downward. This fact effectively more than doubled the required momentum transport by vertically propagating equatorial waves. Observations indicate that mixed Rossby-gravity and Kelvin waves cannot provide sufficient forcing to drive the QBO with the observed periods. Dunkerton reasoned that additional momentum flux must be supplied by a broad spectrum of gravity waves—similar to those postulated by *Lindzen and Holton* [1968].

Although the QBO is a tropical phenomenon, it influences the global stratosphere, as first shown by *Holton and Tan* [1980]. Through modulation of winds, temperatures, and the circulation in the *meridional plane*, the QBO affects

the distribution and transport of greenhouse gases and may be a factor in stratospheric ozone depletion. Thus, an understanding of the QBO and its global effects is necessary for studies of long-term variability or trends in trace gases and aerosols.

2. AN OVERVIEW OF THE QBO AND ITS GLOBAL EFFECTS

2.1. Zonal wind

A composite of the QBO in equatorial zonal winds (Figure 2) [*Pawson et al.*, 1993] shows faster and more regular downward propagation of the westerly *phase*, and the stronger intensity and longer duration of the easterly phase. The mean period of the QBO for data during 1953–1995 is 28.2 months, slightly longer than the 27.7 months from the shorter record in *Naujokat* [1986]. The standard deviation of the mean QBO is also included in Figure 2, showing maxima in variability close to the descending easterly and westerly shear zones (larger for the westerly phase). This mainly reflects deviations in the duration of each phase (as seen in Figure 1).

Dunkerton [1990] showed that the QBO may be synchronized to the annual cycle, demonstrating that the onset of the easterly regime at 50 hPa tends to occur during NH late spring or summer. His analysis is updated in Figure 3, showing the onset of each wind regime at 50 hPa. The easterly and westerly transitions both show a strong preference to occur during April–June.

The latitudinal structure of the QBO in zonal wind is shown in Figure 4, derived from long time series of wind observations at many tropical stations [*Dunkerton and Delisi*, 1985]. The amplitude of the QBO is latitudinally symmetric, and the maximum is centered over the equator, with a meridional half width of approximately 12°. Similar QBO structure is derived from assimilated meteorological analyses, but the amplitude is often underestimated in comparison to radiosonde measurements [*Pawson and Fiorino*, 1998; *Randel et al.*, 1999].

Figure 5 provides a dynamical overview of the QBO, its sources, and its global dynamical effects, as well as a foundation for the discussion of the details of the QBO in the following sections. The diagram span the troposphere, stratosphere, and mesosphere from pole to pole, and shows schematically the differences in zonal wind between easterly and westerly phases of the QBO.

Convection in the tropical troposphere, ranging from the scale of individual clouds through mesoscale convective complexes (spanning more than 100 km) produces a broad spectrum of waves (tan wavy arrows), including gravity, *inertia-gravity*, Kelvin, and Rossby-gravity waves (see Section 3). These waves, with a variety of vertical and horizontal wavelengths and phase speeds, propagate into the stratosphere, transporting easterly and westerly zonal momentum. Most of this zonal momentum is deposited at stratospheric levels, driving the zonal wind anomalies of the QBO. For each wave, the vertical profile of the zonal wind determines the critical level at which the momentum is deposited. The critical levels for these waves depend, in part, on the shear zones of the QBO. Some gravity waves propagate through the entire stratosphere and produce a QBO near the mesopause known as the mesospheric QBO, or *MQBO* (Section 6).

In the tropical stratosphere the time-averaged wind speeds are small, so the easterly minus westerly composite in Figure 5 is similar in appearance to the actual winds during the easterly phase of the QBO. At high latitudes, there is a pronounced annual cycle, with strong westerly winds during the winter season. To the north of the equator in the lower stratosphere, tropical winds alter the effective waveguide for upward and equatorward propagating planetary-scale waves (curved purple arrows). The effect of the zonal wind structure in the easterly phase of the QBO is to focus more wave activity toward the pole, where the waves converge and slow the mean zonal flow. Thus, the polar vortex north of ~45°N shows weaker westerly winds (light blue). The high-latitude wind anomalies penetrate the troposphere and provide a mechanism for the QBO to have a small influence on tropospheric weather patterns (Section 6).

2.2. Temperature and meridional circulation

The QBO exhibits a clear signature in temperature, with pronounced signals in both tropics and extratropics. The tropical temperature QBO is in thermal wind balance with the vertical shear of the zonal winds, expressed for the equatorial *β-plane* as

$$\frac{\partial u}{\partial z} = \frac{-R}{H\beta}\frac{\partial^2 T}{\partial y^2} \qquad (1a)$$

[*Andrews et al.*, 1987, eq. 8.2.2], where u is the zonal wind, T is temperature, z is *log-pressure height* (approximately corresponding to geometric altitude), y is latitude, R is the gas constant for dry air, $H \cong 7$km is the nominal (constant) scale height used in the log-pressure coordinates, and β is the latitudinal derivative of the Coriolis parameter. For QBO variations centered on the equator with meridional scale L, thermal wind balance at the equator is approximated as

$$\frac{\partial u}{\partial z} \sim \frac{-R}{Hb}\frac{T}{L^2} \qquad (1b)$$

The equatorial temperature anomalies associated with the QBO in the lower stratosphere are of the order of ±4 K, maximizing near 30–50 hPa. Figure 6 compares time series (after subtraction of the seasonal cycle) of 30 hPa temperature measurements at Singapore with the corresponding zonal wind vertical shear at 30 hPa, showing good correla-

tion (see also Figure 1). The slope of *du/dz* versus temperature estimated from regression is consistent with a meridional scale $L \sim$ 1000–1200 km (~10° of latitude) [*Randel et al.*, 1999].

Smaller anomalies extend downward, with QBO variations of order of ±0.5 K observed near the tropopause [*Angell and Korshover*, 1964]. The QBO temperature anomalies also extend into the middle and upper stratosphere, where they are out of phase with the lower stratosphere anomalies. Figure 7 shows an example of temperature anomalies associated with an easterly phase of the QBO during NH winter 1994, derived from UKMO stratospheric assimilation data extending to 45 km. Although these data probably underestimate the magnitude of the temperature QBO (the retrievals average over a layer deeper than the temperature anomaly), the out-of-phase vertical structure is a robust feature also observed in long time records of satellite radiance measurements [*Randel et al.*, 1999].

Besides the equatorial maximum in QBO temperature, satellite data reveal coherent maxima over 20–40 degrees latitude in each hemisphere, which are out of phase with the tropical signal. This is demonstrated in Figure 8 showing regression of stratospheric temperatures over 13–22 km (from the Microwave Sounding Unit Channel 4) onto the 30-hPa QBO winds, for the period 1979–1999. One remarkable aspect of the extratropical temperature anomalies is that they are seasonally synchronized, occurring primarily during winter and spring in each hemisphere. Nearly identical signatures are observed in column ozone measurements (Section 5), and this seasonally-synchronized extratropical variability is a key and intriguing aspect of the global QBO. Because low frequency temperature anomalies are tightly coupled with variations in the mean meridional circulation, global circulation patterns associated with the QBO are also highly asymmetric at solstice (arrows in Figure 7). The temperature patterns in Figure 8 furthermore show signals in both polar regions, which are out of phase with the tropics, and maximize in spring in each hemisphere. Although these polar signals are larger than the subtropical maxima, they are not statistically significant in this 1979–1999 record because of enhanced natural variability in polar regions during winter and spring.

The modulation by the QBO of zonal-mean wind (Figure 5) is coupled to modulation of the zonally averaged circulation in the latitude-height plane. The climatological circulation is characterized by large-scale ascent in the tropics, broad poleward transport in the stratosphere, and compensating sinking through the extratropical tropopause [*Holton et al.*, 1995]. The transport of chemical trace species into, within, and out of the stratosphere is the result of both large-scale circulations and mixing processes associated with waves. Chemical processes, such as those resulting in ozone depletion, depend not only on the concentrations of trace species, but may depend critically on temperature. Since the QBO modulates the global stratospheric circulation, including the polar regions, an understanding of the effects of the QBO on both dynamics and the distribution of trace species is an essential component needed to understand global climate variability and change.

Many long-lived trace species, such as N_2O and CH_4, originate in the troposphere and are transported into the stratosphere through the tropical tropopause. Figure 9 provides a summary of the influence of the QBO on the circulation in the latitude-height plane and the transport of chemical trace species. In Figure 9 the contours illustrate schematically the isopleths of an idealized conservative, long-lived, vertically stratified tracer during the NH winter when the equatorial winds are easterly near 40 hPa (matching Figure 5). Upwelling is reflected in the broad tropical maximum in tracer density in the middle to upper stratosphere. The extratropical influences from the QBO result in deviations from hemispheric symmetry.

The heavy arrows illustrate circulation anomalies associated with the QBO (the time-averaged circulation has been removed), which is here assumed to be easterly at 40 hPa. At the equator, the QBO induces ascent (relative to the mean tropical upwelling) through the tropopause, but descent in the middle to upper stratosphere. The lower stratospheric ascent is nearly symmetric about the equator, while the circulation anomaly in the middle stratosphere is larger in the winter hemisphere. This asymmetry is reflected in the asymmetric isopleths of the tracer. In addition to advection by the circulation in the latitude-height plane, the tracer is mixed by wave motions (approximately on isentropic, or constant potential temperature, surfaces). This mixing is depicted by the wiggly horizontal arrows. The descent from the middle stratosphere circulation anomaly creates a "stair-step" pattern in the tracer isopleths between the equator and the subtropics (near 5 hPa). A second stair-step in the mid-latitude winter hemisphere is formed by isentropic mixing in the region of low potential vorticity gradients which surrounds the polar vortex, known as the *"surf zone"* [*McIntyre and Palmer*, 1983]. Mixing may also occur equatorward of the subtropical jet axis in the upper stratosphere, as illustrated by the wavy line near 3 hPa and 10–20°N [*Dunkerton and O'Sullivan*, 1996]. Anomalous transport from the Southern Hemisphere (SH) to the NH near the stratopause is associated with changes in extratropical planetary wave driving (Figure 5). The detailed effects of the QBO on tracer transport are discussed in Section 5.

3. DYNAMICS OF THE QBO

3.1. QBO mechanism

Since the QBO is approximately longitudinally symmetric, it is natural to try to explain it within a model that considers the dynamics of a longitudinally symmetric atmos-

phere. In a rotating atmosphere the temperature and wind fields are closely coupled and correspondingly both heating or mechanical forcing (i.e. forcing in the momentum equations) can give rise to a velocity response. Although, as noted in Section 1, the current view is that mechanical forcing, provided by wave momentum fluxes, is essential for the QBO, the coupling between temperature and wind fields must be taken into account to explain many aspects of the structure.

The essence of the mechanism for the oscillation may be most simply demonstrated in a simple representation of the interaction of vertically propagating gravity waves with a background flow that is itself a function of the vertical [*Plumb*, 1977]. Consider two discrete upward-propagating internal gravity waves, forced at a lower boundary with identical amplitudes but equal but opposite zonal phase speeds. The waves are assumed to be quasi-linear (interacting with the mean flow, but not with each other), steady, hydrostatic, unaffected by rotation, and subject to linear damping. The superposition of these waves corresponds exactly to a single "standing" wave. As each wave component propagates vertically, its amplitude is diminished by damping, generating a force on the mean flow due to convergence of the vertical flux of zonal momentum. This force locally accelerates the mean flow in the direction of the dominant wave's zonal phase propagation. The momentum flux convergence depends on the rate of upward propagation, and hence on the vertical structure in zonal wind speed. Even with two equal but opposite waves in a basic state at rest, the mean flow is an unstable equilibrium; any small deviation from zero will inevitably grow with time.

Plumb [1977] showed that the zonal wind anomalies descend in time, as illustrated in Figure 10. Each wave propagates vertically until its group velocity is slowed and the wave is damped as it encounters a shear zone where $|\overline{u}$ -c| is small. As the shear zone descends (Figure 10a) the layer of eastward winds becomes sufficiently narrow that viscous diffusion destroys the low-level eastward winds. This leaves the eastward wave free to propagate to high levels through westward mean flow (figure 10b), where dissipation and the resulting eastward acceleration gradually build a new eastward regime that propagates downward (Figures 10c,d).

The process just described repeats, but with westerly shear descending above easterly shear, leading to the formation of low-level easterly jet. When the westward jet decays, the westward wave escapes to upper levels, and a new easterly shear zone forms aloft. The entire sequence, as described, represents one cycle of a nonlinear oscillation. The period of the oscillation is determined, among other things, by the eastward and westward momentum flux input at the lower boundary and by the amount of atmospheric mass affected by the waves. In *Plumb's* [1977] *Boussinesq* formulation the QBO period is inversely proportional to momentum flux. A quasi-compressible atmosphere results in a substantially shorter period due to the decrease of atmospheric density with height. If the waves are "underdamped" (able to generate an oscillation at all heights) the QBO period is once again inversely proportional to momentum flux but is also proportional to a density scale height.

Simple representations such as Plumb's capture the essential wave mean-flow interaction mechanism leading the QBO. However they cannot explain why the QBO is an equatorial phenomenon (notwithstanding its important links to the extratropics). Some simple insights on this point come from considering the equations for the evolution of a longitudinally symmetric atmosphere subject to mechanical and thermal forcing. A suitable set of model equations for such a longitudinally symmetric atmosphere is as follows:

$$\frac{\partial u}{\partial t} - 2\Omega \sin\phi v = F \tag{2}$$

$$2\Omega \sin\phi \frac{\partial u}{\partial z} + \frac{R}{aH}\frac{\partial T}{\partial \phi} = 0 \tag{3}$$

$$\frac{\partial T}{\partial t} - w\frac{HN^2}{R} = -\alpha T \tag{4}$$

$$\frac{1}{a\cos\phi}\frac{\partial}{\partial \phi} v\cos\phi + \frac{1}{\rho_0}\frac{\partial}{\partial z}(\rho_0 w) = 0 \tag{5}$$

Here ϕ is longitude, Ω is the angular velocity of the Earth, a is the radius of the Earth and ρ_0 is a nominal basic state density proportional to exp $(-z/H)$. In (4), N^2 is the square of the buoyancy frequency (a measure of static stability), defined as

$$N^2 \equiv \frac{R}{H}\left(\frac{dT_0}{dz} + \frac{\kappa T_0}{H}\right)$$

where T_0 is a reference temperature profile depending only on z and $\kappa = R/c_p$, where c_p is the specific heat of air at constant pressure. Finally u is the longitudinal component of wind, T is the temperature deviation from T_0, and v and w are respectively the latitudinal and vertical components of velocity.

Equation (2) states that the longitudinal acceleration is equal to the applied force, F (which will for the moment be taken to be a given function of latitude, height and time), plus the Coriolis force associated with the latitudinal velocity. The Coriolis force is the important effect of rotation—the response to an applied force is not simply an equivalent acceleration. Instead, part of the applied force is balanced by a Coriolis force—how much depends on how large a latitudinal velocity is excited. Equation (3) is the thermal wind equation coupling the longitudinal velocity field and the temperature field, which follows from the assumption that the flow is in hydrostatic and geostrophic balance. Equation (4) states that the rate of change of temperature is equal to

the diabatic heating plus the adiabatic heating associated with vertical motion. Here the diabatic heating is represented by the term $-\alpha T$, where α is a constant rate, representing long-wave heating or cooling. Equation (5) is the mass-continuity equation.

Equations (2–5) may be regarded as predictive equations for the unknowns $\partial u/\partial t, \partial T/\partial t$, v and w. They may be combined to give a single equation for one of the unknowns, with a single forcing term containing the force F. In order to simplify the calculations and focus on the phenomena of importance, it is convenient to follow *Garcia* [1987] and assume that the time dependence is purely harmonic. Thus we write $F(\phi, z, t) = \mathrm{Re}\left(\hat{F}(\phi,z)e^{i\omega t}\right)$ and consider the response in the longitudinal velocity u, assumed to be of the form $u(\phi,z,t) = \mathrm{Re}\left(\hat{u}(\phi,z)e^{i\omega t}\right)$. (2–5) can then be transformed to a single equation

$$\frac{1}{\cos\phi}\frac{\partial}{\partial\phi}\left(\frac{1}{\cos\phi}\frac{\partial}{\partial\cos\phi}\left(\frac{\cos\phi}{\sin\phi}\hat{u}\right)\right)+ \frac{1}{\rho_0}\frac{\partial}{\partial z}\left(\rho_0\left(1+\frac{\alpha}{i\omega}\right)\frac{4\Omega^2a^2}{N^2}\frac{\sin\phi}{\cos\phi}\frac{\partial\hat{u}}{\partial z}\right) = \frac{1}{i\omega}\frac{1}{\cos\phi}\frac{\partial}{\partial\phi}\left(\frac{1}{\cos\phi}\frac{\partial}{\partial\cos\phi}\left(\frac{\cos\phi}{\sin\phi}\hat{F}\right)\right) \quad (6)$$

The operator acting on $\hat{u}$ on the left-hand side of the equation is elliptic, consistent with the well-known property of rotating, stratified systems that localized forcing gives rise to a non-local response. For an oscillation with period two years, $\omega \sim 10^{-7}s^{-1}$. The Newtonian cooling rate, α, is, for the lower stratosphere, generally taken to be about 5×10^{-7}, corresponding to a time scale of about 20 days. Hence the factor $1 + \alpha/(i\omega)$ appearing in the second term on the left-hand side may be approximated by $\alpha/(i\omega)$.

A scale analysis of (6) shows that when rotational effects are weak, i.e. when $\sin\phi$ is small, the dominant balance will be between the forcing term and the first term on the left-hand side. This implies that the acceleration is equal to the applied force. More generally the second term on the left-hand side will play a major role in the balance, implying that the Coriolis force must be substantially canceling the applied force in (2). Following *Haynes* [1998], a quantitative comparison of the two terms on the left-hand side of (6) may be performed by assuming a height scale D and a latitudinal scale L for the velocity response. Then, at low latitudes, noting that $\sin\phi$ scales as ϕ and hence as L/a, the ratio of the second term on left-hand side of (6) to the first is $4\Omega^2L^4\alpha/(a^2D^2N^2\omega)$. It follows that if $L \ll (aDN/(2\Omega))^{1/2}(\omega/\alpha)^{1/4}$ then the acceleration is approximately equal to the applied force. This might be called the "tropical response"—it occurs if the latitudinal scale L is small enough. On the other hand if $L \gg (aDN/(2\Omega))^{1/2}(\omega/\alpha)^{1/4}$ then the applied force is largely cancelled by the Coriolis torque and most of the response to the applied force appears as a circulation in the height-latitude plane. This might be called the "extratropical response" (though clearly the scaling would require modification if it were to be applied well away from the equator).

The physical reason for the distinction between the tropical and extratropical responses is the link between velocity and temperature fields in a rotating system, expressed by (3), together with the temperature damping implied by (4). At high latitudes an applied force, varying on sufficiently long time scales, will tend to be cancelled by the Coriolis force due to a circulation in the height-latitude plane. This circulation will induce temperature anomalies, upon which the thermal damping will act, effectively damping the velocity response and limiting its amplitude. At low latitudes, on the other hand, the force will give rise to an acceleration, there will be relatively little temperature response and thermal damping will have little effect on the velocity response. It is as if low-latitude velocities have a longer "memory" than high-latitude velocities; anomalies at low latitudes take longer to dissipate. Thus the QBO mechanism might be expected to work only at low latitudes. The *Lindzen and Holton* (1968) experiments in a 2-D model showed that the Coriolis torque reduced the amplitude of the wind oscillation away from the equator. *Haynes* [1998] went further to suggest that it might be the transition from the tropical regime to the extratropical regime that sets the latitudinal width of the QBO, rather than, for example, the latitudinal scale of the waves that provide the necessary momentum flux. Simulations in a simple numerical model where the momentum forcing is provided by a latitudinally broad field of small-scale gravity waves, designed not to impose any latitudinal scale, predicted a transition scale at about 10 degrees.

To summarize, a long-period oscillation that requires the zonal velocity field to respond directly to a wave-induced forced is likely to work only in the tropics, since elsewhere the force will tend to be balanced by the Coriolis torque due to a meridional circulation. For this reason, 1-D models, which omit Coriolis torques altogether, can capture the tropical oscillation. However, they cannot simulate the latitudinal structure that arises in part from the increase of Coriolis torques with latitude.

3.2. Waves in the tropical lower stratosphere

There exists a broad spectrum of waves in the tropics, and the details of which waves are driving the QBO are not entirely settled. Based on observations of wave amplitudes, we now believe that a combination of Kelvin, Rossby-gravity, inertia-gravity and smaller-scale gravity waves provide most of the momentum flux needed to drive the QBO [*Dunkerton*, 1997]. All these waves originate in the tropical

troposphere and propagate vertically to interact with the QBO. Convection plays a significant role in the generation of tropical waves; modes are formed through lateral propagation, refraction, and reflection within an equatorial waveguide, the horizontal extent of which depends on wave properties (e.g., turning points where wave intrinsic frequency equals the local inertial frequency).

Equatorward propagating waves originating outside the tropics, such as planetary Rossby waves from the winter hemisphere, may have some influence in upper levels of the QBO [*Ortland*, 1997]. The lower region of the QBO (~20–23 km) near the equator is relatively well shielded from the intrusion of extratropical planetary waves [*O'Sullivan*, 1997].

Vertically propagating waves relevant to the QBO are either those with slow vertical group propagation undergoing absorption (due to radiative or mechanical damping) at such a rate that their momentum is deposited at QBO altitudes, or those with fast vertical group propagation up to a critical level lying within the range of QBO windspeeds [*Dunkerton*, 1997]. The height at which momentum is deposited depends on the vertical group velocity (supposing for argument's sake that the damping rate per unit time is independent of wave properties). Waves with very slow group propagation are confined within a few kilometers of the tropopause [*Li et al.*, 1997]. Waves with fast vertical group velocity (and phase speeds lying outside the range of QBO windspeeds) propagate more or less transparently through the QBO.

Long-period waves tend to dominate spectra of horizontal wind and temperature. Higher frequency waves are expected to transport momentum to a greater degree than would be suggested by a comparison of temperature variance alone. We can organize the waves relevant to the QBO into three categories:

(1) Kelvin and Rossby-gravity waves, which are equatorially trapped; periods $\gtrsim$ 3days; wavenumbers 1–4 (zonal wavelengths $\gtrsim$10000 km).

(2) *Inertia-gravity waves*, which may or may not be equatorially trapped; periods of ~1–3 days; wavenumber ~4–40 (zonal wavelengths ~1000–10000 km).

(3) Gravity waves; periods $\lesssim$1 day; wavenumber >40 (zonal wavelengths ~10–1000 km) propagating rapidly in the vertical. (Waves with very short horizontal wavelengths ($\leq$10 km) tend to be trapped vertically at tropospheric levels near the altitude where they are forced, and are not believed to play a significant role in middle atmosphere dynamics.)

The observations reviewed below suggest that intermediate and high-frequency waves help to drive the QBO. However, uncertainties remain in the wave momentum flux spectrum, with regard to actual values of flux and the relative contribution from various parts of the spectrum. Although the momentum flux in mesoscale waves is locally very large, it is necessary to know the spatial and temporal distribution of these waves in order to assess their role in the QBO. Available observations are insufficient for this purpose. For intermediate-scale waves, it is unclear what fraction of the waves are important to the QBO without a more precise estimate of their phase speeds, modal structure, and absorption characteristics. Twice-daily rawinsondes provide an accurate picture of vertical structure but have poor horizontal and temporal coverage. Their description of horizontal structure is inadequate, and temporal aliasing may occur, obscuring the true frequency of the waves.

The QBO, in principle, depends on wave driving from the entire tropical belt, but the observing network can only sample a small fraction of horizontal area and time. Thus it is uncertain how to translate the information from local observations of intermediate and small-scale waves into a useful estimate of QBO wave driving on a global scale. Ultimately satellite observations will provide the needed coverage in space and time. These observations have already proven useful for planetary-scale equatorial waves and small-scale extratropical gravity waves with deep vertical wavelength. Significant improvement in the vertical resolution of satellite instruments and their ability to measure or infer horizontal wind components will be necessary, however, before such observations are quantitatively useful for estimates of momentum flux due to intermediate and small-scale waves in the QBO region.

3.2.1. Kelvin and Rossby-gravity waves

Kelvin and Rossby-gravity waves were detected many years ago, using rawinsonde observational data, by *Yanai and Maruyama* [1966] and *Wallace and Kousky* [1968]; these discoveries were important to the development of a modified theory of the QBO by *Holton and Lindzen* [1972]. For reviews of early equatorial wave observations see *Wallace*, [1973]; *Holton*, [1975], *Cornish and Larsen*, [1985], *Andrews et al.*, [1987], and *Dunkerton*, [1997]. Interpretation of disturbances as equatorial wave modes relies on a comparison of wave parameters (e.g., the relation of horizontal scale and frequency), latitudinal structure (e.g., symmetric or antisymmetric about the equator) and phase relationship between variables (e.g., wind components and temperature) with those predicted by theory. The identification of equatorial modes is relatively easy in regions with good spatial coverage so that coherent propagation may be observed.

Long records of rawinsonde data from high-quality stations have been used to derive seasonal and QBO-related variations of Kelvin and Rossby-gravity wave activity near the equator [*Maruyama*, 1991; *Dunkerton*, 1991b, 1993;

Shiotani and Horinouchi, 1993; *Sato et al.*, 1994; *Wikle et al.*, 1997]. The QBO variation of Kelvin wave activity observed in fluctuations of zonal wind and temperature is consistent with the expected amplification of these waves in descending westerly shear zones. Annual variation of Rossby-gravity wave activity is observed in the lowermost equatorial stratosphere and may help to explain the observed seasonal variation of QBO onsets near 50 hPa [*Dunkerton*, 1990].

Equatorially trapped waves have been observed in temperature and trace constituent data obtained from various satellite instruments. Most of these studies dealt with waves in the upper stratosphere relevant to the stratopause semiannual oscillation; a few, however, also observed waves in the equatorial lower stratosphere relevant to the QBO (e.g., *Salby et al.* [1984]; *Randel* [1990]; *Ziemke and Stanford* [1994]; *Canziani et al.* [1995]; *Kawamoto et al.* [1997]; *Shiotani et al.* [1997]; *Mote et al.* [1998]; *Canziani and Holton* [1998]). It is difficult to detect the weak, shallow temperature signals associated with vertically propagating equatorial waves, and satellite sampling usually recovers only the lowest zonal wavenumbers (e.g. waves 1–6). Nevertheless, satellite observations are valuable for their global view, complementing the irregular sampling of the rawinsonde network.

2-D modeling studies [*Gray and Pyle* [1989], *Dunkerton*, 1991a; 1997] showed that Kelvin and Rossby-gravity waves are insufficient to account for the required vertical flux of momentum to drive the QBO. The required momentum flux is much larger than was previously assumed because the tropical stratospheric air moves upward with the Brewer-Dobson circulation. When realistic equatorial upwelling is simulated in the model, the required total wave flux for a realistic QBO is 2–4 times as large as that of the observed large-scale, long-period Kelvin and Rossby-gravity waves. Recent 3-D simulations (e.g., *Takahashi and Boville* [1992]; *Hayashi and Golder* [1994]; *Takahashi* [1996]) described in Section 3.3.2, confirm the need for additional wave fluxes. Therefore it is necessary to understand better from observations the morphology of inertia-gravity and gravity waves and their possible role in the QBO.

3.2.2. Inertia-gravity waves

Eastward propagating equatorial inertia-gravity waves are seen in westerly shear phases of the QBO, while westward propagating waves are seen in easterly shear phases. Observational campaigns using rawinsondes have provided data with high temporal and vertical resolution, so that analysis is possible both for temporal and vertical phase variations.

Cadet and Teitelbaum [1979] conducted a pioneering study on inertia-gravity waves in the equatorial region, analyzing 3-hourly rawinsonde data at 8.5°N, 23.5°W during GATE (Global Atmospheric Research Project Atlantic Tropical Experiment). The QBO was in an easterly shear phase. They detected short vertical wavelength (<1.5 km) inertia-gravity wave-like structure having a period of 30–40 hours. The zonal phase velocity was estimated to be westward.

Tsuda et al. [1994a,b] conducted an observational campaign focusing on waves in the lower stratosphere at Watukosek, Indonesia (7.6°S, 112.7°E) for 24 days in February to March 1990 when the QBO was in a westerly shear phase. Wind and temperature data were obtained with a temporal interval of 6 hours and vertical resolution of 150 m. Figure 11 shows a time and height section of temperature fluctuations with periods shorter than 4 days. Clear downward phase propagation is observed in the lower stratosphere (above about 16 km altitude). The vertical wavelength is about 3 km and wave period is about 2 days. Similar wave structure was seen also for zonal (u) and meridional wind (v) fluctuations. The amplitudes of horizontal wind and temperature fluctuations were about 3 ms^{-1} and 2K, respectively.

Based on hodographic analysis assuming that these fluctuations are due to plane inertia-gravity waves, *Tsuda et al.* [1994b] showed that most waves propagated energy eastward and upward in the lower stratosphere. Similar characteristics are observed in their second campaign in Bandung, Indonesia (107.6°E, 6.9°S) during another eastward shear phase of the QBO (November 1992 to April 1993) [*Shimizu et al.*, 1997].

Statistical studies of equatorial inertia-gravity waves have been made using operational rawinsonde data at Singapore (1.4°N, 104.0°E). *Maruyama* [1994] and *Sato et al.* [1994] analyzed the year-to-year variation of 1–3 day wave activity in the lower stratosphere using data from Singapore spanning ten years. Extraction of waves by their periods has merit since the ground-based wave frequency is invariant during the wave propagation in a steady background field. The QBO can be considered sufficiently steady for these purposes for inertia-gravity waves having periods shorter than several days.

Maruyama analyzed the covariance of zonal wind and the time derivative of temperature for 1–3 day components and estimated the vertical flux of zonal momentum per unit density $\overline{u'w'}$ using the following relation derived from the thermodynamic equation for adiabatic motions:

$$\overline{\frac{\partial T'}{\partial t}u'} = -\left[\frac{\overline{T}N^2}{g}\right]\frac{c}{\hat{c}}\overline{u'w'}, \qquad (7)$$

where T is temperature, t is time, u and w are the zonal and vertical components of wind velocity, c the ground-based horizontal phase speed ($\hat{c}$ =c−$\overline{u}$) the intrinsic horizontal phase speed, $\overline{u}$ the background wind speed, and the overbar indicates a time average. Since $\hat{c}$ is not obtained from the observational data, this estimate is possible only when $\overline{u}$ is small enough to assume $\hat{c}/c \sim 1$. Maruyama showed that the

momentum flux $\overline{u'w'}$ is largely positive and that the magnitude is comparable to that of Kelvin waves in the westerly shear phase of the QBO.

Sato et al. [1994] examined interannual variation of the power and cross spectra of horizontal wind and temperature fluctuations in the period range of 1–20 days at Singapore. They found that spectral amplitudes are maximized around the tropopause for all components in the whole frequency band, although the altitudes of the tropopause maxima are slightly different. The T and u spectra are maximized around 10-day period, corresponding to Kelvin waves. In the lower stratosphere, the wave period shortens, e.g., 9 days at 20 km to 6 days at 30 km. On the other hand, v spectra are maximized around 5 days slightly below the tropopause corresponding to Rossby-gravity waves. The Rossby-gravity wave period also becomes shorter with increasing altitude in the lower stratosphere, consistent with the analysis of *Dunkerton* [1993] based on rawinsonde data at several locations over the tropical Pacific. An important fact is that spectral amplitudes are as large at periods shorter than 2–3 days as for long-period Kelvin waves and Rossby-gravity waves.

The activity of inertia-gravity and Kelvin waves is observed to be synchronized with the QBO. Figure 12 shows power and cross spectra as a function of time averaged over the height region 20–25 km in the lower stratosphere. A lowpass filter with cutoff of 6 months was applied in order to display the relation with the QBO more clearly. Dominant peaks in the power spectra of T and u are observed in the 1–3 day period range during both phases of the QBO and around 10-day period in the westerly shear phase of the QBO. The latter peak corresponds to Kelvin waves.

The quadrature spectra $Q_{Tu}(\omega)$ correspond to the covariance of zonal wind and time derivative of temperature. Thus large negative values observed around 10-day period in the westerly shear phase show the positive $\overline{u'w'}$ associated with Kelvin waves [*Maruyama,* 1991, 1994]. Such tendency is not clear at shorter periods in the quadrature spectra. Clear synchronization with the QBO is seen in the cospectra $C_{Tu}(\omega)$ in the whole range of frequencies. Positive and negative values appear alternately in the westerly and easterly shear phases, respectively, though the negative values are weak around 10-day period. This feature cannot be explained by the classical theory of equatorial waves in a uniform background wind [*Matsuno*, 1966], which predicts that the covariance of T and u should be essentially zero.

Dunkerton [1995] analyzed theoretically and numerically the covariance of T and u for 2-D (plane) inertia-gravity waves in a background wind having vertical shear, and derived the following relation

$$\overline{T'u'} = \left[\frac{\bar{T}N}{2gk|\hat{c}|}\right]\bar{u}_z\left|\overline{u'w'}\right|, \qquad (8)$$

for slowly varying, steady, conservative, incompressible waves. This theory was extended to 3-D equatorially trapped waves [*Dunkerton,* 1998]. According to (8), the covariance is proportional to the vertical shear and vertical flux of horizontal momentum, or radiation stress. The sign of the covariance is determined by the vertical shear, independent of the horizontal and vertical direction of inertia-gravity wave propagation. This is qualitatively consistent with the observation in Figure 12c.

Sato and Dunkerton [1997] estimated momentum fluxes associated with 1–3 day period waves directly and indirectly based on the quadrature and cospectra of T and u components at Singapore obtained by *Sato et al.,* [1994]. Unlike Kelvin waves which propagate only eastward, inertia-gravity waves can propagate both eastward and westward. Thus the net momentum flux estimate from quadrature spectra as obtained by *Maruyama* [1994] may be a residual after cancellation between positive and negative values. On the other hand, cospectra correspond to the sum of absolute values of positive and negative momentum fluxes. Using an indirect estimate of momentum fluxes from cospectra and a direct one from quadrature spectra, positive and negative parts of momentum fluxes can be obtained separately.

The direct estimate for Kelvin waves (5–20 day period) is $2-9\times10^{-3}m^2s^{-2}$ and accords with the indirect estimate within the estimation error, supporting the validity of the indirect method. The result for 1–3 day periods is shown in Figure 13, assuming plane inertia-gravity waves. The indirect estimate of 1–3 day period components for westerly shear is $20-60\times10^{-3}m^2s^{-2}$, while the direct estimate is only $0-4\times10^{-3}m^2s^{-2}$. For easterly shear, the indirect estimate is $10-30\times10^{-3}m^2s^{-2}$, while the direct estimate is almost zero. The discrepancy between the indirect and direct estimates indicates a large cancellation between positive and negative momentum fluxes.

There is ambiguity in the indirect estimate according to the assumed wave structure. If equatorially trapped modes are assumed, the values should be reduced by 30–70%. On the other hand, if there is aliasing from higher frequency waves (wave periods shorter than 1 day for twice-daily data such as rawinsonde data at Singapore), the actual momentum flux should be much larger than shown in Figure 13. Even considering these ambiguities, it appears that intermediate-frequency period gravity or inertia-gravity waves have significant momentum flux compared to Kelvin and Rossby-gravity waves.

Bergman and Salby [1994] calculated equatorial wave activity propagating into the stratosphere based on high-resolution imagery of the global convective pattern and some simple assumptions about the relation of cloud variations to the properties of the waves that would be generated. Figure 14 shows the geographical distribution of the vertical component of *Eliassen-Palm flux* that they derived. The components with periods shorter than 2 days have large

Eliassen-Palm flux, compared with longer period waves. The short-period wave generation is large over the African and American continents and in a broad area from the Indian Ocean to western tropical Pacific.

The analysis of Bergman and Salby does not provide a quantitative estimate of actual wave fluxes, but supports the idea that intermediate and small-scale waves contribute significantly to the QBO. From their analysis we note, first, that the contribution is large relative to that of planetary-scale equatorial waves, by a factor of about 2.5, and second, that most of the activity in smaller-scale waves is associated with zonal phase speeds lying in the range of QBO wind-speeds [*Dunkerton,* 1997].

The excitation of inertia-gravity waves by deep tropical convection occurs either through a process of self-organization, in which waves and convection support one another, or (more simply) as a result of irregular, seemingly random activity as convective elements impinge on a stratified layer above. The self-organization of waves and convection occurs mainly on longer horizontal and temporal scales as illustrated (e.g., *Takayabu et al* [1996], *Wada et al* [1999], and *Wheeler and Kiladis* [1999]).

3.2.3. Gravity waves

Deep convection is also a dominant source for high-frequency gravity waves near the equator. Numerical simulations of convection that include stratospheric altitudes [*Fovell et al.,* 1992; *Alexander et al.,* 1995; *Alexander and Holton,* 1997] generate high-frequency gravity waves that appear prominently above storm clouds (Figure 15). Theory predicts a close association of high-frequency waves in the lower stratosphere and the storms that generate them because the energy propagation direction is most vertically oriented for the highest frequency waves,

$$\hat{\omega} = N \cos \theta \qquad (9)$$

where θ is the angle between the vertical and the lines of constant phase or direction of the group velocity vector. In these simulations, the high-frequency waves carry significant momentum flux suggesting they could play a prominent role in driving the QBO [*Alexander and Holton,* 1997].

Observational studies have identified large-amplitude, high-frequency gravity waves in the stratosphere directly above deep tropospheric convection [*Rottger,* 1980; *Larsen et al.,* 1982; *Sato,* 1992, 1993; *Sato et al.,* 1995]. *Sato* [1993] was able to estimate the vertical momentum flux carried by the waves. These midlatitude observations found significant values of 0.03 Pa, an order of magnitude larger than the estimated time-average, zonal mean flux needed for tropical gravity waves to be important to the QBO [*Dunkerton,* 1997]. Note that momentum flux is properly measured in units of Pascal (Pa), equal to air density times the product of velocity components. In most QBO literature the density term is ignored, and the resulting "flux" is described in units of m^2s^{-2}. Near the tropical tropopause the density is about 0.1 in MKS units, providing an easy conversion between the two definitions of flux.

High-frequency gravity waves have also been detected in aircraft observations in the lower stratosphere. NASA's ER-2 aircraft flies at altitudes up to ~20 km and has participated in numerous campaigns that included tropical flights in the stratosphere. Observations of winds and temperatures onboard have been used to detect gravity waves. Pfister et al. [1986, 1993a,b] detected short horizontal wavelength waves < 150 km in temperature and horizontal wind fields associated with cumulus convection over Panama and Northern Australia. *Pfister et al.* [1993a,b] proposed a "convective topography" mechanism for generating these waves and used a model to estimate the vertical momentum flux that could be generated by this mechanism and the impact such waves might have on the QBO momentum budget. The calculated effect was small (< 10%) compared to estimates of planetary-scale wave driving. Other forcing mechanisms may be active, however, and the effects of high-frequency waves would be under-represented in these calculations [*Dunkerton,* 1997]. The estimates are also uncertain because of unknown geographical distribution and occurrence frequency of convectively-forced gravity waves based on only a few case studies.

Alexander and Pfister [1995] used observations of both the horizontal and vertical winds together to estimate momentum flux along an ER-2 flight path over deep convection north of Australia. The momentum flux emphasizes shorter-period waves. Very large values ~ 0.1 Pa were observed over the deepest highest clouds. More extensive correlations of these data with cloud top temperature were reported by *Alexander et al.* [1999] and are shown in Figure 16. These results suggested that large values of momentum flux are correlated with deep convection and have similar magnitudes to waves generated in 2-D simulations of tropical convection [*Alexander and Holton,* 1997]. While the geographical and seasonal distributions of such fluxes are uncertain, the results nonetheless suggest a potentially important role for high-frequency gravity waves in the QBO.

The gravity waves observed in the low-latitude (~12°S) rawinsonde analyses described by *Allen and Vincent* [1995] showed a seasonal cycle suggesting convection as an important source during the December–February monsoon season. These results represented only one year of observations; however, subsequent analysis of data from Cocos Island, also at ~12°S spanning 6 years, showed a similar correlation with the monsoon season, but it is modulated by QBO winds [*Vincent and Alexander,* 1999]. The months with peak momentum flux were found to coincide with the strongest easterly winds. At these times the waves also propagate predominantly eastward. Parallel theoretical calculations of gravity wave propagation and interaction with the background flow qualitatively support the convective topography mechanism because of the anisotropy observed in wave propagation direction, and because the altitude where the

waves are generated was inferred to be very high, close to the tropopause. *Karoly et al.* [1996] also observed a correlation between inertia-gravity wave activity and deep convection in tropical sounding data.

3.3. Numerical models of the QBO

3.3.1. One-dimensional models

1-D models, in which wind and wave fields are functions of height only have been used to explore many aspects of QBO behavior relevant in the real atmosphere. Sometimes the one-dimensionality may be justified, as in *Holton and Lindzen* [1972], by integrating the dynamical equations in latitude to derive evolution equations for the zonal flow integrated across the tropics. This approach may be acceptable for Kelvin waves, which are known to depend primarily on the near-equatorial wind and which generate a simple profile of the mean-flow forcing. Other equatorial waves, however, are significantly affected by latitudinal shear and produce more complicated latitudinal profiles of mean-flow forcing [*Andrews and McIntyre*, 1976; *Boyd*, 1978; *Dunkerton*, 1983a]. High-frequency gravity waves propagate mostly vertically, and their interaction with the mean flow is more easily described in a 1D model. For these waves the latitudinal dependence of sources is important, however, owing to the seasonally varying distribution of tropical convection [*Allen and Vincent*, 1995]. For these and other reasons the utility of 1-D models is limited and their value lies in their simplicity rather than their realism. *Plumb* [1977] (discussed in Section 3.1) included non-rotating gravity waves in order to demonstrate a number of basic properties of QBO behavior.

1-D models have been used to investigate several aspects of QBO wave forcing, including the effect of scale-dependent radiative damping of the waves *Hamilton* [1981], effects of laterally propagating Rossby waves *Dunkerton* [1983b], the effect of self-acceleration of wave phase speed and of wave saturation [*Tanaka and Yoshizawa*, 1987], upwelling of the tropical Hadley circulation [*Saravanan*, 1990]. Interannual variations of forcing, as might be due to ENSO may cause long-term variations of QBO period by *Geller et al.* [1997]. 1-D models are also useful for interpreting the results of 2-D models [e.g., *Dunkerton* 1997].

3.3.2. Two-dimensional Models

Many important aspects of the QBO behavior can be considered only using models that represent latitude as well as height variation. This applies self-evidently to questions concerning latitudinal structure, but also to wider questions concerning the interaction of the QBO with the annual cycle and the effect of the QBO on tracer distributions (to be discussed in more detail in Section 5).

The first detailed 2-D model analysis of the latitudinal structure, including the circulation in the latitude-height plane (the meridional circulation), was that by *Plumb and Bell* [1982b], who assumed that the wave momentum fluxes were due to equatorial Kelvin waves and mixed Rossby-gravity waves. For the wind field at any instant they calculated the height-latitude structure of the waves on the basis of a linear, steady-state calculation [*Plumb and Bell*, 1982a]. These momentum and heat fluxes were used to force the longitudinally symmetric dynamical equations including thermal damping through a Newtonian cooling term, with the structure of the waves being recalculated at each time step. Their attempt to simulate the QBO in this manner was broadly successful, except that they were limited to cases where the amplitude of the oscillation was only about half of that observed. *Dunkerton* [1985] and *Takahashi* [1987] used different strategies for calculating the wave momentum fluxes and succeeded in simulating oscillations of realistic amplitude. The 2-D models showed explicitly that the QBO meridional circulation was in the sense of sinking at the equator in westerly shear zones and rising at the equator in easterly shear zones. In westerly shear zones the thermal wind equation (2) implies a maximum in temperature at the equator which is maintained against thermal damping by adiabatic heating due to sinking motion. The opposite holds in easterly shear zones. The pattern of shear zones and meridional circulations is shown schematically in Figure 17.

The models mentioned above were focused on the equatorial regions and did not include a realistic seasonal cycle in winds or temperatures. A realistic QBO was achieved by *Gray and Pyle* [1989] in a full radiative-dynamical model (which therefore had a realistic seasonal cycle) only by increasing their parameterized wave momentum forcing by a factor of three larger than could be justified by Kelvin and Rossby-gravity waves alone. This additional forcing was required in order that the QBO wind regimes would propagate downward despite climatological upwelling in the tropics [*Dunkerton*, 1997]. This was additional evidence of the requirement for forcing from waves other than Kelvin and Rossby-gravity waves. *Mengel et al.* [1995] obtained a QBO-like oscillation in a 2-D middle atmosphere model in which eddy momentum transport was due solely to the *Hines* [1997] gravity wave parameterization. Although the QBO simulated in this model was weak and sensitive to vertical diffusion, the parameterization's striking ability to reproduce the entire phase structure of observational equatorial oscillations [*Burrage et al.*, 1996] emphasizes the importance of gravity waves that have a wide range of phase speeds and whose amplitude grows with height.

The 2-D simulations by *Gray and Pyle* [1989] demonstrated that the influence of the QBO extends to all latitudes. For example, the QBO circulation with rising or sinking at the equator is compensated by an opposing circulation off the equator, which gives rise to a temperature anomaly in the subtropics and midlatitudes of opposite sign to that at the equator (see also *Plumb and Bell* [1982b] and *Dunkerton* [1985].) A significant interhemispheric asymmetry in the

timing and amplitude of the subtropical anomalies was also present, due to the interaction of the QBO with the seasonal cycle [*Gray and Dunkerton*, 1990]. The QBO-induced meridional velocity in the winter hemisphere and, correspondingly, the vertical velocity in the subtropics winter hemisphere are substantially larger than those in the summer hemisphere, particularly above ~25 km [*Jones et al.*, 1998; *Kinnersley*, 1998], probably due in part to the asymmetric subtropical angular momentum gradients under solstice conditions.

The meridional circulation affects chemical tracers such as ozone and gives rise to strong QBO signals in such tracers at all latitudes, with significant interhemispheric asymmetry (see Section 5). However, there may also be a significant feedback of the ozone QBO on the dynamics of the QBO, since changes in ozone have radiative implications and, in particular, have a direct effect on short-wave heating. The effect of including the coupling between QBO ozone anomalies and heating rates tends to reduce the heating rate that would otherwise be calculated from a given temperature anomaly in the lower stratosphere [*Hasebe*, 1994, *Li et al.*, 1995, *Kinnersley and Pawson*, 1996, and *Randel et al.*, 1999]. *Hasebe* [1994] argued that this effect must be taken into account in order to explain the observed phase relation in the lower stratosphere between the QBO signals in ozone and wind. In the upper stratosphere the ozone heating enhances the QBO vertical velocity.

Plumb and Bell [1982b] noted that the advective effects of the meridional circulation can account for the observed asymmetry in the descent of easterlies and westerlies (without any need for asymmetry in the waves providing easterly and westerly momentum fluxes). Downward advection of momentum associated with the westerly shear zone enhances the descent of the westerlies, while the upward advection of momentum associated with the easterly winds inhibits the descent of the westerlies. An additional advective effect, since the vertical velocities are maximal near the equator, is to narrow the region of strongest westerly acceleration and to broaden that of strongest easterly acceleration [*Hamilton*, 1984, *Dunkerton and Delisi*, 1985, *Dunkerton*, 1985, *Takahashi*, 1987; *Dunkerton*, 1991].

3.3.3. Three-dimensional models (including mechanistic and GCMs)

In the 1-D and 2-D models discussed above, the waves that contribute to the driving of the QBO must be parameterized. 3-D models offer the possibility of explicit simulation of the waves, without any need for simplifying assumptions that allow parameterization. In "mechanistic" models waves are artificially forced (e.g. by imposed heating fields or imposed lower boundary perturbations). One particular issue where mechanistic models have given important insight concerns whether the easterly momentum forcing needed to account for the equatorial QBO can be supplied by Rossby-gravity waves. A 3-D mechanistic model simulation by *Takahashi and Boville* [1992] in which a Kelvin wave and a Rossby-gravity wave were forced at the lower boundary, gave a good representation of the QBO in the lower stratosphere. However, the amplitudes of the Kelvin wave and, particularly, the Rossby-gravity wave were considerably stronger than the observed values. This added to the evidence that a much broader spectrum of waves was needed.

In general circulation models (GCMs) the waves are generated spontaneously in the model (although that is not to say that the generation processes are necessarily realistic). For various reasons the ability to simulate a realistic QBO is seen as a stringent requirement on a GCM. Firstly, the large apparent contribution of the QBO to interannual variability in the entire middle atmosphere, not just low latitudes (see Section 4) means that, ultimately, if a GCM that includes the middle atmosphere is to be regarded as realistic then it must represent the QBO. Secondly, since the QBO is believed to be partially driven by waves excited by cumulus convection (on a whole range of scales), the ability or inability of a model to simulate the QBO might also have implications for the realism of the simulated tropical tropospheric circulation

The QBO was not simulated in GCMs even if the Kelvin and Rossby-gravity waves had realistic amplitudes (CCM2: *Boville and Randel* [1992]; SKYHI: *Hayashi and Golder* [1994]). Until relatively recently no GCM had successfully simulated the QBO, or an analogous long-period wave-diven oscillation (the term "QBO-like" is used). It appears that simulation of the subtle QBO mechanism puts demanding requirements on a GCM. Here we present an overview of the successful simulations and discuss the main features upon which a successful simulation depends.

The first realistic simulation of the QBO in a GCM was made by *Takahashi* [1996]. He used the CCSR/NIES GCM with horizontal resolution of T21 (triangular truncation at total wavenumber 21, equivalent to a grid spacing of about 600 km, or 5° of latitude) and with a vertical grid spacing of 500 m in the stratosphere. This was an unprecedentedly fine vertical resolution which allowed waves with small vertical wavelengths to propagate vertically and interact with the mean flow; most previous GCMs had a vertical grid spacing of 2 km or more in the stratosphere.

All GCMs, for numerical reasons, include some kind of horizontal diffusion or its equivalent. In this case, to obtain a QBO it was necessary also to reduce the coefficient of the fourth order horizontal diffusion by one order of magnitude from its standard value. The model then produced a QBO-like oscillation with a period of 1.5 years. Other simulations have been made by *Horinouchi and Yoden* [1998] (aqua-planet GCM, period 1.1 years), *Hamilton et al.* [1999] (SKYHI, period 1 year), and *Untch* [1998] (ECMWF, realistic period). Figure 18 shows the most realistic simulation to date [*Takahashi*, 1999], with a period of 2.3 years, using a

horizontal resolution to T42. The horizontal diffusion coefficient had to be reduced by a factor of four from its standard value.

Although several GCMs have produced simulations of the QBO, there is no simple set of criteria that will guarantee a successful simulation. Further, attempts to produce more realistic simulations are difficult (as well as time consuming) because the simulations depend on the subtle interaction of several factors. The simulation of a QBO in a GCM requires fine vertical resolution in the stratosphere, a small diffusion coefficient, moderate to high horizontal resolution, and a convection scheme that generates sufficient waves to drive the QBO.

The vertical grid spacing in the stratosphere must be sufficient to resolve the waves and their interaction with the mean flow. The values used in simulations of the QBO range from 700 m [*Horinouchi et al.*, 1996] to 1500 m [*Untch*, 1998]. Fine horizontal resolution is usually not required. The *Horinouchi et al.* [1996] simulation used a horizontal resolution of only T21. In a T63 simulation, *Untch* [1998] found that a QBO developed, but then disappeared due to a long-term westerly drift in the upper stratosphere. The drift was eliminated and the QBO persisted in T159 simulation. *Hamilton et al.* [1999] found that a horizontal resolution of $2° \times 2.4°$ was needed.

The development of an oscillation of the zonal averaged flow can be prevented by the diffusion that smoothes the meridional structure. All the QBO simulations have diffusion time scales longer than the period of the simulated QBO-like oscillation. Waves propagating upward into the stratosphere are also damped by the diffusion. *Takahashi* [1996] showed that a decrease in the diffusion coefficient increased the power of waves in the stratosphere while having little effect on the troposphere.

As in the real atmosphere, it appears that a broad spectrum of waves supplies the necessary forcing in these simulations. However, For example, *Takahashi et al.* [1997] suggested that the easterly acceleration of the model's QBO was due to gravity waves as well as Rossby waves from the NH winter and Rossby-gravity waves, while westerly acceleration was due to Kelvin and gravity waves. In contrast, in the *Takahashi* [1999] model gravity waves were the dominant forcing for the QBO.

Horinouchi and Yoden [1998] also did a thorough wave analysis. The frequency distribution of the momentum flux and its magnitude were roughly consistent with the observational estimates of *Sato and Dunkerton* [1997] for Singapore (see Section 3.2). In particular, the Kelvin and Rossby-gravity waves played a small role.

The tropospheric source of the waves, which is dominated by latent heat release due to cumulus convection, is a crucial characteristic. Since most GCMs roughly reproduce the climatological mean precipitation, the low-frequency components of the latent heating will be similar. However, transient characteristics of cumulus convection, which are important for the wave excitation, differ greatly among models.

All of the QBO simulations employed the moist convective adjustment scheme except for the model of *Untch* [1998], which used the *Tiedtke* [1989] scheme. The moist convective adjustment scheme tends to produce intermittent grid-scale cumulus convection. The *Takahashi et al.* [1996] T21 model also produced a QBO-like oscillation when the scheme was replaced by the prognostic Arakawa–Schubert scheme [*Nagashima et al.*, 1998], which also tends to produce highly transient grid-scale heating pulses. However, some cumulus parameterizations produce little transient cumulus convection. For example, convection due to the *Zhang and McFarlane* [1995] scheme in the NCAR CCM3 (which has not successfully simulated the QBO) results in a momentum flux to the stratosphere that is quite weak, even though the time-averaged precipitation is very realistic.

A final factor that may affect the ability of a GCM to simulate a QBO is the Brewer–Dobson circulation tropical upwelling. As noted in Section 3.3.1, strong upwelling tends to slow the descent of the QBO. The upwelling in the *Takahashi* [1999] model, which had a realistic period, was a little weaker than the observational estimates of *Mote et al.* [1996]. The *Takahashi* [1997] and *Horinouchi and Yoden* [1998] models, which had shorter periods, had unrealistically weak upwelling. It is possible that in some models unrealistically strong upwelling may prevent the simulation of a QBO.

The most important factor in reproducing the QBO is probably the use of a fine vertical resolution to resolve equatorial gravity waves. The horizontal diffusion should be weak enough not to prevent the evolution of the mean flow oscillation and not to be the primary damping mechanism for the waves. Transient characteristics of tropical cumulus convection are also important since they determine the excitation of the waves. Despite the recent success, those models that reproduced the QBO might have overly active cumulus convection and hence large amplitude of gravity waves with resolved scales. Thus, a parameterization of subgrid-scale gravity waves due to convection might be necessary to produce the QBO with the same waves that drive it in the real atmosphere.

4. DYNAMICAL EFFECTS IN THE EXTRATROPICAL STRATOSPHERE

Any connection between the equatorial QBO and the extratropical atmosphere must be viewed in the context of the seasonal cycle and variability of the extratropical stratosphere. The zonal-mean circulation in the stratosphere undergoes a much stronger seasonal cycle than the troposphere, with an actual reversal of winds in the extratropical

stratosphere. During the winter season the high-latitude stratosphere cools, forming a deep, strong vortex. The strong westerlies are replaced by easterlies with increasing solar heating in the spring and summer.

In both hemispheres the smoothly varying seasonal cycle described above is modified by the effects of planetary-scale waves (herein, simply planetary waves), which are forced largely by land-sea contrasts and surface topography. These waves propagate vertically and meridionally into the winter stratosphere (Figure 5), but are strongly trapped in the mean easterly winds of the summer hemisphere [*Charney and Drazin*, 1961].

The NH has much greater land-sea contrast and larger mountain ranges than the SH, resulting in larger amplitude tropospheric planetary waves. Consequently, the northern winter stratosphere tends to be much more disturbed by planetary waves than the southern stratosphere. Large amplitude waves can rapidly disrupt the northern polar vortex, even in midwinter, replacing eastward winds with westward winds and causing the polar stratosphere to dramatically warm. Such events are called major stratospheric warmings. The transition from westerlies to easterlies in the springtime usually occurs in conjunction with a planetary wave event, and is called the final warming. In the NH, the timing of the final warming is highly variable, and tends to occur during March or April. In the SH the final warming occurs in November–December, with much less interannual variability [*Waugh and Randel*, 1999].

In the NH, the planetary wave amplitudes are just large enough for midwinter sudden warmings to occur during some years but not others. Thus, the northern stratosphere is sensitive to the effects of vertically propagating planetary waves, resulting in large interannual variability in the strength of the polar vortex. It appears that this sensitivity to the upward and equatorward propagation of planetary waves allows the equatorial QBO to influence the polar stratosphere by modulating the flux of wave activity (EP flux) [*Dunkerton and Baldwin*, 1991].

The definitive identification of an extratropical QBO signal has been difficult due to the shortness and limited spatial coverage of data sets. In the NH data up to 10 hPa appear to be reliable beginning in the 1950s. Above the 10-hPa level, and in the SH lower stratosphere, the lack of rawinsonde coverage has limited the production of reliable gridded data to the period beginning in the late 1970s, when satellite temperature retrievals began. Most of the literature on the extratropical influence of the QBO has focused on the NH simply because the data record is longer and more reliable. Part of the difficulty in identifying a NH QBO signal is that the QBO accounts for only a fraction of the variance. In addition to the variability of tropospheric forcing, other signals, such as the 11-year solar cycle, volcanoes, and sea surface temperature anomalies appear to influence the variability of the extratropical stratosphere.

Holton and Tan [1980, 1982] presented strong empirical evidence that the QBO influences the extratropical northern stratosphere by using gridded data for 16 NH winters (1962–1977) to form easterly and westerly phase composites of 50 hPa geopotential. They showed that geopotential height at high latitudes is significantly lower during the westerly phase of the QBO. They also found a statistically significant modulation of the springtime zonal wind in the SH. *Naito and Hirota* [1997] found a robust QBO signal during November–December, but a strong relation to the 11-year solar cycle during January–February, suggesting that solar influence modifies the signal during late winter.

4.1. Mechanism for Extratropical Influence

The modulation of the polar vortex by the QBO (now called the Holton-Tan effect) is relatively easy to understand, at least in general terms. Typically, the dominant direction of wave activity propagation for tropospheric planetary waves is upward and equatorward, and vertical propagation is limited to the waves with the largest spatial scales (primarily waves 1 and 2) [*Charney and Drazin*, 1961]. In the high-latitude stratosphere, these waves distort the vortex from zonal symmetry, and if the amplitudes are large enough, the vortex can be displaced from the pole or disrupted so that easterlies replace westerlies near the pole. Concomitant with large wave amplitudes is the "*breaking*" of planetary waves [*McIntyre and Palmer*, 1983, 1984] leading to the erosion of the vortex and weaker westerly winds.

The state of the zonal-mean circulation in the NH winter stratosphere depends on the degree to which planetary waves affect the polar vortex. In the NH wave amplitudes are large enough that the time-mean vortex is much smaller than it would be in the absence of the waves. By contrast, in the SH, wave amplitudes are much smaller (because both land-sea contrasts and topography are smaller) and the wintertime climatological zonal winds are approximately twice those in the NH. The vertical and meridional propagation of planetary waves depends on the latitude-height structure of the zonal-mean wind, which may be thought of as refracting the waves as they propagate out of the troposphere. Quasi-stationary waves cannot propagate in easterly winds, and the phase of the QBO (in the tropics and subtropics) alters the effective *wave guide* and position of the boundary between easterly and westerly zonal-mean winds (the critical line).

If the mean flow in the tropical stratosphere is westerly, planetary waves are able to penetrate into the tropics and even across the equator without encountering a critical line. By contrast, when the mean flow in the tropical stratosphere is easterly, planetary waves encounter a critical line on the winter side of the equator. Thus, when there are easterly winds in the tropics, the effective wave guide for planetary wave propagation is narrower and the wave activity at mid and high latitudes of the winter hemisphere is stronger. Stronger planetary waves in high latitudes lead to greater

wave-induced drag on the mean flow, reduced westerly winds, and hence a warmer winter stratospheric pole.

4.2. Observations of Extratropical Influence

The effect of the QBO on the strength of the northern winter stratospheric vortex may be seen by comparing composites of extratropical zonal-mean wind made during easterly and westerly phases of the QBO. The QBO phase must be defined precisely, and typically the equatorial mean zonal wind at a particular level is used. *Holton and Tan* [1980] defined the QBO phase using equatorial winds at the 50 hPa level, but other authors have used 45, 40, and 30 hPa. The motivation for picking a particular wind level is to optimize the extratropical signal. In the following figures, the QBO phase was defined [*Wallace et al.*, 1993; *Baldwin and Dunkerton*, 1998a], by using the first two empirical orthogonal functions (EOFs) of the vertical variations of equatorial winds. The QBO definition was adjusted to optimize the extratropical signal in either the NH or SH. The resulting definition of the QBO phase is very similar to the 40 hPa equatorial wind for the NH composites and the 25 hPa wind for the SH composites.

Figure 19 illustrates the difference in zonal mean wind between easterly and westerly QBO composites, using *NCEP* analyses for the period 1978–1996. The difference is formed by calculating separate averages of the January wind data when the QBO is at 40 hPa easterly and westerly, and then taking the difference between these averages. The zonal winds were derived from the geopotential fields using the balance method [*Robinson*, 1986; *Hitchman et al.*, 1987; *Randel*, 1987]. Although this method works well in the extratropics, it is not possible to derive accurate winds in the tropics, where winds have been interpolated between 10°N and 10°S, making the QBO too weak. The northern signal is dominated by a modulation of the polar vortex which extends from the surface to the 1 hPa level. Differences are of the opposite sign south of ~40°N and blend into the upper branch of the tropical QBO.

The features in Figure 19 are not confined to the middle stratospheric levels where the equatorial QBO is defined. Rather, the most prominent features are found above 10 hPa. Correlation analysis of zonal-mean wind in the latitude-height plane [*Baldwin and Dunkerton*, 1991] suggests that the upper level features, including those in the SH near 30°S, represent modulation of the diabatic circulation by the QBO. It is reasonable to suppose that this circulation is weakly modulated by the Holton-Tan oscillation. For example, during the easterly phase of the QBO, polar temperatures are relatively high, implying a stronger cross-equatorial flow and a weak westerly anomaly near 30°S. The feature near 30°S may be interpreted not only as a direct effect of the QBO, but a remote effect of the Holton-Tan wave driving communicated by the mean meridional circulation. This behavior is also seen in numerical models (see Section 4.3).

The statistical significance of the NH winter QBO signal has been addressed by several authors, and was treated in detail by *Baldwin and O'Sullivan* [1995]. The details of such an analysis (definition of the QBO, selection of winter months, level of data) are critical to the outcome of statistical tests. For example, the effect of the QBO is observed to be large in December and January, but weaker in February. Using 1964–1993 NCEP data for DJF at levels up to 10 hPa, they showed that the effect of the QBO (defined by the 40-hPa Singapore wind) is statistically significant at the 0.001 level using 10 hPa geopotential, as measured by the field significance test of *Barnston and Livezey* [1987]. In zonal-mean wind composites the statistical significance of the effect of the QBO increases with height, at least through 10 hPa, with much higher significance at 10 hPa than at 30 hPa.

The NH dipole pattern illustrated in Figure 19 is not unique to the influence of the QBO – it represents the leading mode of variability of the northern winter stratosphere [*Nigam*, 1990; *Dunkerton and Baldwin*, 1992]. During winter, the QBO appears to excite the "northern annular mode (*NAM*; also called the Arctic Oscillation) [*Thompson and Wallace*, 1998, 1999; *Baldwin and Dunkerton*, 1999]. NH QBO composites (of geopotential, wind, temperature, etc.) tend to reflect the degree to which the QBO excites the NAM. One phase of the NAM is represented by a cold, strong vortex, while the opposite phase is represented by a weaker vortex and higher polar temperatures. The dipole in Figure 19 is much more prominent in the stratosphere, and weaker in the troposphere. The connection to the stratosphere is limited to the winter season, but the tropospheric NAM is observed during all seasons. The tropospheric aspects of the NAM, and the tropospheric patterns associated with the QBO will be discussed in Section 6.2.

Figure 20 illustrates the 5-hPa seasonal development of the NH zonal wind composite difference. The extratropical signal begins during autumn in midlatitudes, and reaches a high-latitude maximum during January. The late winter (February and March) composite difference is insignificant north of 40°. The abrupt diminution of the signal indicates that the QBO modulates the strength of the northern winter polar vortex until midwinter, but has little effect on the timing of the final warming.

Major stratospheric warmings are defined as a reversal of the zonal-mean zonal wind at 10 hPa, 60°N to easterly, and higher temperature at the pole than the zonal average at 10 hPa, 60°N. The Holton-Tan effect implies that major warmings should be more common when the QBO is easterly. Unfortunately, such a simple measure is not robust because the definitions of both QBO phase (E/W) and warming (Yes/No) are arbitrary. Using NCEP reanalyzed data from 1958–1999, and a 40-hPa definition of the QBO phase, there were six westerly warmings and ten easterly warm-

ings. However, if the "Berlin" hand-analyzed data are used with a 45-hPa definition of the QBO, and major warmings are defined synoptically, there were ten westerly warmings and eleven easterly warmings [K. Labitzke, personal communication, 2000]. The disparity between these results illustrates that this procedure is too sensitive to the definitions of QBO phase and warmings. Composites, as in Figures 19–20, are more robust, can be used in both hemispheres, and quantify the Holton-Tan effect in both latitude and time.

The SH polar vortex is much stronger, longer-lived, and more quiescent than its NH counterpart. During winter, planetary waves generally do not disrupt the southern vortex in the lower to middle stratosphere. It is not surprising that the observations indicate that the QBO does not significantly modulate the strength of the Antarctic vortex in winter. However, as shown in Figure 21, the QBO modulates the strength of winds in midlatitudes during late autumn, as in the NH. Unlike the NH, the wind modulation is apparent only in midlatitudes throughout the winter and early spring. The striking difference between Figures 21 and 20 is that in the SH, the largest influence of the QBO occurs during late spring (November), at the time of the final warming. In the SH the October vortex is of the same magnitude as the NH vortex in January. Since planetary wave amplitudes are much smaller in the SH, the effect of the QBO is seen only at the vortex periphery until the vortex is relatively small. The 5-hPa observations from Figures 20 and 21 may be compared to the (8-hPa) modeling results of *O'Sullivan and Dunkerton* [1994], discussed in the next section.

4.3. Model Simulations of Extratropical Influence

It is hard to formulate a simple quantitative model for this mechanism (analogous, say, to the Holton-Lindzen model [*Holton and Lindzen*, 1972] for interaction of the equatorial mean flow with vertically-propagating waves). The main complications are (1) the planetary waves propagate both vertically and meridionally, (2) the effects of critical lines on planetary wave propagation are not easy to predict theoretically. In the absence of a simple theory, the effects of the QBO on extratropical waves and mean circulation have been studied extensively in detailed numerical simulation experiments with models of varying complexity.

In purely zonally-symmetric models the response of the flow to near-equatorial momentum forcing is strongly confined to tropical and subtropical latitudes [*Plumb*, 1982]. This also appears to be the case for 2-D models in which the eddy fluxes are parameterized as a simple linear diffusion (e.g., *Gray and Pyle* [1989]).

The effect of the QBO on sudden warmings was investigated in numerical experiments by *Dameris and Ebel* [1990] and *Holton and Austin* [1991]. Both studies used fairly brief integrations of 3-D mechanistic models forced by idealized, rapidly growing midlatitude lower boundary perturbations. They found that the development of the high-latitude stratospheric flow can be very strongly influenced by the tropical winds in the lower stratosphere, although this depends on the strength of the imposed wave forcing. Holton and Austin found that for weak wave forcing the high latitude flow was largely unaffected by the tropical winds, but that this sensitivity to tropical winds increased as the strength of the wave forcing was raised. Within some range of the amplitude of the forcing, the model developed a sudden warming when there were easterly winds in the tropical stratospheric initial conditions, but not when there were westerly winds. As the wave forcing was increased further, sudden warmings occurred regardless of the state of the tropical winds, and the sensitivity of the extratropical flow evolution to tropical winds diminished.

Simplified model studies have the advantage of allowing the relevant parameters (notably the strength of the wave forcing from the troposphere) to be varied in a controlled manner. *O'Sullivan and Salby* [1990] and *Chen* [1996], used models with rather fine horizontal resolution, but limited to a single layer in the vertical. Their experiments were run with simple linear relaxation of the zonal-mean state in order to simulate the effects of radiative transfer in constraining the mean flow in the real atmosphere, and included an imposed wave-1 lower boundary forcing in the winter extratropics. The results showed that the models simulated high latitude effects of the tropical QBO in the same sense as observed. *O'Sullivan and Young* [1992] and *O'Sullivan and Dunkerton* [1994] used a global 3-D mechanistic model forced with a specified wave-1 perturbation at the 10-km lower boundary. The model parameterized radiative effects with a linear relaxation of temperature to an imposed radiative state. Their simulations also included a seasonal cycle. Experiments were repeated with a range of amplitudes of the extratropical wave forcing, for initial conditions in the tropics representative of easterly and westerly QBO phases. The flow in the NH polar region in these simulations was found to be nearly unaffected by the tropical wind through November. In December, January and February, however, there was a significant effect with the time-mean polar vortex in the stratosphere being stronger when the tropical winds were westerly. The contrast in the winter-mean stratospheric polar vortex strength between east and west QBO phases depended strikingly on the amplitude of the wave forcing adopted and on whether the parameterized gravity wave drag was included.

In a GCM the tropospheric forcing of the stratosphere (and its interannual variation) is generated self-consistently within the model. *Hamilton* [1998b] used a GCM run for a continuous 48 year period with a time-varying tropical momentum forcing that produced a 27-month QBO in the equatorial zonal wind with shear zones of realistic magnitude and descending at a realistic speed. Figure 22 shows the January composite zonal mean wind for 20 years with westerly 40 hPa equatorial winds minus that for 20 years

with easterly 40 hPa winds). The results show the tendency for a weaker polar vortex in the east QBO phase. The general features (outside of the tropics) of the composite difference in Figure 22 compare well with the observed January composite shown as Figure 19. Figure 23 shows the easterly and westerly phase composite 28-hPa North Pole temperature for each month from October through April in the model integration. The systematic effects of the tropical QBO on NH polar stratospheric temperature in the model seem to be largely confined to the period December through March. The midwinter differences in Fig. 28 are ~4–5°C, which are comparable to those seen in the observed easterly minus westerly phase composite of *Dunkerton and Baldwin* [1991].

Niwano and Takahashi [1998] have investigated the stratospheric extratropical variability in a version of the Japanese Center for Climate System Research model, which does spontaneously produce a QBO-like oscillation in the tropics with period of about 1.4 years. They analyzed a 14-year integration and calculated January–March composites based on the five most easterly and five most westerly QBO phases as judged by the equatorial zonal wind averaged between 7 and 50 hPa. The results show that on average the NH polar vortex was weaker in the easterly QBO phase, by ~15 ms^{-1} near 70°N at 1 hPa.

In summary, a wide range of models have been applied to the study of influence of the QBO on the extratropical stratosphere. Thus far all studies seem to have focused exclusively on the NH in late autumn through early-spring. The published model studies are unanimous in showing at least some tendency for the strength of the polar vortex through the stratosphere to be positively correlated with the equatorial zonal wind near 40 hPa. These many theoretical model results thus lend credence to the reality of the Holton-Tan effect. All the model studies are idealized to one degree or another, but the one that is most complete (and hence bears detailed comparison with observations) is that of *Hamilton* [1998b]. The results from this study are generally in reasonable agreement with available observations, suggesting that even GCMs that fail to simulate a tropical QBO can have a realistic representation of the wave-modulated interactions between the low and high-latitude stratosphere.

4.4. Interaction of the QBO with other low-frequency signals

The extratropical QBO signal may be identified statistically in a long data record, but it is only part of the large interannual variability of the northern winter stratosphere. Several other signals contribute to variability or interact with the QBO signal to produce other frequencies of variability in the observed data record.

Since upward-propagating planetary waves require westerly mean winds to penetrate the stratosphere, the extratropical influence of the QBO should be limited largely to the period between late autumn and early spring. *Baldwin and Tung* [1994] showed that the QBO modulates the extratropical annual cycle signal so that the signature of the QBO, rather than simply a single spectral frequency peak of ~28 months, includes two additional spectral peaks at the annual frequency plus or minus the QBO frequency. These studies demonstrated that the "3-peak QBO" spectrum [*Tung and Yang*, 1994a] can be expected from the Holton-Tan effect acting to modulate the annual cycle. They considered a harmonic with the period of the QBO that acts to modulate a signal consisting of an annual mean plus a sinusoid with an annual period. The combined signal of the QBO in the extratropics together with the annual cycle can be represented mathematically as

$$(A + B \sin \Omega_{12}t) \times \sin \Omega_{QBO}t \equiv A \sin \Omega_{QBO}t + B/2 \cos (\Omega_{12}-\Omega_{QBO})t - B/2 \cos (\Omega_{12}+\Omega_{QBO})t,$$

where Ω_{12} and Ω_{QBO} denote the annual and tropical QBO frequencies, respectively. With a QBO period of 30 months (the average QBO period during 1979–92, used by Tung and Yang), the last two terms of the above equation represent variations with periods of 20 and 8.6 months. The 30, 20, and 8.6-month spectral peaks were found in ozone [*Tung and Yang*, 1994a,b]; angular momentum and Eliassen-Palm flux [*Baldwin and Tung*, 1994]; and isentropic potential vorticity [*Baldwin and Dunkerton*, 1998a].

Studies using time series of stratospheric temperatures [*Salby et al.*, 1997; *Marquardt*, 1999] suggest that low frequency variability of the middle and upper stratosphere includes a biennial mode with a period of exactly 24 months. Such a purely biennial signal cannot be the result of quasi-biennial forcing. Salby et al. as well as *Baldwin and Dunkerton* [1998a] speculated that a biennial mode might propagate into the stratosphere from the upper troposphere. It is unclear why a biennial mode, which may be found in the troposphere, would be amplified to become important in the polar stratosphere. Baldwin and Dunkerton could find no explanation for such a biennial mode, and noted that the statistical significance of the biennial spectral peak is not high—the mode may simply be an artifact of using a short (32 year) data record that happened to have biennial variability. They noted that the Holton-Tan mechanism would tend to make polar anomalies in PV change sign from year to year. This tendency, together with random chance, could account for the observed biennial mode. If this interpretation is correct, then the biennial mode, in all likelihood, will not continue.

Several researchers have considered that remote effects from El Niño Southern Oscillation (ENSO) could influence the extratropical stratosphere. Such an influence could masquerade as a QBO signal, or at least be difficult to separate from a QBO signal. *Wallace and Chang* [1982] were unable to separate the effects of ENSO and the QBO on the tropical stratosphere in 21 winters of NH 30-hPa geopotential. *Van*

Loon and Labitzke [1987] also found that the phases of the QBO and ENSO tended to coincide. By removing cold and warm ENSO years (keeping years only with weak ENSO anomalies) they displayed results similar to Holton and Tan. Subsequent observational studies (e.g., *Hamilton* [1993]; *Baldwin and O'Sullivan,* [1995]), and modeling [*Hamilton,* 1995] show a consistent picture in which the influence of ENSO on the zonal-mean structure of the vortex is largely confined to the troposphere. In the lower stratosphere, ENSO appears to modulate the amplitudes of large-scale stationary waves.

Decadal variability, possibly related to the 11-year solar cycle, clearly exists in data records which began in the 1950s. *Labitzke* [1987] and *Labitzke and van Loon* [1988] studied the observed late-winter NH circulation classified by both the level of solar activity and the QBO phase. *Naito and Hirota* [1997] found a robust QBO signal during early winter, but they found a strong relation to the solar cycle during late winter. Figure 24 summarizes the solar/QBO results as scatter plots of mean 30-hPa geopotential heights during January and February above the North Pole vs. 10.7 cm solar radio flux (a proxy for the 11 year cycle in solar activity). The data set can be grouped into four categories based on the QBO phase and solar activity level. In years with low solar activity, the polar winter vortex tends to be disturbed and weak when the QBO is easterly, but deeper and undisturbed when the QBO is westerly. In years with strong solar activity, however, westerly phases of the QBO are associated with disturbed winters, whereas easterly phases of the QBO are accompanied with deep and undisturbed polar vortices. Hence, the QBO acts as predicted by *Holton and Tan* [1980] in years with low solar activity, but appears to reverse its behavior during years with high solar activity. Only two cases do not fit into this scheme: 1989 and 1997.

It is the subject of active debate whether or not decadal variability is caused by the 11-year solar cycle, but there is increasing evidence through modeling that the solar cycle has a significant influence on winds and temperatures in the upper stratosphere. Over the 11-year solar cycle, the solar "constant" (i.e., the radiative energy input into the earth's atmosphere summed over the entire spectrum) varies by less than 0.1% [*Willson et al.,* 1986]. Variability in the UV responsible for most of ozone heating is less than 1% [*Rottman,* 1999]. The variability rises to 8% only at wavelengths shorter than 200 nm, but these wavelengths may affect indirectly the ozone chemistry through enhanced production of odd oxygen, which in turn could affect middle atmospheric heating rates and dynamics.

Following earlier solar modeling [*Haigh,* 1994; 1996; 1999] and solar-QBO modeling [*Rind and Balachandran,* 1995; *Balachandran and Rind,* 1995], *Shindell et al.* [1999] used a troposphere-stratosphere-mesosphere GCM with interactive ozone and realistic values of UV forcing to show that ozone changes amplify irradiance changes to affect climate. Circulation changes introduced in the stratosphere penetrated downward, even reaching the troposphere. The modeling studies find a more intense Hadley circulation during solar maximum conditions. They concluded that the observed record of geopotential height variations in the NH are, in part, driven by solar variability.

Figure 20 showed that the observed QBO modulation of zonal wind in the NH middle stratosphere is essentially over by February, and the observations show decadal variability coherent with the solar cycle during January–February. The possibility exists for the QBO to dominate early winter, while solar influence is manifest during late winter. Due to the strong absorption of ozone in the UV occurring in the upper stratosphere and mesosphere, a solar influence on the thermal structure in these regions of the atmosphere is plausible. This, in turn, might affect the strength of the planetary wave driven "extratropical pump" [*Holton et al.,* 1995]. A mechanism involving downward propagation of stratospheric anomalies, through modification of planetary wave propagation from below, is discussed in Section 6.2.

Salby and Callaghan [2000] showed that the QBO westerlies below 30 hPa vary with the solar cycle, as do the easterlies above 30 hPa. Changes in the duration of wind regimes were found to introduce a systematic drift in the QBO phase during northern winter.

Various hypotheses have been proposed to explain the observed stratospheric decadal variability without reference to the solar cycle. These hypotheses rely on the QBO interacting with other signals. *Teitelbaum and Bauer* [1990] and *Salby and Shea* [1991] argued that the wintertime 11-year variability is a byproduct of the analysis procedure which involves the stratification of the data into years with respect to the QBO. *Gray and Dunkerton* [1990] showed the possibility of an 11-year cycle arising from the beating of the QBO with the annual cycle. *Salby et al.* [1997] and *Baldwin and Dunkerton* [1998a] suggested a modulation of the tropical QBO by a biennial extratropical signal (which exists, but has not yet been explained) would result in a period of 11 years. These would provide an explanation of the 11-year variability without referring to the solar variability, although the observed in-phase relation to the solar cycle remains unexplained.

The origin of the observed biennial or decadal variability does not affect the reality of the influence of the QBO on the extratropical stratosphere. The debate centers on the reality of both the solar and biennial signals, and whether or not the observed decadal variability could arise in the absence of solar influence. An alternative explanation was given by *Marquardt* [1999]. By analyzing observed data rather than analytical functions, he showed that the biennial signal can be understood as a natural consequence of the modulation of Tung and Yang's extratropical QBO by an 11-year signal.

5. EFFECTS OF THE QBO ON CHEMICAL CONSTITUENTS

5.1. Background

There is a substantial body of evidence for the influence of the QBO on chemical constituents in the atmosphere. Initial evidence came from ground-based observations of column ozone at two subtropical stations reported by *Funk and Garnham* [1962], which were shown by *Ramanathan* [1963] to be associated with the stratospheric wind oscillation. In an examination of historical ozone data, *Angell and Korshover* [1964] showed that a QBO signal is evident in Shanghai data (31°N) in the 1930s. Subsequent information about the temporal, latitudinal and vertical structure of the ozone QBO has come primarily from satellite observations, due to their global nature and better temporal and spatial sampling. Although no single satellite has been operational for the whole period, the large-scale pattern and evolution of the ozone QBO, including its height structure, has been well characterized over this period, often with overlapping measurements from two or more instruments.

The first simulation of the ozone QBO was carried out by *Reed* [1964] using a simplified linearised model. However, it was not until 1986 that the QBO was studied in a full photochemical model. *Ling and London* [1986] included the QBO variation in zonal wind in a 1-D radiative dynamical photochemical model of the stratosphere. This was soon followed by a 2-D simulation [*Gray and Pyle,* 1989] enabling the modeling of the latitudinal structure and interaction with the annual cycle, and subsequently by 3-D simulations [*Hess and O'Sullivan,* 1995] which included a better representation of the wave-driven transport. Subsequent studies employing both 2-D and 3-D models have increased our understanding of the mechanisms of the ozone QBO, and these are described in more detail in the following sections.

In their 2-D QBO simulation, *Gray and Chipperfield* [1990] also noted QBOs in many of the other trace gases carried in the model, some of which were substantial. Some of these model predictions were confirmed by the subsequent analysis of SAGE II NO_2 measurements [*Zawodny and McCormick,* 1991] and, more recently, by measurements of CH_4, H_2O, HF, HCl and NO from the Halogen Occultation Experiment (HALOE – e.g. [*Luo et al.,* 1997, *Ruth et al.,* 1997, *Randel et al.,* 1998, *Dunkerton,* 1999]). Additionally, there is a well-documented modulation of the distribution of volcanic aerosol in the lower stratosphere (e.g. [*Trepte and Hitchman,* 1992, *Hitchman et al.,* 1994, *Grant et al.,* 1996, *Choi et al.,* 1998]) which has been associated with the QBO.

5.1.1. Ozone: the Equatorial Anomaly

The close association of variations in equatorial column ozone with the zonal wind QBO is illustrated by Figure 25(a) which shows a time-series of SBUV and SBUV/2 equatorial ozone anomalies together with a reference QBO wind time series. The signal varies between ±10 DU, approximately ±4% of the background total column amount. The reference QBO wind time series was calculated by multiplying the observed equatorial stratospheric wind profile with the weighting profile shown in Figure 25b. The latter profile was derived empirically to optimize the fit to column ozone, neglecting volcanic periods. Note the excellent correspondence between the observed ozone anomaly and the reference wind series. Positive anomalies are present when the zonal winds in the lower stratosphere are westerly, while negative anomalies correspond to easterlies. The strongest correlations with ozone are achieved with the weighting profile biased towards the winds around 20–30 hPa winds rather than the 40–50 hPa reference wind normally used in correlations with the extratropical zonal wind [*Dunkerton and Baldwin,* 1991].

The variable period of the equatorial ozone QBO is clearly evident in Figure 26, which shows the latitude time-series of the column ozone anomaly. Note that the equatorial QBO signal is not synchronized with the annual cycle since there is no apparent preferred season in which the anomalies change sign or reach their maximum amplitude.

A mechanism to explain the equatorial column ozone QBO anomaly was first suggested by *Reed* [1964]. The timing of the maximum westerly vertical wind shear at a particular level corresponds to the warmest phase of the temperature QBO on the equator. This is therefore the time of maximum diabatic cooling, which will induce relative sinking of air parcels through isentropic surfaces. This vertical motion occurs in a region of the atmosphere where the ozone mixing ratio increases with height and where the lifetime of ozone is rapidly changing. Below about 28 km the chemical lifetime is relatively long compared with dynamical processes and ozone may be considered to be a long-lived tracer. Above 28 km its chemical lifetime shortens considerably. The relative descent of air through this region produces an increase in the total column of ozone, since at levels above 28 km ozone is replaced by chemical production on relatively short timescales. Thus, the maximum column ozone occurs when the column has been displaced farthest downwards into the lower stratosphere. This will be after the descent of the westerly shear zone i.e. at around the time of maximum westerlies in the lower stratosphere. The converse is true of an easterly shear situation. Mass continuity also requires there to be a return arm to this circulation in the subtropics with upwelling associated with westerly equatorial shear, and downwelling associated with easterly equatorial shear.

While this conventionally accepted mechanism accounts for a large component of the variability, there are nevertheless additional important factors contributing to the column anomaly. Figure 27 shows the height time-series of the QBO

ozone density anomaly (DU/km) from the SAGE II data set. A regression analysis has been applied in order to isolate the QBO variability. Ozone density can be used to visually determine contributions to the column ozone anomaly (simply a sum in the vertical of the ozone density anomalies). The QBO dominates the ozone variability at the equator, with alternating positive and negative anomalies which propagate downwards with time [*Zawodny and McCormick*, 1991, *Hasebe*, 1994, *Randel and Wu*, 1996]. There are two regions of maximum ozone perturbation: in the lower stratosphere (20–27 km) and the middle stratosphere (30–37km). The anomalies at these two levels are approximately a quarter cycle out of phase. There is, therefore, a small contribution to the column from the region above 28 km, which also influences the timing of the maximum column ozone anomaly. The equatorial QBO column ozone signal is simulated reasonably well by models (e.g. [*Ling and London*, 1986, *Gray and Pyle*, 1989, *Tung and Yang*, 1994, *Chipperfield et al.*, 1992, 1994, *Kinnersley and Tung*, 1998, *Jones et al.*, 1998, *Hess and O'Sullivan*, 1995, *Nagashima et al.*, 1998]), particularly when the observed winds are used to force a realistic zonal wind QBO period [*Gray and Ruth*, 1993] and when the effect of the ozone anomaly itself on the heating rate is included [*Hasebe*, 1994, *Li et al.*, 1995, *Huang*, 1996].

Although the origin of the lower level anomaly below 28 km in Figure 27 is conventionally assumed to be due to the vertical advection of ozone as proposed by Reed and described above, there is evidence that vertical advection may not be the only contribution to the lower level anomaly. If only vertical advection were responsible for the ozone anomalies one would expect a quadrature relationship between the anomalies in ozone and vertical velocity and hence also with temperature (since perturbations in temperature and vertical velocity are inversely proportional). Observations of ozone and temperature, however, indicate that they are approximately in phase; *Jones et al.* [1999] have suggested that horizontal, as well as vertical, advection by the induced meridional circulation may contribute to the equatorial ozone QBO, thus explaining the lack of quadrature.

The ozone QBO anomaly above 28 km has been shown to be controlled by changes in the photochemical sources and sinks of ozone, primarily via transport-induced variations of NO_y (the total reactive nitrogen reservoir) [*Chipperfield et al.*, 1992, 1994, *Politowicz and Hitchman*, 1997, *Jones et al.*, 1998].

5.1.2. Ozone: Subtropical and Higher Latitudes

A QBO signal in the subtropics that extends to mid and high latitudes is clearly evident in Figure 26. There is a 180° phase change at around 15° in each hemisphere with the higher latitude anomaly extending at least to 60°N but with its maximum at approximately 30–40° latitude. Broadly, this concurs with the presence of a return arm of the local equatorial QBO circulation described above, with ascent (descent) in the subtropics associated with westerly (easterly) equatorial shear. However, there are two significant departures from the signature one would expect from this simple explanation. Firstly, the theoretical equatorial QBO circulation is confined to low latitudes and cannot explain the presence of an ozone QBO signal poleward of about 30°. Secondly, the timing of the subtropical anomalies is such that they are not symmetric about the equator. The subtropical and higher latitude anomaly maxima and minima in the two hemispheres are approximately six months apart and coincide with the local late winter/spring. This timing is confirmed in Figure 28 in which we show a regression fit of the TOMS column ozone amounts to the 30 hPa Singapore winds [*Randel and Cobb*, 1994]. On average, the subtropical regression anomalies reach their maximum in March and August in the Northern and Southern Hemispheres respectively. However, note from Figure 27 that occasionally there is a "missed" subtropical anomaly e.g. in 1981, 1986 and 1991 in the NH and in 1993 in the SH. There is therefore a change in the "period" of the column ozone QBO as one moves to higher latitudes [*Hilsenrath and Schlesinger*, 1981], with a phase relationship between the equatorial and subtropical anomalies which is constantly changing and is more complicated than a symmetric QBO circulation would imply.

The timing of the subtropical and high latitude anomalies in late winter/spring is highly suggestive of a modulation of the ozone QBO by the annual cycle [*Bowman*, 1989, *Hamilton*, 1989, and *Lait et al.*, 1989]. Early proposed mechanisms for the seasonal synchronization of the subtropical anomalies centered on a modulation of the low latitude ozone anomalies once they had been produced by the classic symmetric QBO circulation. For example, *Holton* [1989] proposed that transport of the equatorial anomaly by the poleward winter circulation could explain the seasonality, while *Gray and Dunkerton* [1990] suggested that downwelling during the winter would preserve the subtropical ozone anomaly while upwelling in summer would destroy it. On the other hand, *Hamilton* [1989] suggested the possibility of a modulation of the seasonally varying eddy transport of ozone into the subtropics. However, more recently, *Jones et al.*, [1998] and *Kinnersley* [1999] have shown that there is a significant modulation of the meridional circulation induced by the QBO itself. This seasonal dependence of the circulation occurs primarily because of nonlinear horizontal advection of zonal momentum in the tropics and subtropics by the mean circulation, which is highly asymmetric during solstice periods. This results in a strongly asymmetric QBO circulation in which the winter hemisphere half of the circulation is substantially reinforced and the summer hemisphere circulation is weakened (Figure 9). Thus, the classic symmetric QBO circulation may not be present except, per-

haps, in the very low stratosphere where horizontal advection by the mean circulation is thought to be weak and at equinox when the mean circulation is at its weakest. The asymmetry in subtropical ozone anomalies therefore arises primarily through its formation by an asymmetric QBO circulation rather than by the subsequent disruption of a symmetric ozone pattern.

The "missed" subtropical and mid-latitude anomalies in 1981, 1986 and 1991 in the NH and in 1993 in the SH (Figure 26b) are thought to be due to the timing of the equatorial QBO relative to the annual cycle. The formation of a significant winter subtropical anomaly requires not only a strong vertical wind shear at the equator so that a strong QBO circulation is induced but also the presence of strong background horizontal advection which will strengthen the winter side of the induced QBO circulation as described above. These conditions need to last for a month or two to allow the ozone distribution to respond to the induced circulation. Hence, if either of these requirements are not present for a sufficient length of time, a significant subtropical anomaly is unlikely to form in that year.

Similarly, if the timing and duration of the equatorial wind QBO is such that it persists in the same phase for two successive winters of either hemisphere, then two anomalies of the same sign will occur in successive winters in the subtropics of that hemisphere. The latter is evident in the SH in 1983/84 and 1988/89. This phenomenon can be thought of as a nonlinear interaction between the annual cycle and the QBO cycle [*Gray and Dunkerton*, 1990], which results in a low frequency modulation of the amplitude of the subtropical and mid-latitude ozone anomaly. Over the period of data used in Figure 28 this causes the SH regression anomaly to be coincidentally larger on average than the NH anomaly. Over a longer time span both anomalies would presumably be of similar size.

A typical latitude-altitude cross-section of the modeled QBO in ozone from the *Jones et al.*, [1998] model is shown in Figure 29 for winter solstice in the NH with an eastward QBO wind maximum at about 26 km in the tropics. In both the tropics and subtropics the QBO in ozone consists of two maxima centered in the lower and middle stratosphere with the tropical and subtropical anomalies approximately 180° out of phase, in agreement with observations. Also in agreement with observations, the modeled anomalies are large in the winter hemisphere and small in the summer hemisphere in both the photochemically and dynamically controlled regions. This is due to the asymmetry in the QBO-induced circulation as illustrated by the corresponding mass streamfunction also shown in Figure 29. The asymmetric ozone anomaly arises directly through advection of ozone at the lower levels and indirectly though the advection of NO_y at the upper levels.

The *Jones et al.* [1998], model did not include extratropical influences such as the QBO modulation of planetary wave breaking. While it produces a good simulation in the tropics and subtropics, the modeled ozone anomalies do not extend as far poleward as suggested by observations. The upper level anomalies inferred from observations maximize between 10°–40°, whereas those in the lower stratosphere extend to at least 60° [*Randel and Wu*, 1996]. The mechanism for the poleward extension of the dynamically controlled ozone anomaly is not well understood, although it likely involves an interaction between the planetary waves and the equatorial QBO. The modulation of planetary wave forcing by the equatorial wind QBO results in a stronger large-scale mean circulation in easterly phase years. Stronger downwelling in the winter mid-latitudes will produce a relatively larger column ozone anomaly in easterly years than westerly years, as observed [*Tung and Yang*, 1994]. On the other hand, the extension of the ozone anomalies to mid and high latitudes in the models of *Gray and Pyle* [1989] and *Kinnersley and Tung* [1998] is a result of the seasonally varying eddy transports in their models, which transfer the subtropical anomalies to higher latitudes. Figure 30 shows the correlation between the simulated ozone anomaly *of Kinnersley and Tung* [1998] and the observed anomaly between 1978 and 1993. At mid latitudes, therefore, a number of factors and feedback processes are found to contribute to the final ozone QBO and the QBO may actually be responsible for a larger part of the observed ozone anomaly than a simple correlation with the wind QBO would suggest.

In addition to the QBO signals in the tropics and mid-latitudes, analysis of TOMS data and other long-term records suggest a further region of QBO influence in the winter polar regions [*Oltmans and London*, 1982, *Garcia and Solomon*, 1987, *Bowman*, 1989, *Lait et al.*, 1989, *Randel and Cobb*, 1994]. The polar ozone QBO is approximately in phase with mid-latitudes and is seasonally synchronized in the same way, with maximum amplitude in springtime. Observational evidence for the polar ozone QBO is less statistically significant than that in the tropics or midlatitudes, at least partly because of the high level of interannual variability in the springtime vortex associated with planetary wave forcing from the troposphere [*Kinnersley and Tung*, 1998]. There is also a suggestion of a feedback loop between the QBO in temperature, the formation of polar stratospheric clouds and hence with the underlying chemical destruction that gives rise to the Ozone Hole [*Poole et al.*, 1989, *Manzini et al.*, 1991, *Butchart and Austin*, 1996].

5.1.3. QBO Anomalies in Other Trace Species

The QBO influences a wide range of other trace gases in the atmosphere, including methane, water vapor, volcanic aerosol and many of the shorter lived species such as NO_2 and N_2O_5. Volcanic aerosol distributions following major eruptions in equatorial latitudes have graphically illustrated the different circulation patterns associated with the two

QBO phases, as shown in Figure 31 from *Trepte and Hitchman* [1992]. In a descending westerly phase (Figure 31a) the aerosol shows a distinctive "double peak" with relative maxima in the subtropics and a minimum at the equator in the region 20–50 hPa structure compared with the descending easterly phase (Figure 31b) which has a single equatorial peak. The heavy arrows indicate the approximate sense of the induced QBO circulations. The near-symmetry of the double peak in the aerosol distribution, in contrast to the emphasis on hemispheric asymmetry in the previous section, is probably due to being so low down in the equatorial stratosphere and hence relatively unaffected by the influence of the asymmetrical mean circulation.

Figure 32 shows the interannual anomalies in H_2O over the equator from HALOE observations [*Randel et al.*, 1998]. The QBO anomaly in H_2O ascends slowly with time, at approximately the rate of ascent of the background mean upwelling, in contrast to the slow descent of the ozone anomaly. In general the global variations in H_2O anomaly mimic those observed in CH_4, but with opposite sign. In the upper stratosphere (35–45 km) these are approximately in-phase with the QBO winds near 30 km. The CH_4 and H_2O variations over this region cancel to a large degree, such that there are much smaller variations in $H_2O+2*CH_4$ (the variable part of total hydrogen); this cancellation confirms the production of water vapor via methane oxidation at these levels and is evidence that these stratospheric anomalies arise via variations in transport.

One region where differences between CH_4 and H_2O anomalies are observed is in the tropical middle stratosphere, where H_2O (and $H_2O+2*CH_4$) show QBO variations over approximately 25–35 km, but none are observed for CH_4. These patterns are equatorially centered (approx. 15°N–S) and are highly correlated with the QBO zonal winds near 20 hPa. One possible mechanism for the tropical H_2O signal is that the QBO temperature variations modulate tropical tropopause temperatures (e.g., *Reid and Gage* [1985]) and hence the magnitude of water vapor entering the lower stratosphere [*Mote et al.*, 1996]. However, the HALOE H_2O anomalies do not show strong coherence between 100 and 30 hPa levels in Figure 32; and the variations at the lowest levels do not exhibit a strong QBO behavior. The mechanism(s) of the middle stratosphere QBO signal in H_2O await(s) clarification.

The measurements of long-lived tracers also show the large effects of the QBO over midlatitudes. Figure 33 shows the January and April CH_4 distributions from HALOE in 1993 (westerly phase) and 1994 (easterly phase). In January 1994 the isolines form a distinctive "staircase" pattern between the tropics and NH midlatitudes that is very different from the January 1993 behavior; this structure is also seen in *MLS* and CLAES data [*Dunkerton and O'Sullivan*, 1996, *O'Sullivan and Dunkerton*, 1997, *Gray and Russell*, 1999, *Gray*, 2000]. *Gray* [2000] has shown that this large asymmetry in QBO anomalies between the hemispheres is consistent with the asymmetric QBO circulation of *Jones et al.*, [1998] and *Kinnersley* [1999] discussed earlier. The detailed staircase pattern in Figure 33c nevertheless results from a complicated interaction of advection by the local QBO circulation and the effects of isentropic mixing at midlatitudes.

In April 1993 (Figure 33b) the distribution displays a distinct "double peak" feature near 0.3–5 hPa, significantly higher than that displayed by the volcanic aerosol in Figure 31. This double peak results from vertical advection by the circulation associated with westerly shear of the semiannual oscillation (*SAO*) [Gray *and Pyle*, 1986, *Sassi et al.*, 1997]. The HALOE observations show a distinct QBO variation in the amplitude of this SAO double peak, with a prominent double peak feature in westerly phase years (e.g. Figure 33b) but a barely discernible one in easterly phase years (e.g. Figure 33d) [*Ruth et al.* 1997, *Randel et al.* 1998]. This is counter-intuitive, since during an easterly QBO phase there is enhanced vertical propagation of eastward propagating waves and hence a stronger SAO westerly wind shear. However, in a 2-D modeling study, *Kennaugh et al.*, [1997] showed that this increased eastward wave forcing also caused the westerly SAO phase to descend much more rapidly during an easterly QBO phase. Hence, the SAO circulation that produces the double peak does not remain at any one level for long enough for the tracers to respond to its presence.

In the January CH_4 distributions, there is also a distinct QBO signal in the steepness of the isolines in the subtropics at around 30 hPa. In 1993 (Figure 33a) they slope gently from equator to mid-latitudes but in 1994 (Figure 33c) the isolines are almost vertical [*Gray and Russell*, 1999]. This difference is not so apparent in the aerosol distributions of Figure 31, probably due to the unusual distribution of tracer gradients immediately after a volcanic eruption, but it is more apparent in composite aerosol measurements [*Hitchman et al.*, 1994]. Again, it is not clear whether this is due to advection by the QBO circulation or to the QBO influence on the equatorward extent of Rossby wave mixing and hence on the sharpness of the PV and tracer gradients at the subtropical edge of the surf zone. Some studies have suggested a sensitivity of isentropic mixing to the QBO [*Dunkerton and Baldwin*, 1991, *O'Sullivan and Young*, 1992; *O'Sullivan and Chen*, 1996; *O'Sullivan and Dunkerton*, 1997] and there is evidence of this in satellite measurements [*Grant et al.*, 1996]. On the other hand, *Waugh* [1996] used analyzed winds and contour advection techniques to make quantitative estimates of mixing in the subtropics, but found no sensitivity to the QBO. This may be due to a lack of reliable wind data in the subtropics. *Gray and Russell* [1999] have pointed out that the strong QBO signature is in the steepness of the isolines and not in the isentropic gradients, which suggests that advection by the QBO circulation is important in setting up this feature. This is supported by the

modeling of *Jones et al.*, [1998] and *Kinnersley* [1999] which reproduce some aspects of this steepening using advective transport only.

The QBO anomalies in the shorter lived species NO_2, as measured by HALOE, are shown in Figure 34. The general pattern of the anomalies in NO are similar to those of NO_2 and reflect QBO-induced changes in the abundance of NO_y in the stratosphere [*Gray and Chipperfield*, 1990; *Jones et al.*, 1998]; the anomalies in NO_y are produced through the influence of vertical advection on the vertical gradient in NO_y (*Chipperfield et al.*, 1994; *Politowicz and Hitchman*, 1997; *Jones et al.*, 1998]. Below about 5 hPa, the amplitude of the QBO in NO_2 is larger than in NO as a result of the influence of the QBO anomalies in temperature on the ratio of the abundance of NO to NO_2, through the reaction $NO + O_3 -> NO_2 + O_2$ [*Gray and Chipperfield*, 1990]. The reason for a large QBO signal in NO above 5 hPa has not yet been investigated. However, it is likely due to the dominant contribution of NO to NO_y at these altitudes.

The pattern of QBO anomaly in HCl observed by HALOE (not shown) is similar to that in NO and NO_2. In their modeling study *Gray and Chipperfield* [1990] found a similarity between the QBO anomaly in NO_y and Cl_y (the total inorganic chlorine reservoir). The anomalies were produced by the influence of vertical advection on the positive vertical gradients in Cl_y and NO_y in the lower and middle stratosphere. In the upper stratosphere, where the vertical gradient in Cl_y is weak, the QBO anomalies in HCl are also weak, providing supporting evidence for this mechanism.

6. THE QBO ABOVE AND BELOW THE STRATOSPHERE

6.1. Mesospheric QBO

Rawinsonde measurements of equatorial winds (to ~30 km, since the 1950s) and rocketsonde wind observations from stations near 8°S and 8°N (to ~60 km, since the 1960s) (as shown in Figure 1). Satellite measurements of equatorial winds in the stratosphere and mesosphere from the High Resolution Doppler Imager (HRDI) on the Upper Atmosphere Research Satellite (UARS), beginning in November, 1991, provide equatorial wind data from 10–40 and 50–115 km. The HRDI data allowed the discovery of a QBO in the upper mesosphere [*Burrage et al.*, 1996], called the mesospheric QBO (MQBO). Monthly mean HRDI equatorial winds are shown in Figure 35 (top panel) confirming the QBO up to 40 km, and the mesospheric SAO from ~55–85 km. By removing the annual and semi-annual harmonics (similar to removing the seasonal cycle in the top panel of Figure 1) a mesospheric QBO centered near 85 km becomes apparent. The wind variations have been confirmed by radar observations at Christmas Island (2°N) during the HRDI period. The HRDI data show that the MQBO extends out to ±30° latitude, with a 180° phase difference with the stratospheric QBO (~40 hPa).

The HRDI data record is too short to reliably confirm that the MQBO is linked to the stratospheric QBO. *Garcia et al.* [1997] suggested that the easterly phase of the mesospheric SAO is usually stronger only when deep easterlies are present. This relationship holds during 1992–1995, but exceptions are found when Christmas Island radar data from 1990–1991 are examined. Mesospheric westerlies do not show marked interannual variability, and they are not correlated with the QBO.

The possibility of a connection to the QBO is strengthened by both modeling and theoretical evidence. *Mayr et al.* [1997] used a 2-D model to simulate oscillations in the equatorial stratosphere and mesosphere resulting from vertically propagating gravity waves. The modeled QBO was not confined to the stratosphere, but showed a QBO in the upper mesosphere, similar to that observed in HRDI data and Christmas Island radar data. The theoretical explanation involves selective critical layer absorption or wave filtering of small-scale gravity waves as they traverse the underlying winds in the stratosphere, together with the complimentary wave breaking at higher altitude levels in the upper mesosphere. This process also generates the SAO in the upper mesosphere.

The amplitudes of the various equatorial oscillations in zonal wind, as a function of height, are summarized in Figure 36. The annual cycle (dotted line) is relatively small in the stratosphere (~5 ms^{-1}). The stratospheric QBO is shown from 16–40 km, peaking near 20 ms^{-1} at about 25 km. The amplitude in the troposphere is small. The amplitude of the QBO between 40 and 70 km is not shown due to uncertainty and difficulty defining what part of the variability is related to the QBO (see Figure 1).

6.2. Effect of the QBO on the extratropical troposphere

In Section 4 it was shown that the QBO, by modulating the wave guide for vertically propagating planetary waves, affects the circulation of the extratropical winter stratosphere. This modulation is more easily seen in the NH, where wave amplitudes are larger and the stratospheric circulation is disrupted by sudden warmings in which the usual westerly middle stratospheric winds become easterly. Figure 19 showed that modulation of the zonal wind by the QBO in the NH in January appears to extend below the tropopause. *Angell and Korshover* [1975] showed a strong correlation between Balboa 50-hPa zonal wind and the displacement of the northern vortex at 300 hPa, near the tropopause. The surface signature of the QBO was first examined by *Holton and Tan* [1980], who showed the difference between 1000-hPa geopotential for the two phases of the QBO. An update of Holton and Tan's calculation, for 1964–1996 data, is shown as Figure 37. The pattern is characterized by modula-

tion of the strength of the polar vortex, and anomalies of the opposite sign at low- to mid-latitudes. The pattern in Figure 37 is essentially similar to that shown by Holton and Tan. *Hamilton* [1998], in a 48-year GCM simulation with an imposed QBO, found that the difference, between QBO phases, of the strength of the upper tropospheric polar vortex was statistically significant.

Disturbances in the extratropical stratosphere affect only ~25% of the vertical column of air, and there is increasing evidence, from observations, numerical models, and conceptual models, that stratospheric anomalies do influence the troposphere. It is not necessary to limit the discussion to the influence of the QBO, but to think of any circulation anomaly in the stratosphere (e.g. due to solar influence, the QBO phase, a volcanic eruption). *Boville* [1984] showed, using a GCM, that a change in the high-latitude zonal wind structure introduced changes in the zonal-mean flow all the way down to the boundary condition that corresponds to the Earth's surface, as well as in wave structures. He concluded that the degree of trapping of the planetary waves in the troposphere is determined by the strength and structure of the stratospheric mean zonal wind, resulting in sensitivity of the troposphere to the stratospheric zonal wind structure. *Boville* [1986] explained further that when the high-latitude winds, especially in the lower stratosphere are strong, it tends to inhibit the vertical propagation of wave activity into the polar stratosphere. If the winds are weak, wave activity can propagate more effectively into the polar stratosphere. The process was found, in a GCM, to be tightly coupled to tropospheric generation of vertically-propagating planetary waves.

Kodera et al. [1990] used both observations and GCM output, to show that anomalies in the mid-latitude upper stratosphere (1 hPa) in December tend to move poleward and downward, reaching the troposphere approximately two months later. In general, these effects can be understood in terms of the modification of the zonal-mean zonal wind, which acts as a wave guide for planetary wave propagation. Stratospheric anomalies tend to induce changes in wave propagation at lower levels, which affect the convergence of the waves, which further modifies the zonal-mean flow. Over time, the net effect appears to be downward (and poleward) movement of the anomalies.

A complementary approach to understanding the downward link to the troposphere has been to examine "modes of variability." Such modes may be thought of as patterns which tend to recur and which account for a large fraction of variability; patterns should be robust and be found through different analysis schemes. For example, the NH winter zonal wind tends to vary in a dipole pattern (e.g., Figure 19). This coupled mode of variability between the northern winter stratosphere and troposphere was discussed by *Nigam* [1990], who examined rotated empirical orthogonal functions (EOFs) of zonal-mean wind. Nigam's result showed that the dominant mode of variability in zonal-mean wind appears as a deep north-south dipole, with a node near 40–45°N (similar to Figure 19). The poleward part of the dipole represents fluctuations in the strength of the polar vortex.

Coupling between the stratosphere and troposphere was further explored by *Baldwin et al.* [1994], who examined geopotential patterns in the middle troposphere that were linked to the stratosphere. Using singular value decomposition (also called maximum covariance analysis) between 500 hPa geopotential and mean zonal wind, they showed that the leading mode had a strong dipole signature in mean zonal wind, extending from the surface to above 10 hPa. The north-south dipole mode accounts for a large fraction of the variance in zonal wind, and is found by a variety of techniques.

The leading mode of variability of the northern extratropical troposphere/stratosphere is characterized by a deep, zonally-symmetric or "annular" structure [*Thompson and Wallace,* 1999]. This dipole mode in zonal-mean zonal wind is coupled to a horizontal wave structure of geopotential anomalies in the troposphere. The surface pattern resembles the North Atlantic Oscillation, but is more symmetric in longitude. *Thompson and Wallace* [1998] showed that the surface pattern corresponds to the leading EOF of wintertime monthly-mean sea level pressure. The entire mode, throughout the troposphere and stratosphere, is known as the Northern Annular Mode (NAM). The surface NAM pattern is also know as the Arctic Oscillation [*Thompson and Wallace,* 1998], and is broadly similar to the QBO signature shown in Figure 37, suggesting that the QBO may act to modulate the deep structure of the NAM. It is now becoming clear that all of the studies of modes of NH variability produce patterns that are essentially slight variants of the NAM. The NAM represents a dominant, robust, naturally occurring mode of variability, and if the QBO phase can affect the NAM in the stratosphere, it can be expected that there would be a surface signature of the QBO.

The NAM is closely linked to stratospheric sudden warmings [*Baldwin and Dunkerton,* 1999], and every major warming shows a clear signature in the magnitude of the NAM. This relationship can be expected because both phenomena, in the stratosphere, relate to the strength of the polar vortex. As the strength of the stratospheric polar vortex changes, the surface NAM signature tends to vary. Baldwin and Dunkerton examined this relationship and demonstrated that large, sustained variations in the strength of the stratospheric polar vortex tend to propagate downward to the earth's surface. The time for propagation from 10 hPa to the surface was found to be variable, but averaged about three weeks. They also examined the relationship between the QBO and the NAM, which was found to be strongest during December in the middle stratosphere, and weaker as winter progressed. The QBO appears to be a factor that influences

the NAM. That influence tends to appear as modulation of the strength of the polar vortex, from the lower mesosphere to the Earth's surface [*Baldwin and Dunkerton*, 2000].

6.3. Effects of the QBO on the tropical troposphere

Because the QBO has its maximum amplitude over the equator, it is logical to inquire whether this oscillation has any effect on the underlying tropical troposphere. In this regard, it is important to keep two things in mind. First, the zonal wind and temperature anomalies of the QBO do not penetrate significantly below the tropopause (Figure 1). The temperature QBO at the tropopause is small relative to the annual cycle. Second, it is known that the tropical troposphere has a quasi-biennial oscillation of its own, uncorrelated with the stratospheric QBO [*Yasunari*, 1985; *Gutzler and Harrison*, 1987; Kawamura, 1988; *Lau and Sheu*, 1988; *Moron et al.*, 1995; *Shen and Lau*, 1995]. Unlike the latter, the "tropospheric QBO" is irregular in time, asymmetric in longitude, and propagates slowly eastward, with largest amplitude near the Maritime Continent.

Although *Yasunari* [1989] suggested that the tropospheric oscillation is coherent with the stratospheric QBO, his results and those of other authors tend to disprove the claim. For example, the Hovmoller plot of biennially filtered upper tropospheric winds has an irregular variation in longitude and time, with at least two apparently distinct oscillations in the Pacific and Atlantic sectors, neither of which correlate well with the stratospheric QBO. The oscillation is a bit too fast over the Atlantic, and bit to slow over the Pacific. On the basis of a longer record, some authors view the stratospheric and tropospheric QBOs as completely unrelated [*Barnett*, 1991; *Xu*, 1992]. As far as linear correlations are concerned, tropospheric and stratospheric QBOs do not exhibit a consistent phase relationship over several decades. Their morphologies are so different that it is difficult to see any obvious connection.

On the other hand, a more subtle relationship (either nonlinear or multivariate) might exist between these phenomena. There is evidence that ENSO warm events affect the rate of QBO westerly descent [*Maruyama and Tsuneoka*, 1988]. This effect is dynamically plausible [*Dunkerton*, 1990; *Geller et al.*, 1997] but would not result in any linear correlation. Perhaps in a similar way, the stratospheric QBO influences the underlying troposphere, its effect mixed with that of other phenomena or constrained to operate nonlinearly only at certain times and places.

The most promising connection between the stratospheric QBO and tropical troposphere is found in the interannual variation of Atlantic hurricane activity [*Gray*, 1984a,b; *Shapiro*, 1989; *Hess and Elsner*, 1994; *Landsea et al.*, 1998; *Elsner et al.*, 1999]. Strong hurricanes originating in the tropical Atlantic occur significantly more frequently in seasons when the overlying QBO is westerly or becoming westerly near 50 hPa. The reverse is true in the opposite phase of the QBO. The stratospheric QBO remains one of several predictors of Atlantic hurricane activity in seasonal forecasts issued by W. Gray and collaborators at Colorado State University: http://typhoon.atmos.colostate.edu/forecasts/.

It is unclear whether the QBO has a similar influence on typhoons in the western Pacific [*Chan*, 1995; *Baik and Paek*, 1998; *Lander and Guard*, 1998]. The dynamics of hurricane formation are somewhat different in the two oceanic regions.

A convincing explanation of the QBO's effect on hurricane activity has not been given. Suggestions were made concerning the effect of lower stratospheric vertical wind shear on penetrative convection associated with strong storms [*Gray et al.*, 1992a,b], the effect on lower stratospheric static stability [*Knaff*, 1993], and the effect of QBO winds on the position of critical levels for tropical easterly waves [*Shapiro*, 1989]. Evidence supporting a role of the QBO in hurricane activity is derived from multiple regression in which the predictors are chosen subjectively from experience. The possibility that other forms of quasi-biennial variability might equally well explain the Atlantic hurricane connection has not been explored [*Shapiro*, 1989].

Other apparent effects of the QBO in the troposphere include the remarkable finding of *Chao* [1989] that the Earth's length of day has an interannual variation coherent with the stratospheric QBO's angular momentum. This result reflects the fact that atmospheric angular momentum is intimately connected to the rotation rate of the Earth. In a similar vein, *Del Rio and Cazenave* [1994] discuss a possible effect on polar motion. *Fontaine et al.* [1995] found that contrasting precipitation regimes in west Africa are associated with the stratospheric QBO. *Collimore et al.* [1998] showed a correlation, albeit imperfect, between the QBO and deep convective activity in regions of strong convection. In the realm of much smaller signals, *Hamilton* [1983] found quasi-biennial variability in the amplitude of the semidiurnal surface pressure oscillation. These and other published and unpublished evidences of the QBO's effect on the tropical troposphere remain tantalizing enough for further study, and demonstrate that the stratospheric QBO should be properly simulated in models of the tropical atmosphere.

7. CONCLUSIONS

In a paper summarizing work on the then recently discovered QBO, *Reed* [1967] stated:

> *"Perhaps a simple explanation will soon be found, and what now seems an intriguing mystery will be relegated to the category of a meteorological freak. Or perhaps the phenomenon will prove to have a*

greater significance than we now might envisage, either because of some intrinsic property it possesses or because of its effect on other related areas of research."

With the benefit of more than 3 decades of QBO related research, we can now say assuredly that the QBO is more than a meteorological "freak." Indeed, as we have tried to demonstrate in this review, it does have importance beyond that envisaged in the 1960s, both for its inherent fluid dynamical characteristics and for its relevance to issues of global atmospheric climate and chemistry.

The QBO is a spectacular demonstration of the role of wave, mean-flow interactions in the fluid dynamics of a rotating stratified atmosphere. As has been elegantly argued by *McIntyre* [1993], what makes the dynamics of a rotating stratified atmosphere special is the ubiquitous occurrence of wave motions, and the fact that wave propagation and wave refraction are generally accompanied by a transport of momentum. The QBO could not exist if it were not for momentum transfer by wave propagation and refraction. The dependence of wave refraction on the mean flow provides the mechanism whereby wave-induced momentum fluxes in the equatorial stratosphere can produce a feedback onto the mean flow. In the QBO not only do the oscillating waves interact with the mean flow to produce a flow rectification, but also the rectified flow itself oscillates on a period completely different from that of the driving waves.

Figure 1 shows that the QBO, which in the 1960s was regarded by some as likely to be merely a transient phenomenon, is a very persistent feature of the circulation of the equatorial stratosphere. We now have direct observations of 20 full cycles of the oscillation, and there is indirect evidence covering a much longer time. By study of long-term variations in the solar semidiurnal tidal signal in surface pressure at equatorial stations (which is sensitive to the zonal winds in the stratosphere) *Hamilton* [1983] and *Teitelbaum et al.* [1995] have argued that the QBO must have existed for at least the past 120 years.

This robust nature of the QBO suggests that similar phenomena should be present on other planets with rotating stratified atmospheres and equatorial convection zones. Indeed an analogous oscillation, the quasiquadrennial oscillation (QQO), has been documented in the equatorial atmosphere of Jupiter [*Leovy et al.*, 1991, *Friedson*, 1999The observed meridional scale of the QQO on Jupiter ~7° latitude is about 1/2 that of the terrestrial QBO. For the parameters given by Friedson, this is consistent with the transition scale discussed in Section 3.1, provided that the vertical scale of the forcing is set at 12 km, rather than the 4-km value appropriate for the terrestrial QBO.]. *McIntyre* [1994] has suggested that a similar oscillation may occur in the solar interior.

The possibility of broader implications of the QBO for other areas of research, as suggested by Reed in the above quotation, has certainly proved to be true. As discussed in Section 6.2, the influence of the QBO on interannual climate variations in the extratropical troposphere and the stratosphere is a major subject of current interest. Attempts to better understand and predict trends and variability of atmospheric ozone also require careful consideration of direct and indirect effects of the equatorial QBO on the ozone layer (see Section 5). Thus, models of interannual climate variability and of global stratospheric chemistry both should include the effects of the QBO either explicitly or through some parameterization.

Unfortunately, simulation of the QBO remains a great challenge for general circulation models. Many such models are currently being used for prediction of climate trends and variability associated with human induced changes in the concentrations of various greenhouse gases. Yet, as discussed in Section 3.3.2, most such models are unable to spontaneously generate a realistic QBO. The atmosphere, however, has no such difficulties. A skeptic might argue that the absence of such a robust global-scale dynamical phenomenon is evidence that the models are still far from reality in some important respects. The arguments presented above suggest that gravity waves generated by equatorial convection are essential to forcing of the QBO. This in turn suggests that among other things, better parameterization of the dynamics of convective systems is required if GCMs are to routinely reproduce the fascinating wave, mean-flow feedback interactions that result in the equatorial QBO.

GLOSSARY

β-plane: An approximation of the Coriolis parameter in which $f = f_0 + \beta y$, where beta is a constant. The Coriolis parameter varies linearly in the north-south direction.

Boussinesq limit: A simplification in which density is treated as a constant except where it is coupled to gravity in the buoyancy term of the vertical momentum approximation.

Coriolis Parameter: $f = 2\Omega \sin \phi$, where Ω is the rotation rate of the earth, and ϕ is latitude.

Critical level or line: For a wave propagating on a mean flow, the point at which the wave's phase speed equals the mean flow speed in the direction of wave propagation.

Easterly: From the east.

Eastward: To the east.

Eliassen-Palm (EP) flux: The Eliassen-Palm flux [*Eliassen and Palm*, 1961; *Edmon et al.*, 1980] is a measure of the propagation of wave activity in the latitude-height plane. The convergence of the EP flux is a measure of the (retarding) force exerted by the waves on the zonal-mean flow.

GCM: General Circulation Model

Gravity waves: Oscillations usually of high frequency and short horizontal scale, relative to synoptic-scale motions, that arise in a stably stratified fluid when parcels are displaced vertically.

Inertia-gravity waves: Low-frequency gravity waves that are substantially affected by the Coriolis force.

Kelvin Waves: At the equator, eastward propagating waves with negligible meridional velocity component and Gaussian latitudinal structure in zonal velocity, geopotential, and temperature, symmetric about the equator.

Log-pressure height: A vertical coordinate which is proportional to the logarithm of pressure. It is approximately equal to physical height.

Meridional plane: The latitude-height plane.

Mixed Rossby-gravity waves: Westward propagating waves with meridional velocity maximum on the equator, symmetric about the equator. Zonal wind, geopotential, and temperature are antisymmetric.

MLS: Microwave Limb Sounder

MQBO: Mesospheric quasi-biennial oscillation

NAM: Northern Annular Mode.

NCEP: National Centers for Environmental Prediction (Washington, DC, USA)

Phase of the QBO: Easterly or westerly as defined by the equatorial winds at a precise level. Historically, the level has been 50 to 30 hPa, with 40 hPa being typical.

Planetary-scale waves: Tropical or extratropical disturbances with low zonal wave number (1–3), e.g., equatorial Kelvin waves or Rossby waves in the winter stratosphere.

Planetary wave breaking: Rossby waves owe their existence to meridional gradients in potential vorticity, which provide a restoring force to allow propagation of the waves. In the wintertime stratosphere, the polar vortex provides steep meridional gradients of PV, surrounded by small gradients. At the edge of the vortex, there is overturning (in the meridional direction of PV by Rossby waves as their amplitudes become large. This "wave breaking" results in long, drawn-out tongues of PV and irreversible mixing of PV at small scales.

Rossby waves: See planetary-scale waves.

SAO: Semi-annual oscillation, with a period of six months.

Surf zone: See Rossby wave breaking.

Wave guide: The path of propagation of these waves is analogous to the propagation of light through a medium with a variable index of refraction. For planetary-scale waves, the index of refraction depends on the zonally-averaged zonal wind.

Westerly: From the west.

Westward: To the west.

Zonal: Longitudinal. The zonal wind is positive from the west.

ACKNOWLEDGEMENTS

This review was the outgrowth of a workshop held in March, 1998 in La Jolla, CA, sponsored by the World Climate Research Program (WCRP) Stratospheric Processes and their Role in Climate (SPARC) Initiative and NASA's Atmospheric Chemistry Modeling and Analysis Program. We wish to thank Sandy Grant and Susan Ball for preparing the manuscript and Charles McLandress for comments. The NCEP/NCAR Reanalysis data were provided by the NOAA-CIRES Climate Diagnostics Center. The Singapore zonal wind data were provided by Barbara Naujokat (Free University Berlin). MPB's research was supported by NSF's Climate Dynamics and Large-scale Dynamic Meteorology Program. MPB and TJD were supported by NASA's SR&T Program for Geospace Sciences and NOAA's Office of Global Programs. MJA was supported by NSF's Physical Meteorology Program. WJR was supported by NCAR (sponsored by NSF) and NASA's ACMAP and UARS Programs.

REFERENCES

Alexander, M.J., and L. Pfister, Gravity wave momentum flux in the lower stratosphere over convection, *Geophys. Res. Lett.*, *22*, 2029–2032, 1995.

Alexander, M.J., J.R. Holton, and D.R. Durran, The gravity wave response above deep convection in a squall line simulation, *J. Atmos. Sci.*, *52*, 2212–2226, 1995.

Alexander, M.J., and J.R. Holton, A model study of zonal forcing in the equatorial stratosphere by convectively induced gravity waves, *J. Atmos. Sci.*, *54*, 408–419, 1997.

Alexander, M.J., J. Beres, and L. Pfister, Tropical stratospheric gravity waves and cloud correlations, *J. Geophys. Res.* ***(submitted)*, 1999.**

Allen, S.J., and R.A. Vincent, Gravity waves activity in the lower atmosphere: seasonal and latitudinal variations, *J. Geophys. Res.*, *100*, 1327–1350, 1995.

Andrews, D.G., and M.E. McIntyre, Planetary waves in horizontal and vertical shear; the generalized Eliassen–Palm relation and the mean zonal acceleration, *J. Atmos. Sci.*, *33*, 2031–2048, 1976.

Andrews, D.G., J.R. Holton, and C.B. Leovy, *Middle Atmosphere Dynamics*, 489 pp., Academic Press, 1987.

Angell, J.K., and J. Korshover, Quasi-biennial variations in temperature, total ozone, and tropopause height, *J. Atmos. Sci.*, *21*, 479–492, 1964.

Angell, J.K., and J. Korshover, Evidence for a quasi-biennial variation in eccentricity of the North Polar vortex, *J. Atmos. Sci.*, **–, 634**–635, 1975.

Baik, J.–J., and J.–S. Paek, a climatology of sea surface temperature and the maximum intensity of western north Pacific tropical cyclones, *J. Meteor. Soc. Japan*, *76*, 129–137, 1998.

Balachandran, N.K., and D.Rind, Modeling the effects of UV variability and the QBO on the troposphere-stratosphere system. Part I: The middle atmosphere, *J. Climate*, *8*, 2058–2079, 1995.

Baldwin, M.P., and T.J. Dunkerton, Quasi-biennial oscillation above 10 mb, *Geophys. Res. Lett.*, *18*, 1205–1208, 1991.

Baldwin, M.P., X. Cheng, and T.J. Dunkerton, Observed correlation between winter-mean tropospheric and stratospheric circulation anomalies, *Geophys. Res. Lett.*, *21*, 1140–1144, 1994.

Baldwin, M.P., and K.–J. Tung, Extra-tropical QBO signals in angular momentum and wave forcing, *Geophys. Res. Lett.*, *21*, 2717–2720, 1994.

Baldwin, M.P., and D. O'Sullivan, Stratospheric effects of ENSO-related tropospheric circulation anomalies, *J. Climate*, *4*, 649–667, 1995.

Baldwin, M., and T. Dunkerton, Biennial, quasi-biennial, and decadal oscillations of potential vorticity in the northern stratosphere, *J. Geophys. Res.*, *103*, 3919–3928, 1998a.

Baldwin, M.P., and T.J. Dunkerton, Quasi-biennial modulations of the southern hemisphere stratospheric polar vortex, *Geophys. Res. Lett.*, *25*, 3343–3346, 1998b.

Baldwin, M.P., and T.J. Dunkerton, Downward propagation of the Arctic Oscillation from the stratosphere to the troposphere, *J. Geophys. Res.*, 30,937–30,946, 1999.

Baldwin, M.P., and T.J. Dunkerton, Propagation of annular modes from the mesosphere to the Earth's surface, *Nature*, submitted, 2000.

Barnett, T.P., The interaction of multiple time scales in the tropical climate system, *J. Climate*, *4*, 269–285, 1991.

Barnston, A.G., and R.E. Livezey, A closer look at the effect of the 11-year solar cycle and the QBO on the northern hemisphere 700 mb height and extratropical North American surface temperature, *J. Climate*, *2*, 1295–1313, 1987.

Bergman, J.W., and M.L. Salby, Equatorial waves activity derived from fluctuations in observed convection, *J. Atmos. Sci.*, *51*, 3791–3806, 1994.

Booker, J.R., and F.B. Bretherton, The critical layer for internal gravity waves in a shear flow, *J. Fluid Mech.*, *27*, 513–539, 1967.

Boville, B.A., The influence of the polar night jet on the tropospheric circulation in a GCM, *J. Atmos. Sci.*, *41*, 1132–1142, 1984.

Boville, B.A., Wave-mean flow interactions in a general circulation model of the troposphere and stratosphere, *J. Atmos. Sci.*, *43*, 1711–1725, 1986.

Boville, B.A., and W.J. Randel, Equatorial waves in a stratospheric CGM: effects of vertical resolution, *J. Atmos. Sci.*, *49*, 785–801, 1992.

Bowman, K.P., Global patterns of the quasi biennial oscillation in total ozone, *J. Atmos. Sci.*, *46*, 3328–3343, 1989.

Boyd, J.P., The effects of latitudinal shear on equatorial waves, Part 1: theory and methods, *J. Atmos. Sci.*, *35*, 2236–2258, 1978.

Burrage, M.D., R.A. Vincent, H.G. Mayr, W.R. Skinner, N.F. Arnold, and P.B. Hays, Long-term variability of the equatorial middle atmosphere zonal wind, *J. Geophys. Res.*, *101*, 12,847–12,854, 1996.

Butchart, N., and J. Austin, On the relationship between the quasi biennial oscillation, total chlorine and the severity of the Antarctic ozone hole, *Quart. J. Roy. Meteor. Soc.*, *122*, 183–217, 1996.

Cadet, D., and H. Teitelbaum, Observational evidence of internal inertia-gravity waves in the tropical stratosphere, *J. Atmos. Sci.*, *36*, 892–907, 1979.

Canziani, P.O., J.R. Holton, E. Fishbein, and L. Froidevaux, Equatorial Kelvin wave variability during 1992 and 1993, *J. Geophys. Res.*, *100*, 5193–5202, 1995.

Canziani, P.O., and J.R. Holton, Kelvin waves and the quasi-biennial oscillation: An observational analysis, *J. Geophys. Res.*, *103* (31), 509–531, 521, 1998.

Chan, J.C.L., Tropical cyclone activity in the western north Pacific in relation to the stratospheric quasi-biennial oscillation, *Mon. Wea. Rev.*, *123*, 2567–2571, 1995.

Chao, B.F., Length-of-day variations caused by El Nino — southern oscillation and quasi-biennial oscillation, *Science*, *243*, 923–926, 1989.

Charney, J.G., and P.G. Drazin, Propagation of planetary-scale disturbances from the lower into the upper atmosphere, *J. Geophy. Res.*, *66*, 83–109, 1961.

Chen, P., The influences of zonal flow on wave breaking and tropical-extratropical interaction in the lower stratosphere, *J. Atmos. Sci.*, *53*, 2379–2392, 1996.

Chipperfield, M.P., L.J. Gray, J.S. Kinnersley, and J. Zawodny, A two dimensional model study of the QBO signal in SAGE II NO2 and 03, *Geophys. Res. Letts.*, *21*, 589–592, 1994.

Choi, W., W.B. Grant, J.H. Park, K.–M. Lee, H. Lee, and J.M.R. III, Role of the quasi biennial oscillation in the transport of aerosols from the tropical stratosphere reservoir to mid-latitudes, *J. Geophys. Res.*, *103*, 6033–6042, 1998.

CIRA-1986, Part II Middle Atmosphere Models, D. Rees, J.J. Barnett, K. Labitzke (ed.), *Advances in Space Research (COSPAR)*, 10, Number 12, 1990.

Collimore, C.C., M.H. Hitchman, and D.W. Martin, Is there a quasi-biennial oscillation in tropical deep convection?, *Geophys. Res. Lett.*, *25*, 333–336, 1998.

Cornish, C.R., and M.F. Larsen, A review of synoptic scale wave perturbations in the equatorial stratosphere, *J. Atmos. Terr. Phys.*, *47*, 769–780, 1985.

Dameris, M., and A. Ebel, The quasi-biennial oscillation and major stratospheric warmings: A three-dimensional model study, *Annales Geophysicae*, *8*, 79–85, 1990.

Del Rio, R.A., and A. Cazenave, Interannual variations in the Earth's polar motion for 1963–1991: Comparison with atmospheric angular momentum over 1980–1991, *Geophys. Res. Lett.*, *21*, 2361–2364, 1994.

Dunkerton, T.J., Wave transience in a compressible atmosphere, part 2: transient equatorial waves in the biennial oscillation, *J. Atmos. Sci.*, *38*, 298–307, **1981b.**

Dunkerton, T.J., The evolution of latidudinal shear in Rossby-gravity wave, mean flow interaction, *J. Geophys. Res.*, *88*, 3836–3842, 1983a.

Dunkerton, T.J., Laterally-propagating Rossby waves in the easterly acceleration phase of the quasi-biennial oscillation, *Atmos- Ocean*, *21*, 55–68, 1983b.

Dunkerton, T.J., A two-dimensional model of the quasi-biennial oscillation, *J. Atmos. Sci.*, *42*, 1151–1160, 1985.

Dunkerton, T.J., and D.P. Delisi, Climatology of the equatorial lower stratosphere, *J. Atmos. Sci.*, *42*, 376–396, 1985.

Dunkerton, T.J., Annual variation of deseasonalized mean flow acceleration in the equatorial lower stratosphere, *J. Meteor. Soc. Japan*, *68*, 499–508, 1990.

Dunkerton, T.J., Nonlinear propagation of zonal winds in an atmosphere with Newtonian cooling and equatorial wavedriving, *J. Atmos. Sci.*, *48*, 236–263, 1991a.

Dunkerton, T.J., Intensity variation and coherence of 3–6 day equatorial waves, *Geophys. Res. Lett.*, *18*, 1469–1472, 1991b.

Dunkerton, T.J., and M.P. Baldwin, Quasi-biennial modulation of planetary-wave fluxes in the Northern Hemisphere winter, *J. Atmos. Sci.*, *48*, 1043–1061, 1991.

Dunkerton, T.J., Observation of 3–6 day meridional wind oscillations over the tropical Pacific, 1973–1992: vertical structure and interannual variability, *J. Atmos. Sci.*, *50*, 3292–3307, 1993.

Dunkerton, T.J., Horizontal buoyancy flux of internal gravity waves in vertical shear, *J. Meteor. Soc. Japan*, *73*, 747–755, 1995.

Dunkerton, T.J., and D.J. O'Sullivan, Mixing zone in the tropical stratosphere above 10 mb, *Geophys. Res. Lett.* (23), 2497–2500, 1996.

Dunkerton, T.J., The role of gravity waves in the quasi-biennial oscillation, *J. Geophys. Res.*, *102*, 26,053–26,076, 1997.

Dunkerton, T.J., Quasi-biennial and sub-biennial variations of stratospheric trace constituents derived from HALOE observations, *J. Atmos. Sci.*, in press, 2000.

Ebdon, R.A., Notes on the wind flow at 50 mb in tropical and subtropical regions in January 1957 and in 1958, *Quart. J. Royal Meteor. Soc.*, *86*, 540–542, 1960.

Ebdon, R.A., and R.G. Veryard, Fluctuations in equatorial stratospheric winds, *Nature*, *189*, 791–793, 1961.

Edmon, H.J., B.J. Hoskins, and M.E. McIntyre, Eliassen–Palm cross sections for the troposphere, *J. Atmos. Sci.*, *37*, 2600–2616, 1980.

Eliassen, A., and E.E. Palm, On the transport of energy in stationary mountain waves, *Geophys. Publ.*, *22*, 1–23, 1961.

Elsner, J.B., A.B. Kara, and M.A. Owens, Fluctuations in north Atlantic hurricane frequency, *J. Climate*, *12*, 427–437, 1999.

Fontaine, B., S. Janicot, and V. Moron, Rainfall anomaly patterns and wind field signals over west Africa in August, *J. Climate*, *8*, 1503–1510, 1995.

Fovell, R., D. Durran, and J.R. Holton, Numerical simulations of convectively generated stratospheric gravity waves, *J. Atmos. Sci.*, *49*, 1427–1442, 1992.

Friedson, A.J., New observations and modelling of a QBO-like oscillation in Jupiter's stratosphere, *Icarus*, *137*, 34–55, 1999.

Funk, J.P., and G.L. Garnham, Australian ozone observations and a suggested 24 month cycle, *Tellus*, *14*, 378–382, 1962.

Garcia, R.R., On the mean meridional circulation of the middle atmosphere, *J. Atmos. Sci.*, *41*, 2113–2125, 1987.

Garcia, R.R., and S. Solomon, A possible relationship between interannual variability in Antarctic ozone and the quasi biennial oscillation, *Geophys. Res. Letts.*, *14*, 848–851, 1987.

Garcia, R.R., T.J. Dunkerton, R.S. Lieberman, and R.A. Vincent, Climatology of the semiannual oscillation in the tropical middle atmosphere, *J. Geophys. Res.*, *102*, 26,019–26,032, 1997.

Geller, M.A., W. Shen, M. Zhang, and W.–W. Tan, Calculations of the stratospheric quasi-biennial oscillation for time-varying wave forcing, *J. Atmos. Sci.*, *54*, 883–894, 1997.

Grant, W.B., E.V. Browell, C.S. Long, L.L. Stowe, R.G. Grainger, and A. Lambert, Use of volcanic aerosols to

study the tropical stratospheric reservoir, *J. Geophy. Res.*, *101*, 3973–3988, 1996.

Gray, L.J., and J.A. Pyle, A two-dimensional model of the quasi-biennial oscillation in ozone, *J. Atmos. Sci.*, *46*, 203–220, 1989.

Gray, L.J., and M.P. Chipperfield, On the interannual variability of trace gases in the middle atmosphere, *Geophys. Res. Lett.*, *17*, 933–936, 1990.

Gray, L.J., and T.J. Dunkerton, The role of the seasonal cycle in the quasi biennial oscillation of ozone, *J. Atmos. Sci.*, *47*, 2429–2451, 1990.

Gray, L.J., and S.L. Ruth, The modeled latitudinal distribution of the ozone quasi biennial oscillation using observed equatorial winds, *J. Atmos. Sci.*, *50*, 1033–1046, 1993.

Gray, L.J., and J.M. Russell III, Interannual variability of trace gases in the subtropical winter stratosphere, *J. Atmos. Sci.*, *56*, 977–993, 1999.

Gray, L.J., 2000

Gray, L.J., S.J. Phipps, T.J. Dunkerton, M.P. Baldwin, E.F. Drysdale, and M.R. Allen, The influence of the equatorial upper stratosphere on northern Hemisphere stratospheric sudden warmings, *Q. J. Royal Meteor. Soc.*, submitted, 2000.

Gray, W.M., Atlantic seasonal hurricane frequency. Part I: El nino and 30 mb quasi-biennial oscillation influences, *Mon. Wea. Rev.*, *112*, 1649–1668, 1984a.

Gray, W.M., Atlantic seasonal hurricane frequency. Part II: forecasting its variability, *Mon. Wea Rev.*, *112*, 1669–1683, 1984b.

Gray, W.M., J.D. Sheaffer, and J.A. Knaff, Hypothesized mechanism for stratospheric QBO influence on ENSO variability, *Geophys. Res. Lett.*, *19*, 107–110, 1992a.

Gray, W.M., J.D. Sheaffer, and J.A. Knaff, Influence of the stratospheric QBO on ENSO variability, *J. Meteor. Soc. Japan*, *70*, 975–995, 1992b.

Graystone, P., Meteorological office discussion — tropical meteorology, *Meteor. Mag.*, *88*, 113–119, 1959.

Gutzler, D.S., and D.E. Harrison, The structure and evolution of seasonal wind anomalies over the near-equatorial eastern Indian and western Pacific oceans, *Mon. Wea. Rev.*, *115*, 169–192, 1987.

Haigh, J.D., The role of stratospheric ozone in modulating the solar radiative forcing of climate, *Nature*, *370*, 544–546, 1994.

Haigh, J.D., The impact of solar variability on climate, *Science*, *272*, 981–984, 1996.

Haigh, J.D., A GCM study of climate change in response to the annual 11-year solar cycle, *Q.J. Roy. Meteorol. Soc.*, *125* (817–892), 1999.

Hamilton, K., The vertical structure of the quasi-biennial oscillation: observations and theory, *Atmos. – Ocean*, *19*, 236–250, 1981.

Hamilton, K., Quasi-biennial and other long-period variations in the solar semidiurnal barometric oscillation: observations, theory and possible application to the problem of monitoring changes in global ozone, *J. Atmos. Sci.*, *40*, 2432–2443, 1983.

Hamilton, K., Mean wind evolution through the quasi-biennial cycle of the tropical lower stratosphere, *J. Atmos. Sci.*, *41*, 2113–2125, 1984.

Hamilton, K., Interhemispheric asymmetry and annual synchronisation of the ozone quasi biennial oscillation, *J. Atmos. Sci.*, *46*, 1019–1025, 1989.

Hamilton, K., An examinaton of observed southern oscillation effects in the northern hemisphere stratosphere, *J. Atmos. Sci.*, *50*, 3468–3473, 1993.

Hamilton, K., Interannual variability in the Northern Hemisphere winter middle atmosphere in control and perturbed experiments with the GFDL SKYHI general circulation model, *J. Atmos. Sci.*, *52(1)*, 44–66, 1995.

Hamilton, K., Observations of tropical stratospheric winds before World War II. *Bull. Amer. Meteorol. Soc.*, 79, 1367-1371, 1998a.

Hamilton, K., Effects of an imposed quasi-biennial oscillation in a comprehensive troposphere-stratosphere-mesosphere general circulation model, *J. Atmos. Sci.*, *55*, 2393–2418, 1998b.

Hamilton, K., R.J. Wilson, and R. Hemler, Middle atmosphere simulated with high vertical and horizontal resolution versions of a GCM: Improvement in the cold pole bias and generation of a QBO-like oscillation in the tropics, *J. Atmos. Sci.*, *56*, 3829–3846, 1999.

Hasebe, F., Quasi-biennial oscillations of ozone and diabatic circulation in the equatorial stratosphere, *J. Atmos. Sci.*, *51*, 729–745, 1994.

Hayashi, Y., and D.G. Golder, Kelvin and mixed Rossby-gravity waves appearing in the GFDL 'SKYHI' general circulation and the FGGE dataset: implications for their generation mechanism and role in the QBO, *J. Meteor. Soc. Japan*, *72*, 901–935, 1994.

Haynes, P.H., The latitudinal structure of the quasi-biennial oscillation, *Quart. J. Roy. Meteorol. Soc.*, *124* (2645–2670), 1998.

Hess, J.C., and J.B. Elsner, Extended-range hindcasts of tropical-origin Atlantic hurricane activity, *Geophys. Res. Lett.*, *21*, 365–368, 1994.

Hess, P.G., and D. O'Sullivan, A three dimensional modelling study of the extratropical quasi biennial oscillation in ozone, *J. Atmos. Sci.*, *52*, 1539–1554, 1995.

Hilsenrath, E., and B.M. Schlesinger, Total ozone seasonal and interannual variations derived from the 7 year Nimbus-4 BUV dataset, *J. Geophys. Res.*, *86*, 12,087–12,096, 1981.

Hines, C.O., Doppler-spread parameterization of gravity wave momentum deposition in the middle atmosphere .

2: Broad and quasi-monochromatic spectra, and implementation, *J. Atmos. Terr. Phys.* 59, 387-400, 1997.

Hirota, I., Equatorial waves in the upper stratosphere and mesosphere in relation to the semiannual oscillation of the zonal wind, *J. Atmos. Sci.*, *35*, 714–722, 1978.

Hitchman, M.H., C.B. Leovy, J.C. Gille, and P.L. Baily, Quasi-stationary asymmetric circulations in the equatorial lower mesosphere, *J. Atmos. Sci.*, *44*, 2219–2236, 1987.

Hitchman, M.H., M. McKay, and C.R. Trepte, A climatology of stratospheric aerosol, *J. Geophys. Res.*, *99*, 20,689–20,700, 1994.

Holton, J.R., and R.S. Lindzen, An updated theory for the quasi-biennial cycle of the tropical stratosphere, *J. Atmos. Sci.*, *29*, 1076–1080, 1972.

Holton, J.R., *The Dynamic Meteorology of the Stratosphere and Mesosphere*, 319 pp., Amer. Meteor. Soc., 1975.

Holton, J.R., and H.–C. Tan, The influence of the equatorial quasi-biennial oscillation on the global circulation at 50 mb, *J. Atmos. Sci.*, *37*, 22,00–22,08, 1980.

Holton, J.R., and H.–C. Tan, The quasi-biennial oscillation in the Northern Hemisphere lower stratosphere, *J. Meteor. Soc. Japan*, *60*, 140–148, 1982.

Holton, J.R., Influence of the annual cycle in meridional transport on the quasi biennial oscillation in total ozone, *J. Atmos. Sci.*, *46*, 1434–1439, 1989.

Holton, J.R., and J. Austin, The influence of the QBO on sudden stratospheric warmings, *J. Atmos. Sci.*, *48*, 607–618, 1991.

Holton, J.R., P.H. Hayes, M.E. McIntyre, A.R. Douglass, R.B. Hood, and L. Pfister, Stratosphere-troposphere exchange, *Rev. Geophys.*, *33*, 403–439, 1995.

Horinouchi, T., and S. Yoden, Excitation of transient waves by localized episode heating in the tropics and their propagation in the middle atmosphere, *J. Meteor. Soc. Japan*, *74*, 189–210, 1996.

Horinouchi, T., and S. Yoden, Wave-mean flow interaction associated with a QBO-like oscillation simulated in a simplified GCM, *J. Atmos. Sci.*, *55*, 502–526, 1998.

Huang, T.Y.W., The impact of solar radiation on the quasi-biennial oscillation of ozone in the tropical stratosphere, *Geophys. Res. Letts.*, *23(22)*, 3211–3214, 1996.

Jones, D.B.A., H.R. Schneider, and M.B. McElroy, Effects of the quasi-biennial oscillation on the zonally averaged transport of tracers, *J. Geophys. Res.*, *103*, 11,235–11,249, 1998.

Jones, D.B.A., H.R. Schneider, and M.B. McElroy, An analysis of the mechanisms for the QBO in ozone in the tropical and subtropical lower stratosphere, ***Submitted to J. Geophys. Res.***, 1999.

Karoly, D.J., G.L. Roff, and M.J. Reeder, Gravity wave activity associated with tropical convection detected in TOGA COARE sounding data, *Geophys. Res. Lett.*, *23*, 261–264, 1996.

Kawamoto, N., M. Shiotani, and J.C. Gille, Equatorial Kelvin waves and corresponding tracer oscillations in the lower stratosphere as seen in LIMS data, *J. Meteor. Soc. Japan*, *75*, 763–773, 1997.

Kawamura, R., Quasi-biennial oscillation modes appearing in the tropical sea water temperature and 700 mb zonal wind, *J. Meteor. Soc. Japan*, *66*, 955–965, 1988.

Kinnersley, J.S., and S. Pawson, The descent rates of the shear zones of the equatorial QBO, *J. Atmos. Sci.*, *53*, 1937–1949, 1996.

Kinnersley, J.S., and K.K. Tung, Modeling the global interannual variability of ozone due to the equatorial QBO and to extratropical planetary wave variability, *J. Geophys. Res.*, *94*, 11,559–11,571, 1998.

Kinnersley, J.S., On the seasonal asymmetry of the lower and middle latitude QBO circulation anomaly, *J. Atmos. Sci.*, *56*, 1942–1962, 1999.

Knaff, J.A., Evidence of a stratospheric QBO modulation of tropical convection, ?????? Colorado State University, 1993.

Kodera, K., K. Yamazaki, M. Chiba, and K. Shibata, Downward propagation of upper stratospheric mean zonal wind perturbation to the troposphere, *Geophys. Res. Lett.*, *17*, 1263–1266, 1990.

Labitzke, K., Sunspots, the QBO, and the stratospheric temperature in the north polar region, *Geophys. Res. Lett.*, *14*, 535–537, 1987.

Labitzke, K., and H. van Loon, Association between the 11-year solar cycle, the QBO and the atmosphere. Part I: The troposphere and stratosphere in the northern hemisphere in winter, *J. Atmos. Terr. Phys.*, *50*, 197–206, 1988.

Lait, L.R., M.R. Schoeberl, and P.A. Newman, Quasi-biennial modulation of the Antarctic ozone depletion, *J. Geophy. Res.*, *94*, 11559–11571, 1989.

Lander, M.A., and C.P. Guard, A look at global tropical cyclone activity during 1995: contrasting high Atlantic activity with low activity in other basins, *Mon. Wea. Rev.*, *126*, 1163–1173, 1998.

Landsea, C.W., G.D. Bell, W.M. Gray, and S.B. Goldenberg, The extremely active 1995 Atlantic hurricane season: environmental conditions and verification of seasonal forecasts, *Mon. Wea. Rev.*, *126*, **1174–??**, 1998.

Larsen, M.F., W.E. Schwartz, and R.F. Woodman, Gravity wave generation by thunderstorms observed with a vertically-pointing 430 MHz radar, *Geophys. Res. Lett.*, *9*, 571–574, 1982.

Lau, K.–M., and P.J. Sheu, Annual cycle, quasi-biennial oscillation, and southern oscillation in global precipitation, *J. Geophys. Res.*, *93*, 10,975–10,988, 1988.

Leovy, C.B., A.J. Friedson, and G.S. Orton, The quasiquadrennial oscillation of Jupiter's equatorial stratosphere, *Nature*, *354*, 380–382, 1991.

Li, D., K.P. Shine, and L.J. Gray, The role of ozone-induced diabatic heating anomalies in the quasi-biennial oscillation, *Quart. J. Roy. Meteor. Soc.*, *121*, 937–943, 1995.

Li, X., P.L. Read, and D.G. Andrews, Mode selection, wave breaking and parametric sensitivity in the quasi-biennial oscillation, *Quart. J. Roy. Meteor. Soc.*, *123*, 2041–2068, 1997.

Lindzen, R.S., and J.R. Holton, A theory of the quasi-biennial oscillation, *J. Atmos. Sci.*, *25*, 1095–1107, 1968.

Lindzen, R.S., Vertical momentum transport by large-scale disturbances in the equatorial lower stratosphere, *J. Meteor. Soc. Japan*, *48*, 81–83, 1970.

Lindzen, R.S., On the development of the theory of the QBO, *Bull. Amer. Meteor.*, *68*, 329–337, 1987.

Ling, X.–D., and J. London, The quasi biennial oscillation of ozone in the tropical middle stratosphere: a one dimensional model, *J. Atmos. Sci.*, *43*, 3122–3136, 1986.

Luo, M., J.M.R. III, and T.Y.W. Huang, Halogen Occultation Experiment obervations of the quasi biennial oscillation and the effects of Pinatubo aerosols in the tropical stratosphere, *J. Geophys. Res.*, *102*, 19,187–**19,219 & 198, 1997**.

Manzini, E., G. Visconti, G. Pitari, and M. Verdecchia, An estimate of the Antarctic ozone modulation by the QBO, *Geophys. Res. Lett.*, *18*, 175–178, 1991.

Marquardt, C., QBO-related extratropical variability in the northern hemisphere stratosphere: Biennial Oscillation versus Triple Peak Spectra, , **1999 (in preparation).**

Maruyama, T., Large-scale disturbances in the equatorial lower stratosphere, *J. Meteor. Soc. Japan*, *45*, 196–199, 1967.

Maruyama, T., and Y. Tsuneoka, Anomalously short duration of the easterly wind phase of QBO at 50 hPa in 1987 and its relation with an El Nino event, *J. Meteor. Soc. Japan*, *69*, 219–232, 1988.

Maruyama, T., Annual and QBO-synchronized variations of lower-stratospheric equatorial wave activity over Singapore during 1961–1989, *J. Meteor. Soc. Japan*, *69*, 219–232, 1991.

Maruyama, T., Upward transport of westerly momentum due to disturbances of the equatorial lower stratosphere in the period range of about 2 days — Singapore data analysis for 1983–1993, *J. Meteor. Soc. Japan*, *72*, 423–432, 1994.

Maruyama, T., The quasi-biennial oscillation (QBO) and equatorial waves — a historical review, *Papers Meteor. Geophys.*, *48*, 1–17, 1997.

Matsuno, T., Quasi-geostrophic motions in the equatorial area, *J. Meteor. Soc. Japan*, *44*, 25–43, 1966.

Mayr, H.G., J.G. Mengel, C.O. Hines, K.L. Chan, N.F. Arnold, C.A. Reddy, and H.S. Porter, The gravity wave Doppler spread theory applied in a numerical spectral model of the middle atmosphere, 2, Equatorial oscillations, *J. Geophys. Res.*, *102*, 26,093–26,105, 1997.

McIntyre, M.E., and T.N. Palmer, Breaking planetary waves in the stratosphere, *Nature*, *305*, 593–600, 1983.

McIntyre, M.E., and T.N. Palmer, The 'surf zone' in the stratosphere, *J. Atmos. Terr. Phys.*, *46*, 825–849, 1984.

McIntyre, M.E., On the role of wave propagation and wave breaking in atmosphere-ocean dynamics, in *In Theoretical and Applied Mechanics 1992*, edited by J.S. S. R. Bodner, A. Solan and Z. Hashin, pp. 281–304, Elsevier Science Publishers B. V., Amsterdam, New York, 1993.

McIntyre, M.E., McIntyre, M. E., 1994: The quasi-biennial oscillation (QBO): some points about the terrestrial QBO and the possibility of related phenomena in the solar interior, in *In The Solar Engine and its Influence on the Terrestrial Atmosphere and Climate*, edited by E. Nesme–Ribes, pp. 293–320, Springer–Verlag, 1994.

Mengel, J.G., H.G. Mayr, K.L. Chan, C.O. Hines, C.A. Reddy, N.F. Arnold, and H.S. Porter, Equatorial oscillations in the middle atmosphere generated by small scale gravity waves, *Geophys. Res. Lett.*, *22*, 3027–30, 1995.

Moron, V., B. Fontaine, and P.Roucou, Global equatorial variability of 850 and 200 hPa zonal winds from rawinsondes between 1963 and 1989, *Geophys. Res. Lett.*, *22*, 1701–1704, 1995.

Mote, P.W., K.H. Rosenlof, M. McIntyre, E.S. Carr, J.C. Gille, J.R. Holton, J.S. Kinnersley, H.C. Pumphrey, J.M. Russell, and J.W. Waters, An atmospheric tape recorder: The imprint of tropical tropopause temperatures on stratospheric water vapor, *J. Geophys. Res.*, *101*, 3989–4006, 1996.

Mote, P.W., T.J. Dunkerton, and H.C. Pumphrey, Subseasonal variations in lower stratospheric water vapor, *Geophys. Res. Lett.*, *25*, 2445–2448, 1998.

Nagashima, T., M. Takahashi, and F. Hasebe, The first simulation of an ozone QBO in a general circulation model, *Geophys. Res. Letts.*, *25*, 3131–3134, 1998.

Naito, Y., and I. Hirota, Interannual variability of the northern winter stratospheric circulation related to the QBO and the solar cycle, *J. Meteor. Soc. Japan*, *75*, 925–937, 1997.

Naujokat, B., An update of the observed quasi-biennial oscillation of the stratospheric winds over the tropics, *J. Atmos. Sci.*, *43*, 1873–1877, 1986.

Nigam, S., On the structure of variability of the observed tropospheric and stratospheric zonal-mean wind, *J. Atmos. Sci.*, *47*, 1799–1813, 1990.

Nitta, T., Statistical study of tropical wave disturbances in the tropical Pacific region, *J. Meteor. Soc. Japan*, *48*, 47–60, 1970.

Niwano, M., and M. Takahashi, Notes and Correspondence: The influence of the equatorial QBO on the Northern Hemisphere winter circulation of a GCM, *J. Meteor. Soc. Japan*, *76(3)*, 1998, 453–461.

O'Sullivan, D., and M.L. Salby, Coupling of the quasi-biennial oscillation and the extratropical circulation in the

stratosphere through planetary wave transport, *J. Atmos. Sci.*, *47*, 650–673, 1990.

O'Sullivan, D., and R.E. Young, Modeling the quasi-biennial oscillation's effect on the winter stratospheric circulation, *J. Atmos. Sci.*, *49*, 2437–2448, 1992.

O'Sullivan, D., and T.J. Dunkerton, Seasonal development of the extratropical QBO in a numerical model of the middle atmosphere, *J. Atmos. Sci.*, *51*, 3706–3721, 1994.

O'Sullivan, D., and P. Chen, Modeling the QBO's influence on isentropic tracer transport in the subtropics, *J. Geophys. Res.*, *101*, 6811–6821, 1996.

O'Sullivan, D., and T.J. Dunkerton, The influence of the quasi-biennial oscillation on global constituent distributions, *J. Geophys. Res.*, *102*, 21,731–21,743, 1997.

O'Sullivan, D.J., Interaction of extratropical Rossby waves with westerly quasi-biennial oscillation winds, *J. Geophys. Res.*, *102*, 19,461–19,469, 1997.

Oltmans, S.J., and J. London, The quasi biennial oscillation in atmospheric ozone, *J. Geophys. Res.*, *87*, 8981–8989, 1982.

Ortland, D.A., Rossby wave propagation into the tropical stratosphere observed by the High Resolution Doppler imager, *Geophys. Res. Lett.*, *24*, 1999–2002, 1997.

Palmer, C.E., The general circulation between 200 mb and 10 mb over the Equatorial Pacific, *Weather*, *9*, 3541–3549, 1954.

Pawson, S., and M. Fiorino, A comparison of reanalyses in the tropical stratosphere, Part 1: Thermal structure and the annual cycle, *Clim. Dyn.*, *14*, 631–644, 1998.

Pawson, S., K. Labitzke, R. Lenschow, B. Naujokat, B. Rajewski, M. Wiesner, and R.–C. Wohlfart, Climatology of the Northern Hemisphere Stratosphere Derived from Berlin Analyses. Part 1: Monthly Means. Meteorolog. Abhaudlunger, Freie Univeritat Berlin, Series A, Vol. 7, No. 3., 1993.

Pfister, L., W. Starr, R. Craig, M. Loewenstein, and M. Legg, Small scale motions observed by aircraft in the tropical lower stratosphere: evidence for mixing and its relationship to large scale flows, *J. Atmos. Sci.*, *43*, 3210–3225, 1986.

Pfister, L., S. Scott, M. Loewenstein, S. Bowen, and M. Legg, Mesoscale disturbances in the tropical stratosphere excited by convection: observations and effects on the stratospheric momentum budget, *J. Atmos. Sci.*, *50*, 1058–1075, 1993a.

Pfister, L., K.R. Chan, T.P. Bui, S. Bowen, M. Legg, B. Gary, K. Kelly, M. Proffitt, and W. Starr, Gravity waves generated by a tropical cyclone during the STEP tropical field program: a case study, *J. Geophys. Res.*, *98*, 8611–8638, 1993b.

Plumb, R.A., The interaction of two internal waves with the mean flow: implications for the theory of the quasi-biennial oscillation, *J. Atmos. Sci.*, *34*, 1847–1858, 1977.

Plumb, R.A., and A.D. McEwan, The instability of a forced standing wave in a viscous stratified fluid: a laboratory analogue of the quasi-biennial oscillation, *J. Atmos. Sci.*, *35*, 1827–1839, 1978.

Plumb, R.A., Zonally symmetric Hough modes and meridional circulations in the middle atmosphere, *J. Atmos. Sci.*, *39*, 983–991, 1982.

Plumb, R.A., and R.C. Bell, Equatorial waves in steady zonal shear flow, *Quart. J. Roy. Meteor. Soc.*, *108*, 313–334, 1982a.

Plumb, R.A., and R.C. Bell, A model of the quasi-biennial oscillation on an equatorial beta-plane, *Quart. J. Roy. Meteor. Soc.*, *108*, 335–352, 1982b.

Politowicz, P.A., and M.H. Hitchman, Exploring the effects of forcing the quasi biennial oscillation in a two dimensional model, *J. Geophys. Res.*, *102*, 16,481–16,497, 1997.

Poole, L.R., S. Solomon, M.P. McCormick, and M.C. Pitts, The interannual variability of polar stratospheric clouds and related parameters in Antarctica during September and October, *Geophys. Res. Letts.*, *16*, 1157–1160, 1989.

Ramanathan, K.R., Bi-annual variation of atmospheric ozone over the tropics, *Quart. J. Roy. Meteor. Soc.*, *89*, 540–542, 1963.

Randel, W.J., The evaluation of winds from geopotential height data in the stratosphere, *J. Atmos. Sci.*, *44*, 3097–3120, 1987.

Randel, W.J., Kelvin wave induced trace constituent oscillations in the equatorial stratosphere, *J. Geophys. Res.*, *95*, 18,641–18,652, 1990.

Randel, W.J., and J.B. Cobb, Coherent variations of monthly mean column ozone and lower stratospheric temperature, *J. Geophys. Res.*, *99*, 5433–5447, 1994.

Randel, W.J., and F. Wu, Isolation of the ozone QBO in SAGE II data by singular decomposition, *J. Atmos. Sci.*, *53*, 2546–2559, 1996.

Randel, W.J., F. Wu, J.M.R. III, A. Roche, and J. Waters, Seasonal cycles and QBO variations in stratospheric CH_4 and H_2O observed in UARS HALOE data, *J. Atmos. Sci.*, *55*, 163–185, 1998.

Randel, W.J., F. Wu, R. Swinbank, J. Nash, and A. O'Neill, Global QBO circulation derived from UKMO stratospheric analyses, *J. Atmos. Sci.*, *56*, 457–474, 1999.

Reed, R.J., W.J. Campbell, L.A. Rasmussen, and R.G. Rogers, Evidence of a downward propagating annual wind reversal in the equatorial stratosphere, *J. Geophys. Res.*, *66*, 813–818, 1961.

Reed, R.J., A tentative model of the 26-month oscillation in tropical latitudes, *Quart. J. Roy. Meteor. Soc.*, *90*, 441–466, 1964.

Reed, R.J., The structure and dynamics of the 26-month oscillation, in *Proc. Intern. Symp. Dynamics of large Scale Processes in the Atmosphere*, pp. 376–387, Moscow, Russia, 1967.

Reid, G.C., and K.S. Gage, Interannual variations in the height of the tropical tropopause, *J. Geophys. Res.*, *90*, 5629–5635, 1985.

Rind, D., and N.K. Balachandran, Modeling the effects of UV variability and the QBO on the troposphere-stratosphere system. Part II: The troposphere, *J. Climate*, *8*, 2080–2095, 1995.

Robinson, W., The application of quasi-geostrophic Eliassen-Palm flux to the analysis of stratospheric data, *J. Atmos. Sci.*, *43*, 1017–1023, 1986.

Rottger, J., Structure and dynamics of the stratosphere and mesosphere revealed by VHF radar investigations, *Pageoph.*, *118*, 494–527, 1980.

Rottman, G., Solar ultraviolet irradiance and its temporal variability, *J. Atmos. Solar-Terr. Physics*, *61*, 37–44, 1999.

Ruth, S., R. Kennaugh, L.J. Gray, and J.M.R. III, Seasonal, semiannual and interannual variability seen in measurements of methane made by UARS Halogen Occultation Experiment, *J. Geophys. Res.*, *102*, 16,189–16,199, 1997.

Salby, M.L., D.L. Hartmann, P.L. Bailey, and J.C. Gille, Evidence for equatorial Kelvin modes in Nimbus-7 LIMS, *J. Atmos. Sci.*, *41*, 220–235, 1984.

Salby, M., and D. Shea, Correlations between solar activity and the atmosphere: An unphysical explanation, *J. Geophys. Res.*, *96*, 22,579–22,595, 1991.

Salby, M., P. Callaghan, and D. Shea, Interdependence of the tropical and extra-tropical QBO: Relationship to the solar cycle versus a biennial oscillation in the stratosphere, *J. Geophys. Res.*, *102*, 29,789–29,798, 1997.

Salby, M., and P. Callaghan, Connection between the solar cycle and the QBO: The missing link, *J. Climate*, 13, 328–338, 2000.

Saravanan, R., A multiwave model of the quasi-biennial oscillation, *J. Atmos. Sci.*, *47*, 2465–2474, 1990.

Sassi, F., R.R. Garcia, and B.A. Boville, The stratopause semiannual oscillation in the NCAR Community Climate Model, *J. Atmos. Sci.*, *50*, 3608–3624, 1993.

Sato, K., Vertical wind disturbances in the afternoon of midsummer revealed by the MU radar, *Geophys. Res. Lett.*, *19*, 1943–1946, 1992.

Sato, K., Small-scale wind disturbances observed by the MU radar during the passage of Typhoon Kelly, *J. Atmos. Sci.*, *50*, 518–537, 1993.

Sato, K., F. Hasegawa, and I. Hirota, Short-period disturbances in the equatorial lower stratosphere, *J. Meteor. Soc. Japan*, *72*, 859–872, 1994.

Sato, K., H. Hashiguchi, and S. Fukao, Gravity waves and turbulence associated with cumulus convection observed with the UHF/VHF clear-air Doppler radars, *J. Geophys. Res.*, *100*, 7111–7119, 1995.

Sato, K., and T.J. Dunkerton, Estimates of momentum flux associated with equatorial Kelvin and gravity waves, *J. Geophys. Res.*, *102*, 26,247–26,261, 1997.

Shapiro, L.J., The relationship of the quasi-biennial oscillation to Atlantic tropical storm activity, *Mon. Wea. Rev.*, *117*, 1545–1552, 1989.

Shen, S., and K.–M. Lau, Biennial oscillation associated with the east Asian summer monsoon and tropical sea surface temperatures, *J. Meteor. Soc. Japan*, *73*, 105–124, 1995.

Shimizu, A., and T. Tsuda, Radiosonde observations of equatorial atmosphere dynamics over Indonesia, *J. Geophys. Res.*, *102*, 26,159–26,172, 1997.

Shindell, D., D. Rind, N.B. Balanchandran, J. Lean, and P. Lonergan, Solar cycle variability, ozone and climate, *Science*, *284*, 305–308, 1999.

Shiotani, M., and T. Horinouchi, Kelvin wave activity and the quasi-biennial oscillation in the equatorial lower stratosphere, *J. Meteor. Soc. Japan*, *71*, 175–182, 1993.

Shiotani, M., J.C. Gille, and A.E. Roche, Kelvin waves in the equatorial lower stratosphere as revealed by Cryogenic Limb Array Etalon Spectrometer temperature data, *J. Geophys. Res.*, *102*, 26,131–26,140, 1997.

Takahashi, M., A two-dimensional numerical model of the quasi-biennial oscillation, *J. Meteor. Soc. Japan*, *65*, 523–535, 1987.

Takahashi, M., and B.A. Boville, A three-dimensional simulation of the equatorial quasi-biennial oscillation, *J. Atmos. Sci.*, *49*, 1020–1035, 1992.

Takahashi, M., Simulation of the stratospheric quasi-biennial oscillation using a general circulation model, *Geophys. Res. Lett.*, *23*, 661–664, 1996.

Takahashi, M., N. Zhao, and T. Kumakura, Equatorial waves in a general circulation model simulating a quasi-biennial oscillation, *J. Meteor. Soc. Japan*, *75*, 529–540, 1997.

Takahashi, M., The first realistic simulation of the stratospheric quasi-biennial oscillation in a general circulation model, *Geophys. Res. Lett.*, *26*, 1307–1310, 1999.

Takayabu, Y.N., K.–M. Lau, and C.–H. Sui, Observation of a quasi-2-day wave during TOGA COARE, *Mon. Wea. Rev.*, *124*, 1892–1913, 1996.

Tanaka, H., and N. Yoshizawa, A slowly-varying model of the quasi-biennial oscillation involving effects of transience, self-acceleration and saturation of equatorial waves, *J. Atmos. Sci.*, *44*, 1427–1436, 1987.

Teitelbaum, H., and P. Bauer, Stratospheric temperature eleven years variation: Solar cycle influence or stroboscopic effect?, *Ann. Geophys.*, *8*, 239–242, 1990.

Teitelbaum, H., F. Vial, and P. Bauer, The Stratospheric Quasi-Biennial Oscillation Observed In The Semidiurnal Ground Pressure Data, *Ann. Geophys .— Atmos. Hydros. and Space Sci.*, *13(7)*, 740–744, 1995.

Thompson, D.W.J., and J.M. Wallace, The Arctic Oscillation signature in the wintertime geopotential height and temperature fields, *Geophys. Res. Lett.*, *25*, 1297–1300, 1998.

Thompson, D.W.J., and J.M. Wallace, Annular modes in the extratropical circulation. Part I: Month-to-month variability. *J. Climate* 13, 1000–1016, 2000.

Tiedtke, M., A comprehensive mass flux scheme for cumulus parameterization in large-scale models, *Mon. Wea. Rev., 117*, 1779–800, 1989.

Trepte, C.R., and M.H. Hitchman, Tropical stratospheric circulation deduced from satellite aerosol data, *Nature, 355*, 626–628, 1992.

Tsuda, T., Y. Murayama, H. Wiryosumarto, S.W.B. Harijono, and S. Kato, Radiosonde observations of equatorial atmospheric dynamics over Indonesia, 1, equatorial waves and diurnal tides, *J. Geophys. Res., 99*, 10,491–10,506, 1994a.

Tsuda, T., Y. Murayama, H. Wiryosumarto, S.W.B. Harijono, and S. Kato, Radiosonde observations of equatorial atmospheric dynamics over Indonesia, 2, characteristics of gravity waves, *J. Geophys. Res., 99*, 10,507–10,516, 1994b.

Tung, K., and H. Yang, Global QBO in circulation and ozone. Part I: Reexamination of observational evidence, *J. Atmos. Sci., 51*, 2699–2707, 1994.

Tung, K., and H. Yang, Global QBO in circulation and ozone. Part II: A simple mechanistic model, *J. Atmos. Sci., 51*, 2708–2721, 1994.

Untch, A., Simulation of the quasi-biennial oscillation with the ECMWF model, in *Research activities in the atmospheric and oceanic modelling*, pp. 6.26–6.27, WMO, Geneva, 1998.

van Loon, H., and K. Labitzke, The Southern Oscillation. Part V: The anomalies in the lower stratosphere of the Northern Hemisphere in winter and a comparison with the Quasi-Biennial Oscillation, *Mon. Wea. Rev., 115*, 357–369, 1987.

Vincent, R.A., and M.J. Alexander, Gravity waves in the tropical lower stratosphere: An observational study of seasonal and interannual variability, *J. Geophys. Res.* 105, 17,971–17,982, 2000.

Wada, K., T. Nitta, and K. Sato, Equatorial inertia-gravity waves in the lower stratosphere revealed by TOGA-COARE IOP data, *J. Meteor. Soc. Japan (in press)*, 1999.

Wallace, J.M., and J.R. Holton, A diagnostic numerical model of the quasi-biennial oscillation, *J. Atmos. Sci., 25*, 280–292, 1968.

Wallace, J.M., and V.E. Kousky, Observational evidence of Kelvin waves in the tropical stratosphere, *J. Atmos. Sci., 25*, 900–907, **1968.**

Wallace, J.M., and V.E. Kousky, On the relation between Kelvin waves and the quasi-biennial oscillation, *J. Meteor. Soc. Japan, 46*, 496–502, **1968. <<a,b??>**

Wallace, J.M., General circulation of the tropical lower stratosphere, *Rev. Geophys. Space Phys., 11*, 191–222, 1973.

Wallace, J.M., and F.–C. Chang, Interannual variability of the wintertime polar vortex in the northern hemisphere middle stratosphere, *J. Meteor. Soc. Japan, 60*, 149–155, 1982.

Wallace, J.M., R.L. Panetta, and J. Estberg, Representation of the equatorial stratospheric quasi-biennial oscillation in EOF phase space, *J. Atmos. Sci., 50*, 1751–1762, 1993.

Waugh, D.W., Seasonal variation of isentropic transport out of the tropical stratosphere, *J. Atmos. Sci., 101*, 4007–4023, 1996.

Waugh, D.W., and W.J. Randel, Climatology of Arctic and Antarctic polar vortices using elliptical diagnostics, *J. Atmos. Sci., 56*, 1594–1613, 1999.

Wikle, C.K., R.A. Madden, and T.–C. Chen, Seasonal variations of upper tropospheric and lower stratospheric equatorial waves over the tropical Pacific, *J. Atmos. Sci., 54*, 1895–1909, 1997.

Willson, R., H. Hudson, C. Frohlich, and R. Brusa, Long-term downward trend in total solar irradiance, *Science, 234*, 1114–1117, 1986.

Xu, J.–S., On the relationship between the stratospheric quasi-biennial oscillation and the tropospheric southern oscillation, *J. Atmos. Sci., 49*, 725–734, 1992.

Yanai, M., and T. Maruyama, Stratospheric waves disturbances propagating over the equatorial Pacific, *J. Meteor. Soc. Japan, 44*, 291–294, 1966.

Yasunari, T., Zonally propagating modes of the global east-west circulation associated with the southern oscillation, *J. Meteor. Soc. Japan, 63*, 1013–1029, 1985.

Yasunari, T., A possible link of the QBOs between the stratosphere, troposphere and sea surface temperature in the tropics, *J. Meteor. Soc. Japan, 67* (**483–??**), 1989.

Zawodny, J.M., and M.P. McCormick, Stratospheric aerosol and gases experiment II measurements of the quasi biennial oscillations in ozone and nitrogen dioxide, *J. Geophy. Res., 96*, 9371–9377, 1991.

Zhang, G.J., and N.A. McFarlane, Sensitivity of climate simulations to the parameterization of cumulus convection in the Canadian Climate Centre General Circulation Model, *Atmosphere–Ocean, 33*, 407–446, 1995.

Ziemke, J.R., and J.L. Stanford, Quasi-biennial oscillation and tropical waves in total ozone, *J. Geophys. Res., 99*, 23,041–23,056, 1994.

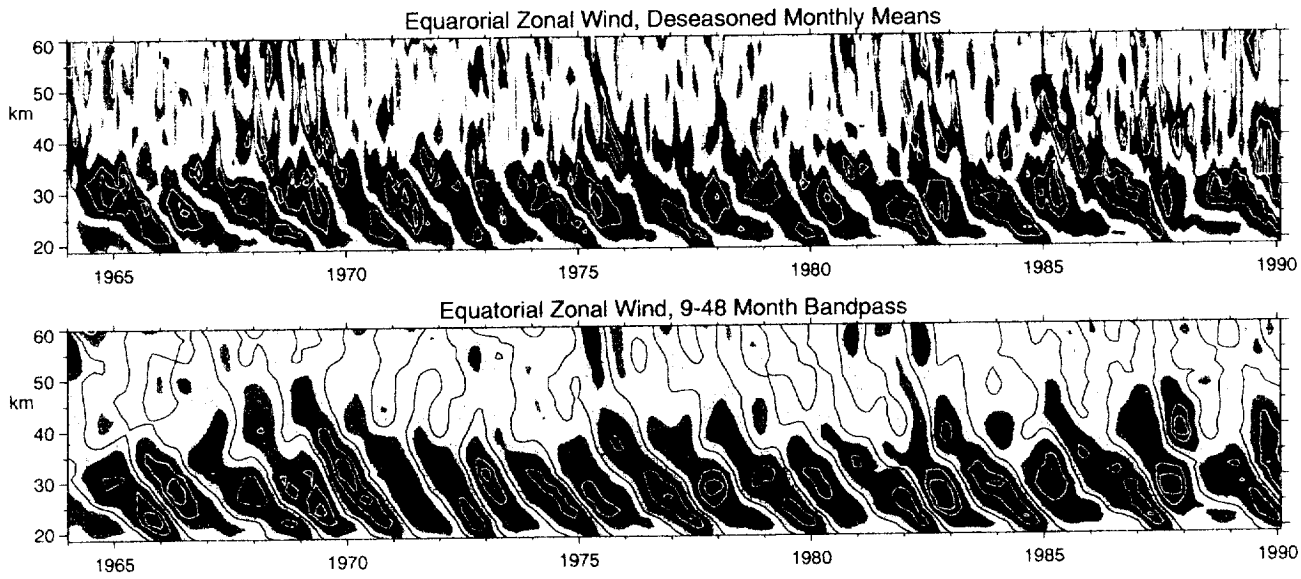

Figure 1. Time-height section (top) of the monthly-mean zonal wind component (ms^{-1}), with the seasonal cycle removed, for 1964–1990. Below 31 km equatorial radiosonde data are used: Canton Island (2.8°N, 1964–August 1967), Gan/Maledive Islands (0.7°S, September 1967–December 1975), and Singapore (1.4°N, January 1976–1990). Above 31 km rocketsonde data from Kwajalein (8.4°N) and Ascension Island (8.6°S) are shown. The contour interval is 6 ms^{-1} with the band between -3 and +3 unshaded. Red represents positive (westerly) winds. After *Gray et al.*, 2000. In the bottom panel the data are bandpass filtered to retain periods between 9 and 48 months.

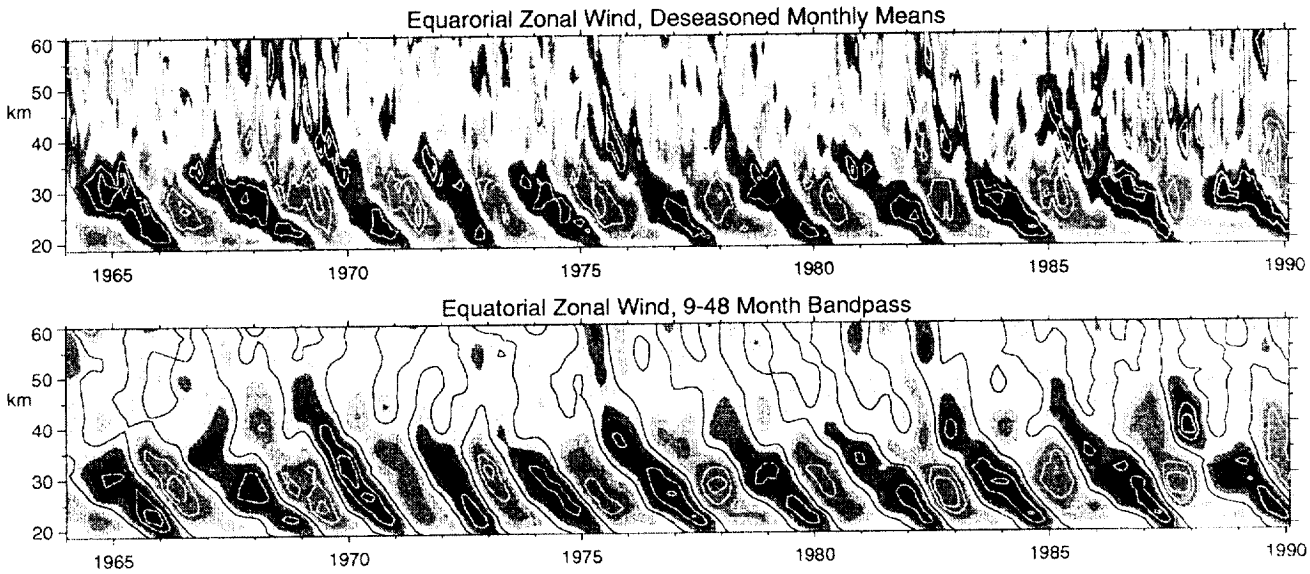

Figure 1. Time-height section (top) of the monthly-mean zonal wind component (ms^{-1}), with the seasonal cycle removed, for 1964–1990. Below 31 km equatorial radiosonde data are used: Canton Island (2.8°N, 1964–August 1967), Gan/Maledive Islands (0.7°S, September 1967–December 1975), and Singapore (1.4°N, January 1976–1990). Above 31 km rocketsonde data from Kwajalein (8.4°N) and Ascension Island (8.6°S) are shown. The contour interval is 6 ms^{-1} with the band between -3 and +3 unshaded. Red represents positive (westerly) winds. After *Gray et al.*, 2000. In the bottom panel the data are bandpass filtered to retain periods between 9 and 48 months.

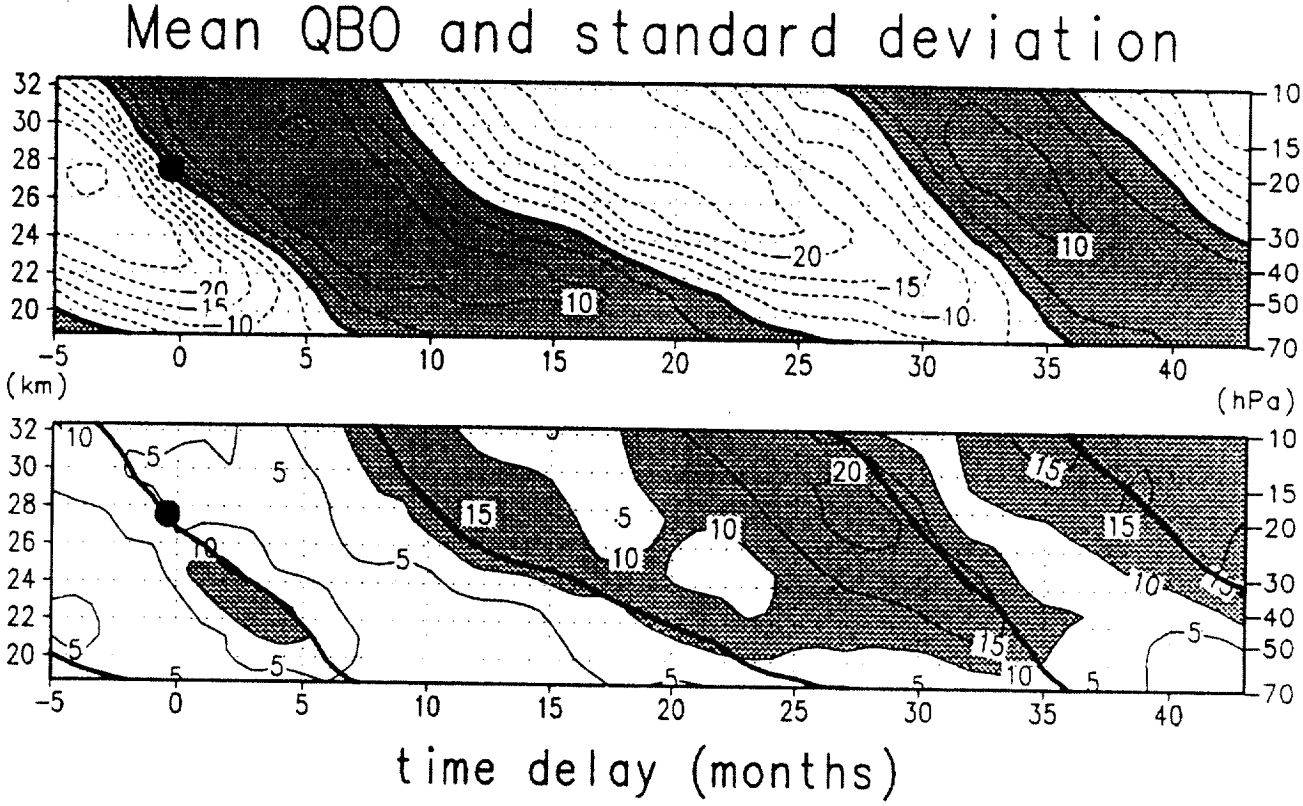

Figure 2. The mean QBO (ms^{-1}) obtained by averaging relative to the time of onset of QBO westerlies at 20 hPa, from 5 months before this time until 43 months afterward (top) and the standard deviation about this mean (bottom). Westerlies are shaded. From *Pawson et al.*, [1993].

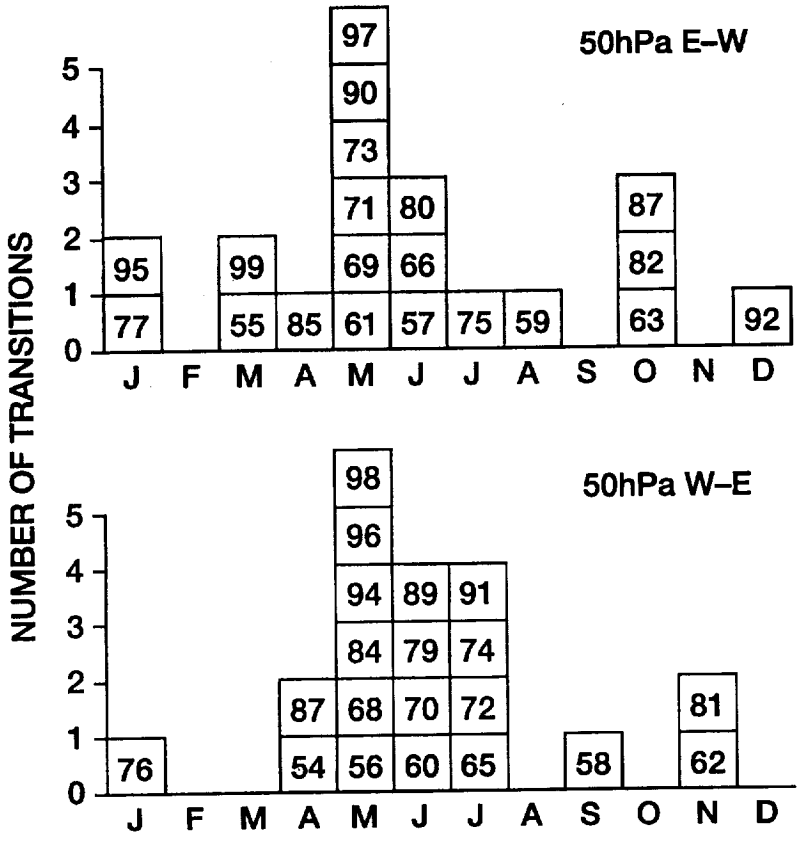

Figure 3. Histograms of the number of transitions (zero crossings) at 50 hPa grouped by month. Individual years are listed in the boxes. Easterly to westerly transitions are displayed in the top panel, while westerly to easterly transitions are shown in the bottom panel. After *Pawson et al.*, [1993].

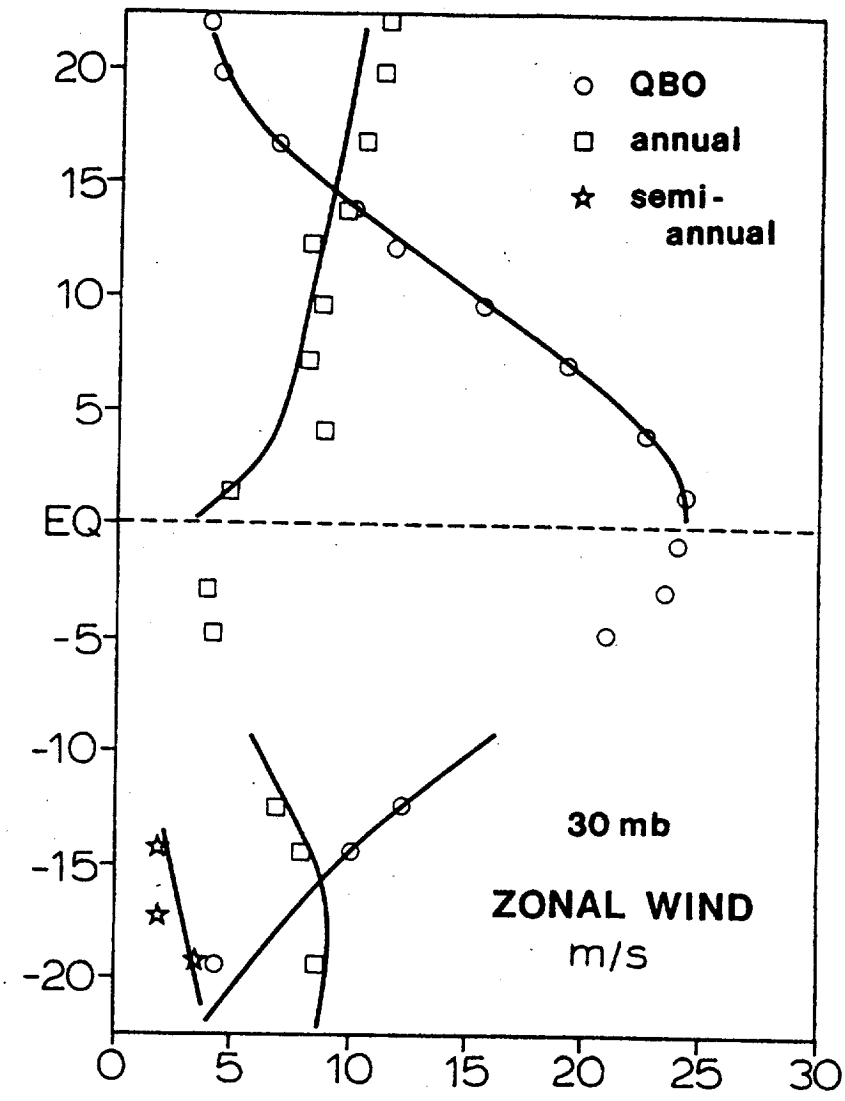

Figure 4. Harmonic analysis of 30-hPa zonal wind, showing the amplitude of the annual cycle (squares), semiannual cycle (stars), and residual deseasoned component (circles). Symbols show individual radiosonde station amplitudes. Solid lines are based on binned data. From *Dunkerton and Delisi* [1985].

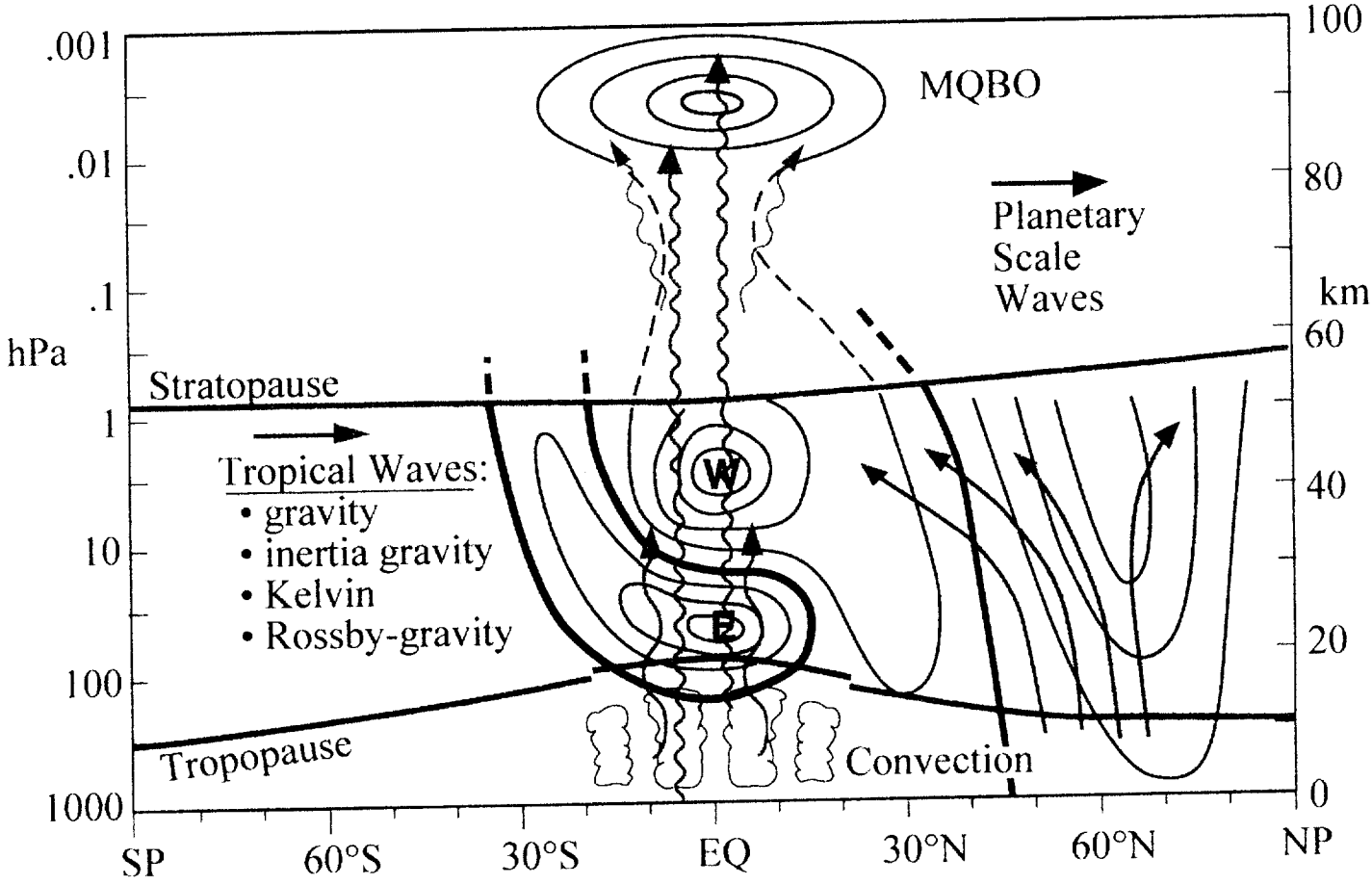

Figure 5. Dynamical overview of the QBO during the northern winter. The propagation of various tropical waves are depicted by tan arrows, with the QBO driven by upward-propagating gravity, inertia-gravity, Kelvin, and Rossby-gravity waves. The propagation of planetary-scale waves (purple arrows) is shown at mid-to high latitudes. Black contours indicate the difference in zonal-mean zonal winds between easterly and westerly phases of the QBO where the QBO phase is defined as easterly by the 40-hPa equatorial wind. Easterly anomalies are light blue and westerly anomalies are pink. In the tropics the contours are similar to the observed wind values when the QBO is easterly. The mesospheric QBO (MQBO) is shown above ~80 km, while wind contours between ~50–80 km are dashed due to observational uncertainty.

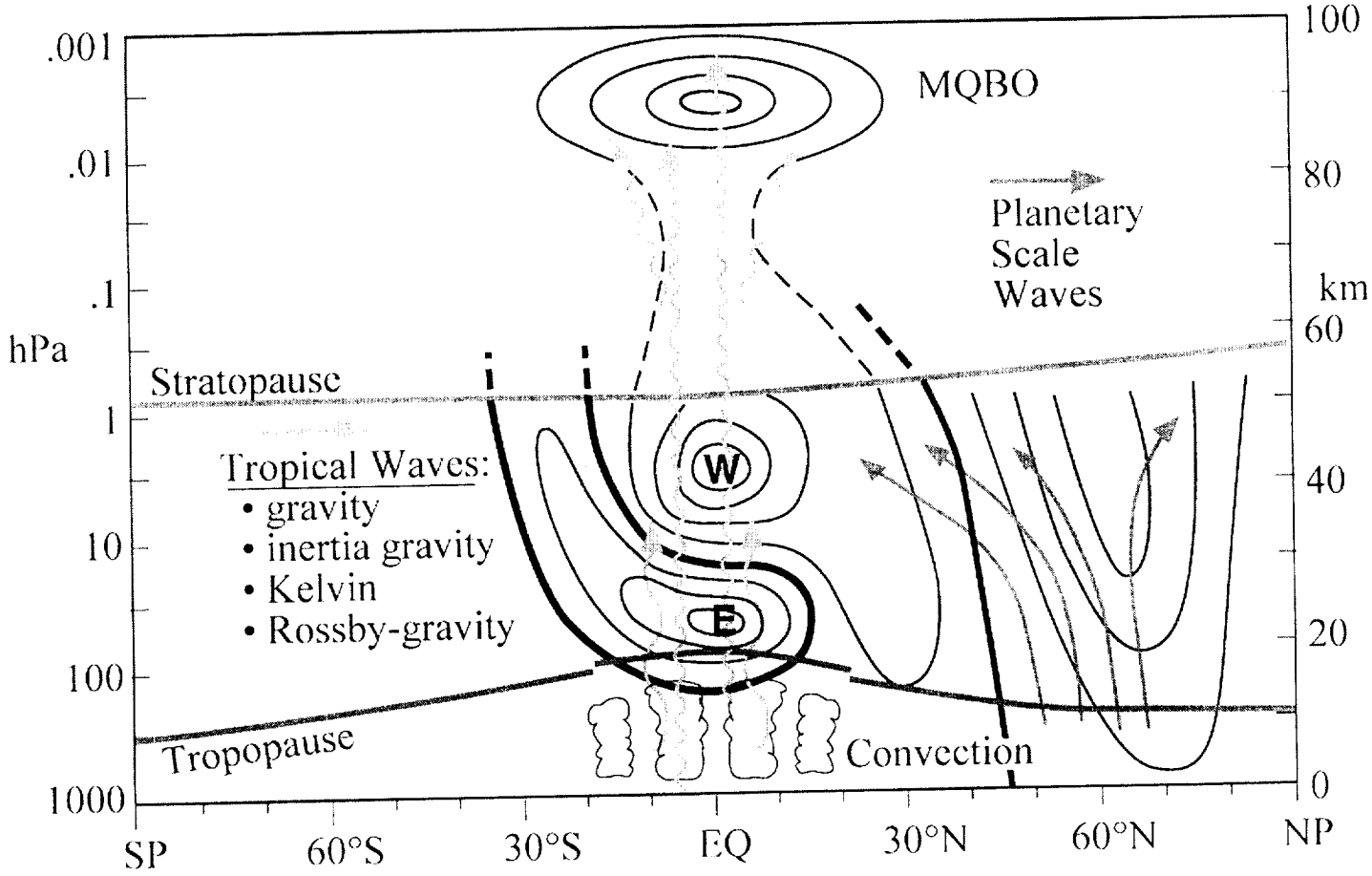

Figure 5. Dynamical overview of the QBO during the northern winter. The propagation of various tropical waves are depicted by tan arrows, with the QBO driven by upward-propagating gravity, inertia-gravity, Kelvin, and Rossby-gravity waves. The propagation of planetary-scale waves (purple arrows) is shown at mid-to high latitudes. Black contours indicate the difference in zonal-mean zonal winds between easterly and westerly phases of the QBO where the QBO phase is defined as easterly by the 40-hPa equatorial wind. Easterly anomalies are light blue and westerly anomalies are pink. In the tropics the contours are similar to the observed wind values when the QBO is easterly. The mesospheric QBO (MQBO) is shown above ~80 km, while wind contours between ~50–80 km are dashed due to observational uncertainty.

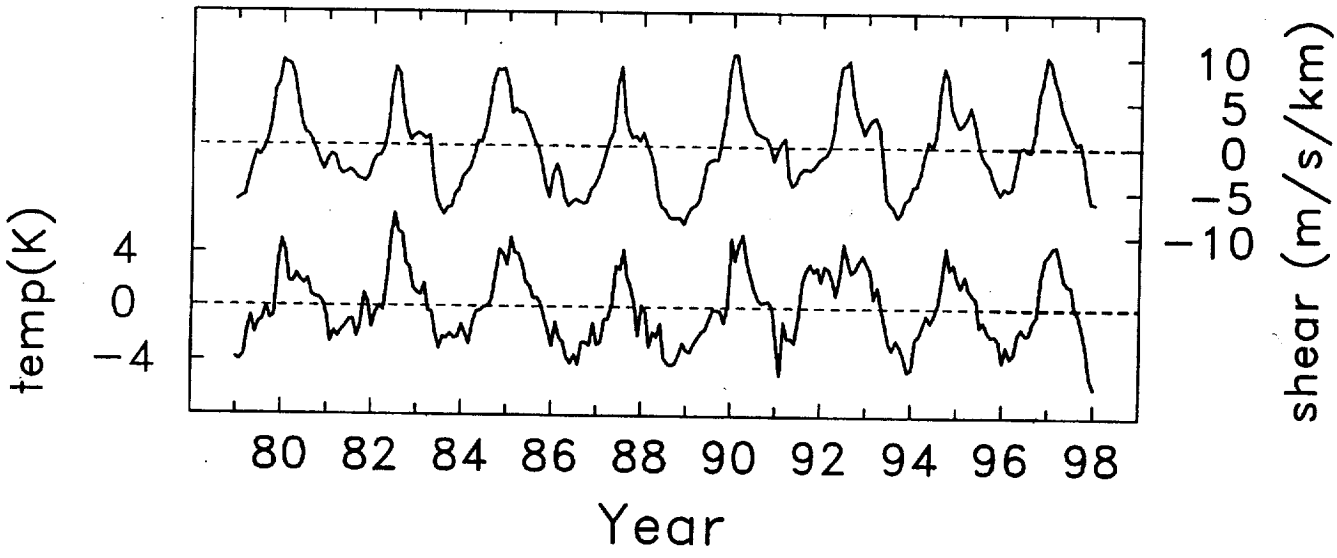

Figure 6. Equatorial temperature anomalies associated with the QBO in the 30-50 hPa layer (bottom) and vertical wind shear (top).

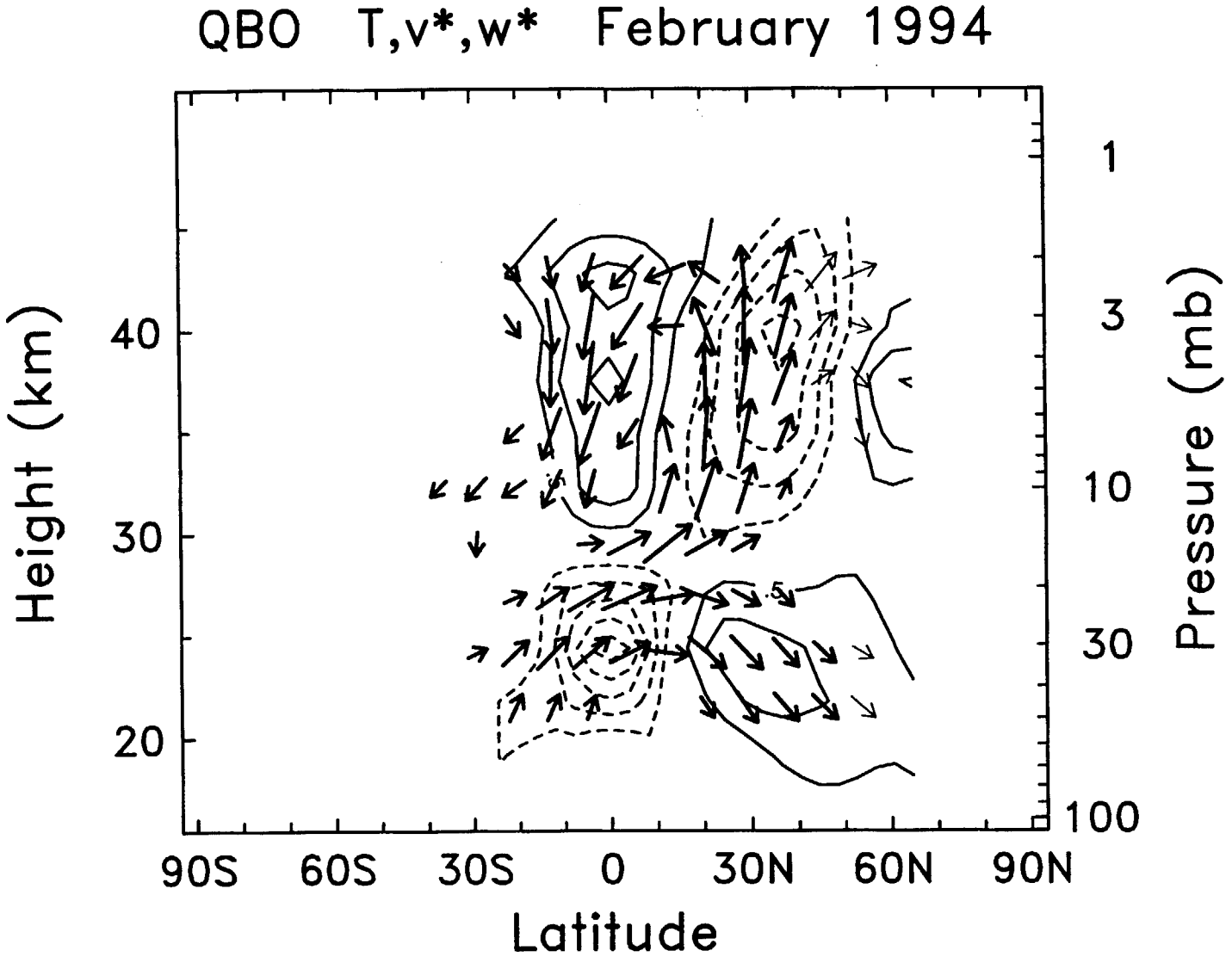

Figure 7. Cross sections of QBO anomalies in February 1994. Temperature anomalies are contoured (+/- 0.5, 1.0, 1.5,...K) and components of the residual mean circulation (v, w) as vectors (scaled by an arbitrary function of latitude. From *Randel et al.* [1999].

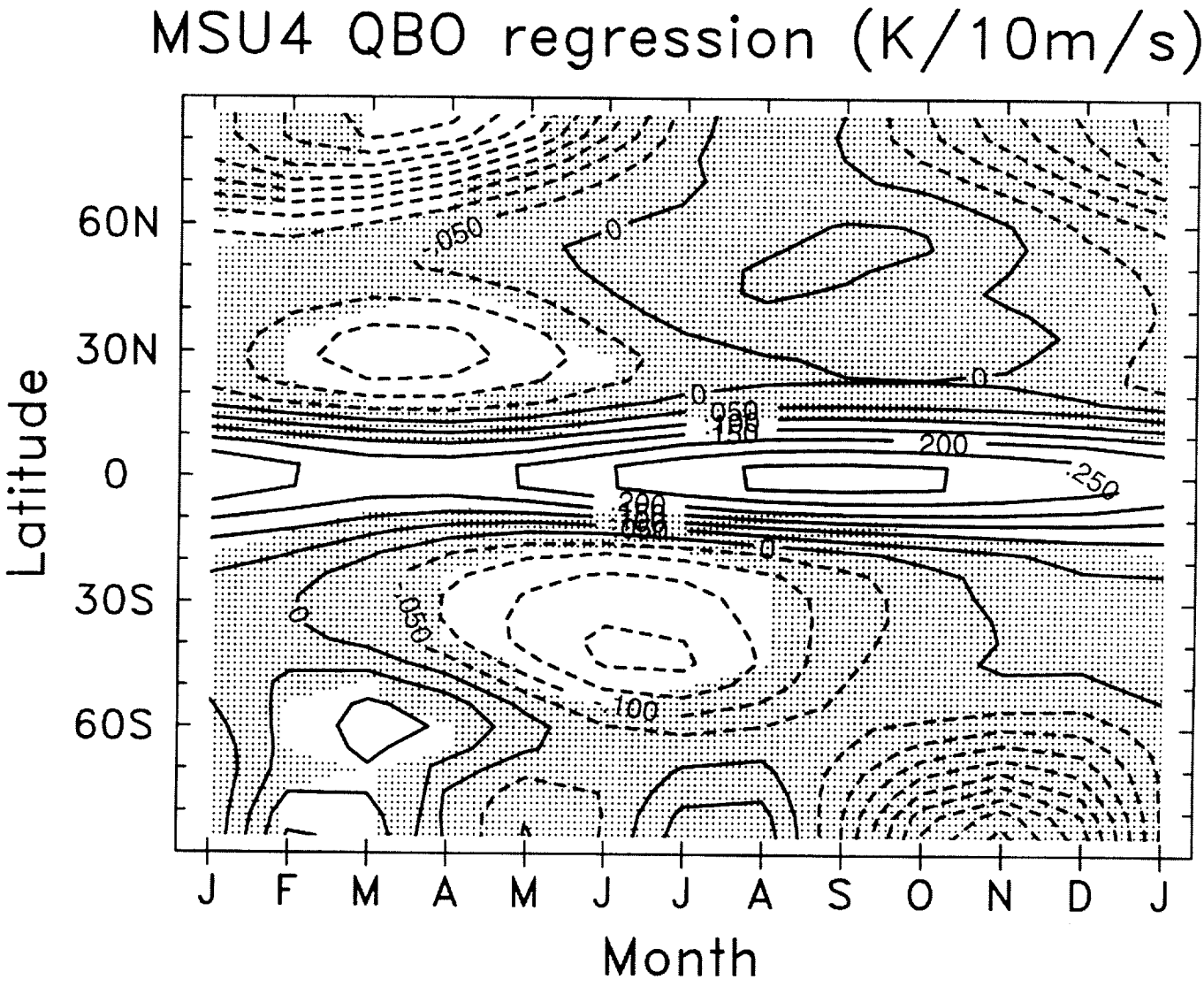

Figure 8. QBO regression using 13-22-km MSU temperature data for 1979–1998. Stippling denotes regions where the statistical fits are different from zero at the 2σ level. Updated from *Randel and Cobb* [1994].

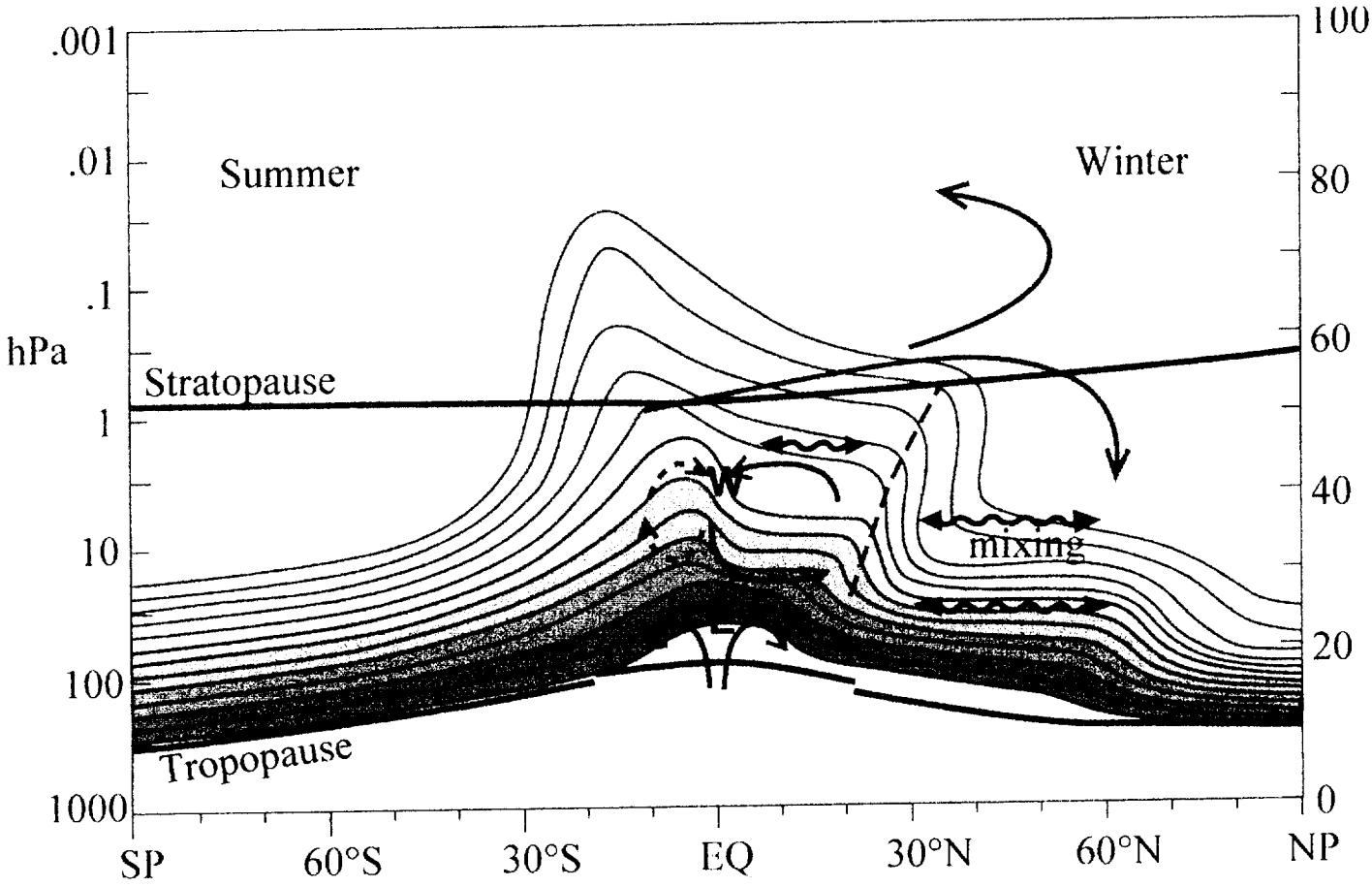

Figure 9. Overview of tracer transport by QBO wind anomalies and mean advection. Contours illustrate schematically the isopleths of a conservative tracer during the northern winter when the QBO is in its east phase at 40 hPa (matching Figure 5). Tropical upwelling causes the broad maximum in tracer density in the middle to upper equatorial stratosphere, while the QBO causes deviations from hemispheric symmetry. Red arrows near the equator depict circulation anomalies from the QBO. The circulation anomaly in the equatorial lower stratosphere is approximately symmetric, while the anomaly in the upper stratosphere is much stronger in the winter hemisphere. The descent near the equator (~5 hPa) and ascent to the north (~5 hPa, 10°N) combine to produce a "stair-step" pattern. A second stair step is formed in midlatitudes by horizontal mixing.

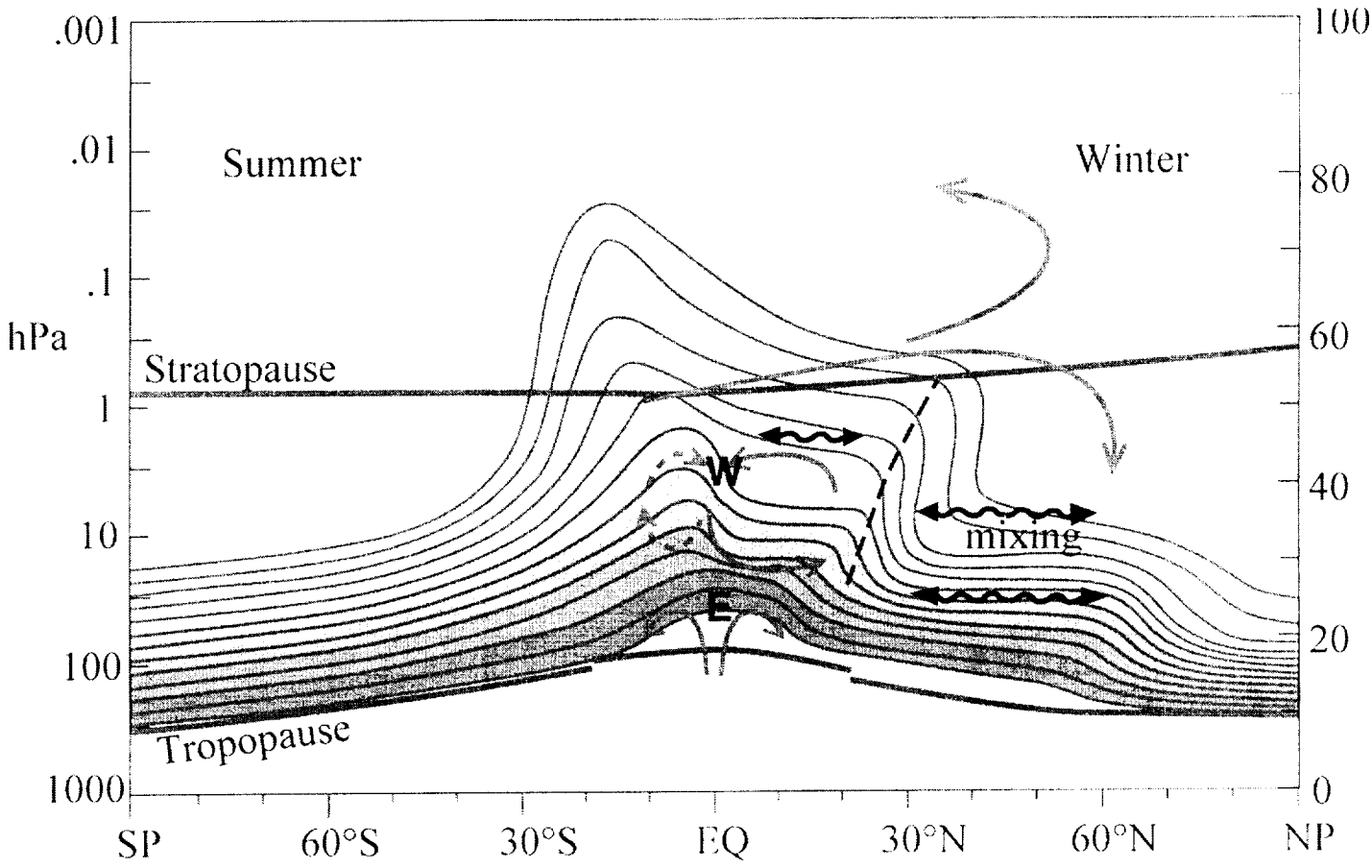

Figure 9. Overview of tracer transport by QBO wind anomalies and mean advection. Contours illustrate schematically the isopleths of a conservative tracer during the northern winter when the QBO is in its east phase at 40 hPa (matching Figure 5). Tropical upwelling causes the broad maximum in tracer density in the middle to upper equatorial stratosphere, while the QBO causes deviations from hemispheric symmetry. Red arrows near the equator depict circulation anomalies from the QBO. The circulation anomaly in the equatorial lower stratosphere is approximately symmetric, while the anomaly in the upper stratosphere is much stronger in the winter hemisphere. The descent near the equator (~5 hPa) and ascent to the north (~5 hPa, 10°N) combine to produce a "stair-step" pattern. A second stair step is formed in midlatitudes by horizontal mixing.

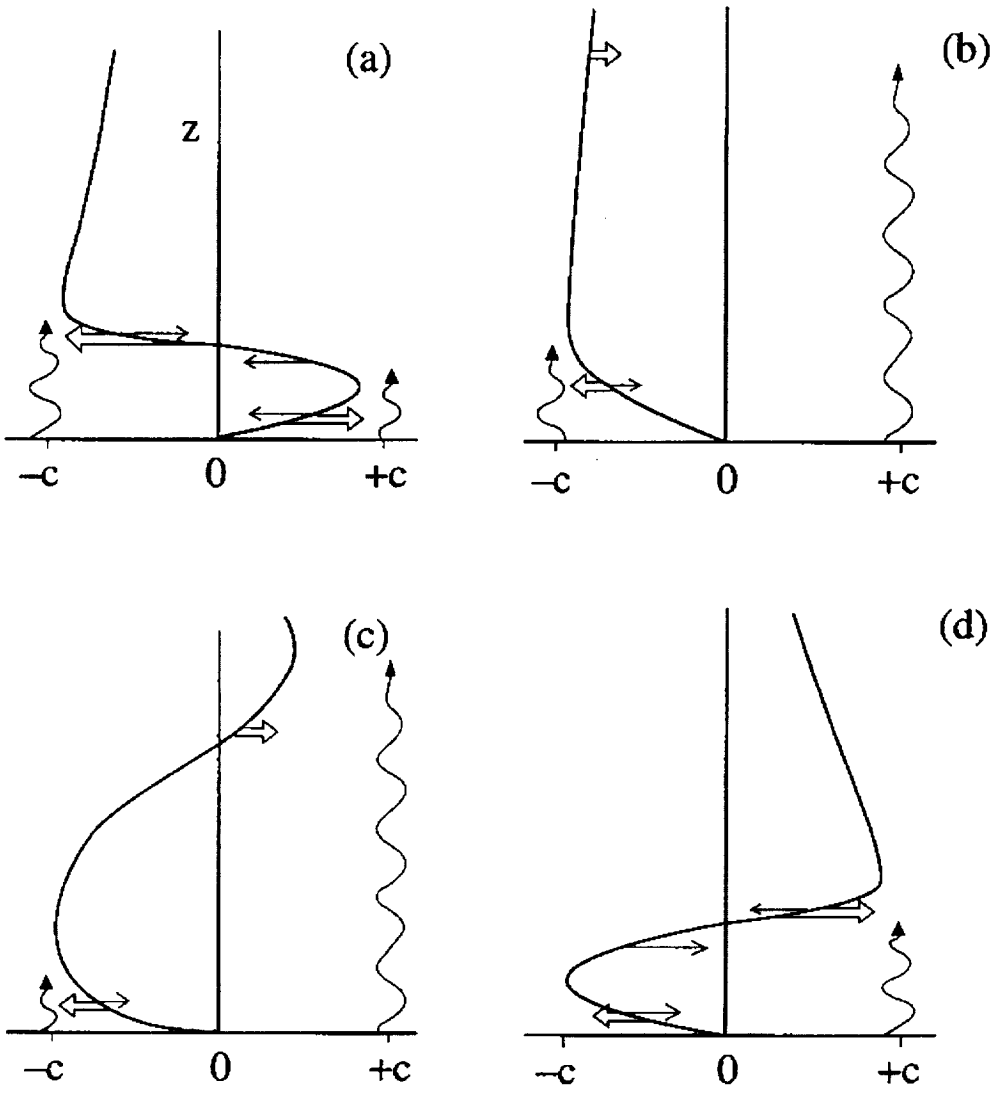

Figure 10. Schematic representation of the evolution of the mean flow in Plumb's analog of the QBO. Six stages of a complete cycle are shown. Double arrows show wave-driven acceleration and single arrows show viscously driven accelerations. Wavy lines indicate relative penetration of eastward and westward waves. (After *Plumb* [1984]).

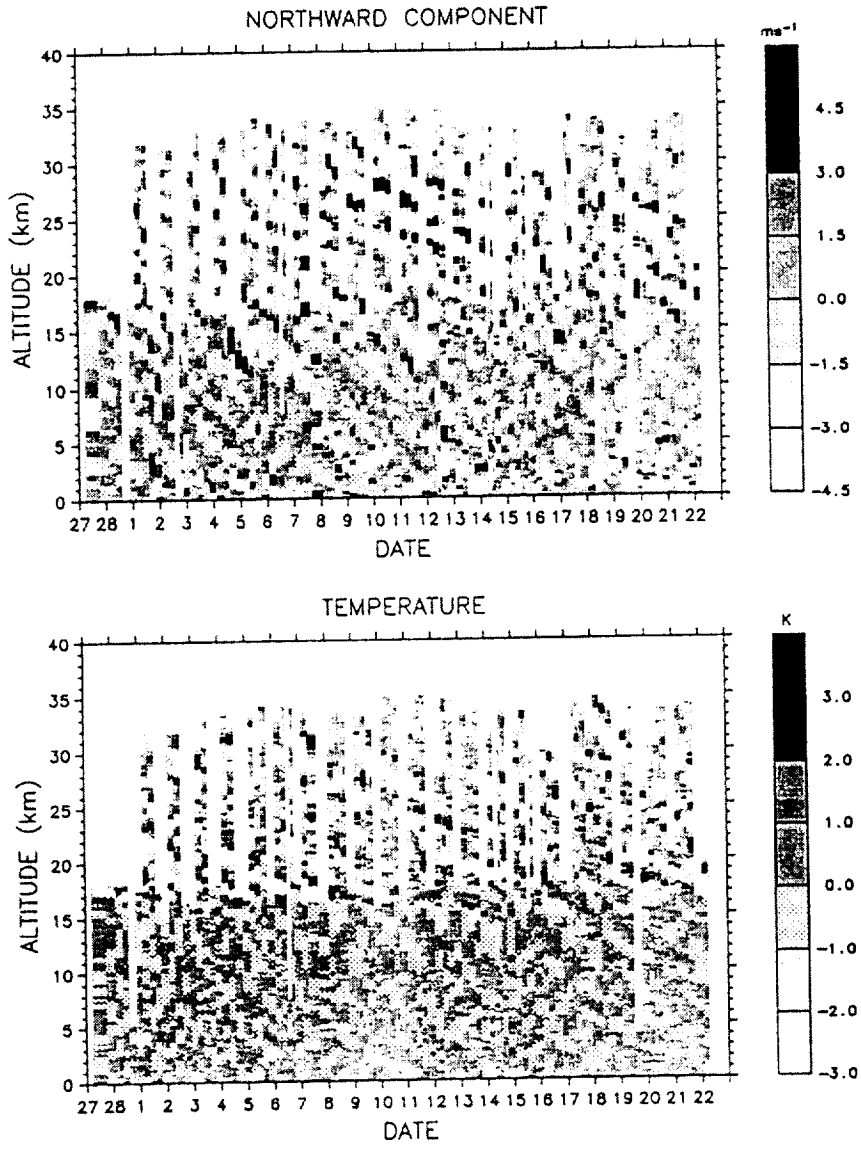

Figure 11. A time-height section of short-period (< 4 days) northward component (top) and temperature component (bottom) at Watukosek, Indonesia (7.6°S, 112.7°E) for 24 days in February to March 1990. From *Tsuda et al.* [1994b].

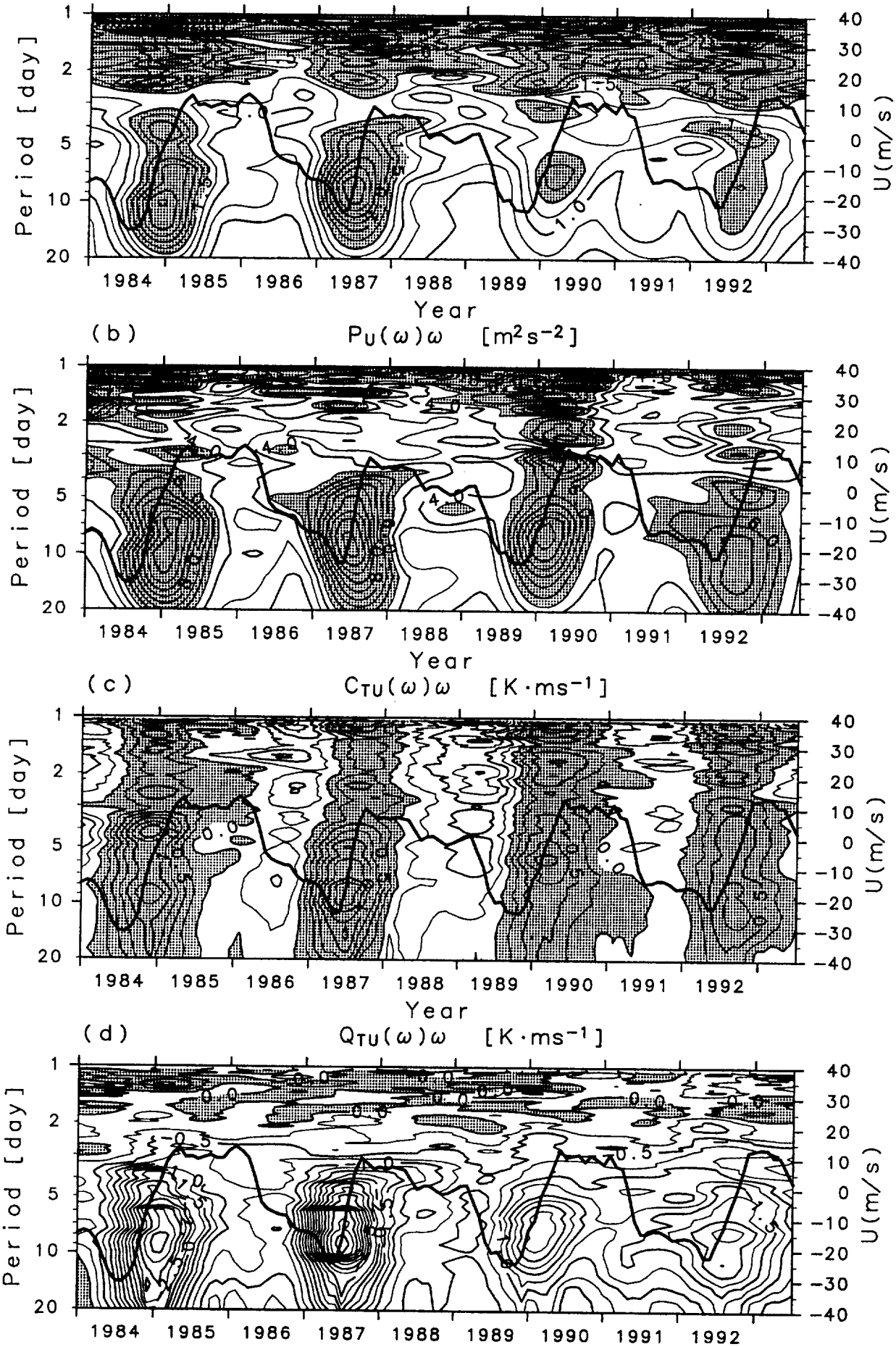

Figure 12. Power spectra for (a) T and (b) u fluctuations at Singapore as a function of time, averaged for a height region of 20–25 km. (c) Cospectra and (d) quadrature spectra of T and u components are also shown. The thick solid line represents a QBO reference time series. From *Sato and Dunkerton* [1997].

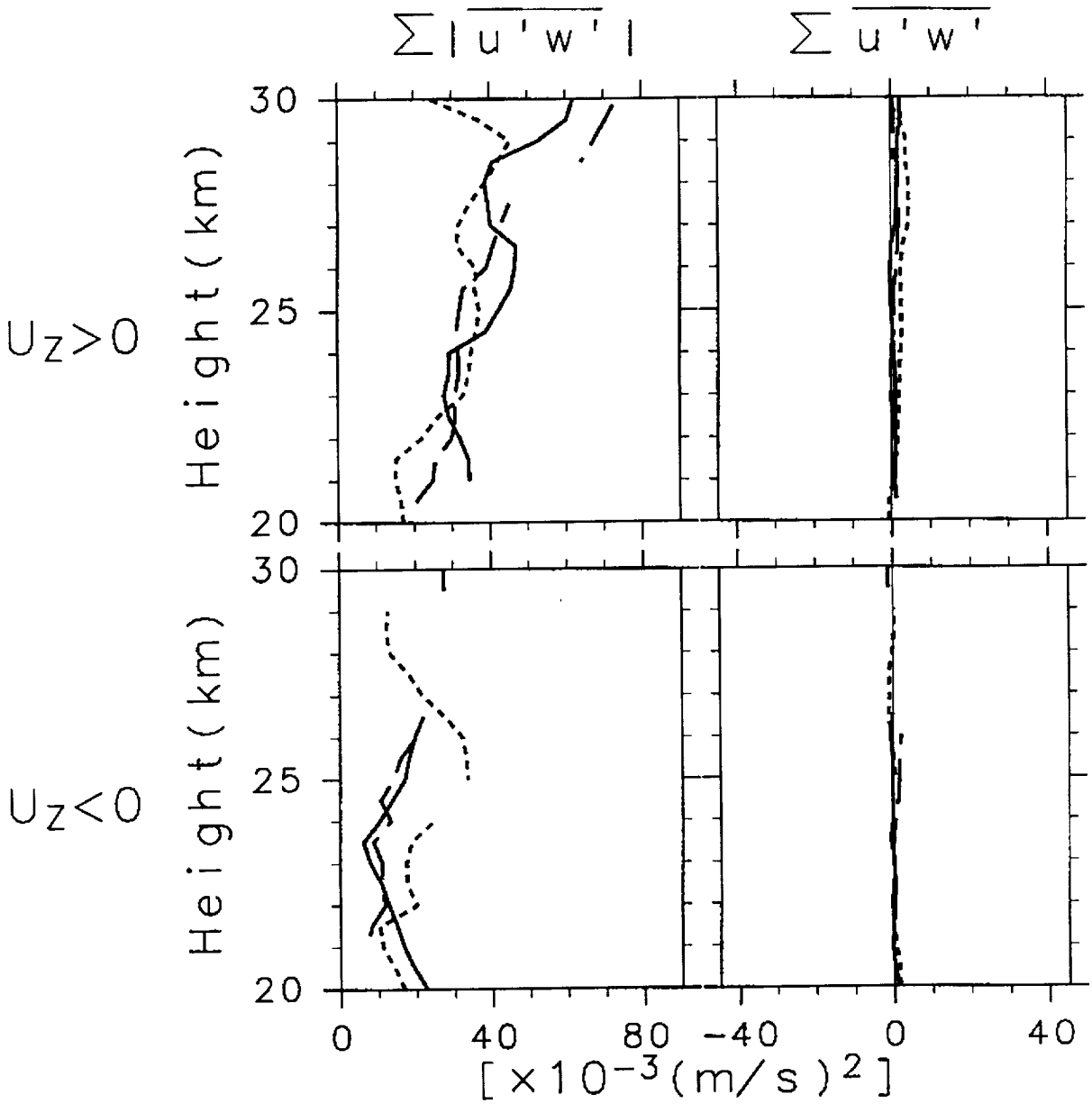

Figure 13 Momentum flux estimates for short-period (1–3 days) component in the (a) westward and (b) eastward shear phases. Left panels show indirect estimates corresponding to a sum of absolute values of positive and negative momentum fluxes. Right panels show direct estimates corresponding to net momentum fluxes. From *Sato* [1997].

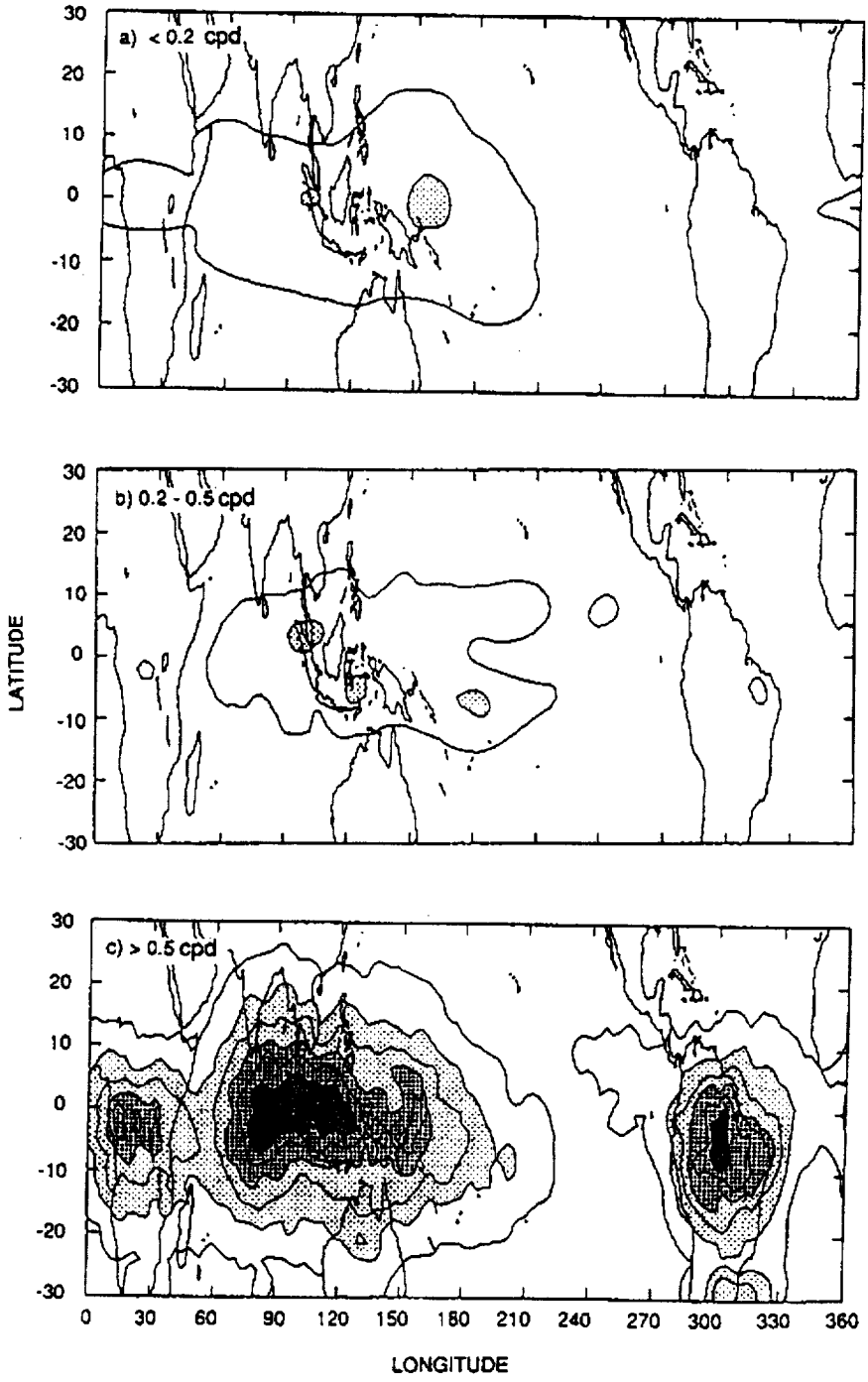

Figure 14. Geographical distribution of vertical component of Eliassen-Palm flux of equatorial waves with periods (a) longer than 5 days, (b) of 2–5 days, and (c) shorter than 2 days estimated based on high-resolution imagery of the global convective pattern constructed from six satellites. Shown here is the frequency-integrated absolute value of the Eliassen-Palm flux. Units are arbitrary and contour increments are linear. From *Bergman and Salby* [1994].

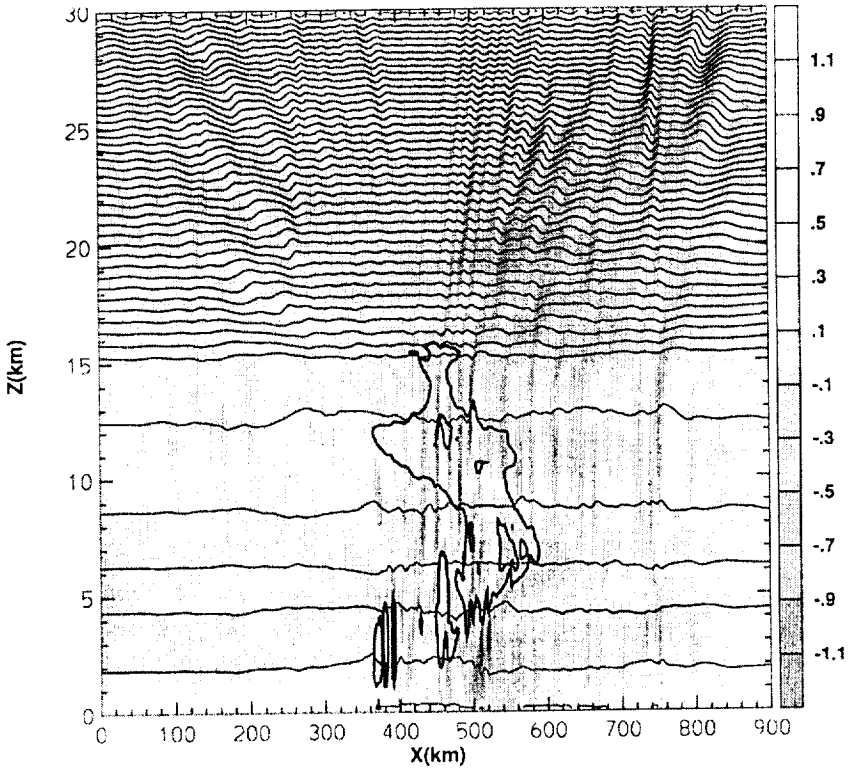

Figure 15. Stratospheric gravity waves above a simulation of tropical convection. The shading shows vertical velocities. The scale runs from $\pm$ 1.2 ms^{-1} to enhance the wave perturbations in the stratosphere, but maximum values in the troposphere exceed $\pm$ 5 ms^{-1}. Potential temperature contours at 10K intervals (thin lines) and the outline of the storm cloud (heavy lines) are also shown [*Alexander and Holton,* 1997].

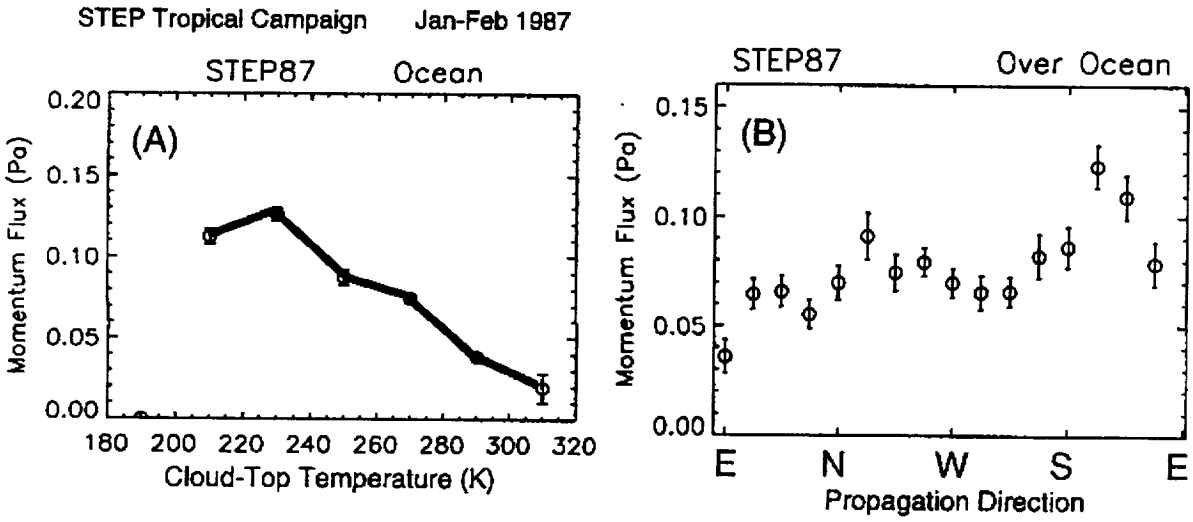

Figure 16. (a) Gravity wave momentum flux in the stratosphere vs. cloud-top temperature below for oceanic flights north of Australia during Jan-Feb 1987. (b) Shows the directional distribution of the momentum fluxes in these observations.

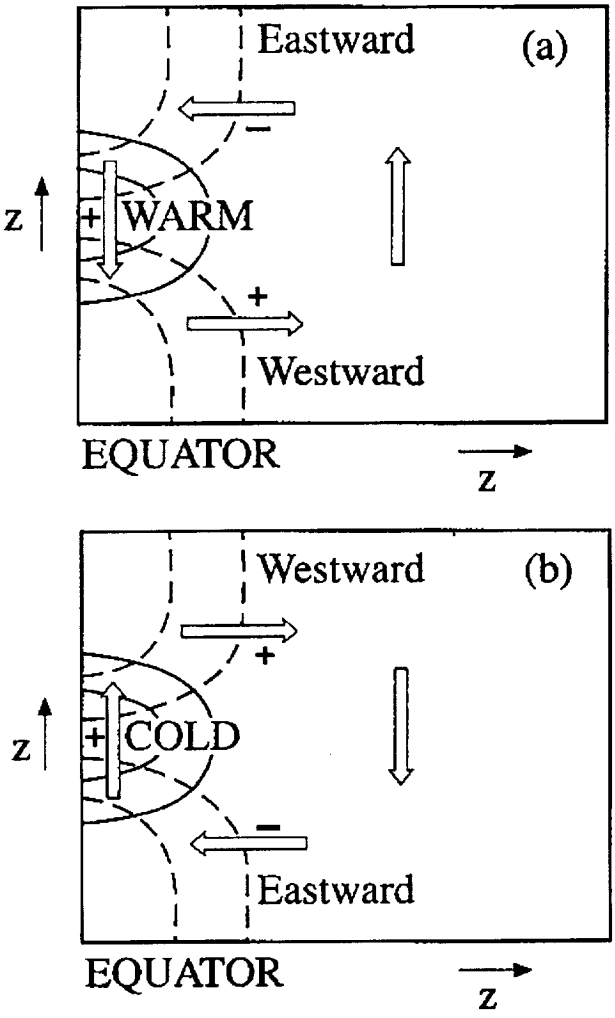

Figure 17. Schematic latitude-height sections showing the mean meridional circulation associated with the equatorial temperature anomaly of the QBO. Solid contours show temperature anomaly isotherms, dashed contours are zonal wind isopleths. Plus and minus designate signs of zonal wind accelerations driven by the mean meridional circulation. (a) Westerly shear zone, b) easterly shear zone. After *Plumb and Bell* [1982b].

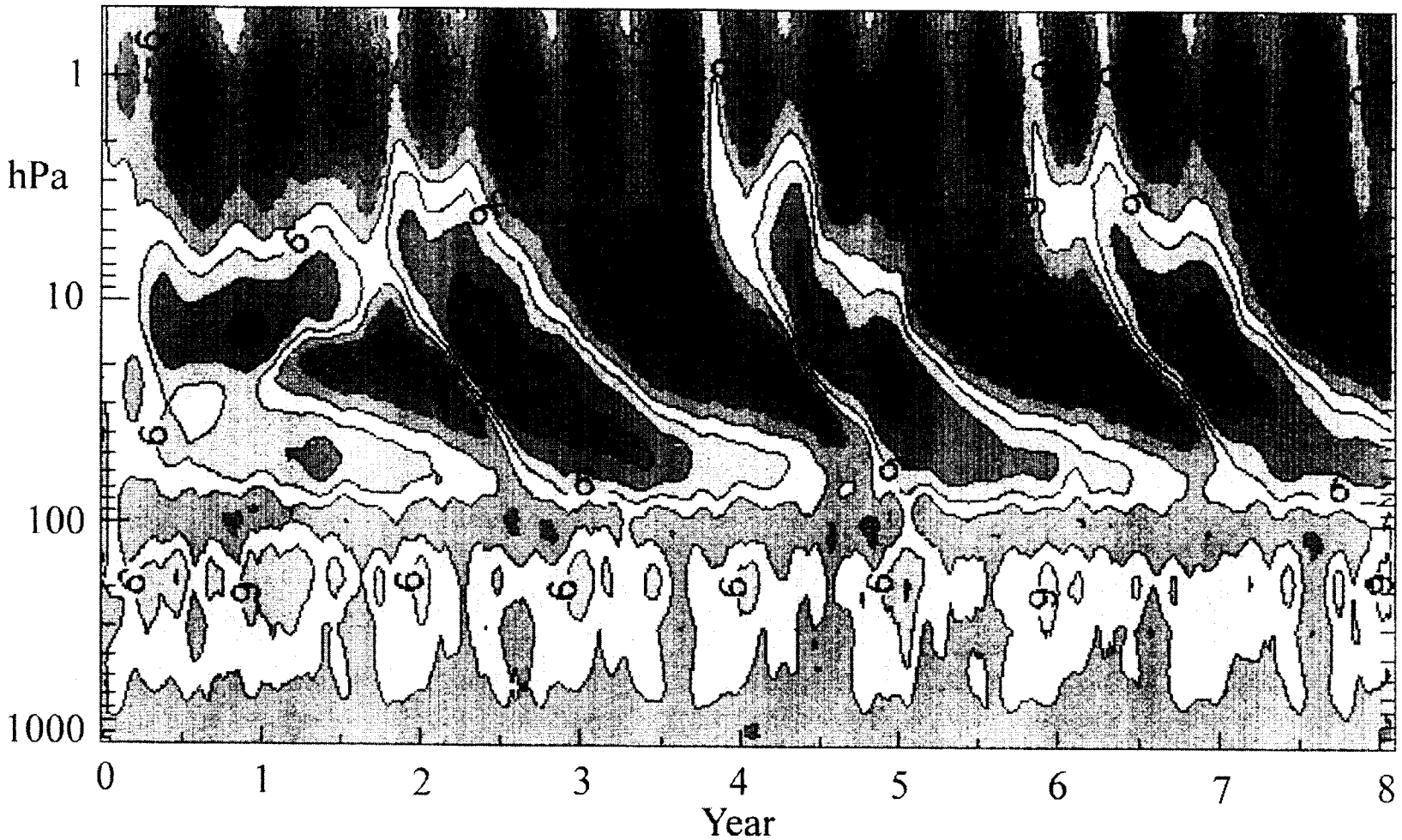

Figure 18. Time-height section of the zonal-mean zonal wind over the equator simulated by *Takahashi* [1999]. The time coordinate ranges from day 0 (1 January with a 360-day model year) to day 1830. The contour interval is 6 ms^{-1}. Red and blue shading represents westerly and easterly winds, respectively.

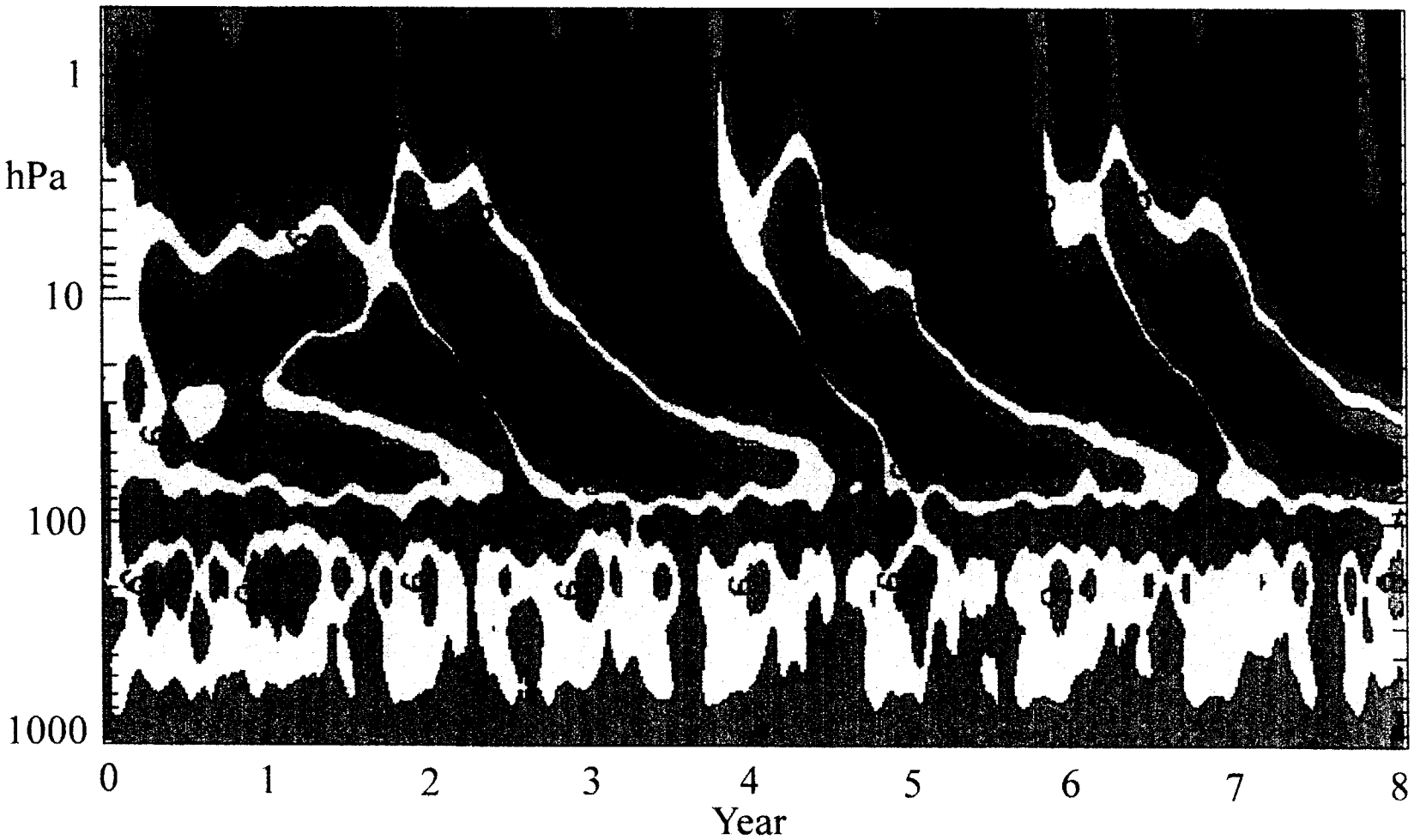

Figure 18. Time-height section of the zonal-mean zonal wind over the equator simulated by *Takahashi* [1999]. The time coordinate ranges from day 0 (1 January with a 360-day model year) to day 1830. The contour interval is 6 ms^{-1}. Red and blue shading represents westerly and easterly winds, respectively.

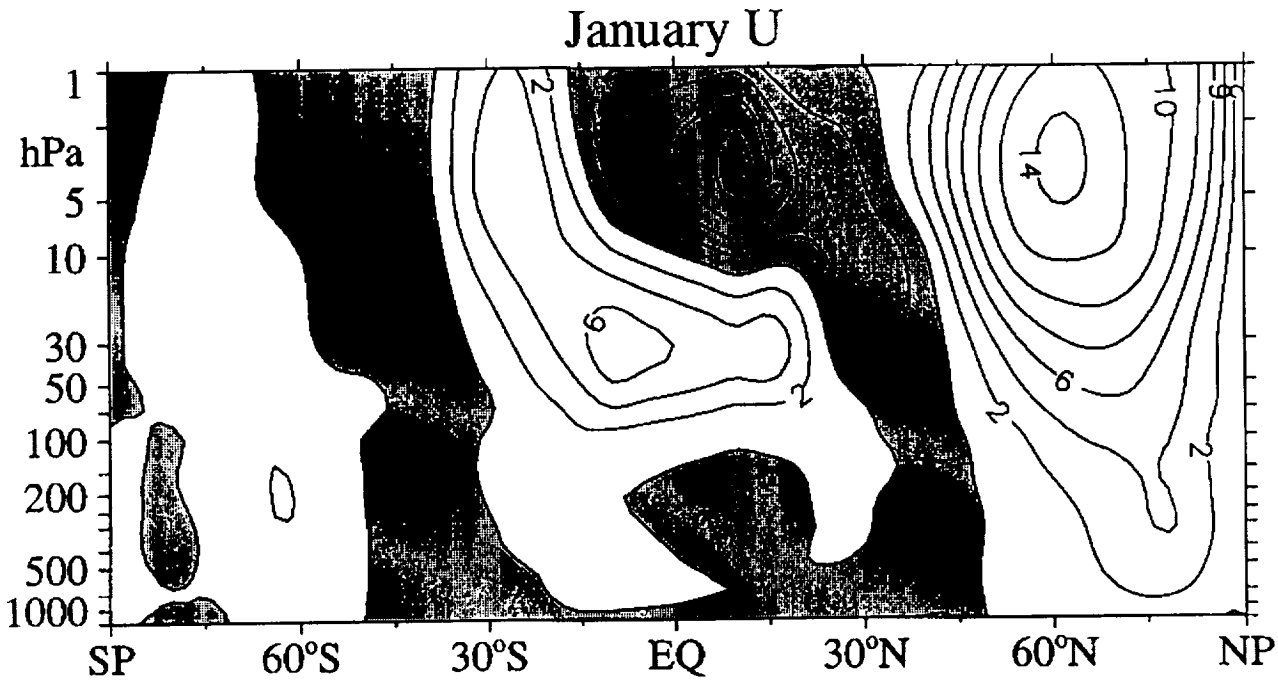

Figure 19. January latitude-height zonal-mean wind difference between the average of all years with westerly QBO and those with easterly QBO. The phase of the QBO is optimized for the NH, and is defined using the EOF technique of [*Baldwin and Dunkerton*, 1998b], and is nearly equivalent to using 40-hPa equatorial winds. The contour interval is 2 ms^{-1} and negative values are shaded. From *Baldwin and Dunkerton* [1998b].

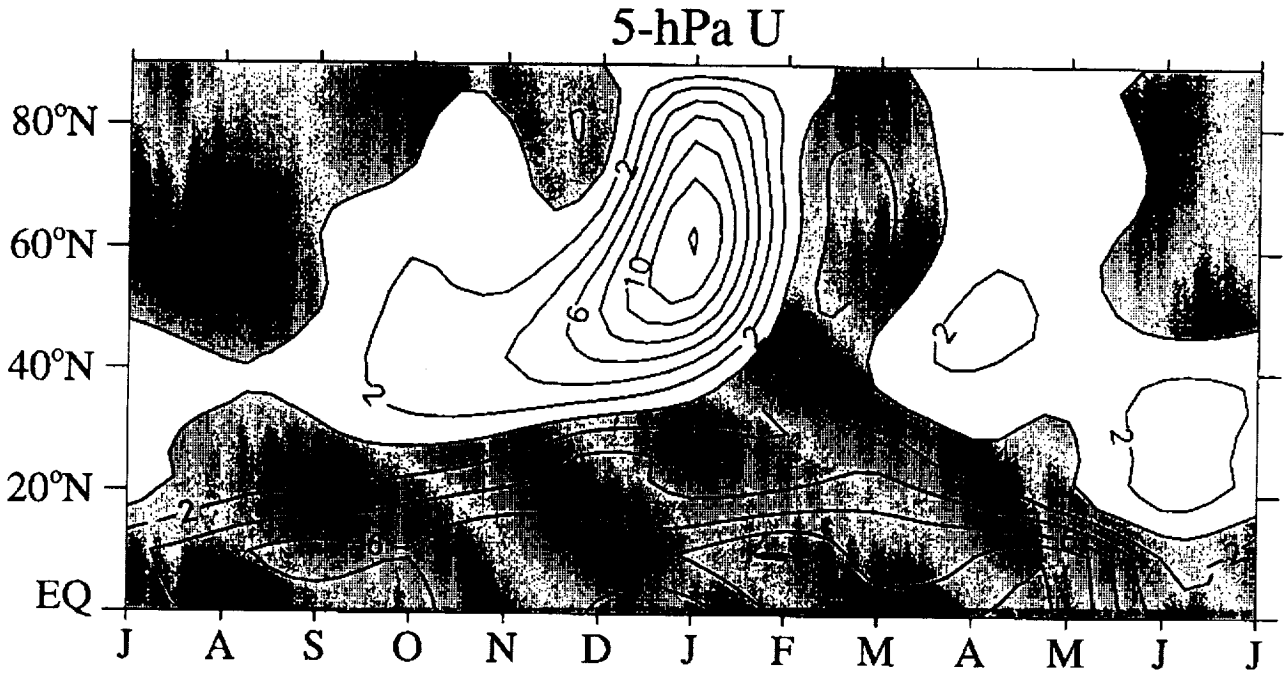

Figure 20. NH 5-hPa month-latitude zonal-mean wind difference between the average of all years with westerly QBO and those with easterly QBO. The phase of the QBO is defined as in Figure 19 and the data are monthly means. The contour interval is 2 ms^{-1} and negative values are shaded. From *Baldwin and Dunkerton* [1998b].

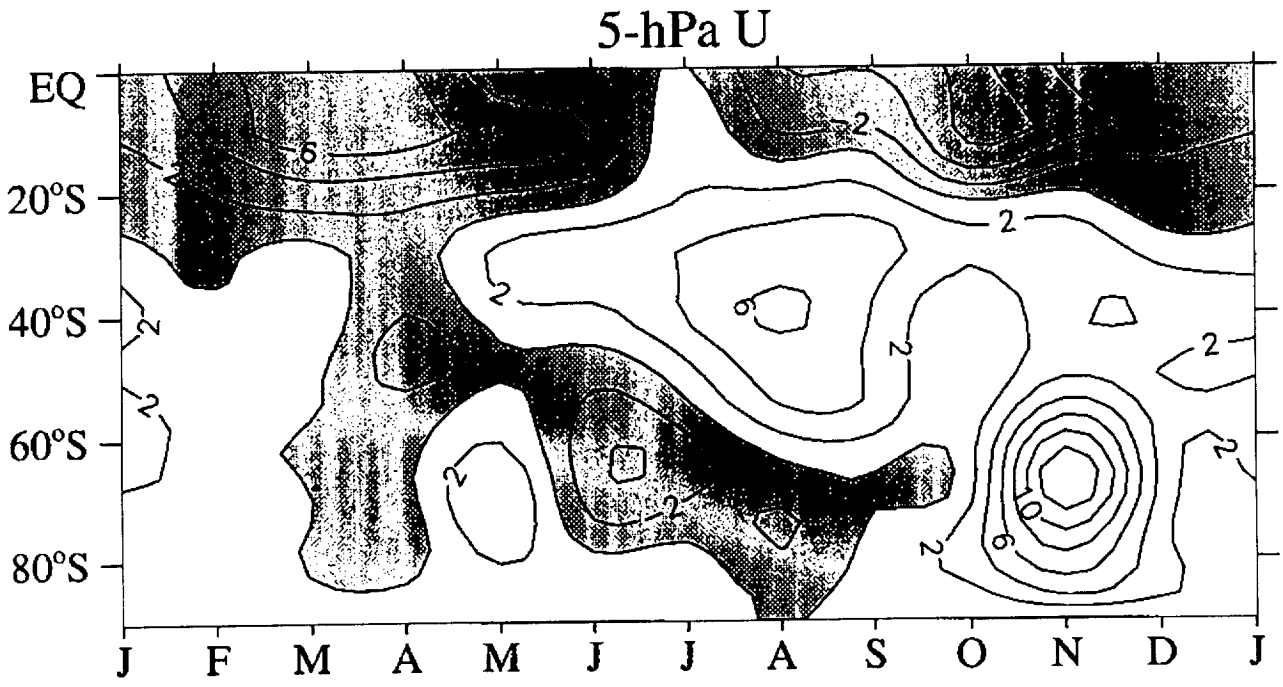

Figure 21. SH 5-hPa month-latitude zonal-mean wind difference between the average of all years with westerly QBO and those with easterly QBO. The calculation is as in Figure 20, except the phase of the QBO is optimized for the SH, which is nearly equivalent to using 25 hPa equatorial winds. From *Baldwin and Dunkerton* [1998b].

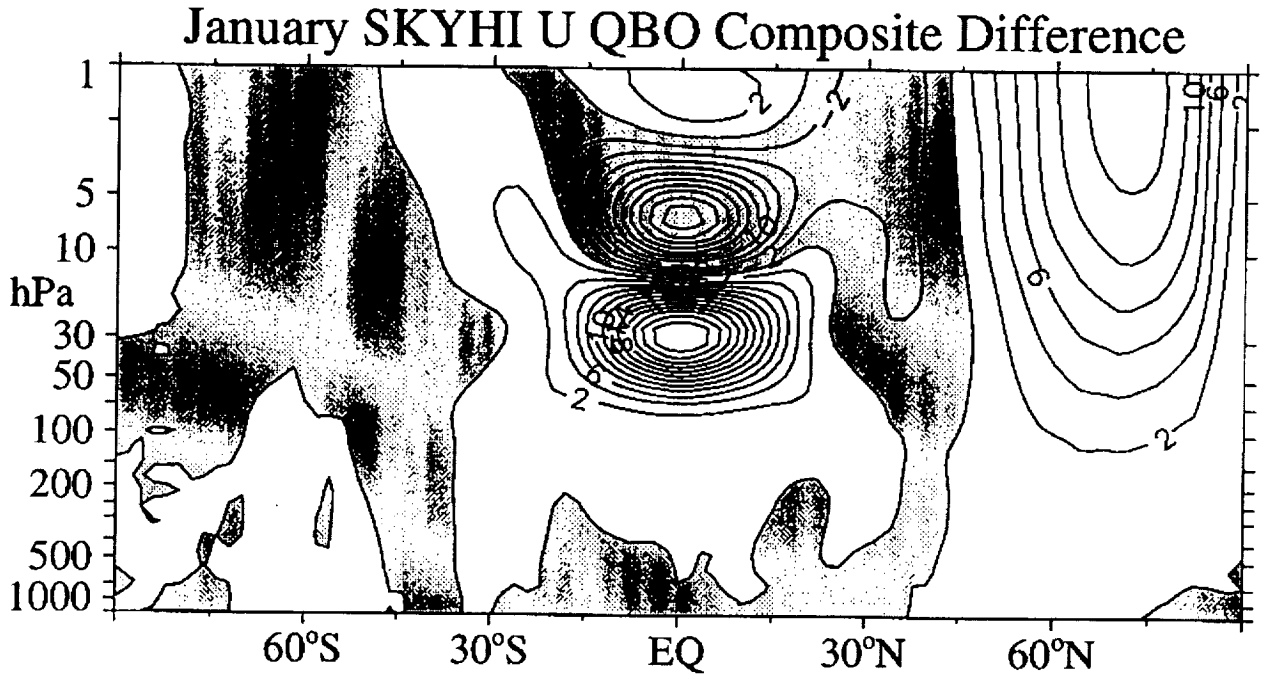

Figure 22. Westerly minus easterly phase composite of the zonal-mean zonal wind in January from the 48 year GCM integration described in Hamilton [1998]. The composite was made based on the 20 Januarys with most westerly equatorial winds at 40 hPa and the 20 Januarys with most easterly equatorial 40 hPa winds. Results are shown here to 1 hPa but the model domain actually extends to 0.01 hPa.

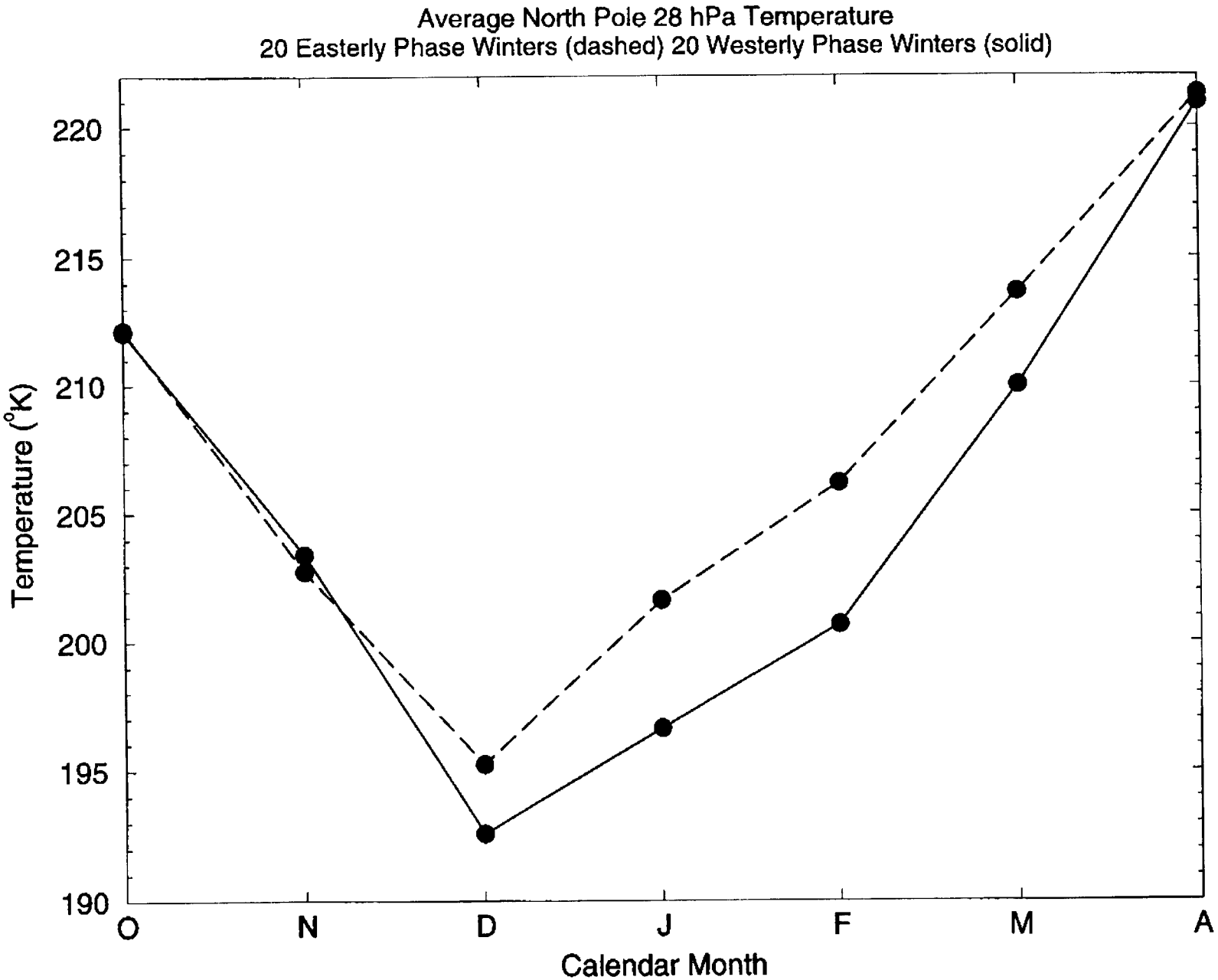

Figure 23. North Pole 28 hPa temperatures for each month from October through April in the 48 year GCM experiment of Hamilton [1998] composited by QBO phase. Results are shown averaged over the 20 years with most easterly (dashed) 40 hPa equatorial winds (for the December-February period) and for the 20 years with most westerly equatorial 40 hPa winds.

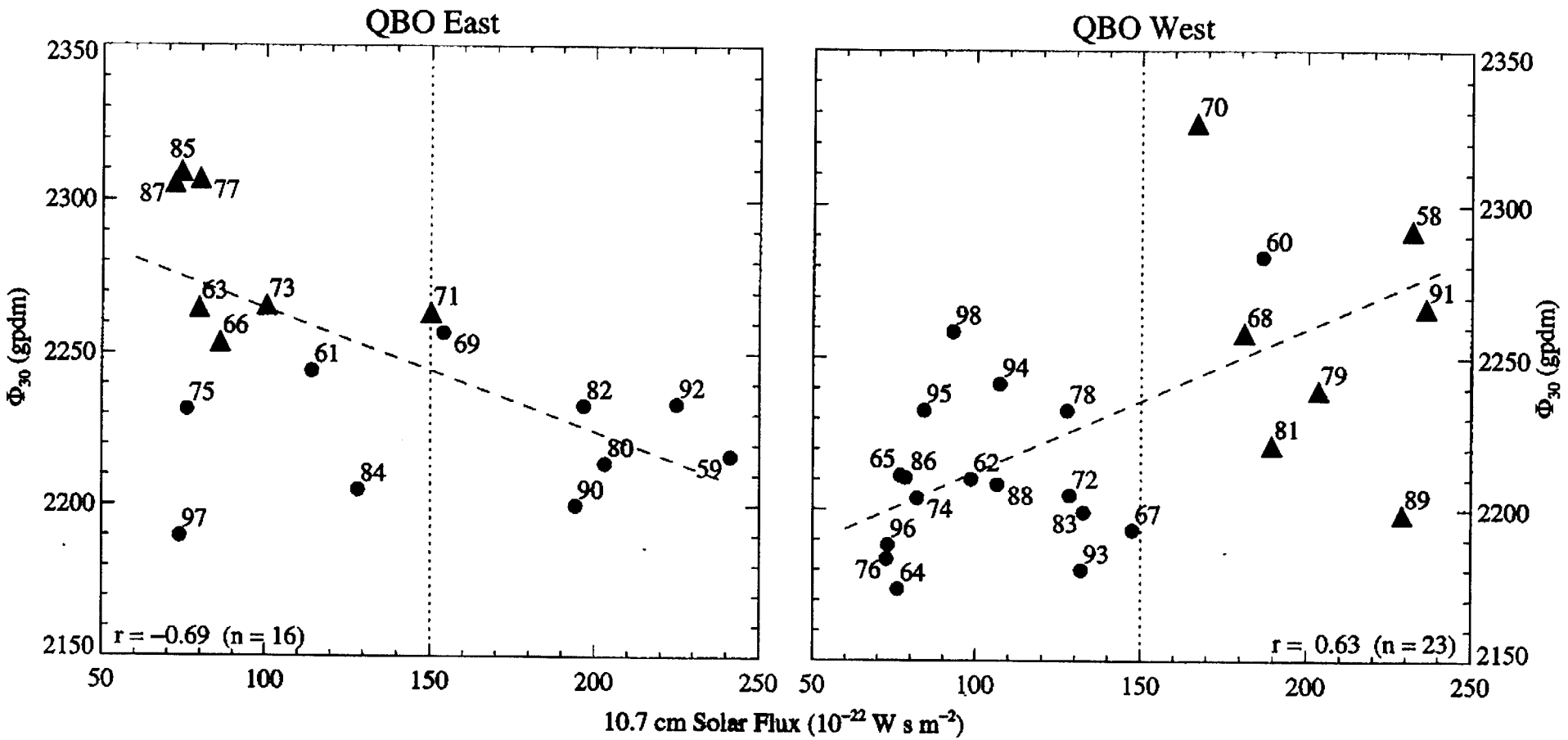

Figure 24. Scatter plots of mean January and February 30 hPa geopotential heights at the North Pole between 1958 and 1998 for years with easterly tropical QBO (left) and westerly (right), respectively (after van *Loon and Labitzke* [1994], updated). Years during which major midwinter or final warmings occurred in January or February are denoted by triangles. Linear correlations are given in the lower left and right corner of each plot, and the linear fit through each of the data sets is denoted by the dashed lines. Note that two outliers (1989 and 1997) were not used in the statistical calculations.

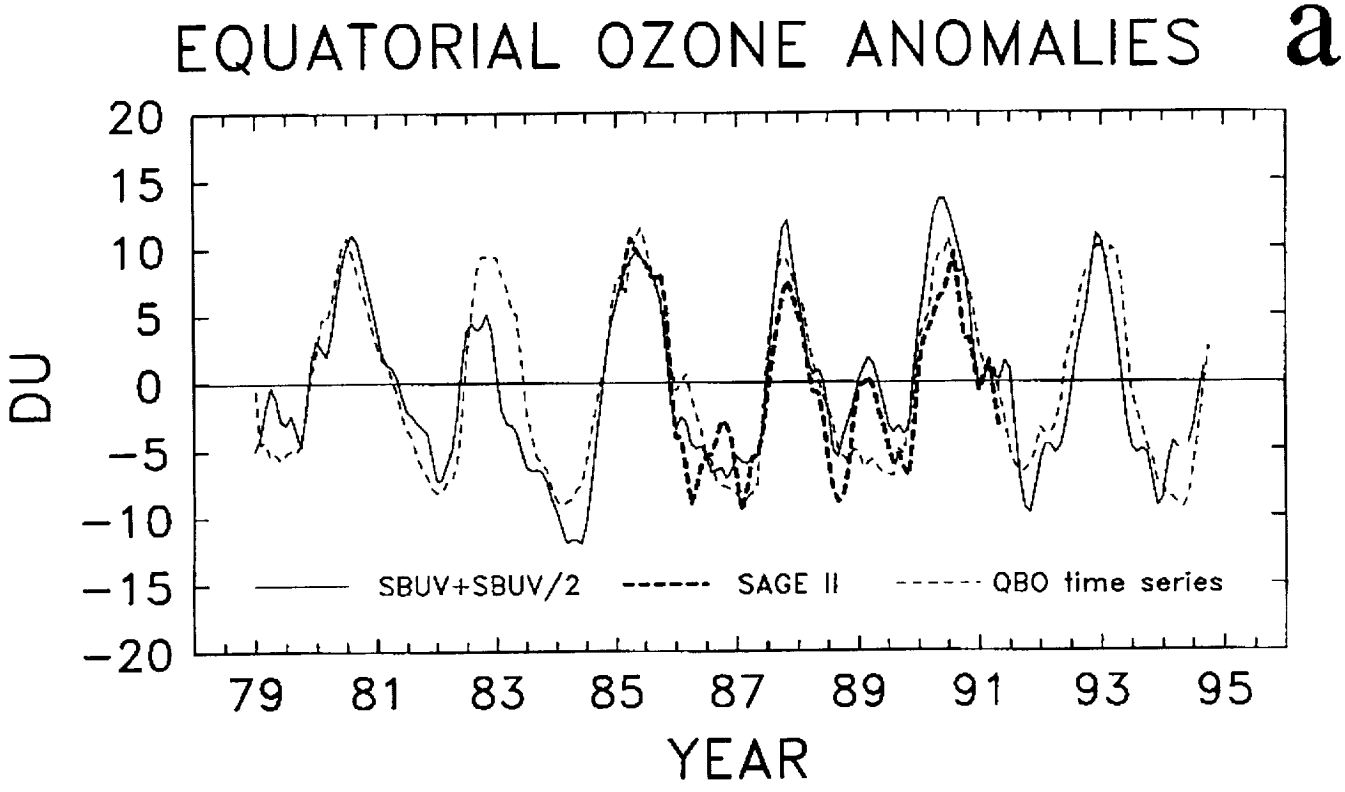

Figure 25. (a) Time-series of equatorial ozone anomaly in percent (solid line) from SBUV and SBUV/2 together with a reference QBO wind time series (dotted line) compiled by multiplying the observed winds at Singapore by the weighting profile shown in (b). From *Randel and Wu* [1996].

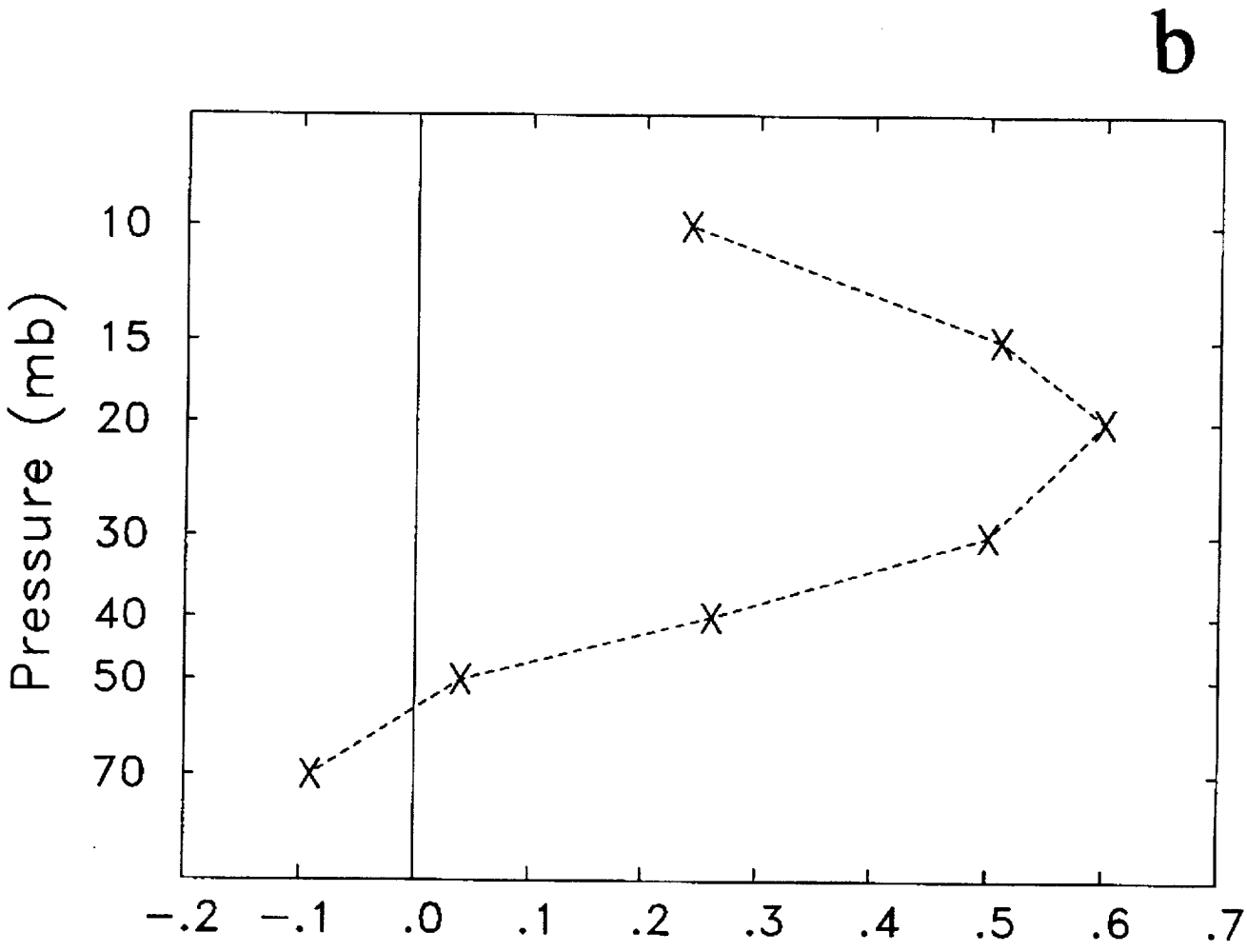

25(6)

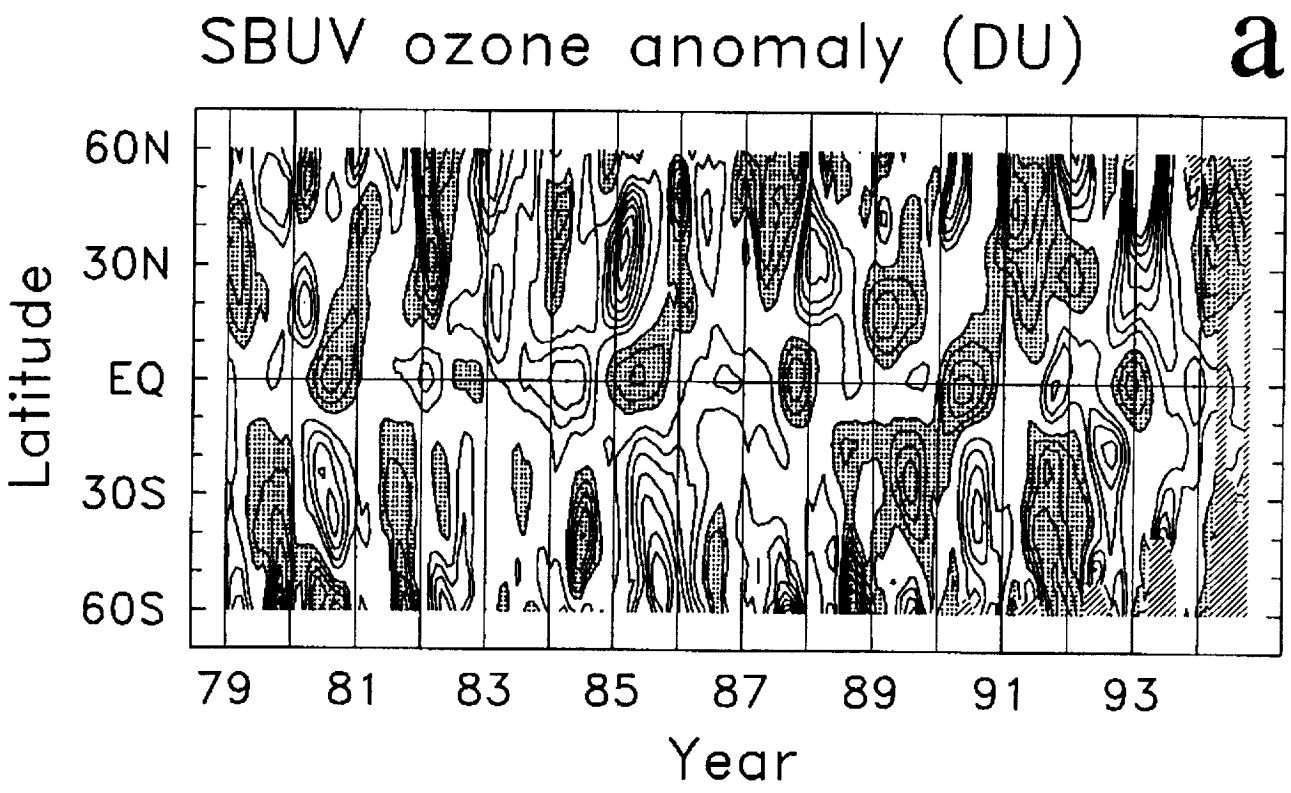

Figure 26. Latitude-time sections of column ozone anomalies from combined SBUV-SBUV/2 data. (a) Full anomalies defined as deseasonalized and detrended over 1979-94, and (b) the QBO component derived by seasonally varying regression analysis. Data in all panels have been multiplied by cos (latitude) to account for area weighting. Contour interval is 3 DU, with zero contours omitted and positive values shaded. Diagonal hatching denotes unreliable data. Vertical lines denote January of each year. From *Randel and Wu* [1996].

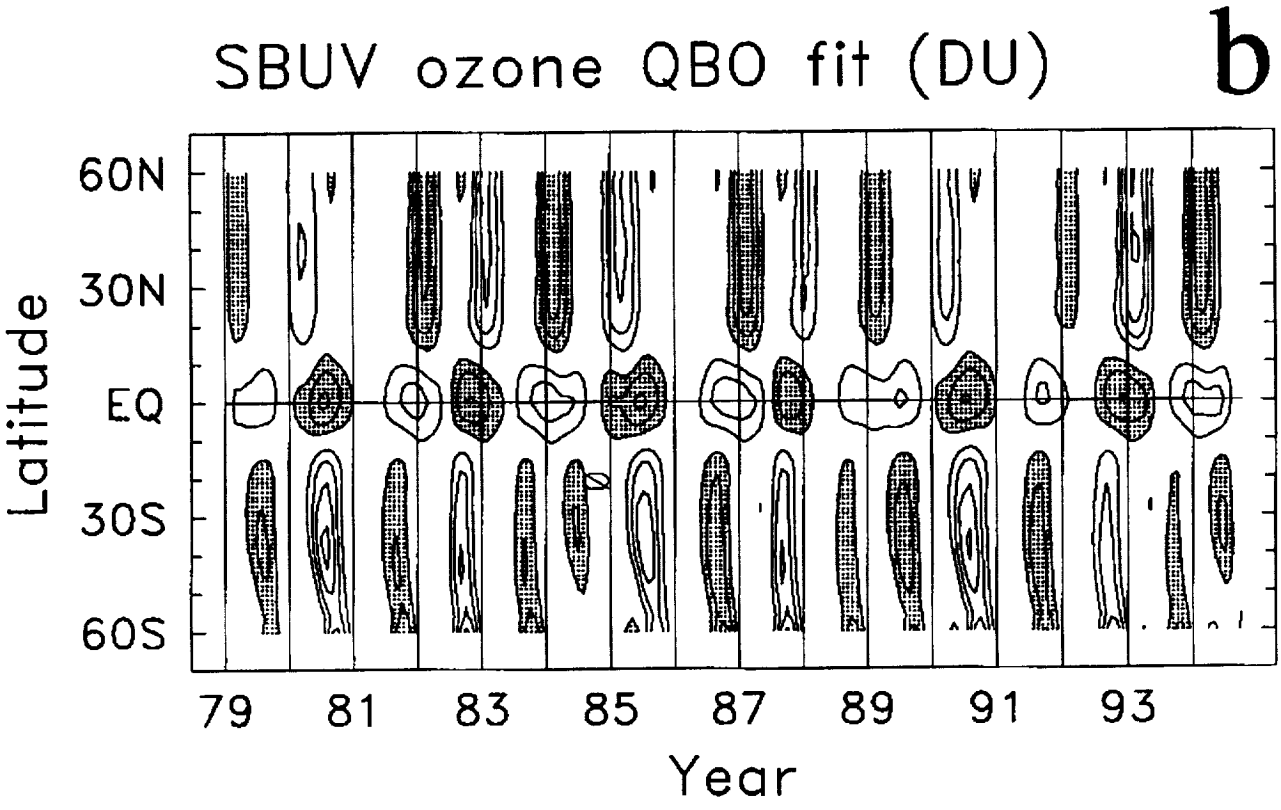
SBUV ozone QBO fit (DU)
b
60N
30N
EQ
30S
60S
Latitude
79
81
83
85
87
89
91
93
Year

2616

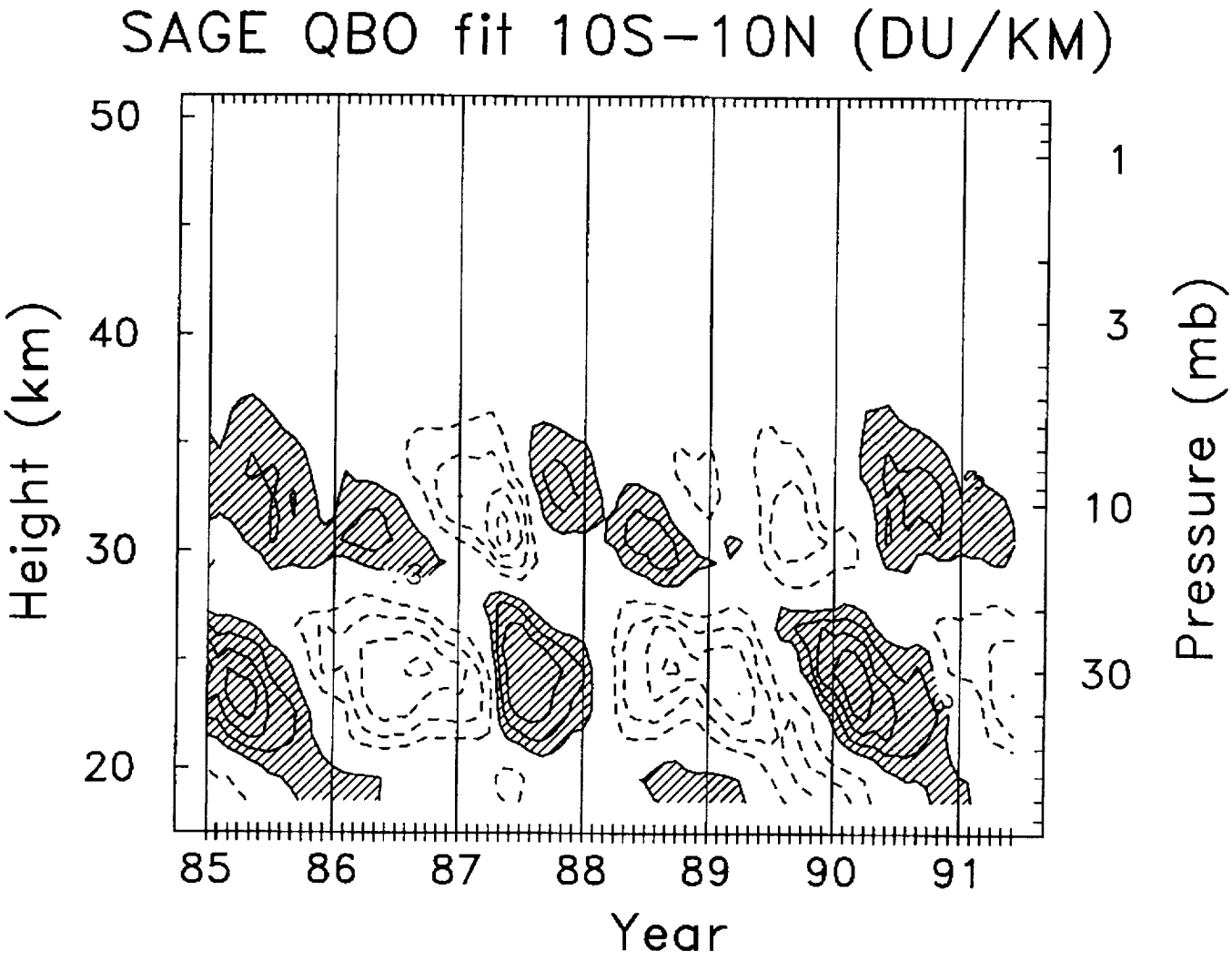

Figure 27. Height – time series of interannual anomalies ozone density (DU/km) derived using a regression analysis to isolate the QBO variation. Contour intervals are 0.3 DU/km with zero contours omitted and positive values shaded. From *Randel and Wu* [1996].

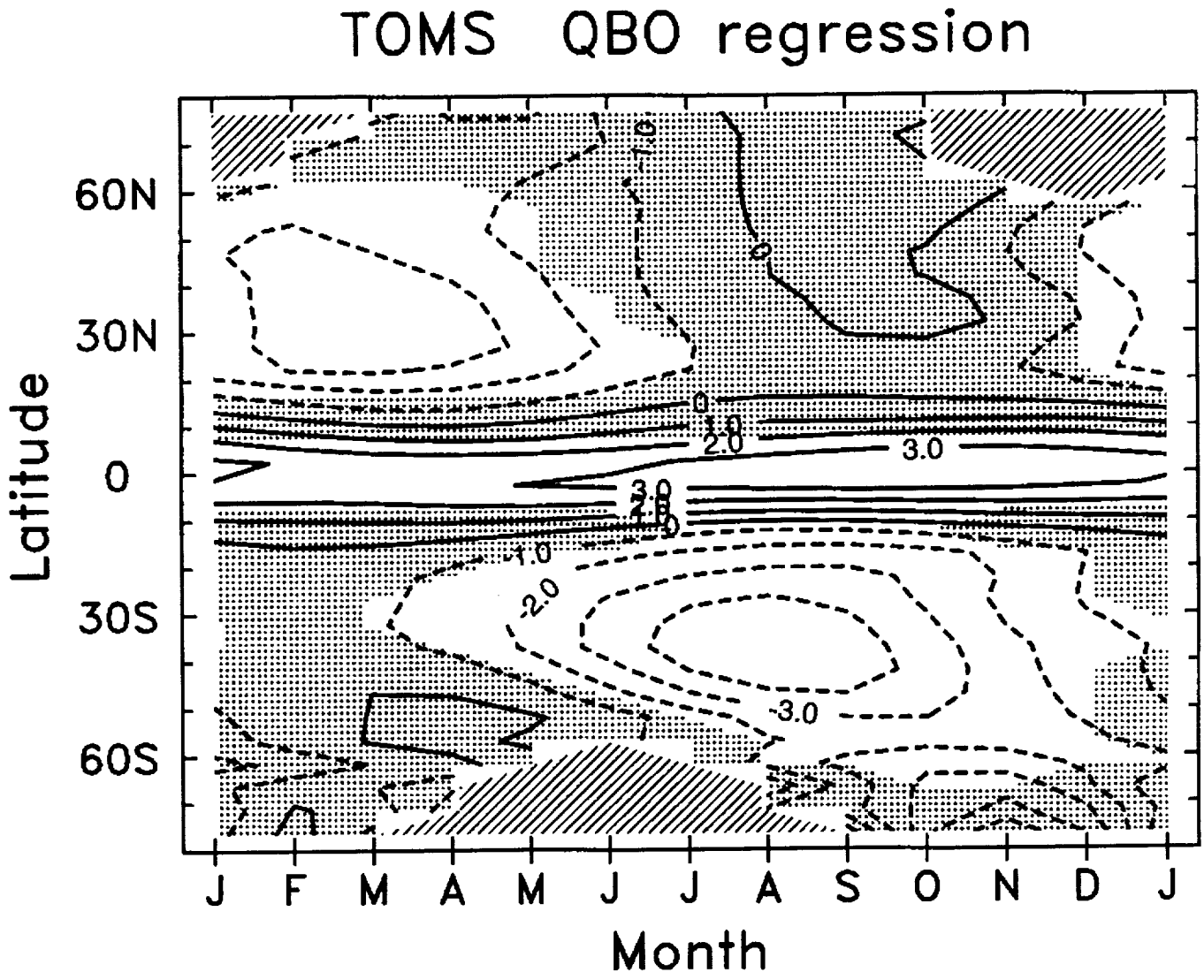

Figure 28. Latitude – time section of QBO-associated regression fit of zonal mean column ozone (DU) from the TOMS instrument to the 30 hPa Singapore winds for the period 1979-1994. Stippling denotes regions where the statistical fits are different from zero at the 2σ level. Hatched regions denote the polar night, where no ozone data are available. Updated from *Randel and Cobb* [1994].

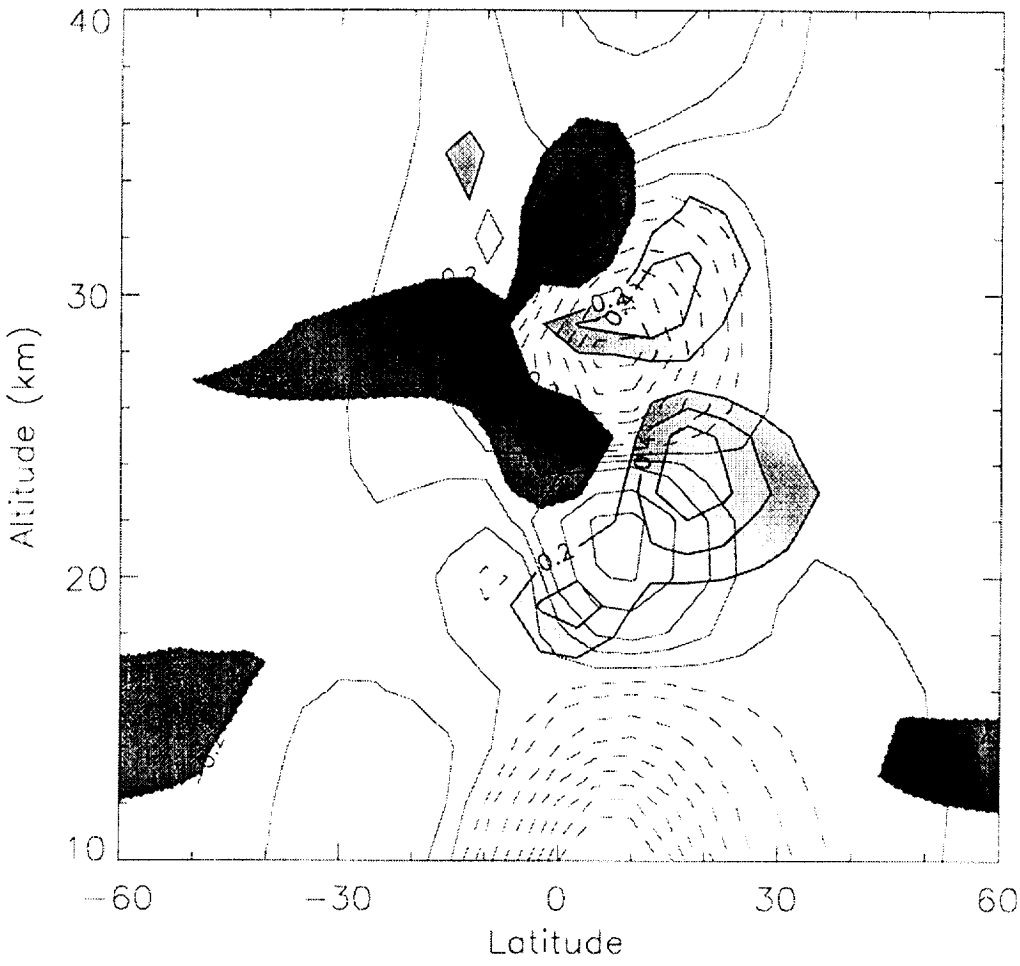

Figure 29. QBO anomaly in ozone (DU/km) in January from the 2-d model of *Jones et al.* [1998] together with the corresponding mass streamfunction. Contour intervals are 0.2 DU/km, with zero contours omitted. Positive (negative) ozone anomaly values are lightly (darkly) shaded. Solid contours indicate positive streamfunction.

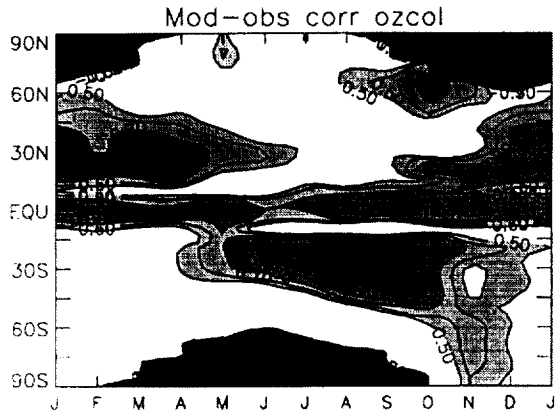

Figure 30. Correlation of detrended TOMS monthly mean ozone column with the ozone column from the model of *Kinnersley and Tung* [1998] (forced by the observed Singapore wind) covering the period November 1978 – April 1993 (contour interval 0.1).

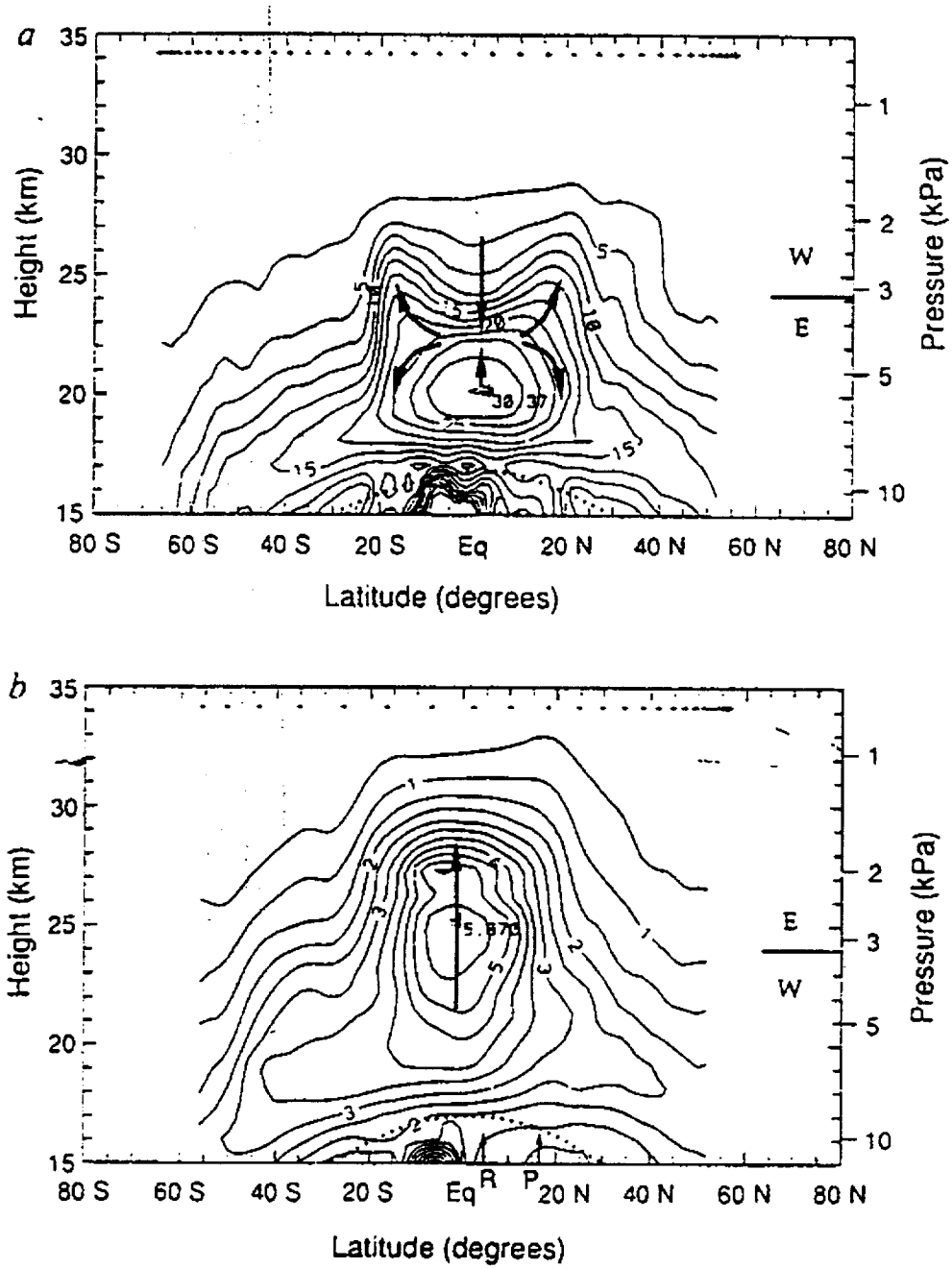

Figure 31. Height-latitude cross-sections of observed aerosol extinction ratio for two 40 day periods representative of the two phases of the QBO. (a) Westerly shear phase centered on 11 November 1984 (contour interval 2.5). (b) Easterly shear phase centered on 4 October 1988 (contour interval 0.5). From *Trepte and Hitchman* [1992].

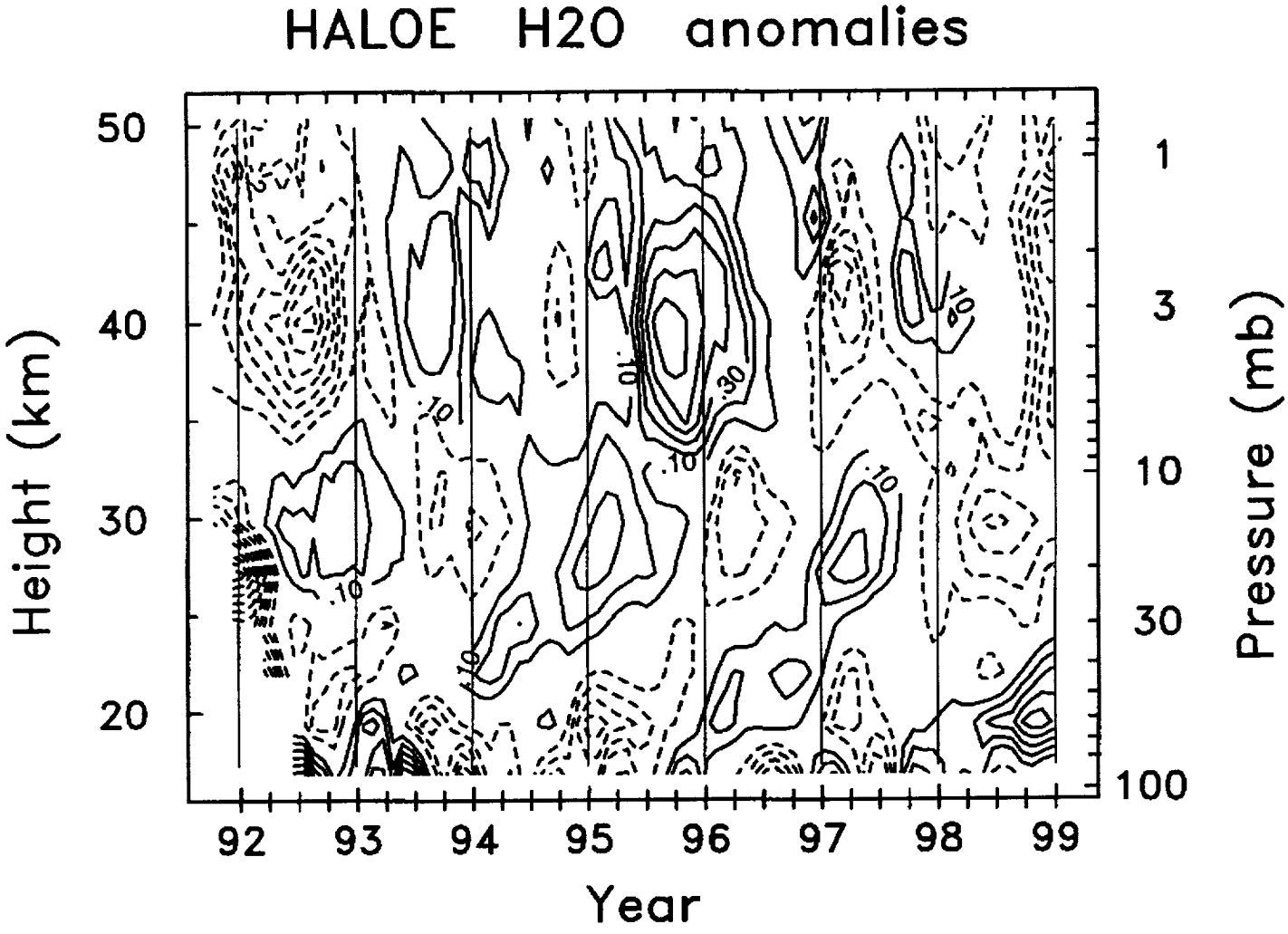

Figure 32. Height-time sections of interannual anomalies in H_2O over the equator from the HALOE instrument. The contour interval is 0.1 ppmv with zero contour omitted. From *Randel et al.*, [1998].

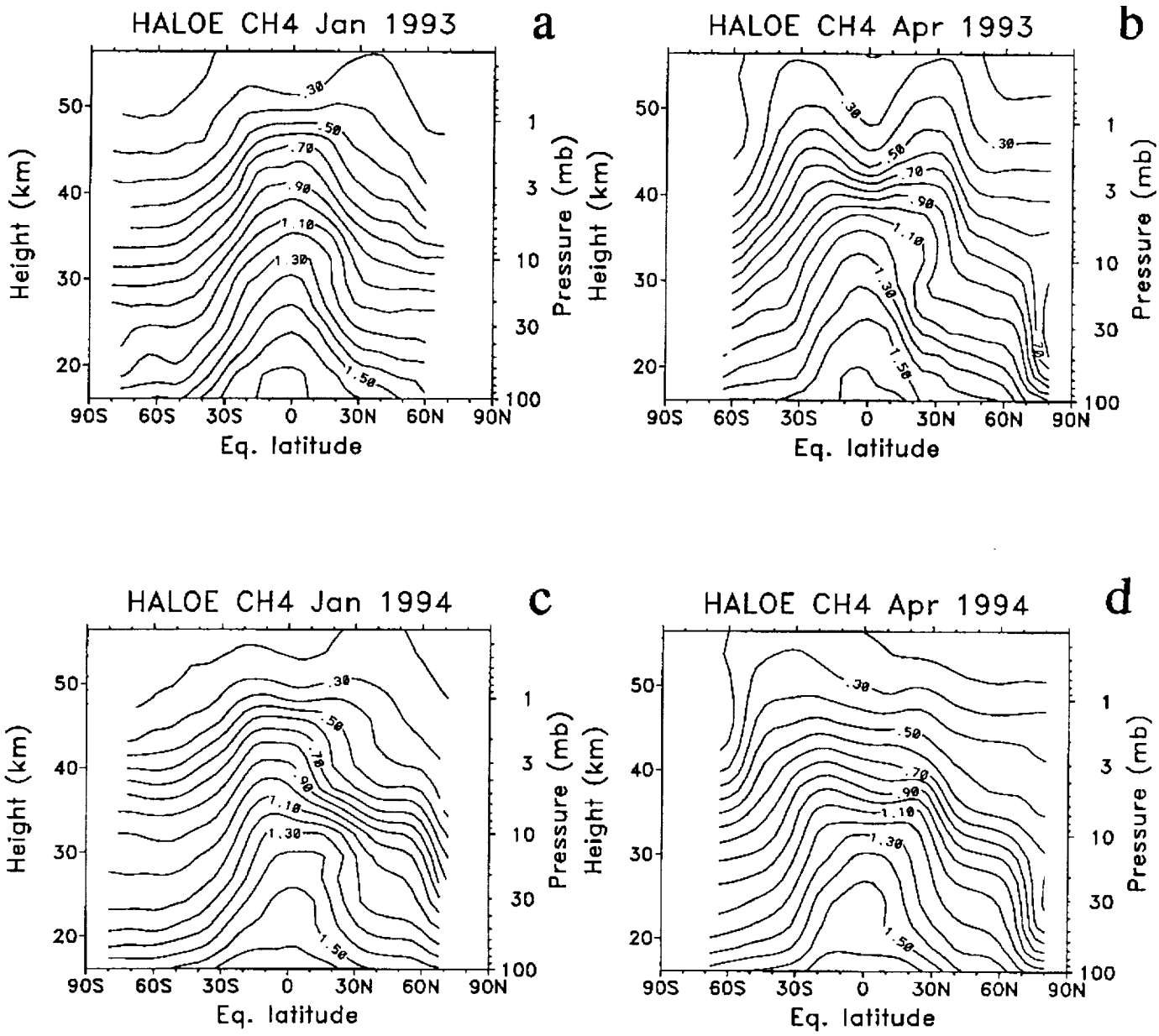

Figure 33. Height versus equivalent latitude cross sections of methane in January and April 1993 and 1994, from HALOE observations. Contour interval of 0.1 ppbv. Linear trends have been removed from each time series. From *Gray and Russell* [1999].

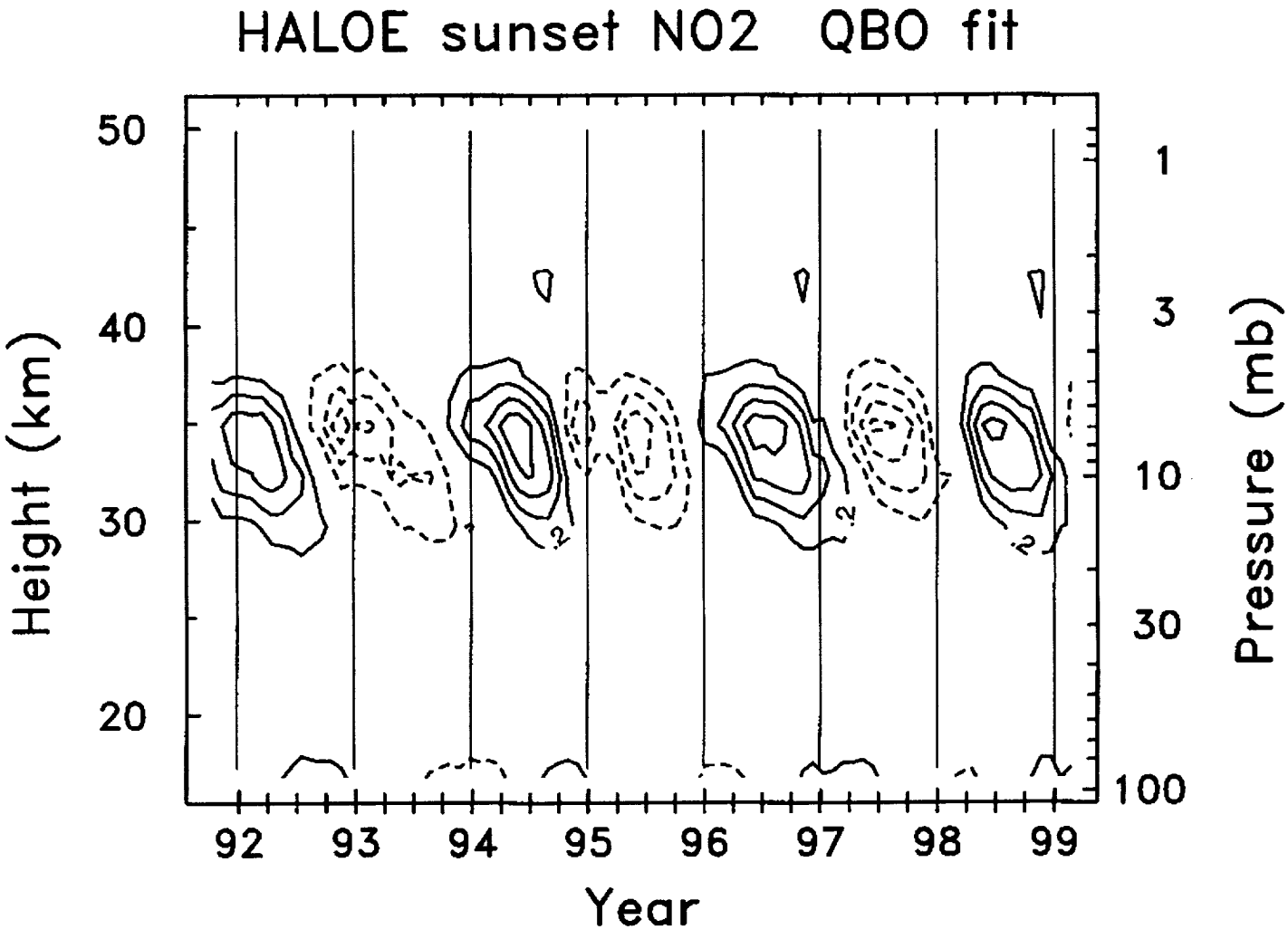

Figure 34. Height – time cross-section of the QBO anomalies in NO_2 in the 10°S–10°N latitude band derived from HALOE observations. The contour interval is 0.2 ppbv, and zero contours omitted. These anomalies have been derived from regression analyses, following *Randel and Wu* [1996].

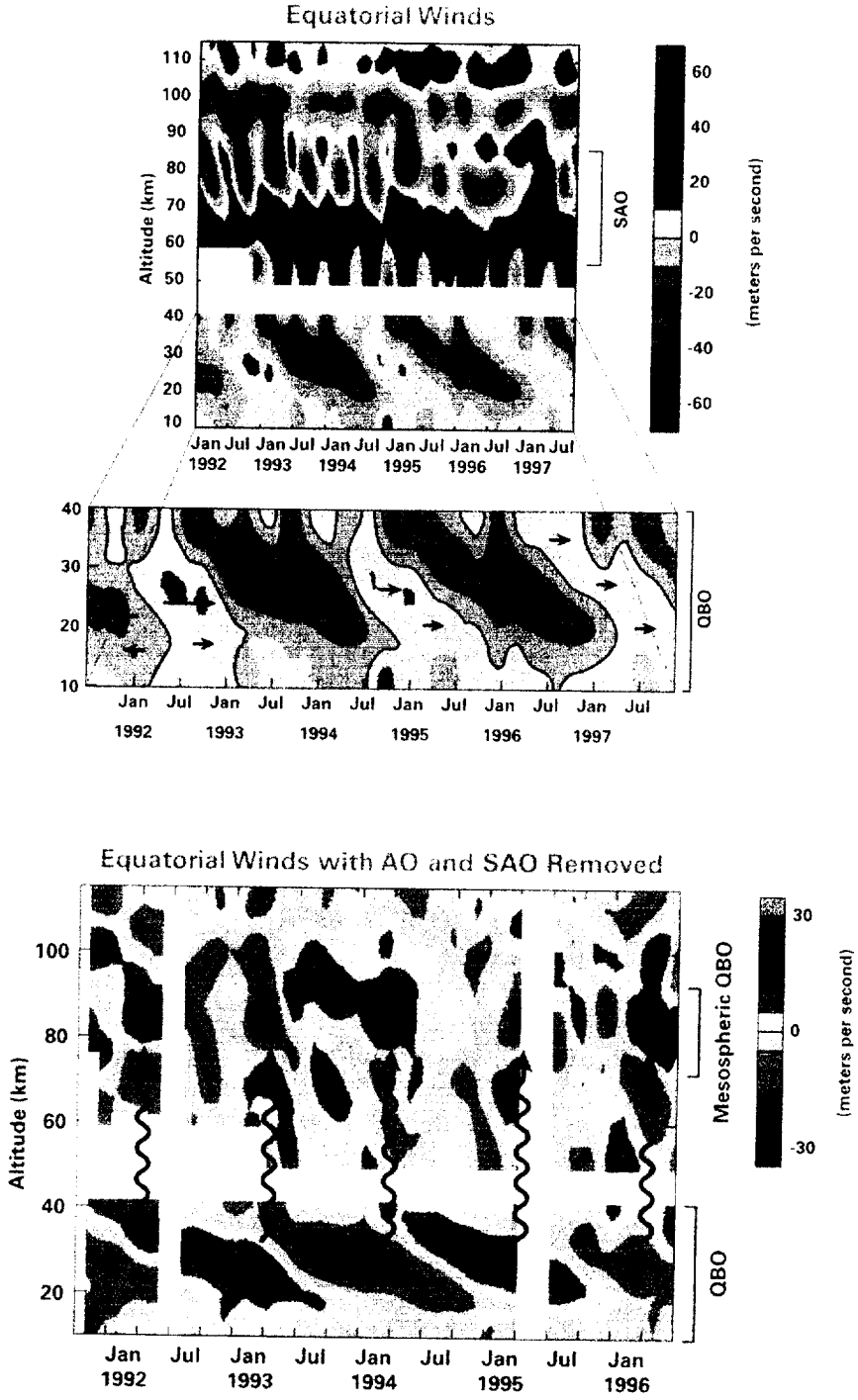

Figure 35. (TOP) HRDI measurements of the zonally averaged zonal eastward (westerly) winds in the tropical stratosphere and mesosphere (left) from 1992 to 1998. The lower figure shows the QBO from 20-40 km as descending easterly (green to blue) and westerly (red to yellow) winds. In the lower mesosphere (60-80 km) the wind structure is dominated by the semiannual oscillation (SAO), a twice-yearly reversal in the winds. (BOTTOM) Removing the SAO and the annual oscillation (upper figure) shows that the influence of the QBO extends into the mesosphere (80 km). Mesospheric wind changes occur coincident with the change of the QBO winds near 30 km. This coupling between the mesosphere and the stratosphere is believed to be caused by small-scale upward moving atmospheric waves, as indicated by wiggly arrows. From the UARS brochure, modified from the original provided by M. Burrage and D. Ortland. Courtesy M. Schoeberl.

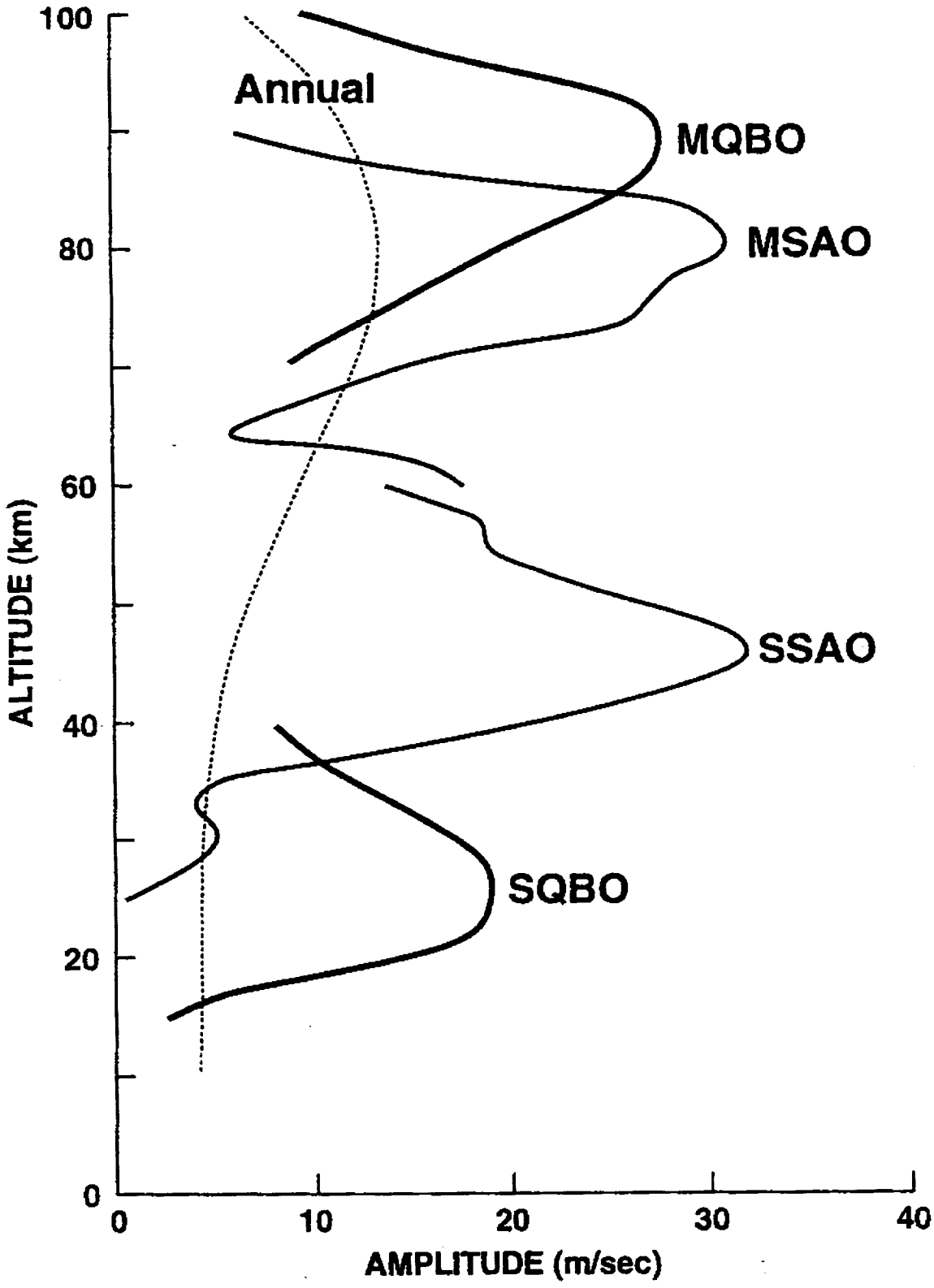

Figure 36. Vertical distribution of the amplitude of the MQBO, MSAO, SSAO, SQBO and annual component at the equator. MQBO is based on the UARS/HRDI observation [*Burrage et al.*, 1996]. SAO is based on the rocket observation at Ascension Island [*Hirota*, 1978] and the annual component is after *CIRA* -1986.

Figure 37. Difference in 1000-hPa geopotential composites (meters) between westerly and easterly QBO composites. December-February monthly-mean NMC data for 1964–1996 are used.

REPORT DOCUMENTATION PAGE

Form Approved
OMB No. 0704-0188

1. AGENCY USE ONLY *(Leave blank)*	2. REPORT DATE	3. REPORT TYPE AND DATES COVERED
	1 November 2000	Final Report June 5, 1997 – June 4, 2000

4. TITLE AND SUBTITLE
Decadal Variability and Temperature Trends in the Middle Atmosphere From Historical Rocketsonde Data

5. FUNDING NUMBERS
NASW-97010

6. AUTHORS
Dr. Timothy Dunkerton

7. PERFORMING ORGANIZATION NAME(S) AND ADDRESS(ES)
Northwest Research Associates, Inc.
P.O. Box 3027
Bellevue, WA 98009-3027

8. PERFORMING ORGANIZATION REPORT NUMBER
NWRA-CR-00-R226

9. SPONSORING/MONITORING AGENCY NAME(S) AND ADDRESS(ES)
NASA/Goddard Space Flight Center
Attn: Mr. Joseph Kroener
Office of Headquarters Operations, Code 210.H
Greenbelt Road
Greenbelt, MD 20771

10. SPONSORING/MONITORING AGENCY REPORT NUMBER

11. SUPPLEMENTARY NOTES

12a. DISTRIBUTION/AVAILABILITY STATEMENT

12b. DISTRIBUTION CODE

13. ABSTRACT *(Maximum 200 words)*

Observational studies were performed using historical rocketsonde data to investigate long-term temperature trends, solar-cycle variations, and interactions between tropical and extratropical latitudes in the middle atmosphere. Evidence from tropical, subtropical, and midlatitude North American rocketsonde stations indicated a consistent downward trend over 25 years, with a solar cycle component superposed. The trend is about -1.4 to-2.0 K per decade and the amplitude of the decadal oscillation is about1.1 K. Prior to trend derivation it was necessary for us to correct temperatures for aerodynamic heating in the early years. The empirically derived correction profile agrees well with a theoretical profile of Krumins and Lyons. A study was also performed of the correlation between equatorial winds and north polar temperatures in winter, showing that the entire stratospheric wind profile near the equator -- including the quasi-biennial oscillation (QBO) and stratopause semiannual oscillation (SAO) -- is important to the extratropical flow, not merely the QBO component as previously thought. A strong correlation was discovered between winter polar temperatures and equatorial winds in the upper stratosphere during the preceding September, suggesting a role for the second cycle of the SAO.

14. SUBJECT TERMS
Rocektsonde, QBO, Temperature Trend

15. NUMBER OF PAGES

16. PRICE CODE

17. SECURITY CLASSIFICATION OF REPORT	18. SECURITY CLASSIFICATION OF THIS PAGE	19. SECURITY CLASSIFICATION OF ABSTRACT	20. LIMITATION OF ABSTRACT
Unclassified	Unclassified	Unclassified	UL